

**Synthetic Studies of Functional
Zinc Phthalocyanines and
Boron Dipyrromethenes**

LIU, Jianyong

**A Thesis Submitted in Partial Fulfillment of the
Requirements for the Degree of Doctor of Philosophy**

**In
Chemistry**

March 2009

UMI Number: 3392269

All rights reserved

INFORMATION TO ALL USERS

The quality of this reproduction is dependent upon the quality of the copy submitted.

In the unlikely event that the author did not send a complete manuscript and there are missing pages, these will be noted. Also, if material had to be removed, a note will indicate the deletion.



UMI 3392269

Copyright 2010 by ProQuest LLC.

All rights reserved. This edition of the work is protected against unauthorized copying under Title 17, United States Code.



ProQuest LLC
789 East Eisenhower Parkway
P.O. Box 1346
Ann Arbor, MI 48106-1346

Thesis/Assessment Committee

Professor Tony K. M. Shing (Chair)

Professor Dennis K. P. Ng (Thesis Supervisor)

Professor Qian Miao (Committee Member)

Professor Kwok-Yin Wong (External Examiner)

Professor Kevin Burgess (External Examiner)

Abstract

This thesis describes my synthetic studies on several series of functional zinc(II) phthalocyanines and boron dipyrromethenes (BODIPYs). Their applications as efficient photosensitizers in photodynamic therapy and light harvesting systems have also been explored.

Chapter 1 presents an overview of phthalocyanines including their general synthesis, properties, and applications. Special attention has been placed on the unsymmetrical analogues, and those which are efficient photosensitizers in photodynamic therapy. A brief account on BODIPYs as another versatile class of functional dyes is also given.

Chapter 2 describes the synthesis, spectroscopic characterization, photophysical properties, and in vitro photodynamic activities of three novel amphiphilic zinc(II) phthalocyanines substituted with one or two 3,4,5-tris(3,6,9-trioxadecoxy)benzoxy group(s). These compounds exhibit significantly higher photodynamic activities toward HepG2 and HT29 cell lines. The α -substituted analogue is particularly potent with IC_{50} values as low as 0.02 μ M. The higher photodynamic activity of this compound can be attributed to its lower aggregation tendency in the culture media as shown by absorption spectroscopy and higher cellular uptake as suggested by the stronger intracellular fluorescence, resulting in a higher efficiency to generate reactive oxygen species inside the cells.

The related studies of a series of novel di- α -substituted zinc(II) phthalocyanines having two biocompatible triethylene glycol methyl ether chains or glycerol moieties are described in **Chapter 3**. Compared with the unsubstituted analogue, these compounds have a red-shifted Q band, and exhibit a relatively weaker fluorescence emission and higher efficiency to generate singlet oxygen. As a result, these compounds are promising candidates for photodynamic therapy. In vitro studies on HepG2 and HT29 cells have shown that they are highly photocytotoxic with IC₅₀ values as low as 0.06 μ M.

Chapter 4 focuses on a related series of 1,4-disubstituted zinc(II) phthalocyanines. These compounds possess two oligoethylene glycol methyl ether chains with various length at the 1,4-di- α -positions. The effects of the chain length on their aggregation, photophysical properties, cellular uptake, and in vitro photodynamic activities have been explored.

Chapter 5 presents the synthesis, characterization, and photophysical properties of another series of zinc(II) phthalocyanines conjugated with one, two or four isopropylidene protected glucofuranose unit(s) through a tetraethylene glycol linker. With these hydrophilic substituents, these macrocycles are highly soluble in common organic solvents and biological media. Their in vitro photodynamic activities toward HT29 and HepG2 cells have also been evaluated. Compared with the tetra-glucosylated phthalocyanines, which are almost nonphotocytotoxic, the mono- and di-glucosylated analogues exhibit a higher photodynamic activity. The di- α -substituted analogue is particularly potent with IC₅₀ values as low as 0.03 μ M.

Chapter 6 reports the synthesis, characterization, and photophysical properties of two novel conjugates of subphthalocyanine substituted axially with a BODIPY or distyryl-BODIPY moiety. Both systems absorb over a broad range in the visible region. They also exhibit a highly efficient photo-induced energy transfer process either from the excited BODIPY to the subphthalocyanine core or from the excited subphthalocyanine to the distyryl-BODIPY unit. The energy transfer quantum yields are close to unity for both of these conjugates.

Chapter 7 describes the preparation and photophysical properties of another two BODIPY and monostyryl-BODIPY conjugates which are linked to a silicon(IV) phthalocyanine core. These conjugates serve as excellent artificial photosynthetic models for the study of energy and electron transfer processes. Depending on the axial substituents, these conjugates exhibit predominantly a photo-induced energy or electron transfer process in toluene.

^1H and $^{13}\text{C}\{^1\text{H}\}$ NMR spectra of all the new compounds and crystallographic data are given in the Appendix.

摘要

本論文報導了一些功能鋅酞菁和氟硼二吡咯染料的合成研究。這些化合物作為有效光敏劑在光動力治療和光捕獲系統中的應用也被探索。

第一章概述了酞菁，特別是不對稱酞菁的合成、性質和應用。這些酞菁化合物作為有效光敏劑在光動力治療上的應用也被討論。此外，本章也簡單介紹了另一類多功能發光染料—氟硼二吡咯。

第二章報導了三個“3 + 1”不對稱兩親性鋅酞菁的合成、光譜特徵和光物理性質。這些化合物對人類肝癌細胞 HepG2 和腸腺癌細胞 HT29 的光毒作用也被探討。這些新型酞菁，尤其是 α 取代酞菁顯示了很高的體外光動力活性，它們的 IC_{50} 值可低至 0.02 μM 。

第三章報導了一系列二 α 取代鋅酞菁。這些酞菁在 1, 4 二 α 位置上包含有兩條生物相容的三(乙二醇)鏈或甘油單位。相比無取代鋅酞菁，這些化合物具有紅移的 Q 帶吸收，相對更弱的螢光發光和更高的單線態氧量子產率。相應地，它們對 HepG2 和 HT29 細胞顯示了很高的光動力活性，其 IC_{50} 值可低至 0.06 μM 。

作為第三章的延續，第四章描述了一系列 1, 4-二取代聚乙二醇酞菁。乙二醇鏈的長度對酞菁聚集、光物理性質、細胞吸收和體外光動力活性的影響也被研究。

第五章闡述了一系列糖連酞菁的合成、光譜表徵和光物理性質。這些酞菁含有一、二或四個丙酮保護的呋喃葡萄糖單位，在一般有機溶劑和生物介質中具有很高的溶解性。此外，這些化合物對 HepG2 和 HT29 細胞的光動力活性也被探討。相比無光毒作用的四取代糖連酞菁。一、二取代糖連酞菁顯示了高的光動力活性，特別是 5.9，其 IC_{50} 值低至 $0.03 \mu\text{M}$ 。

第六章合成並表徵了兩個通過共價鍵相連的亞酞菁-氟硼二吡咯共軛物。這兩個化合物在可見光區具有非常寬廣的吸收。它們也展現了一個非常高效的光誘導能量轉移過程，要麼從激發態的氟硼二吡咯到亞酞菁，要麼從激發態的亞酞菁到二苯乙烯基取代的氟硼二吡咯。

第七章報導了兩個通過共價鍵相連的硅酞菁-氟硼二吡咯共軛物，包括他們的合成、表徵和光物理性質。取決於軸上取代的氟硼二吡咯，這兩個化合物在甲苯中展現了一個主要的光誘導能量或電子轉移過程。

附錄 A 列出所有新化合物的核磁氫譜和碳譜，X 衍射晶體結構測定資料詳見附錄 B。

Acknowledgment

Firstly, I would like to express my deepest gratitude to my supervisor, Prof. Dennis K. P. Ng, for his guidance, inspiration, patience, and support during my postgraduate studies. Over the past three years, he has taught me a lot in various aspects, including presentation of data and arguments effectively in a simple but yet scientific way and composition and review of academic papers. He provided me the opportunity to attend the 12th International Symposium of Novel Aromatic Compounds (ISNA12) held in Japan, which enriched my academic life and widened my horizon. He also gave me great assistance during the preparation of my graduate seminars and this thesis. To him, let me say "many thanks" again.

This research work was made possible only with the efforts of many people. Prof. Wing-Ping Fong, Elaine Y. M. Chan, and Crystal M. H. Chan of the Department of Biochemistry, CUHK, and Prof. Gigi P. C. Lo and Xiongjie Jiang of the Department of Chemistry, CUHK performed the cytotoxicity and cellular uptake experiments in Chapter 2 to 5. Prof. Xiyou Li of the Department of Chemistry, Shandong University measured the fluorescence quantum yields and lifetimes of the compounds reported in Chapter 6. Dr. Eugeny A. Ermilov of the Institut für Physik, Photobiophysik, Humboldt-Universität zu Berlin performed the time-resolved fluorescence and transient absorption spectroscopic studies of the compounds reported in Chapter 7. Betty H. S. Yeung helped me to prepare some precursors during the summer of 2007. To all these people, I give them my gratitude.

Thanks are also given to my lab-mates, past and present, including Dr. Xuebing Leng, Dr. Bill C. F. Choi, Dr. Ming Bai, Prof. Wubiao Duan, Prof. Jiandong

Huang, Dr Baozhong Zhao, Dr. Hu Xu, Hui He, Janet T. F. Lau, Qunling Fang, and Venus Y. S. Huang for their friendship and helpful discussion.

Last but not the least, I would like to thank my parents, my wife, and my friends for their continuous care, support, understanding, and encouragement during these years.

Table of Contents

| | |
|---|------|
| Abstract | i |
| Abstract (in Chinese) | iv |
| Acknowledgment | vi |
| Table of Contents | viii |
| List of Figures | xiii |
| List of Schemes | xix |
| List of Tables | xxi |
| Abbreviations | xxii |
| Chapter 1 Introduction | 1 |
| 1.1 Phthalocyanine | 1 |
| 1.1.1 General | 1 |
| 1.1.2 Synthesis of Unsymmetrical Phthalocyanines | 3 |
| 1.1.2.1 Synthesis of A ₃ B-type Phthalocyanines | 5 |
| 1.1.2.2 Synthesis of A ₂ B ₂ -type Phthalocyanines | 12 |
| 1.1.3 Phthalocyanines as Efficient Photosensitizers for Photodynamic Therapy | 16 |
| 1.1.3.1 Silicon(IV) Phthalocyanines | 19 |
| 1.1.3.2 Aluminum(III) Phthalocyanines | 22 |
| 1.1.3.3 Zinc(II) Phthalocyanines | 24 |
| 1.1.4 Glycosylated Photosensitizers | 28 |
| 1.1.4.1 Glycosylated Phthalocyanines | 31 |

| | | |
|------------------|--|-----------|
| 1.2 | Boron Dipyrromethenes (BODIPYs) | 34 |
| 1.2.1 | General | 34 |
| 1.2.2 | Light Harvesting Systems Based on BODIPYs | 36 |
| 1.2.2.1 | BODIPYs as the Core | 36 |
| 1.2.2.2 | BODIPYs as the Antenna | 39 |
| 1.2.2.3 | BODIPYs as Both the Core and Antenna | 46 |
| 1.3 | References | 48 |
| Chapter 2 | Synthesis, Characterization, and in vitro Photodynamic Activities of Novel Amphiphilic Zinc(II) Phthalocyanines Bearing Oxyethylene-Rich Substituents | 57 |
| 2.1 | Introduction | 57 |
| 2.2 | Results and Discussion | 58 |
| 2.2.1 | Molecular Design and Chemical Synthesis | 58 |
| 2.2.2 | Spectroscopic Characterization and Photophysical Properties | 61 |
| 2.2.3 | In vitro Photodynamic Activities | 66 |
| 2.3 | Conclusion | 69 |
| 2.4 | Experimental Section | 70 |
| 2.4.1 | General | 70 |
| 2.4.2 | Photophysical Studies | 71 |
| 2.4.3 | Synthesis | 72 |
| 2.4.4 | In vitro Studies | 79 |
| 2.4.4.1 | Cell Lines and Culture Conditions | 79 |
| 2.4.4.2 | Photocytotoxicity Assay | 79 |

| | | |
|------------------|---|------------|
| 2.4.4.3 | Fluorescence Microscopic Studies | 80 |
| 2.5 | References | 81 |
| Chapter 3 | Synthesis, Characterization, and in vitro Photodynamic | 83 |
| | Activities of Di-α-Substituted Zinc(II) Phthalocyanine Derivatives | |
| 3.1 | Introduction | 83 |
| 3.2 | Results and Discussion | 84 |
| 3.2.1 | Synthesis and Characterization | 84 |
| 3.2.2 | Electronic Absorption and Photophysical Properties | 89 |
| 3.2.3 | In vitro Photodynamic Activities | 92 |
| 3.3 | Conclusion | 97 |
| 3.4 | Experimental Section | 97 |
| 3.4.1 | General | 97 |
| 3.4.2 | Synthesis | 97 |
| 3.5 | References | 104 |
| Chapter 4 | Highly Photocytotoxic 1,4-Dipegylated Zinc(II) | 107 |
| | Phthalocyanines. Effects of the Chain Length on the in vitro | |
| | Photodynamic Activities | |
| 4.1 | Introduction | 107 |
| 4.2 | Results and Discussion | 107 |
| 4.2.1 | Molecular Design and Synthesis | 107 |
| 4.2.2 | Electronic Absorption and Photophysical Properties | 111 |
| 4.2.3 | In vitro Photodynamic Activities | 115 |
| 4.3 | Conclusion | 120 |

| | | |
|------------------|--|------------|
| 4.4 | Experimental Section | 121 |
| 4.4.1 | General | 121 |
| 4.4.2 | Synthesis | 121 |
| 4.5 | References | 127 |
| Chapter 5 | Effects of the Number and Position of the Substituents on the | 130 |
| | in vitro Photodynamic Activities of Glucosylated Zinc(II) Phthalocyanines | |
| 5.1 | Introduction | 130 |
| 5.2 | Results and Discussion | 131 |
| 5.2.1 | Synthesis and Characterization | 131 |
| 5.2.2 | Electronic Absorption and Photophysical Properties | 137 |
| 5.2.3 | In vitro Photodynamic Activities | 139 |
| 5.3 | Conclusion | 145 |
| 5.4 | Experimental Section | 146 |
| 5.4.1 | General | 146 |
| 5.4.2 | Synthesis | 147 |
| 5.5 | References | 157 |
| Chapter 6 | Highly Efficient Energy Transfer in | 160 |
| | Subphthalocyanine-BODIPY Conjugates | |
| 6.1 | Introduction | 160 |
| 6.2 | Results and Discussion | 162 |
| 6.2.1 | Preparation and Characterization | 162 |
| 6.2.2 | Electronic Absorption and Photophysical Properties | 167 |
| 6.3 | Conclusion | 174 |

| | | |
|---|---|-----|
| 6.4 | Experimental Section | 174 |
| 6.4.1 | General | 174 |
| 6.4.2 | Photophysical Studies | 175 |
| 6.4.3 | Synthesis | 175 |
| 6.4.4 | X-ray Crystallographic Analysis of 6.2 , 6.4·H₂O , and 6.5·CH₂Cl₂ | 179 |
| 6.5 | References | 181 |
| Chapter 7 Switching the Photo-induced Energy and Electron Transfer Processes in BODIPY-Phthalocyanine Conjugates | | 183 |
| 7.1 | Introduction | 183 |
| 7.2 | Results and Discussion | 185 |
| 7.2.1 | Preparation and Characterization | 185 |
| 7.2.2 | Electronic Absorption and Photophysical Properties | 187 |
| 7.3 | Conclusion | 197 |
| 7.4 | Experimental Section | 198 |
| 7.4.1 | General | 198 |
| 7.4.2 | Photophysical Studies | 198 |
| 7.4.3 | Electrochemical Studies | 199 |
| 7.4.4 | Synthesis | 199 |
| 7.5 | References | 202 |
| Appendix A NMR Spectra of New Compounds | | 204 |
| Appendix B Crystallographic Details for 6.2, 6.4·H₂O, and 6.5·CH₂Cl₂ | | 255 |

List of Figures

| | | |
|---------------------|---|----|
| Figure 1.1. | General structures of metallophthalocyanines and metalloporphyrins. | 2 |
| Figure 1.2. | Selected examples of unsymmetrically substituted phthalocyanines. | 4 |
| Figure 1.3. | The photophysical mechanism of photodynamic therapy. | 18 |
| Figure 1.4. | Structure of Pc4. | 19 |
| Figure 1.5. | Structures of silicon(IV) phthalocyanines 1.47 and 1.48. | 21 |
| Figure 1.6. | A series of silicon(IV) phthalocyanines substituted axially with one or two 1,3-bis(dimethylamino)-2-propoxy group(s). | 21 |
| Figure 1.7. | Some examples of sulfonated aluminum(III) phthalocyanines. | 23 |
| Figure 1.8. | Some examples of hydroxy zinc(II) phthalocyanines. | 26 |
| Figure 1.9. | Selected examples of carboxy zinc(II) phthalocyanines. | 27 |
| Figure 1.10. | Structures of substituted fluorinated phthalocyanines 1.70. | 28 |
| Figure 1.11. | Structures of glycosylated pyropheophorbide 1.71, mono-glycosylated porphyrin 1.72, and glycoconjugated sapphyrin 1.73. | 30 |
| Figure 1.12. | Structures of porphyrin-guanine conjugate 1.74 and thio-glycosylated perfluoroporphyrin 1.75. | 31 |
| Figure 1.13. | Some examples of glycosylated phthalocyanines. | 32 |
| Figure 1.14. | Structures of glucoconjugated silicon(IV) phthalocyanines 1.80 and 1.81. | 33 |
| Figure 1.15. | General structure of BODIPYs | 35 |

| | | |
|---------------------|---|----|
| Figure 1.16. | Structures of BODIPY-antracene conjugates 1.85-1.89. | 37 |
| Figure 1.17. | Structures of BODIPY-pyrene conjugates 1.90-1.92. | 38 |
| Figure 1.18. | Structures of BODIPY-polycycle triads 1.93-1.95. | 39 |
| Figure 1.19. | Molecular photonic wire 1.96 and molecular optoelectronic gates 1.97 and 1.98. | 40 |
| Figure 1.20. | Structures of BODIPY-porphyrin conjugates 1.99-1.102. | 41 |
| Figure 1.21. | Structures of light harvesting arrays 1.103-1.106. | 42 |
| Figure 1.22. | A stepwise energy transfer in the supramolecular triad 1.107. | 43 |
| Figure 1.23. | Structures of some tin(IV) porphyrins axially substituted BODIPY fluorophores. | 44 |
| Figure 1.24. | Structure of pentad 1.112 containing four BODIPY donors and a perylenediimide (PDI) acceptor. | 45 |
| Figure 1.25. | Energy transfer followed by electron transfer in the supramolecular triad 1.113. | 46 |
| Figure 1.26. | Structures of FRET cassettes 1.114 and 1.115 composed of two kinds of BODIPY fluorophores. | 47 |
| Figure 1.27. | Structure of energy cassette 1.116 containing three kinds of BODIPY fluorophores. | 47 |
| Figure 1.28. | Structure of the molecular switch 1.117. | 48 |
| Figure 2.1. | The aromatic region of the ^1H NMR spectra of 2.7 , 2.8 , and 2.11 in CDCl_3 . | 63 |
| Figure 2.2. | Electronic absorption spectra of 2.8 at different concentrations in DMF. | 64 |

| | | |
|--------------------|---|----|
| Figure 2.3. | Comparison of the rates of decay of DPBF in DMF using 2.7 , 2.8 , 2.11 , and ZnPc as the photosensitizers. | 65 |
| Figure 2.4. | Effects of 2.7 , 2.8 , and 2.11 on HT29 and HepG2 cells in the absence and presence of light. | 66 |
| Figure 2.5. | Electronic absorption spectra of 2.7 , 2.8 , and 2.11 in the DMEM culture medium. | 68 |
| Figure 2.6. | Electronic absorption spectra of 2.7 , 2.8 , and 2.11 in the RPMI culture medium. | 68 |
| Figure 2.7. | Fluorescence microscopic images of HT29 tumor cells being incubated with 2.7 , 2.8 , and 2.11 for 2 h. | 69 |
| Figure 3.1. | ^1H - ^1H COSY spectrum of 3.4d in DMSO- d_6 . | 87 |
| Figure 3.2. | ^1H NMR spectrum of 3.7b in CDCl_3 with a trace amount of pyridine- d_5 . | 89 |
| Figure 3.3. | Electronic absorption spectra of 3.4b in DMF at different concentrations. | 90 |
| Figure 3.4. | Comparison of the rates of decay of DPBF in DMF using 3.4a-3.4d , 3.7a-3.7b , and ZnPc as the photosensitizers. | 92 |
| Figure 3.5. | Effects of 3.4a and 3.7a on HT29 and HepG2 cells in the absence and presence of light. | 93 |
| Figure 3.6. | Electronic absorption spectra of 3.4a and 3.7a in the DMEM culture medium. | 95 |
| Figure 3.7. | Electronic absorption spectra of 3.4a and 3.7a in the RPMI culture medium. | 95 |

| | | |
|--------------------|--|-----|
| Figure 3.8. | Visualization of intracellular fluorescences of HT29 after incubation with 3.4a-3.4d and 3.7a-3.7b for 2 h. | 96 |
| Figure 4.1. | Electronic absorption spectra of 4.3a at different concentrations in DMF. | 112 |
| Figure 4.2. | Electronic absorption spectra of 4.3a and 4.3f in thin solid films. | 112 |
| Figure 4.3. | Comparison of the rates of decay of DPBF in DMF, using 4.3a-4.3c , 4.3e-4.3f , and ZnPc as the photosensitizers. | 114 |
| Figure 4.4. | Effects of 4.3a-4.3c and 4.3e-4.3f on HT29 and HepG2 cells in the absence and presence of light. | 116 |
| Figure 4.5. | The effects of chain length on the photocytotoxicity of 4.3a-4.3c and 4.3e-4.3f for HT29 and HepG2 cells. | 117 |
| Figure 4.6. | Electronic absorption spectra of 4.3a-4.3c and 4.3e-4.3f in the DMEM culture medium. | 118 |
| Figure 4.7. | Electronic absorption spectra of 4.3a-4.3c and 4.3e-4.3f in the RPMI culture medium. | 119 |
| Figure 4.8. | Fluorescence microscopic images of HT29 cells after incubation with 4.3a-4.3c and 4.3e-4.3f for 2 h. | 120 |
| Figure 5.1. | HPLC analysis of the purified 5.5 and 5.10 . | 137 |
| Figure 5.2. | Electronic absorption spectra of ZnPc(α -PGlu) ₂ (5.9) at different concentrations in DMF. | 138 |
| Figure 5.3. | Effects of 5.6 , 5.9 , 5.10 , and 5.16 on HT29 and HepG2 cells in the absence and presence of light. | 141 |

| | | |
|---------------------|---|-----|
| Figure 5.4. | Electronic absorption spectra of 5.4-5.6 , 5.9 , 5.10 , and 5.16 in the DMEM culture medium. | 142 |
| Figure 5.5. | Fluorescence spectra of 5.4-5.6 , 5.9 , 5.10 , and 5.16 in the DMEM culture medium. | 143 |
| Figure 5.6. | Electronic absorption spectra of 5.4-5.6 , 5.9 , 5.10 , and 5.16 in the RPMI culture medium. | 143 |
| Figure 5.7. | Fluorescence spectra of 5.4-5.6 , 5.9 , 5.10 , and 5.16 in the RPMI culture medium. | 144 |
| Figure 5.8. | Fluorescence microscopic images of HT29 cells after being incubated with 5.6 , 5.9 , 5.10 , and 5.16 for 2 h. | 145 |
| Figure 6.1. | Energy transfer processes in the subphthalocyanine-BODIPY conjugates. | 162 |
| Figure 6.2. | The enlarged high-resolution ESI mass spectrum of 6.5 . | 164 |
| Figure 6.3. | Molecular structure of 6.2 . | 165 |
| Figure 6.4. | Molecular structure of 6.4 . | 166 |
| Figure 6.5. | Molecular structure of 6.5 . | 166 |
| Figure 6.6. | Normalized absorption spectra of 6.1 , 6.4 , and 6.6 in toluene. | 168 |
| Figure 6.7. | Normalized absorption spectra of 6.2 , 6.5 , and 6.6 in toluene. | 168 |
| Figure 6.8. | Overlap between the fluorescence spectrum of 6.1 and the absorption spectrum of 6.6 in toluene. | 169 |
| Figure 6.9. | Overlap between the fluorescence spectrum of 6.6 and the absorption spectrum of 6.2 in toluene. | 170 |
| Figure 6.10. | Fluorescence spectra of 6.1 , 6.4 , and 6.6 in toluene ($\lambda_{\text{ex}} = 470$ nm). | 172 |

| | | |
|---------------------|--|-----|
| Figure 6.11. | Normalized (at 563 nm) absorption and excitation (monitored at 570 nm) spectra of 6.4 in toluene. | 172 |
| Figure 6.12. | Fluorescence spectra of 6.2 , 6.5 , and 6.6 in toluene ($\lambda_{\text{ex}} = 515$ nm). | 173 |
| Figure 6.13. | Normalized (at 647 nm) absorption and excitation (monitored at 653 nm) spectra of 6.5 in toluene. | 174 |
| Figure 7.1. | Photo-induced energy or electron transfer process in the BODIPY-phthalocyanine conjugates. | 184 |
| Figure 7.2. | ESI-Mass spectrum of compound 7.5 . | 187 |
| Figure 7.3. | Normalized absorption spectra of 6.1 , 7.2 , and 7.7 in toluene. | 188 |
| Figure 7.4. | Normalized absorption spectra of 7.4 , 7.5 , and 7.7 in toluene. | 189 |
| Figure 7.5. | Fluorescence spectra of 6.1 , 7.2 , and 7.7 in toluene ($\lambda_{\text{ex}} = 480$ nm). | 190 |
| Figure 7.6. | Normalized absorption (at 613 nm) and excitation (monitored at 687 nm) spectra of 7.2 in toluene. | 191 |
| Figure 7.7. | Fluorescence spectra of 7.2 and 7.7 in toluene ($\lambda_{\text{ex}} = 615$ nm). | 192 |
| Figure 7.8. | Fluorescence spectra of 7.4 , 7.5 , and 7.7 in toluene ($\lambda_{\text{ex}} = 530$ nm). | 194 |
| Figure 7.9. | Fluorescence spectra of 7.5 and 7.7 in toluene ($\lambda_{\text{ex}} = 615$ nm). | 195 |
| Figure 7.10. | Transient absorption spectra of 7.5 in toluene at different delay times. | 196 |

List of Schemes

- Scheme 1.1.** Statistical condensation of two different phthalonitriles affords a mixture of six phthalocyanines. 5
- Scheme 1.2.** Synthesis of fullerene-fused phthalocyanines **1.17**. 6
- Scheme 1.3.** Synthesis of an unsymmetrical water-soluble phthalocyanine for covalent labeling of an oligonucleotide. 7
- Scheme 1.4.** Synthesis of phthalocyanine **1.23** by statistical condensation. 8
- Scheme 1.5.** Synthesis of an A₃B-type phthalocyanine via the ring expansion approach. 10
- Scheme 1.6.** Preparation of the A₃B-type phthalocyanine **1.30** by a polymer supported method. 11
- Scheme 1.7.** A silica gel support was used to prepare the A₃B-type phthalocyanine **1.33**. 12
- Scheme 1.8.** Synthesis of the ABAB-type phthalocyanine **1.36** using 1,3,3-trichloroisoindoline **1.34** as a precursor. 13
- Scheme 1.9.** Preparation of the ABAB-type phthalocyanine **1.38** using 5-neopentoxy-1*H*-isoindole-1,3(2*H*)-dithione (**1.37**) as a precursor. 14
- Scheme 1.10.** Preparation of the ABAB-type phthalocyanine **1.41** by statistical condensation. 15
- Scheme 1.11.** Synthesis of the "adjacent" phthalocyanine **1.43** via the "half-Pc" intermediate. 15
- Scheme 1.12.** Synthesis of the "side-strapped" phthalocyanine **1.45**. 16

| | | |
|---------------------|--|-----|
| Scheme 1.13. | Synthesis of the mono-sulfonated zinc(II) phthalocyanine 1.58 . | 25 |
| Scheme 1.14. | An alternative synthetic route for the mono-sulfonated zinc(II) phthalocyanine 1.60 . | 25 |
| Scheme 1.15. | Synthesis of the unsymmetrical glycosylated zinc(II) phthalocyanine 1.84 . | 34 |
| Scheme 2.1. | Synthesis of phthalocyanines 2.7 and 2.8 . | 60 |
| Scheme 2.2. | Synthesis of phthalocyanine 2.11 . | 61 |
| Scheme 3.1. | Synthesis of 1,4-disubstituted zinc(II) phthalocyanines 3.4a-3.4c . | 85 |
| Scheme 3.2. | Synthesis of tetrahydroxy zinc(II) phthalocyanine 3.4d . | 85 |
| Scheme 3.3. | Synthesis of benzo-fused zinc(II) phthalocyanines 3.7a-3.7b . | 86 |
| Scheme 4.1. | Synthesis of phthalocyanines 4.3a-4.3d . | 109 |
| Scheme 4.2. | Synthesis of phthalocyanines 4.3e and 4.3f . | 110 |
| Scheme 5.1. | Synthesis of tetra- β -glucosylated phthalocyanines 5.4 and 5.5 . | 132 |
| Scheme 5.2. | Synthesis of mono- β -glucosylated phthalocyanine 5.6 . | 133 |
| Scheme 5.3. | Synthesis of di- α -glucosylated phthalocyanines 5.9 and 5.10 . | 134 |
| Scheme 5.4. | Synthesis of di- β -glucosylated phthalocyanine 5.16 . | 135 |
| Scheme 6.1. | Synthesis of conjugates 6.4 and 6.5 . | 163 |
| Scheme 6.2. | Synthesis of subphthalocyanine 6.6 as a reference compound. | 167 |
| Scheme 7.1. | Synthesis of bis(BODIPY) substituted phthalocyanine 7.2 . | 185 |
| Scheme 7.2. | Synthesis of bis(mono-styryl BODIPY) substituted phthalocyanine 7.5 . | 186 |
| Scheme 7.3. | Synthesis of phthalocyanine 7.7 as a reference compound. | 188 |

List of Tables

| | | |
|-------------------|--|-----|
| Table 2.1. | Electronic absorption and photophysical data for 2.7 , 2.8 , and 2.11 in DMF. | 64 |
| Table 2.2. | Comparison of the IC ₅₀ values of phthalocyanines 2.7 , 2.8 , and 2.11 against HT29 and HepG2 cells. | 67 |
| Table 3.1. | Electronic absorption and fluorescence data for 3.4a-3.4d and 3.7a-3.7b in DMF. | 91 |
| Table 3.2. | IC ₅₀ values of 3.4a-3.4d and 3.7a-3.7b against HT29 and HepG2 cells. | 94 |
| Table 4.1. | Electronic absorption and photophysical data for phthalocyanines 4.3a-4.3c and 4.3e-4.3f . | 114 |
| Table 4.2. | Comparison of the IC ₅₀ values of phthalocyanines 4.3a-4.3c and 4.3e-4.3f against HT29 and HepG2 cells. | 116 |
| Table 5.1. | Electronic absorption and photophysical data for all the glucosylated phthalocyanines in DMF. | 139 |
| Table 5.2. | Comparison of the IC ₅₀ values of phthalocyanines 5.6 , 5.9 , 5.10 , and 5.16 against HT29 and HepG2 cells. | 140 |
| Table 6.1. | Absorption and fluorescence data for the dyads 6.4 and 6.5 , and the reference compounds 6.1 , 6.2 , and 6.6 in toluene. | 171 |
| Table 6.2. | Crystallographic data for 6.2 , 6.4·H₂O , and 6.5·CH₂Cl₂ . | 180 |
| Table 7.1. | Absorption and fluorescence data for the triads 7.2 and 7.5 , and the reference compounds 6.1 , 7.4 , and 7.7 in toluene. | 193 |

Abbreviations

General:

| | |
|-----------------|--|
| ϵ | Molar absorptivity |
| λ_{em} | Emission Maximum |
| λ_{max} | Absorption maximum |
| Φ_{Δ} | Singlet oxygen quantum yield |
| Φ_{ENT} | Energy transfer quantum yield |
| Φ_F | Fluorescence quantum yield |
| Φ_T | Triplet state quantum yield |
| τ_F | Fluorescence lifetime |
| τ_T | Triplet state lifetime |
| BODIPY | Boron dipyrromethene |
| ca. | Coarse approximation |
| Calcd. | Calculated |
| DBU | 1,8-Diazabicyclo[5.4.0]undec-7-ene |
| DDQ | 2,3-Dichloro-5,6-dicyano- <i>p</i> -benzoquinone |
| DMAE | N,N-Dimethylaminoethanol |
| DMF | N,N-Dimethylformamide |
| DMSO | Dimethyl sulformamide |
| DPBF | 1,3-Diphenylisobenzofuran |
| EET | Excitation energy transfer |
| equiv. | Equivalent |
| eT | Electron transfer |

| | |
|------------------|--|
| h | Hours |
| H ₂ P | Metal free porphyrin |
| HPLC | High performance liquid chromatography |
| ICT | Intramolecular charge transfer |
| ISC | Intersystem crossing |
| lit. | Literature value |
| PDI | Perylenediimide |
| PDT | Photodynamic therapy |
| ROS | Reactive oxygen species |
| r.t. | Room temperature |
| SubPc | subphthalocyanine |
| TFA | Trifluoroacetic acid |
| THF | Tetrahydrofuran |
| TLC | Thin layer chromatography |
| UV | Ultraviolet |
| Vis | Visible |
| v/v | Volume to volume ratio |
| ZnP | zinc(II) porphyrin |
| ZnPc | Unsubstituted zinc(II) phthalocyanine |

Nuclear Magnetic Resonance (NMR) Data:

| | |
|-------------------|--------------------------|
| { ¹ H} | Proton decouple |
| δ | Chemical shift |
| <i>J</i> | Coupling constant in Hz |
| COSY | Correlation spectroscopy |

ppm Part per million

s Singlet

d Doublet

t Triplet

dd Doublet of doublet

m Multiplet

br s Broad signal

Mass Spectrometric (MS) Data:

M^+ Molecular ion

ESI Electrospray ionization

FAB Fast atom bombardment

HRMS High resolution mass spectroscopy

MALDI-TOF Matrix assisted laser desorption/ionization

– time of flight

Chapter 1

Introduction

1.1 Phthalocyanines

1.1.1 General

Phthalocyanines were derived from the Greek terms naphtha (rock oil) and cyanine (dark blue). The metal-free unsubstituted derivative was discovered accidentally by Braun and Tcherniac in 1907 as a byproduct in the reaction of phthalamide and acetic anhydride.¹ This class of pigments exhibit unusual stability toward alkaline, acid, and heat. Their structures remained unknown until Linstead et al., who used the technique of elemental analysis, molecular mass determination, and oxidative degradation to show that phthalocyanines are symmetrical macrocycles containing a highly conjugated π system with four imino-isoindoline units (Figure 1.1).² Similar to porphyrins, phthalocyanines exhibit an aromatic behavior due to the directly conjugated 18 π electrons. With the additional fused benzene rings, they absorb strongly in the red visible region (at ca. 670 nm) and in the near-ultraviolet region (at ca. 340 nm), giving an intense characteristic greenish blue color. Due to their intense color, and high thermal and chemical stability, phthalocyanines were first employed as green and blue colorants in the photographic, printing, plastics, and textile industries.³ Their intriguing optical and electrical properties also enable them to be used in various technological avenues such as photoconductors, optical recording materials, chemical sensors, and catalysts for oxidative degradation of pollutants.⁴

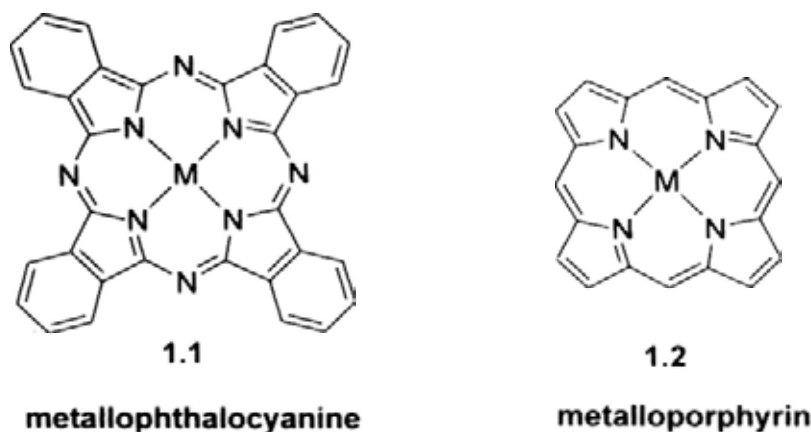


Figure 1.1. General structures of metallophthalocyanines and metalloporphyrins.

Apart from these applications, phthalocyanines are also promising photosensitizing agents for photodynamic therapy (PDT). In contrast to porphyrins, they have stronger absorptions in the red visible region which allows a deeper light penetration into tissues. They also possess favorable photo-physical and chemical properties which can be altered through incorporation of appropriate substituents either on the periphery of the macrocycle or at the axial positions linked to the metal center. However, phthalocyanines tend to aggregate which will shorten the excited state lifetimes and decrease the singlet oxygen quantum yield by dissipating the energy through internal conversion.⁵ This problem can be overcome by incorporating large and bulky substituents or using emulsifying detergents such as Cremophor EL and poly(ethylene glycol), serum or plasma proteins.⁶ The photophysical properties of phthalocyanines are also strongly influenced by the central metal ion. Complexation of phthalocyanines with an open shell or paramagnetic metal ion such as Cu^{2+} , Co^{2+} , Fe^{2+} , Ni^{2+} , VO^{2+} , Cr^{3+} , and Pd^{2+} results in shortening of the excited state lifetimes due to the effects of the unpaired electron(s), which in turn makes the compounds photoinactive.⁷ Phthalocyanines containing a closed d shell or diamagnetic metal ion such as Zn^{3+} , Al^{3+} , and Ga^{3+} have high triplet state quantum yields ($\Phi_T > 0.4$) and

long triplet lifetimes ($\tau_T > 200$ us).⁵ The triplet state of these metallophthalocyanines varies in energy from 110 to 126 kJ mol⁻¹, which is sufficient to trigger the formation of singlet oxygen (94 kJ mol⁻¹). As a consequence, these metallophthalocyanines usually also have high singlet oxygen quantum yields ($\Phi_{\Delta} = \text{ca. } 0.3 - 0.5$),⁵ and are therefore desirable photosensitizers.

1.1.2 Synthesis of Unsymmetrical Phthalocyanines

Among the various functional phthalocyanines, unsymmetrical analogues are of particular interest. Some unsymmetrical phthalocyanines can be used as building blocks for artificial photosynthetic systems.⁸ The dyads **1.3** and **1.4** are two of the recent examples. Push-pull unsymmetrical phthalocyanines substituted with electron donating and accepting groups can exhibit large second-order nonlinear optical responses, and are therefore potentially useful for various optoelectronic devices.⁹ Compounds **1.5-1.8** are some of the examples which have been reported recently. Amphiphilic unsymmetrical phthalocyanines such as **1.9-1.11** are excellent candidates for the formation of well-ordered films by the Langmuir-Blodgett (LB) technique.¹⁰ These phthalocyanines are also promising photosensitizers for photodynamic therapy as a result of their enhanced cellular uptake.¹¹ An additional remarkable feature of unsymmetrical phthalocyanines is their ability to form a wide range of condensed phases with controlled molecular architectures, such as liquid crystals and other self-organized supramolecules.^{12,13} Compounds **1.12-1.14** are some of the examples that can form these supramolecular structures.

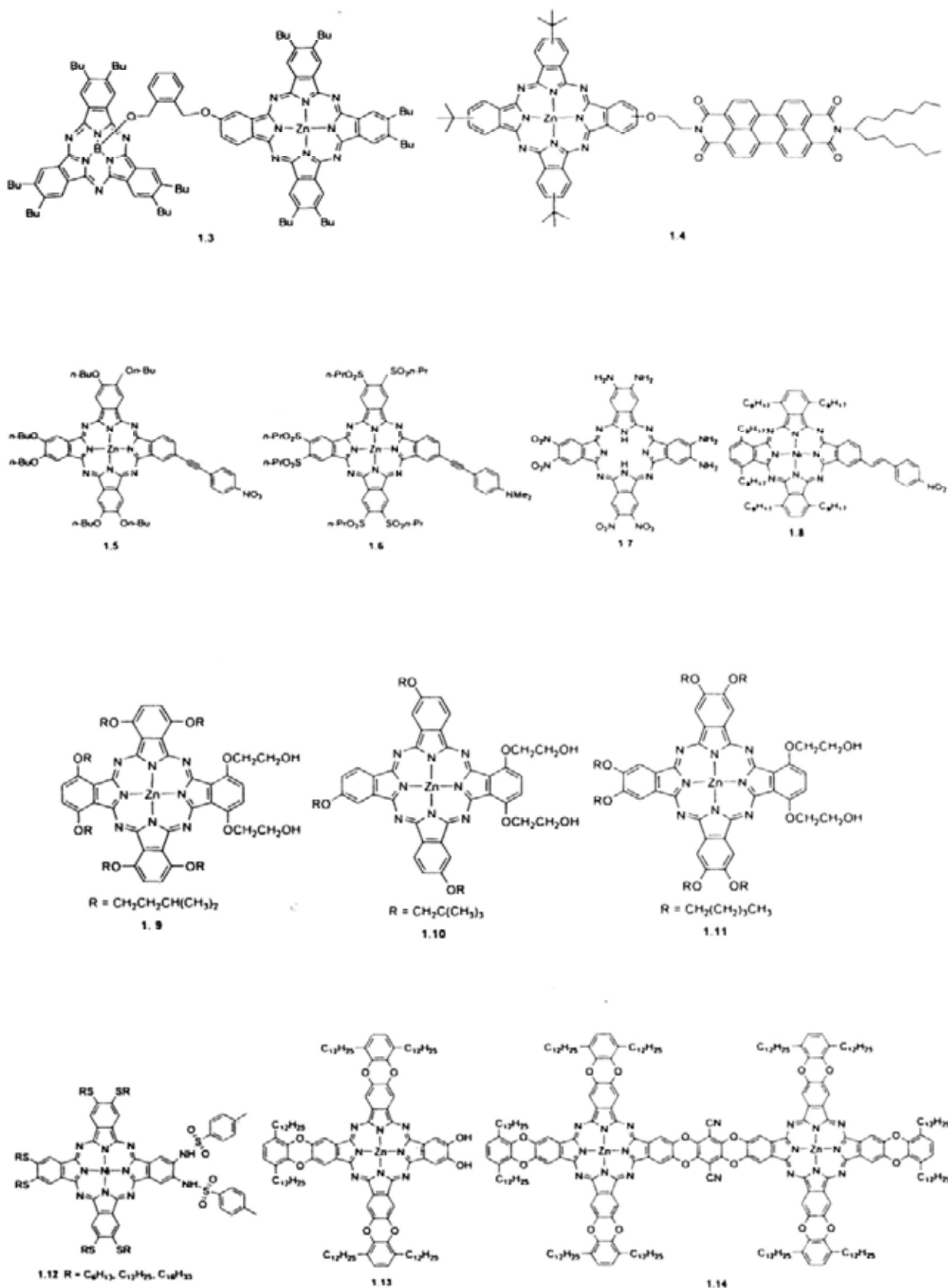


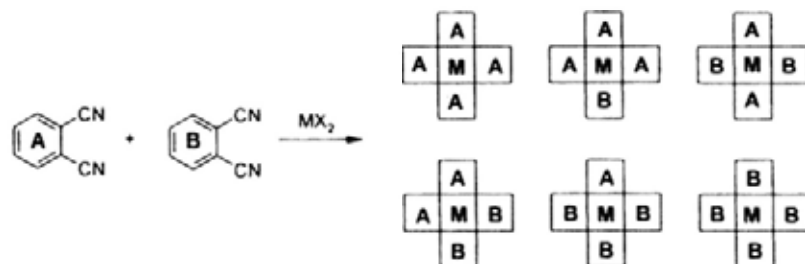
Figure 1.2. Selected examples of unsymmetrically substituted phthalocyanines.

Owing to the unique properties and great potential of unsymmetrical phthalocyanines, these compounds have been extensively studied over the last decade. I have also focused on this class of compounds and studied their use as efficient photosensitizers for PDT. In the following sub-sections, different synthetic pathways to unsymmetrical phthalocyanines with different substitution patterns will be discussed. The properties of some of these unsymmetrical phthalocyanines will also be described briefly.

1.1.2.1 Synthesis of A_3B -type Phthalocyanines

(i) Statistical Condensation

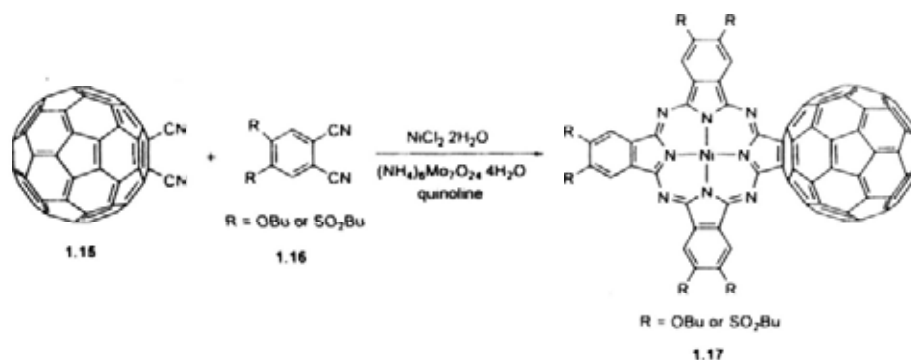
Being a straightforward procedure, statistical condensation is widely used to synthesize this class of compounds. A nonselective mixed cyclization of two different phthalonitriles or 1,3-diiminoisoindolines (A and B) generally affords six compounds as shown in Scheme 1.1. An extensive and tedious chromatographic separation procedure is usually required to isolate the desired A_3B -type macrocycle from the statistical mixture.¹⁴ Due to the high aggregation tendency of phthalocyanine molecules, the separation can become very difficult. Introduction of bulky groups on the periphery of phthalocyanines may facilitate the separation and purification processes.



Scheme 1.1. Statistical condensation of two different phthalonitriles affords a mixture of six phthalocyanines.

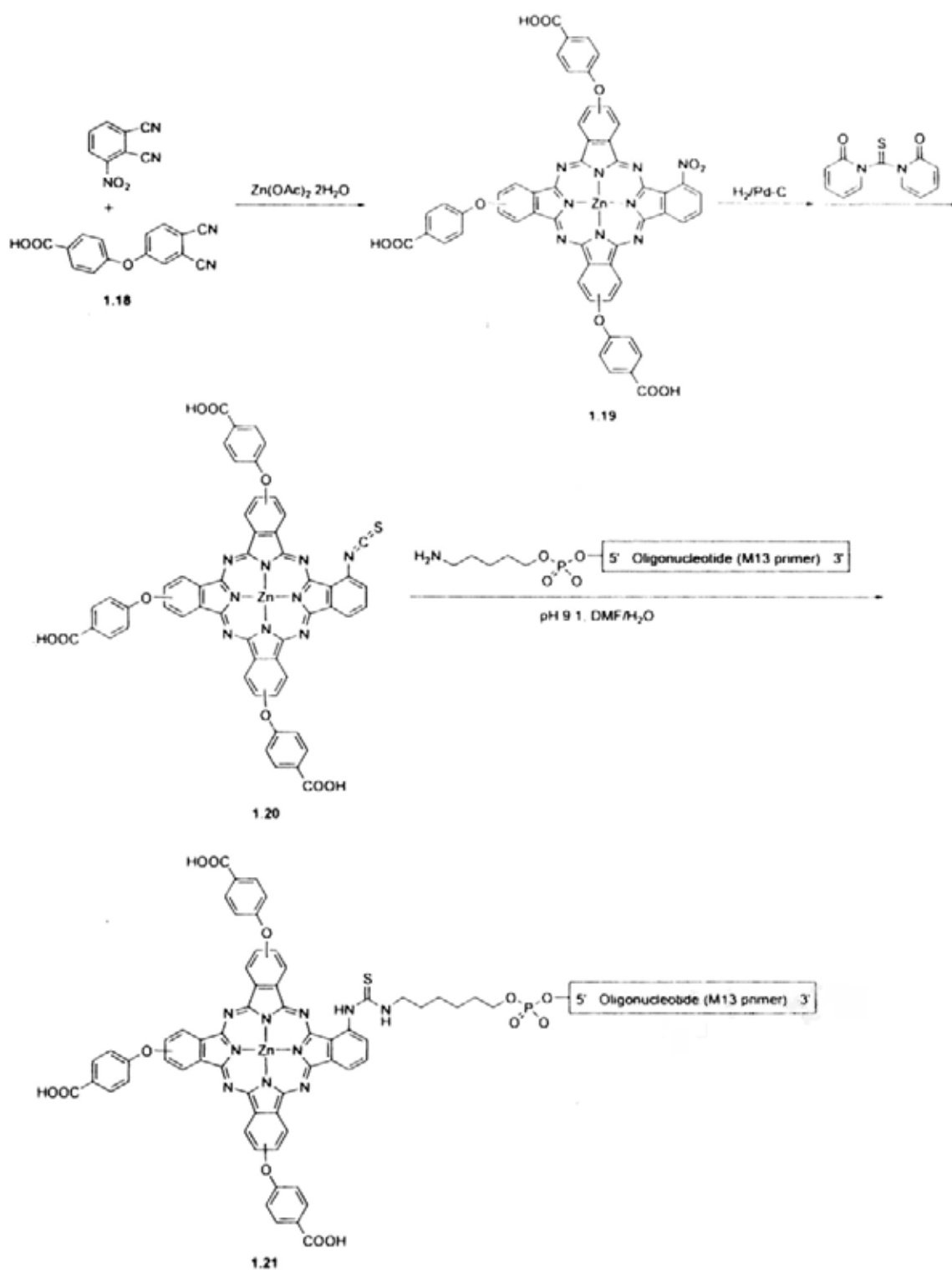
The stoichiometry of the two phthalonitriles used is also critical in these mixed cyclization reactions. Normally, one of the reactants is employed in excess, for example in a 3:1 molar ratio to promote the formation of the A₃B-type product. Under this condition, the theoretical yields of the products are as follows: A₄ (33%), A₃B (44%), and the other condensation products (23%).¹⁵ However, the experimental isolable yields of the desired products are usually lower and in the range of 10 to 20%.

Scheme 1.2 shows one of the examples of these mixed cyclization reactions. Treatment of 1,2-dicyanofullerene **1.15** with 4,5-dibutoxy- or 4,5-bis(butylsulfonyl) phthalonitrile (**1.16**) in a 1:2 ratio in the presence of NiCl₂·2H₂O yielded the C₆₀-tetraazachlorin conjugates **1.17**,¹⁶ which could be purified by repeated silica gel and size exclusion chromatography. The butyloxy or butylsulfonyl groups were introduced at the peripheral positions to increase the solubility of the complexes.



Scheme 1.2. Synthesis of fullerene-fused phthalocyanines **1.17**.

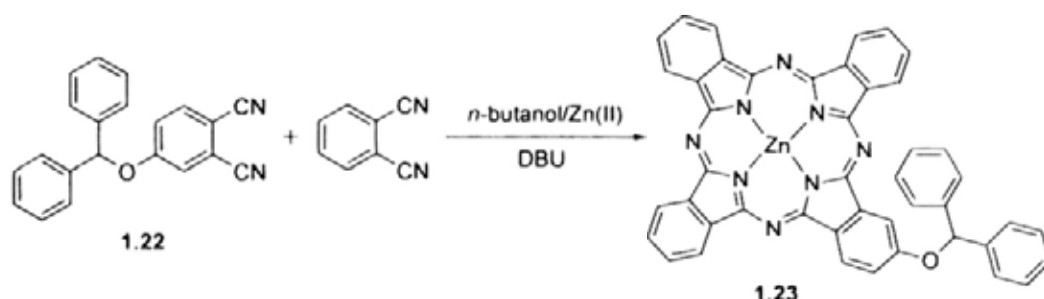
As another example, the A₃B-type phthalocyanine **1.19** was prepared by cross condensation of 3-nitrophthalonitrile and 4-(4-carboxyphenoxy)phthalonitrile (**1.18**) (Scheme 1.3).¹⁷ Having three hydrophilic carboxyl groups, this dye is soluble in water. The nitro group can be readily converted to the reactive isothiocyanate group, which can then be further coupled with an amine-containing oligonucleotide (Scheme 1.3).



Scheme 1.3. Synthesis of an unsymmetrical water-soluble phthalocyanine for covalent labeling of an oligonucleotide.

The distribution of products will also depend on the reactivity of the phthalonitrile precursors. For this reason, the ratio of the reactants used should be altered by considering their relative reactivity. A lower molar ratio of A:B should be

used if A is more reactive than B, while the opposite is applied if B is more reactive than A.¹⁸ For example, Leznoff et al. performed the mixed cyclization of 4-(diphenylmethoxy) phthalonitrile (**1.22**) with unsubstituted phthalonitrile in 1:1 ratio to give a mixture of all the statistical products. By changing the ratio to 10:1, the A₃B-type phthalocyanine **1.23** was isolated as the main product in 50% yield (Scheme 1.4).^{11b}



Scheme 1.4. Synthesis of phthalocyanine **1.23** by statistical condensation.

Steric interactions also affect the composition of products. By using phthalonitriles bearing bulk groups at the 3,6-positions, fewer cyclized products will be formed because the steric hindrance prevents these groups coming in adjacent position. Cook et al. employed a ratio of 1:9 for the condensation of 3,6-disubstituted phthalonitriles (**B**) with other phthalonitriles (**A**).¹⁹ Although this ratio led to an increase in the amount of A₄-type product and a decrease in the amount of the desired A₃B-type product, the formation of other side products was less readily. So the target A₃B-type product could be isolated readily from the reaction mixture.

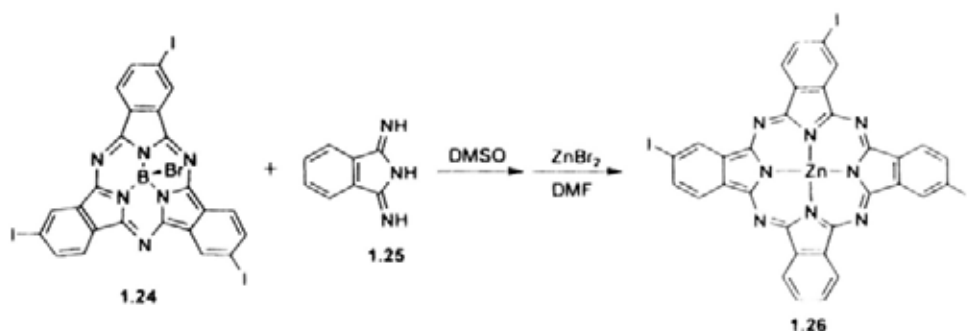
Purification of unsymmetrical phthalocyanines usually requires tedious chromatographic separation procedures. By using phthalonitriles with different solubility properties, it may facilitate the separation process. For example, McKeown et al. demonstrated that an efficient chromatographic separation could be achieved

when alkylated phthalonitriles were treated with oligo(oxyethylene)-substituted phthalonitriles.²⁰ The presence of large dendritic substituents could also facilitate the separation of the desired A₃B-type phthalocyanines.²¹

Despite the low selectivity of this statistical condensation, it is still the most commonly used method for preparing A₃B-type phthalocyanines. Satisfactory results can be achieved by a careful control of the reaction conditions. However, the A₂B₂-type derivatives are hardly prepared by this method because the separation of the two isomers (AABB-adjacent and ABAB-opposite) is very difficult by general chromatographic methods.

(ii) The Ring Expansion Approach from Subphthalocyanines

Apart from the statistical approach, A₃B-type phthalocyanine can also be prepared by the ring expansion reactions of subphthalocyanines (SubPcs). This method was developed in the late 1980s by Kobayashi and others.²² Subphthalocyanines are lower homologues of phthalocyanines composed of three isoindole subunits containing boron as the central atom. These macrocycles contain an aromatic delocalized 14 π -electron system and a C_{3v} cone-shaped structure. They can be synthesized by treating the corresponding phthalonitriles with BCl₃ or other boron derivatives.²³ The ring expansion reactions of SubPc are believed to be caused by the formation of stable phthalocyanines. Upon elimination of the axial ligand of SubPc (i.e., SubPc \rightarrow SubPc⁺ + X⁻), the structure changes from a shuttlecock-shape to a more planar form which leads to stabilization of the π system. Scheme 1.5 shows a typical example for the preparation of A₃B-type phthalocyanine using this approach.²⁴



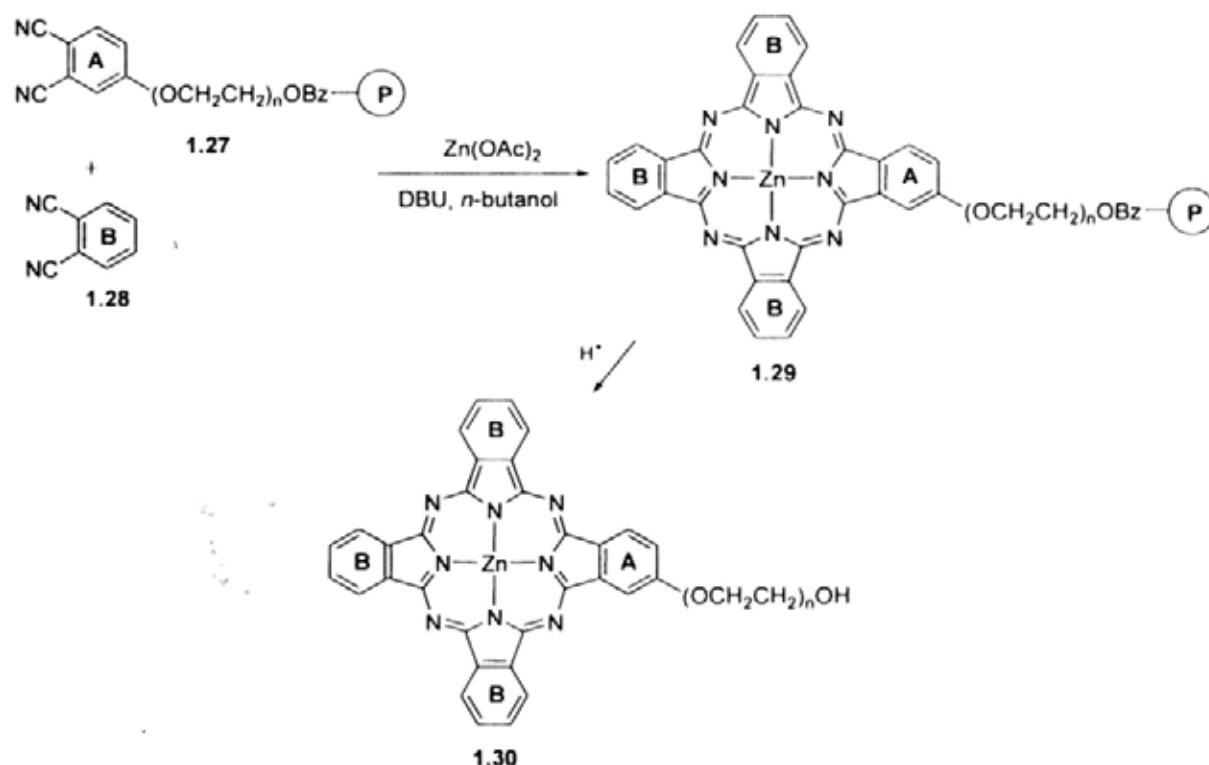
Scheme 1.5. Synthesis of an A₃B-type phthalocyanine via the ring expansion approach.

The efficiency of this synthetic method depends greatly on the reaction conditions and the characteristics of the starting materials.²⁵ For example, addition of a metal template to the reaction mixture can increase the yield of the A₃B-type product.^{25a} Subphthalocyanines react with less reactive phthalonitrile derivatives in the presence of a strong base such as 1,8-diazabicyclo[5.4.0]undec-7-ene (DBU) also give predominantly the A₃B-type phthalocyanines.^{25a} The reactions between less reactive subphthalocyanines, which have no substituent or electron-withdrawing groups, and diiminoisoindoline derivatives having electron-donating substituents usually give the best results, both in terms of the yield and the selectivity. Hence, for some A₃B-type phthalocyanines, the subphthalocyanine expansion method is a unique and efficient approach.

(iii) Polymer Supported Method

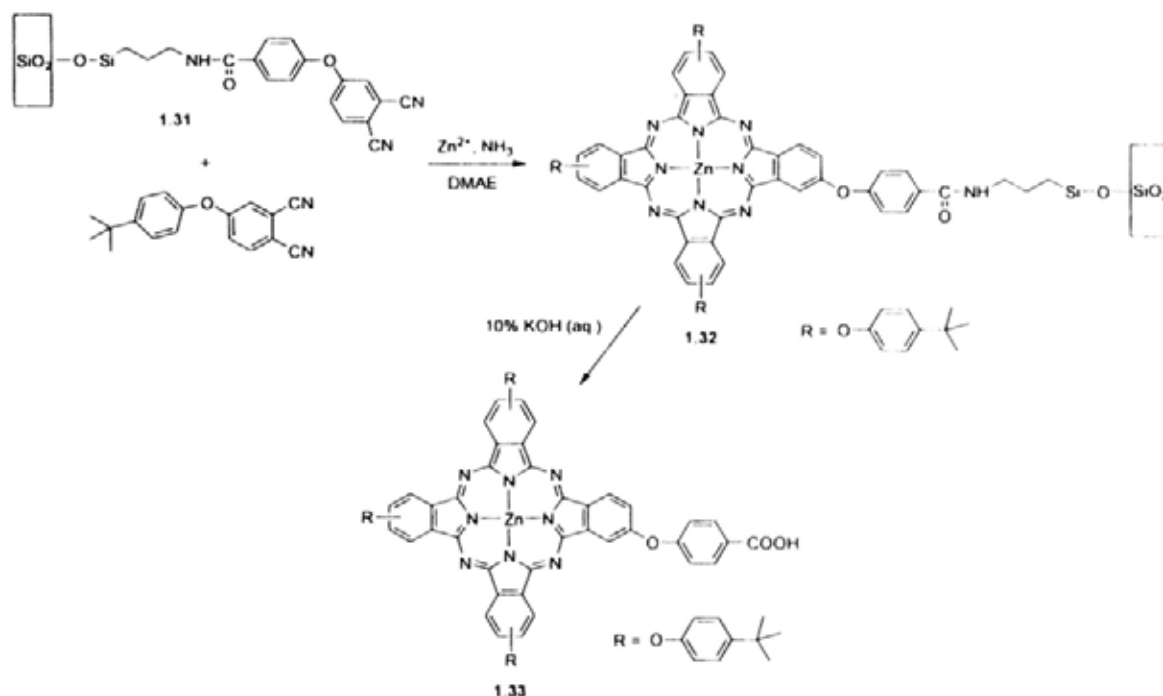
Another approach for the selective preparation of A₃B-type phthalocyanines involves a solid phase support.²⁶ In this method, a 1,3-diiminoisoindoline or phthalonitrile is first attached to a polymer support. This insoluble polymer-bound precursor then reacts with a large excess of another unbound phthalonitrile or 1,3-diiminoisoindoline to give a polymer-bound A₃B-type phthalocyanine. The soluble

B_4 -type phthalocyanine can be removed readily by simply washing with an organic solvent. After treatment with acid, the A_3B -type phthalocyanine is released from the polymer. Scheme 1.6 shows a typical example of the preparation of an A_3B -type phthalocyanine by this methodology.^{26d}



Scheme 1.6. Preparation of the A_3B -type phthalocyanine **1.30** by a polymer supported method.

Apart from this polymer-bound method, Wöhrle et al. introduced a modified silica gel as another kind of support for these solid-phase reactions.²⁷ As shown in Scheme 1.7, the phthalonitrile **1.31** linked to a modified silica gel reacts with 4-(4-*tert*-butylphenoxy)phthalonitrile to give phthalocyanine **1.32**. The insoluble crude product was filtered and washed with acetone and water in a Soxhlet apparatus. The desired A_3B -type phthalocyanine **1.33** was released by alkaline hydrolysis of **1.32** in THF/ H_2O .



Scheme 1.7. A silica gel support was used to prepare the A_3B -type phthalocyanine 1.33.

This approach is restricted to phthalonitriles and diiminoisoindolines which can be linked to a solid support and the phthalocyanines formed can be subsequently released. This method has not been commonly used so far. It is envisaged that with the development of solid-phase technology, this may become an effective route to prepare A_3B -type phthalocyanines in future.

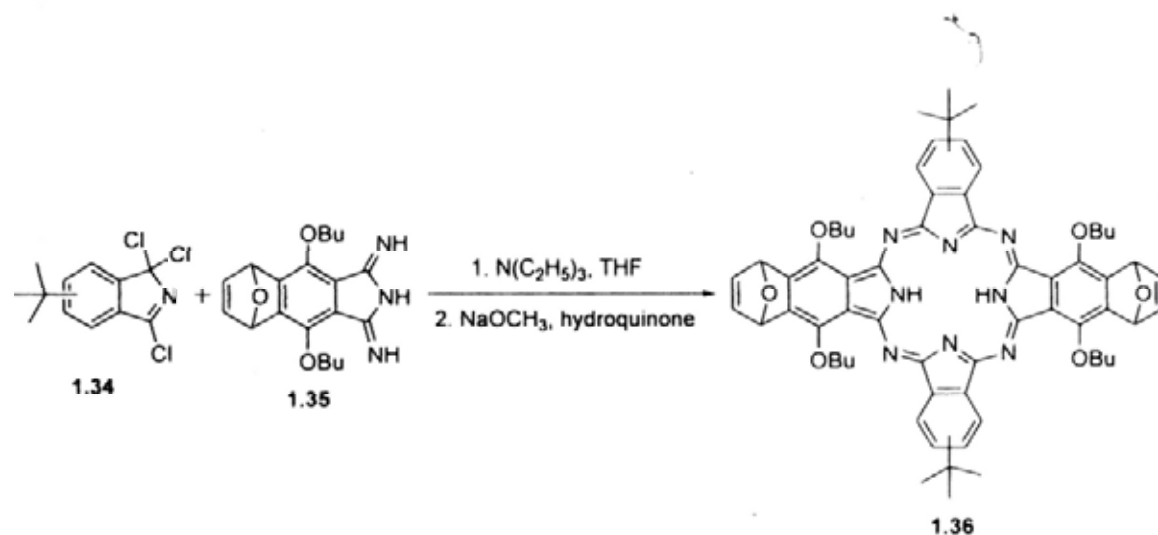
1.1.2.2 Synthesis of A_2B_2 -type Phthalocyanines

The A_2B_2 -type phthalocyanines have special applications. For example, the ABAB-type (opposite) analogues are good building blocks to prepare ladder-type structures,²⁸ while the AABB-type (adjacent) counterparts can be used as second-order nonlinear optical chromophores.²⁹ In addition, these compounds are also promising candidates as photosensitizers for photodynamic therapy as a result of their

amphiphilic nature. However, as mentioned above, it is very difficult to separate these two isomers because they have similar solubility and are frequently eluted out in the same fraction. Hence, some unusual synthetic approaches have been developed for the controlled preparation of these isomers.

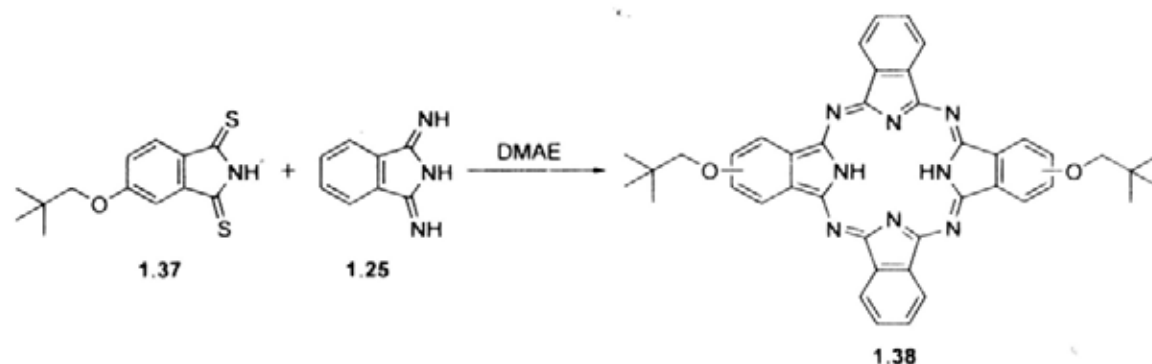
(i) Preparation of "Opposite" Phthalocyanines (ABAB-type)

Based on a patented method,³⁰ Young et al. reported a rather general approach to prepare "opposite" or crosswise-substituted phthalocyanines.³¹ In this procedure, 1,3,3-trichloroisoidindoline **1.34** was treated with 1,3-diiminoisoidindoline **1.35** in the presence of a base and a reducing agent. The ABAB-type phthalocyanine **1.36** was formed via reductive coupling of these precursors (Scheme 1.8).²⁹ By considering the experimental conditions and the stepwise nature of the synthetic procedure, the authors concluded that six of the nitrogen atoms in the phthalocyanine ring came from the diimino starting material without cleavage, while the remaining two nitrogen atoms were derived from the trichloro-compound.



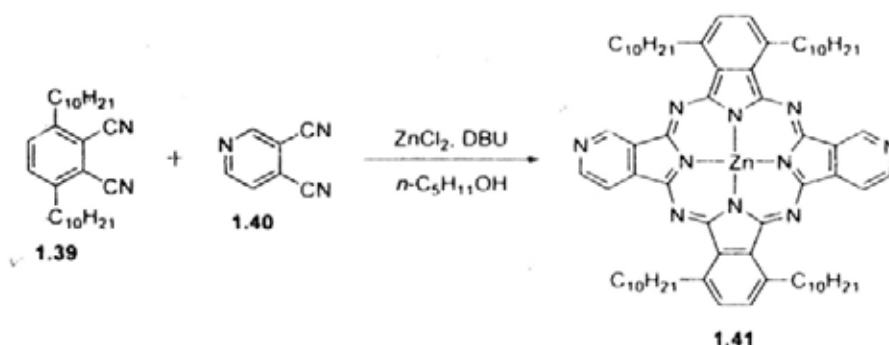
Scheme 1.8. Synthesis of the ABAB-type phthalocyanine **1.36** using 1,3,3-trichloroisoidindoline **1.34** as a precursor.

Beside this approach, another synthetic strategy was reported by Leznoff et al. to prepare this kind of compounds.³² As shown in Scheme 1.9, condensation 5-neopentoxy-1*H*-isoindeole-1,3(2*H*)-dithione (**1.37**) with 1,3-diiminoisindoline (**1.25**) in a 1:1 molar ratio in *N,N*-dimethylaminoethanol (DMAE) affords the unsymmetrical ABAB-type phthalocyanine **1.38** together with trace amounts of the other cyclized products.



Scheme 1.9. Preparation of the ABAB-type phthalocyanine **1.38** using 5-neopentoxy-1*H*-isoindeole-1,3(2*H*)-dithione (**1.37**) as a precursor.

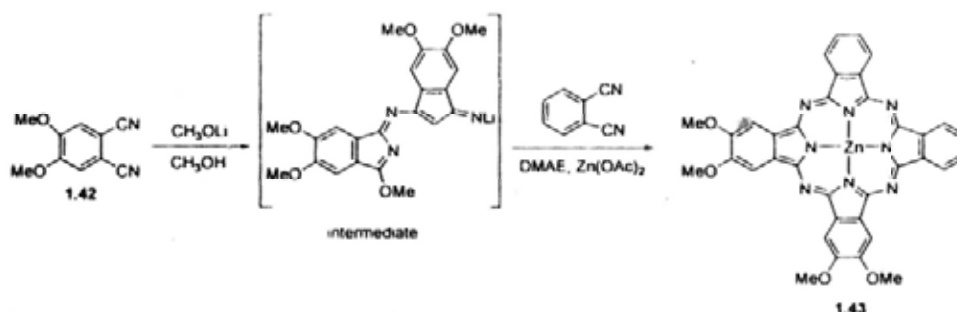
Although statistical condensation usually gives inseparable AABB and ABAB-type isomers, the formation of ABAB-type product may be promoted by using phthalonitriles with bulky substituents at the 3 and 6 positions. For example, Sakamoto et al. employed 3,6-didecylphthalonitrile (**1.39**) as a bulky precursor to condense with phthalonitrile **1.40** to give the ABAB-type product **1.41** in 17% yield (Scheme 1.10).³³



Scheme 1.10. Preparation of the ABAB-type phthalocyanine **1.41** by statistical condensation.

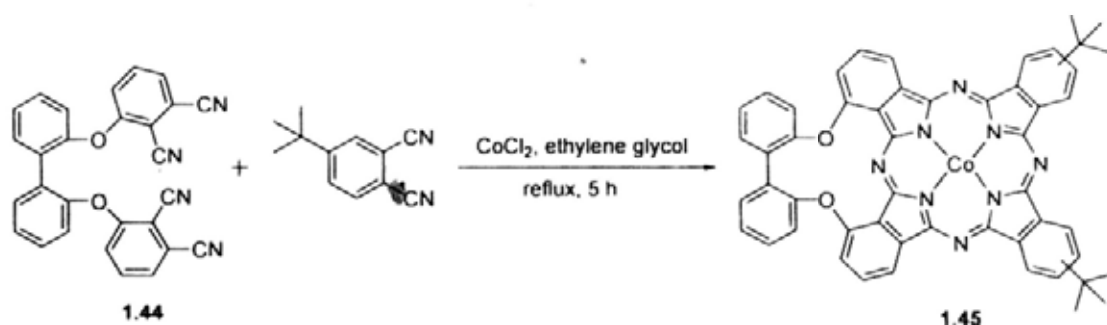
(ii) Preparation of “Adjacent” Phthalocyanines (AABB-type)

In 1997, Leznoff et al. reported a “half-Pc” approach to prepare this class of compounds.³⁴ In this method, a “half-Pc” intermediate was isolated and subsequently treated with another phthalonitrile under mild conditions. The preparation of “half-Pc” intermediates had been reported previously by Oliver and Smith,³⁵ but they proposed that only phthalonitriles bearing strongly electron-withdrawing groups could produce such stable intermediates. However, in the work reported by Leznoff et al., phthalonitrile **1.42**, which does not have strong electron acceptors, can react with lithium methoxide in refluxing methanol to give the half-Pc intermediate, which can further react with the unsubstituted phthalonitrile in the presence of zinc(II) acetate to afford the AABB-type phthalocyanine **1.43** in 28% yield.³⁴



Scheme 1.11. Synthesis of the “adjacent” phthalocyanine **1.43** via the “half-Pc” intermediate.

An alternative synthetic pathway to AABB-type phthalocyanine was established by Kobayashi et al. in 1993.³⁶ It involves the use of *bis*(phthalonitrile) linked by an appropriate bridging group, such as 2,2'-diphenyl (compound **1.44**). The steric constraint prevents the formation of opposite isomer during the cyclization. Additionally, the distance between the two phenoxy groups is close enough to facilitate intramolecular cyclization, avoiding the formation of oligomeric phthalocyanines. Treatment of these bis(phthalonitrile)s with other phthalonitriles can also give “adjacent” phthalocyanines in reasonably good yields. A typical example is shown in Scheme 1.12.



Scheme 1.12. Synthesis of the “side-strapped” phthalocyanine **1.45**.

1.1.3 Phthalocyanines as Efficient Photosensitizers for Photodynamic Therapy

The use of light and dyes to treat medical conditions can be dated back to three thousand years ago, but it was only in the last century that photodynamic therapy (PDT) was developed.³⁷ A German medical student Rabb reported the killing of the microorganism *paramecia* with the combination of acridine and light in the end of 19th century.³⁸ A few years later, von Tappeiner and Jesionek treated skin tumors with topically applied eosin and white light.³⁹ This marked the beginning of PDT. PDT is an innovative approach for the treatment of a range of cancers and wet age-related macular degeneration.⁴⁰ The treatment involves a combined action of a

photosensitizer, light, and oxygen. Each component is harmless by itself, but when combined they can lead to the generation of reactive oxygen species (ROS) causing cellular and tissue damage. Photosensitizers are photosensitive compounds which can be preferentially retained in malignant cells or tissues. After a cancer has been identified, a photosensitizer can be administered into body by various means, such as intravenous injection or topical application to the skin. Upon illumination with light, the photosensitizer is activated, and then the energy is transferred to molecular oxygen to generate ROS, resulting in biochemical attack on the cancer cells. Because of the high reactivity and short lifetime of ROS, their biochemical reactions take place only in the immediate locale of the photosensitizer. So the preferential uptake of the photosensitizer by the diseased tissues and the ability to confine the activation of the photosensitizer by restricting the illumination to a specific region with modern fiber optics and endoscopy are the dual selectivity of PDT.

PDT has several potential advantages over traditional cancer treatment methods.^{40f} Firstly of all, it is comparatively non-invasive and can be targeted accurately, mainly through the precise application of light. In addition, repeated doses can be given to patients without the total-dose limitations associated with radiotherapy. It also does not have multidrug resistant problem which is the main drawback of chemotherapy.⁴¹ The healing process usually results in little or no scarring. Furthermore, PDT can usually be done in an outpatient or day-care setting, which is convenient to patients. Finally, this method does not have significant and long-term side-effects.

The photophysical mechanism of PDT is shown in Figure 1.3. Upon illumination, the photosensitizer at its singlet state is excited to the excited singlet state. This excited state interacts with surroundings leading to photobleaching and a rapid lose of

its energy via intersystem crossing (ISC) to populate the much longer-lived triplet state. The excited triplet state then interacts with tissue oxygen in either a Type I or Type II mechanism. In Type I mechanism, an electron transfer reaction occurs leading to the generation of oxygen radical anions as the reactive oxygen species. Alternatively, the triplet state can undergo an energy transfer with oxygen to form singlet oxygen and this process is classified as the Type II mechanism. Singlet oxygen is a highly reactive oxygen species that can react rapidly with numerous biologically important substrates, resulting in oxidative damage and ultimately cell death. It is generally agreed that the Type II mechanism predominates during PDT and singlet oxygen is the most important cytotoxic species produced.

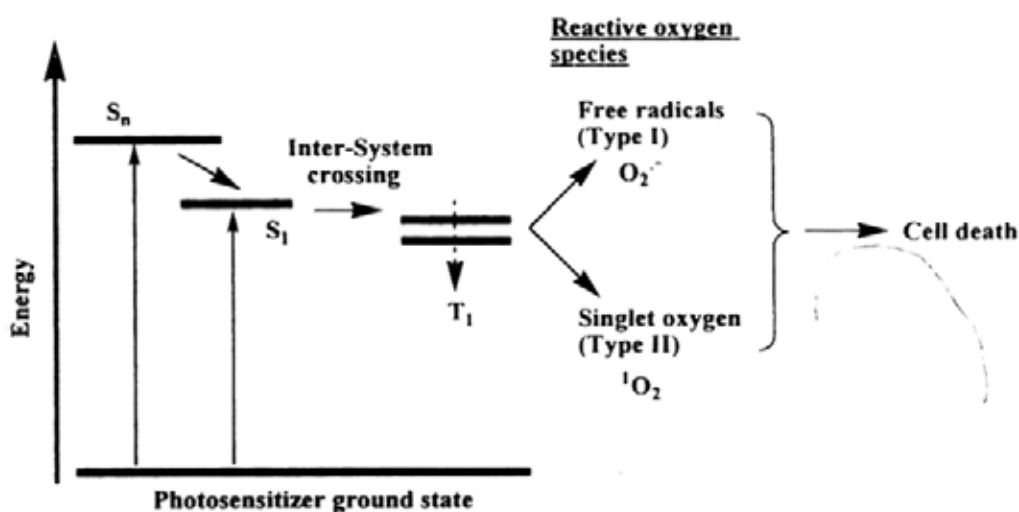


Figure 1.3. The photophysical mechanism of photodynamic therapy.

Porphyrin derivatives are traditional photosensitizers. These compounds, however, are not considered to be ideal for the use in PDT. Among the limitations, the slow clearance and weak absorption in the body's therapeutic window (650 – 800 nm) are the two major drawbacks.⁴² Therefore, there is an impetus for the development of non-porphyrin photosensitizers which have stronger absorption in the red visible

region, and improved photophysical and photobiological properties.⁴³ Among the various classes of macrocyclic compounds being evaluated as second-generation photosensitizers,^{5b,40f,40g} phthalocyanines are of particular interest because of their strong absorptions in the red visible region, high efficiency to generate reactive oxygen species, and ease of chemical modification and formulation.^{5b,44} Some of these compounds, such as the silicon(IV) phthalocyanine Pc4 (**1.46**), a liposomal preparation of zinc(II) phthalocyanine (CGP55847), and a mixture of sulfonated aluminum(III) phthalocyanines (Photosense) are presently in clinical trials.^{44b}

These three potential drugs represent three major classes of phthalocyanines which can be used for PDT, namely silicon(IV), aluminum(III), and zinc(II) phthalocyanines. A brief overview of these three classes of phthalocyanines is given in the following sections, focusing on the unsymmetrical analogues.

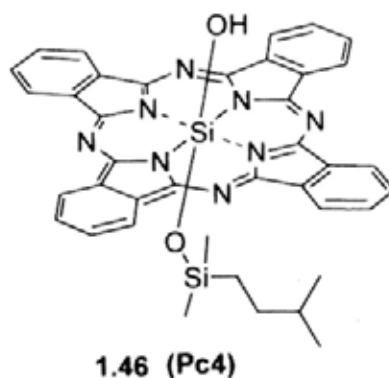


Figure 1.4. Structure of Pc4.

1.1.3.1 Silicon(IV) Phthalocyanines

Phthalocyanines with a Group IV metal center can be modified via the attachment of axial substituents. These phthalocyanines have advantages over other peripherally substituted phthalocyanines because they do not exhibit isomerism. The

axial ligands not only can increase the solubility, but also can prevent aggregation of the phthalocyanines.

Among the silicon(IV) phthalocyanines, Pc4 (**1.46**), which contains an aminosiloxy group and a hydroxyl group, has received much attention. In a structure-activity relationship study, the *in vitro* photoactivity of Pc4 has been compared with those of other analogues.⁴⁵ It has been found that the axial hydroxyl ligand is not essential for efficient photosensitization, and an elongated diaminosiloxy axial ligand generally is less desirable than the short analogue. While there is no significant difference in cellular uptake between Pc4 and the aluminum analogues, the former is about 3-fold more active toward V-79 Chinese hamster lung fibroblast.⁴⁶ This can be attributed to the difference in the intracellular distribution and the aggregation state of the phthalocyanines.⁴⁷

In *in vivo* studies, Pc4 shows a high activity in causing the regression of the RIF-1 tumor at low drug dosage with little cutaneous photosensitivity.⁴⁸ Pc4 is also effective in killing HIV and other envelope viruses as well as blood borne parasites, rendering this compound to be used in the photosensitization of red blood cells and platelet concentrates.⁴⁹ Recently the photoactivity of Pc4 has been studied in a human tumor model, namely the ovarian epithelial carcinoma OVCAR-3 transplanted SC in athymic nude mice.⁵⁰ The results are also very encouraging.

Recently, a comparable study of the photodynamic activities of phthalocyanines **1.47** and **1.48** toward two cell variants of B₁₆ melanoma has been performed.⁵¹ Upon excitation with 776 nm diode laser light, the unsymmetrical analogue **1.48** appears to be a markedly more efficient photosensitizer, likely reflecting its higher cellular uptake and less intracellular aggregation.

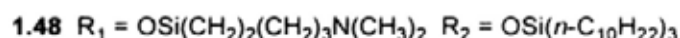
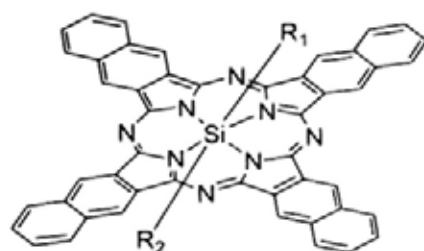


Figure 1.5. Structures of silicon(IV) phthalocyanines 1.47 and 1.48.

Ng et al. have recently prepared a series of silicon(IV) phthalocyanines substituted axially with one or two 1,3-bis(dimethylamino)-2-propoxy group(s) (Figure 1.6).^{11f} Among these compounds, the unsymmetrical amphiphilic analogues 1.50 exhibit a high photocytotoxicity against human hepatocellular carcinoma HepG2 and murine macrophage J774 cells. This can be attributed to the high cellular uptake and/or efficiency to generate singlet oxygen.

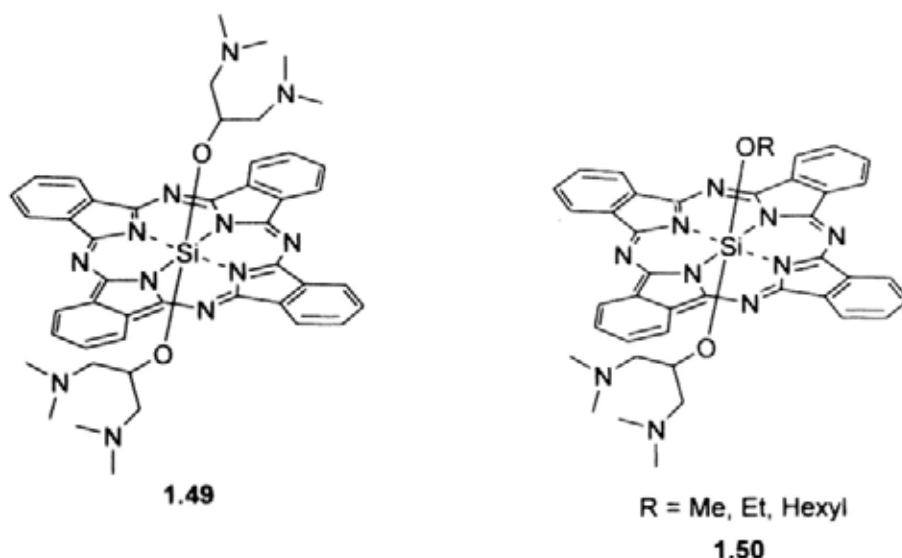


Figure 1.6. A series of silicon(IV) phthalocyanines substituted axially with one or two 1,3-bis(dimethylamino)-2-propoxy group(s).

1.1.3.2 Aluminum(III) Phthalocyanines

Aluminum(III) phthalocyanines have one axial ligand instead of two in silicon(IV) phthalocyanines. These compounds are generally soluble in organic solvents. Axial substituents such as polyethylene glycol (M_{wt} 2000) and poly(vinyl alcohol) (M_{wt} 13000-23000) have been used to render water solubility to the compounds.⁵² These compounds can induce regression in EMT-6 and Colo-26 tumor.

Apart from these polymeric systems, unsymmetrical water-soluble sulfonated aluminum(III) phthalocyanines **1.51-1.55** have also received much attention. The relationships of the structures and photodynamic efficiency of these compounds, both *in vitro* and *in vivo*, have also been examined. The amphiphilic *cis*-disulfonated aluminum(III) phthalocyanine **1.53** is the most active one among the various derivatives because of its highest cellular uptake properties.⁵³ The subcellular localization of differently sulfonated aluminum(III) phthalocyanines against human melanoma cells has also been studied by confocal laser scanning microscopy. It shows that the mono-sulfonated phthalocyanine **1.55** and the di-sulfonated analogues **1.53** and **1.54** localize diffusely in the cytoplasm, while the tri- and tetra-sulfonated compounds **1.52** and **1.51** are found in association with lysosomes. However, translocation from the lysosomes to the cytoplasm has been observed at high concentration of the dyes and low laser light exposure.⁵⁴ Also, the correlation of subcellular and intratumoral localization of these sulfonated aluminum(III) phthalocyanines has been reported.⁵⁵

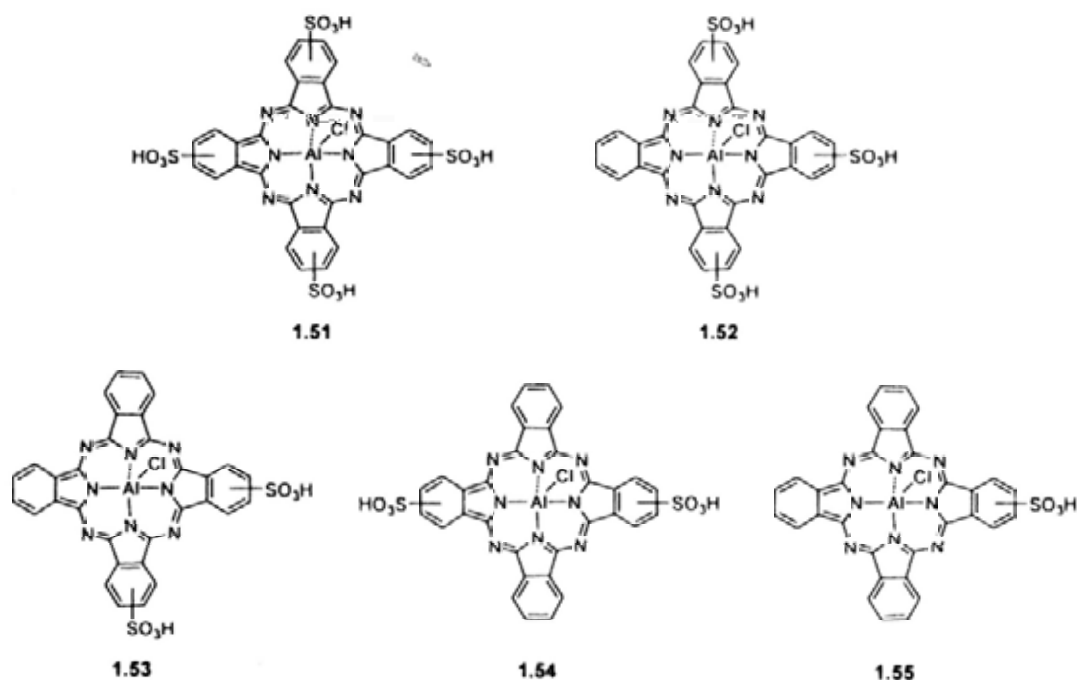


Figure 1.7. Some examples of sulfonated aluminum(III) phthalocyanines.

In *in vivo* studies, it has been found that the disulfonated aluminum(III) phthalocyanine **1.53** and the tetrasulfonated derivative **1.51** (to a lesser extent) accumulate preferentially in tumor associated macrophages rather than in malignant or other tumor associated cells.⁵⁶ The disulfonated phthalocyanines **1.53** has been shown to induce tumor regression via direct tumor cell killing rather than damage to the tumor microvasculature, which is in contrast to the action of Photofrin.⁵⁷ A mixture of chloro aluminum(III) phthalocyanines bearing 2 to 4 sulfonato groups, called Photosense, is presently used in Russia for PDT in clinic.

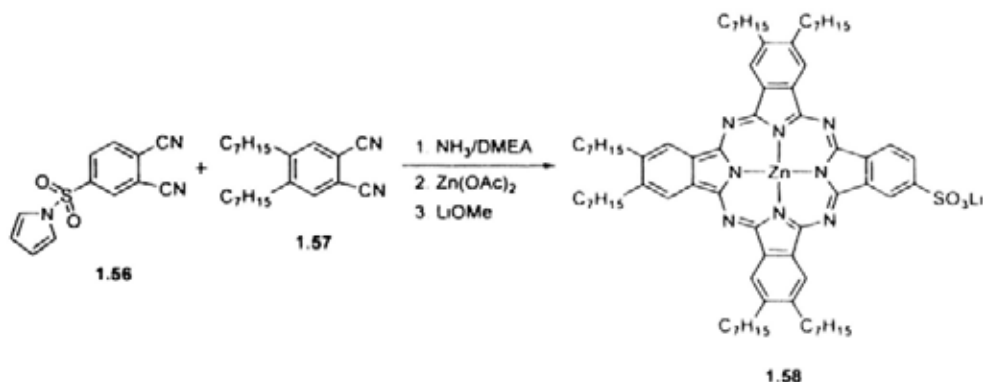
As aluminum congeners, gallium(III) phthalocyanines with different sulfonate groups have also been studied for their *in vitro* photodynamic activities.⁵⁸ The photocytotoxicities of these complexes against V-79 Chinese hamster lung fibroblast are slightly lower than those of the aluminum analogues, which may reflect the effects of the central metal ion on the yield and lifetime of the excited dye.

1.1.3.3 Zinc(II) Phthalocyanines

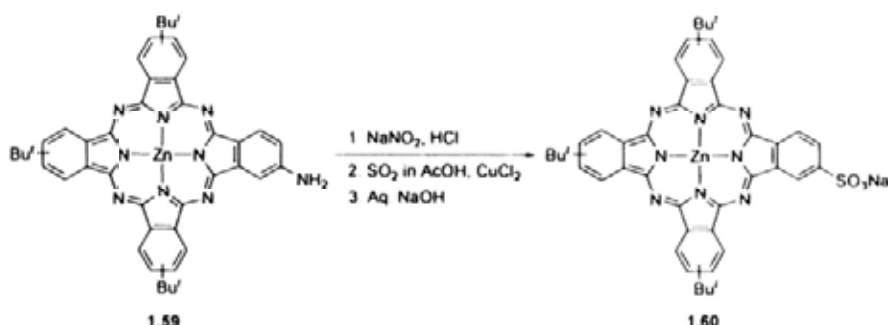
The unsubstituted zinc(II) phthalocyanine is poorly soluble in common organic solvents and aqueous media. Hence, to allow it to be used in PDT, it needs to be formulated as an emulsion or conjugated with proteins, such as unilamellar liposomal,^{59a} low density lipo-protein,^{59b} and bovine serum albumin (BSA).^{59c}

Water-soluble sulfonated zinc(II) phthalocyanines have received much attention as PDT agents since they do not require any other additional vehicles for drug delivery. These compounds can simply be prepared by direct sulfonation of the unsubstituted zinc(II) phthalocyanine with fuming sulfuric acid.⁶⁰ This reaction gives a complex mixture of many isomeric and differently sulfonated phthalocyanines, even though the reaction is carefully controlled. The direct sulfonation leads to substitution at both the 3- and 4-positions of the phthalic subunit. The complexity of the reaction mixture renders a very tedious purification procedure which requires reverse-phase high performance liquid chromatography (HPLC) with a mixture of phosphate-buffered water and methanol as the mobile phase.

Two improved strategies for the preparation of sulfonated phthalocyanines were reported by Busch et al. and Leznoff et al., respectively.^{61,62} Mixed condensation of 1-(3,4-dicyanophenylsulfonyl) pyrrole (**1.56**) with unsubstituted phthalonitrile led to the formation of the corresponding monosulfonated phthalocyanine.⁶² The product, however, was highly insoluble and difficult to be separated by chromatography. To increase the solubility, **1.56** was condensed with 4,5-diheptylphthalonitrile (**1.57**) to give compound **1.58** in 10% overall yield (Scheme 1.13). The monosulfonated phthalocyanine **1.60** was prepared by substitution of the monoamino phthalocyanine **1.59** using the Meerwein procedure (Scheme 1.14).⁶³



Scheme 1.13. Synthesis of the mono-sulfonated zinc(II) phthalocyanine **1.58**.



Scheme 1.14. An alternative synthetic route for the mono-sulfonated zinc(II) phthalocyanine **1.60**.

In addition to these mono-sulfonated phthalocyanines, some tri-sulfonated phthalocyanines have also been prepared by van Lier et al. via the subphthalocyanine approach.⁶⁴

Similar to the aluminum(III) phthalocyanine series, the degree of sulfonation greatly affects the *in vitro* and *in vivo* photocytotoxicity and the photochemical properties of the zinc derivatives.^{59,65} It has been found that decreasing the degree of sulfonation increases the degree of hydrophobicity of the phthalocyanine and leads to a higher photodynamic activity both *in vitro* and *in vivo* against V-79 Chinese hamster cells and EMT-6 mouse mammary tumor.^{65,66} The higher photoactivity is a result of better cellular uptake properties.⁶⁷ Hence the isomeric mixture of sulfonated zinc(II) phthalocyanines obtained through direct sulfonation of zinc(II)

phthalocyanine was found to be 10-fold more active than the homogeneous tetra-sulfonated analogue prepared via the condensation of 4-sulfophthalic acid.⁶⁵

Leznoff et al. have prepared the hydroxy phthalocyanines **1.61-1.65** and studied the relationships between the sites of substitution and the photodynamic activity.^{11b} Compared with the tetrahydroxy analogue **1.61**, compounds **1.62-1.65** exhibit higher photodynamic activities against the Chinese hamster V-79 fibroblasts in the order: 2-hydroxy (**1.62**) > 2,3-dihydroxy (**1.63**) > 2,9-dihydroxy (**1.64**) > 2,9,16-trihydroxy (**1.65**). The trend parallels with the decrease in hydrophobicity of the compounds. An *in vivo* study against EMT-6 mouse mammary tumor shows that the 2,9-dihydroxy isomer **1.64** exhibits the highest photodynamic activity. The monohydroxy derivative **1.62** and the 2,3-dihydroxy isomer **1.63** show a lower potency, while the tetrahydroxy analogue **1.61** fails to induce tumor cure.

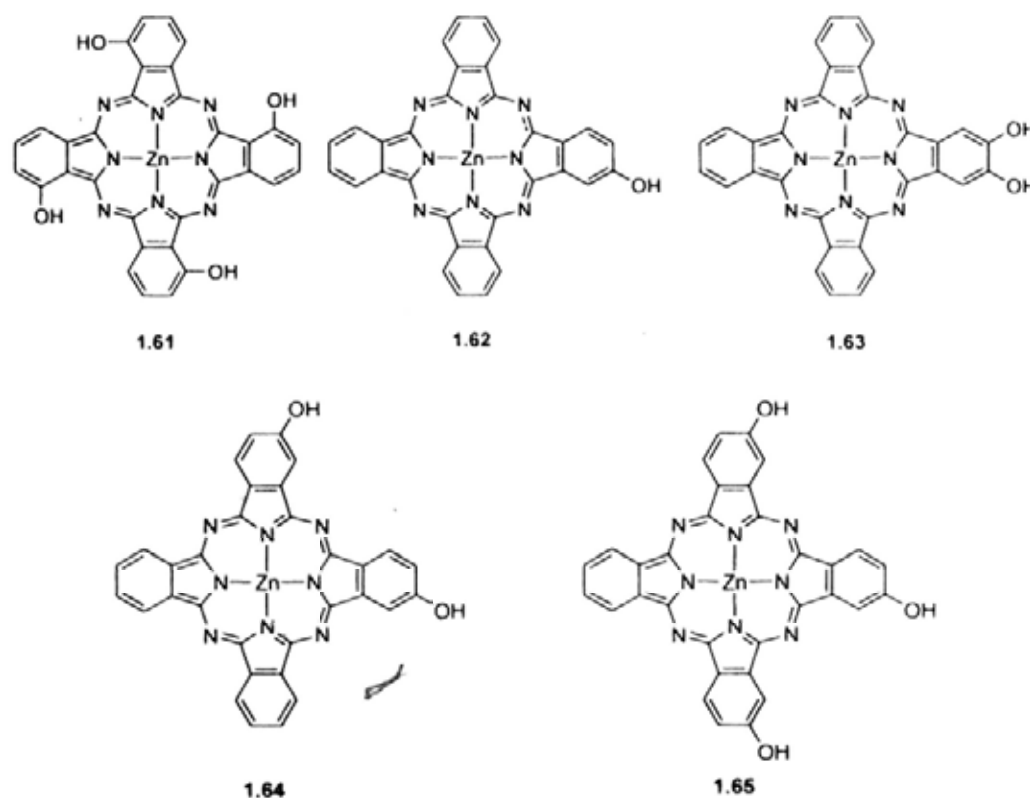


Figure 1.8. Some examples of hydroxy zinc(II) phthalocyanines.

Two amphiphilic carboxy zinc(II) phthalocyanines **1.66** and **1.67** were also synthesized.⁶⁸ Their photodynamic efficiencies toward HeLa cells were compared with those of hydrophobic hexadecafluorophthalocyanine **1.68** and hydrophilic octacarboxyphthalocyanine **1.69**.⁶⁸ The unsymmetrical analogues had a remarkably higher photodynamic effect among the phthalocyanines used. The effect is apparently caused by the fact that these two unsymmetrical phthalocyanines are mainly accumulated in the hydrophobic lipid membrane and are in the photoactive monomer form in HeLa cells.

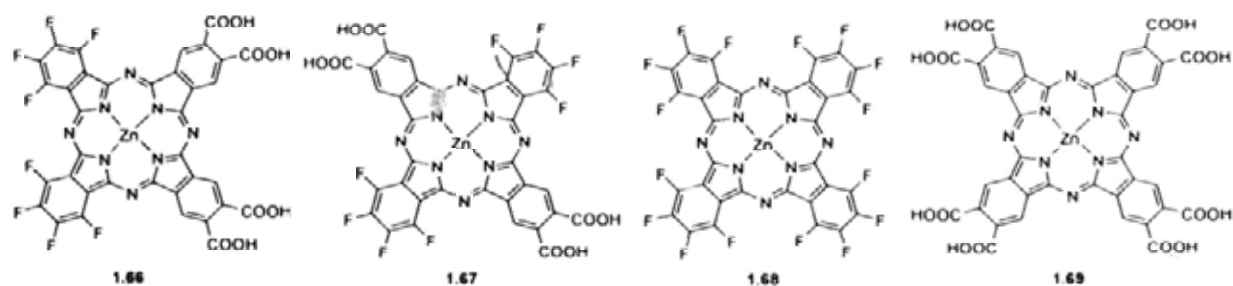
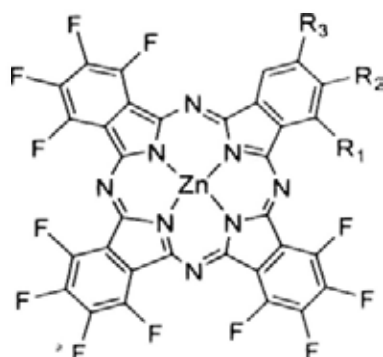


Figure 1.9. Selected examples of carboxy zinc(II) phthalocyanines.

Recently, a series of unsymmetrically substituted fluorinated phthalocyanines **1.70** have been synthesized via the ring expansion approach. Study on their photodynamic activities has shown that the unsymmetrically substituted dodecafluorinated phthalocyanines are more potent toward MRT-6 mouse mammary tumor cells than the symmetrical hexadeca-substituted derivative **1.68**.⁶⁹



1.70: $R_1 = R_3 = \text{H}$, $R_2 = t\text{-butyl, NO}_2, \text{I, H}$

Figure 1.10. Structures of substituted fluorinated phthalocyanines 1.70.

1.1.4 Glycosylated Photosensitizers

In addition to the photophysical properties, the cellular uptake and selectivity are other important issues in the design of photosensitizers. Over the past two decades, some common biomolecules have been conjugated to photosensitizers with a view to enhancing their photodynamic activity and targeting property. Among these carriers, low-density lipoproteins (LDLs) are one of the examples giving promising results.⁷⁰ Viral proteins, which are widely used as vectors in gene therapy, have also been conjugated to phthalocyanines.⁷¹ Recently, glycosylated photosensitizers have gained considerable attention due to their potential targeting property toward the glucose transporters which are overexpressed in cancer cells.

Malignant cells are known to have accelerated metabolism which requires a high glucose uptake. Transport of glucose across the plasma membrane of mammalian cells is the first rate-limiting step for glucose metabolism and is mediated by facilitative glucose transporter (GLUT) proteins. Increased glucose transport in malignant cells has been associated with increased and deregulated expression of glucose transporter proteins. Hence overexpression of GLUT1 and/or GLUT3 is a characteristic identified in many cancerous cells.⁷² For example, elevated GLUT1

expression has been described in many cancers, including (hepatic, breast, endometrial, and cervical carcinoma).⁷³ Owing to this feature, it is believed that glycoconjugation may enhance the selectivity and efficacy of photosensitizers.

In 1997, Carré et al. used a *meso*-arylglycosylporphyrin to inhibit the growth of the yeast *Saccharomyces cerevisiae*.⁷⁴ Later, other glycoconjugated photosensitizers including porphyrins,^{75,76} hypocreli,⁷⁷ and chlorins⁷⁸ were also reported. Zheng et al. used near-infrared confocal microscopy to show that glycosylated pyropheophorbide **1.71** was selectively taken up by 9L glioma cells.⁷⁹ In the presence of 50 mM α -D-glucose, the fluorescence of **1.71** was drastically decreased. This competitive experiment showed that the glycosylated species **1.71** is taken up via GLUT.

Besides the common monosaccharides, glycosamine moieties can also be introduced to increase the uptake. Barberi-Heyob et al. prepared a series of glucosylated chlorins and porphyrins substituted with an *O*-acetylated glucosamine group.⁸⁰ It was found that the mono-glucosylated porphyrin **1.72** has the highest uptake by HT29 human adenocarcinoma cells, which is 11.5-fold higher than tetraphenylporphyrin. The subcellular localization studied by confocal fluorescence microscopy showed that compound **1.72** is accumulated mainly inside the endoplasmic reticulum, not in the mitochondria or lysosome. Endoplasmic reticulum is known to play a central role in the biosynthesis, segregation, and transport of proteins and lipids, as well as in the release of intracellular stores of calcium.⁸¹ Therefore the destruction of endoplasmic reticulum is fatal to the tumor cells, and this mechanism is different from the photochemical damage of mitochondria by photosensitizers, which can cause the release of cytochrome *c* and eventually lead to apoptosis of the cancerous cells.

Besides the porphyrinoid compounds, expanded porphyrins such as sapphyrins were also conjugated with sugars. Sessler's group prepared the glycoconjugated sapphyrin **1.73**, of which the uptake was studied by comparing the intensities of the Raman bands of the free and bound states.⁸² They found that **1.73** has a higher uptake compared with related photosensitizers based on porphyrins and texaphyrins.

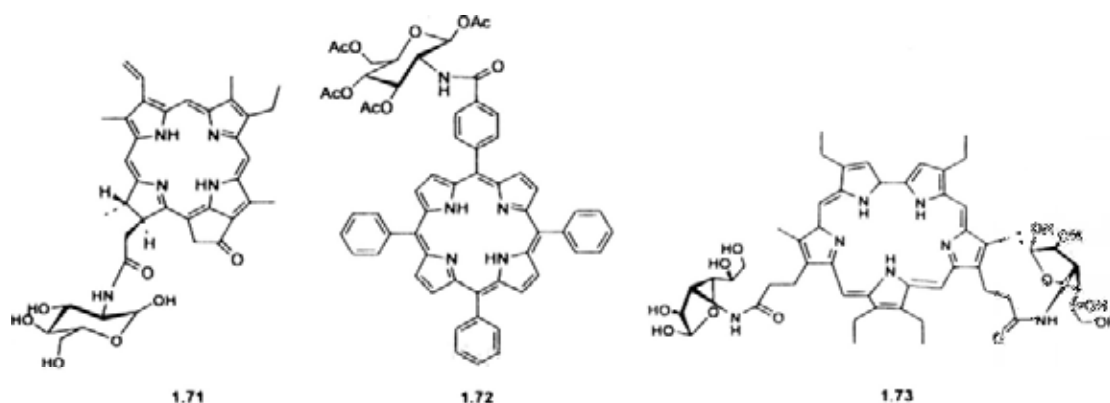


Figure 1.11. Structures of glycosylated pyropheophorbide **1.71**, mono-glucosylated porphyrin **1.72**, and glycoconjugated sapphyrin **1.73**.

In addition to *in vitro* studies, the *in vivo* distribution of some glycosylated photosensitizers was also reported. Volka et al. investigated the photochemical properties and biolocalization of the porphyrin-guanine **1.74** and the sapphyrin-sugar conjugate **1.73**.⁸³ It was found that **1.73** has a high selectivity and is localized in xenographic tumor tissues over other normal mouse tissues. While the distribution kinetics of the porphyrin-guanine **1.74** conjugate was different, it was rapidly released from most of the tissues including tumor in several days after injection. By contrast, the sapphyrin-sugar analogue showed a much slower clearance from the tissues and greater tumor retention. This showed that glycosylation may improve the *in vivo* tumor affinity as well as the cellular uptake.

Recently, a series of tetrapyrrolic macrocycles with different sugar substituents and substitution pattern have been reported. These include tetraphenylporphyrins substituted with sugars such as xylose and arabinose.⁸⁴ To further enhance the selectivity and efficacy, some photosensitizers have been incorporated with more than one target groups. For example, the thio-glycosylated cationic perfluoroporphyrin **1.75** incorporates both sugar and cationic moieties. The latter is believed to have a higher specificity toward the mitochondria and can enhance the solubility of the photosensitizer in aqueous medium.⁸⁵ Although the compound has a little dark toxicity, it is rather potent toward HT29 cells with an LD₉₀ value of 5 μ M.

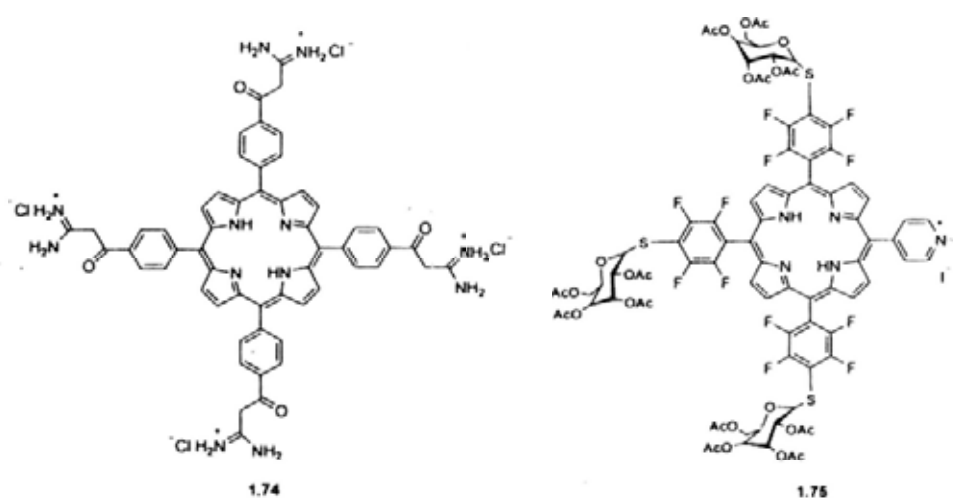


Figure 1.12. Structures of porphyrin-guanine conjugate **1.74** and thio-glycosylated perfluoroporphyrin **1.75**.

1.1.4.1 Glycosylated Phthalocyanines

Although a substantial number of glycosylated photosensitizers have been prepared, glycoconjugated phthalocyanines are extremely rare. To my knowledge, only a few sugar-containing phthalocyanines have been reported so far. Compounds **1.76** and **1.77** were firstly prepared, but they were only briefly characterized and their

photodynamic activities were not evaluated.⁸⁶ Recently, our group has prepared silicon(IV) phthalocyanines **1.78** and **1.79** with one or two galactose substituent(s) by typical substitution reactions.⁸⁷ These compounds exhibit a high photodynamic activity against HepG2 cells with IC_{50} values down to 0.1 μ M.

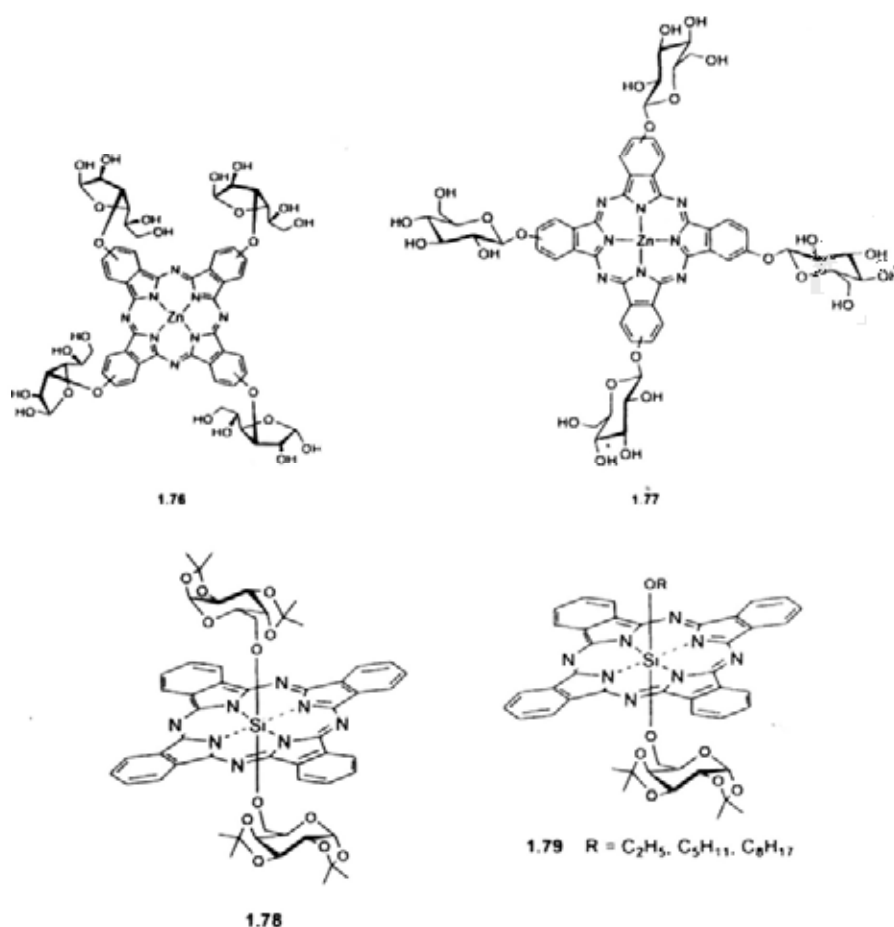


Figure 1.13. Some examples of glycosylated phthalocyanines.

In addition, two glucoconjugated silicon(IV) phthalocyanines **1.80** and **1.81** have also been prepared and examined for their photo-physical and biological properties.⁸⁸ With two axial 1,2:5,6-di-*O*-isopropylidene- α -D-glucopyranose substituents linked to the silicon center through the tetraethylene glycol chain, both compounds are highly photocytotoxic against HT29 and HepG2 cells, particularly the non-chlorinated phthalocyanine **1.80**, of which the IC_{50} values are as low as 5.5 nM.

The lower photodynamic activity of the chlorinated derivative ($IC_{50} = 17.2-21.3$ nM) can be attributed to its higher aggregation tendency in the biological media, leading to a lower efficiency to generate reactive oxygen species (ROS) inside the cells. Fluorescence microscopic studies have also revealed that compound **1.80** has a high and selective affinity to the lysosomes, but not the mitochondria, of HT29 cells.

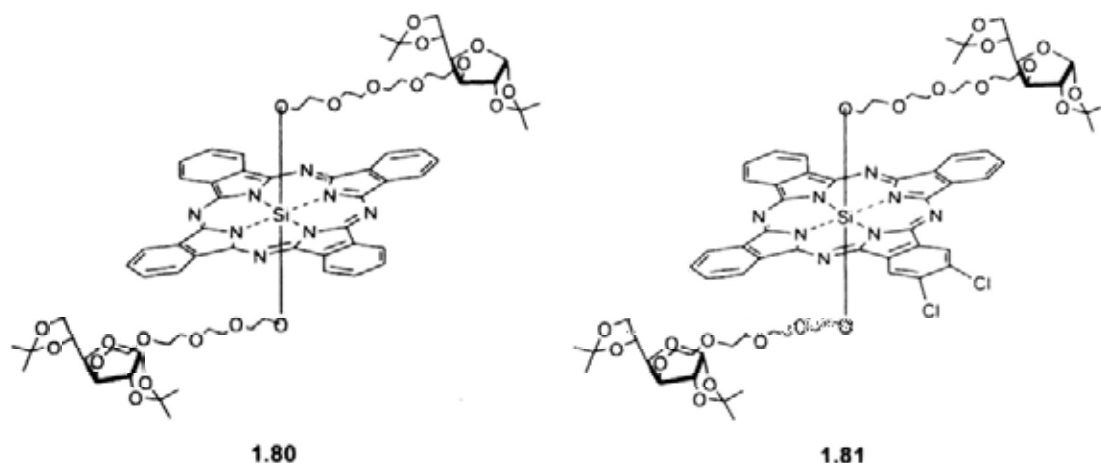
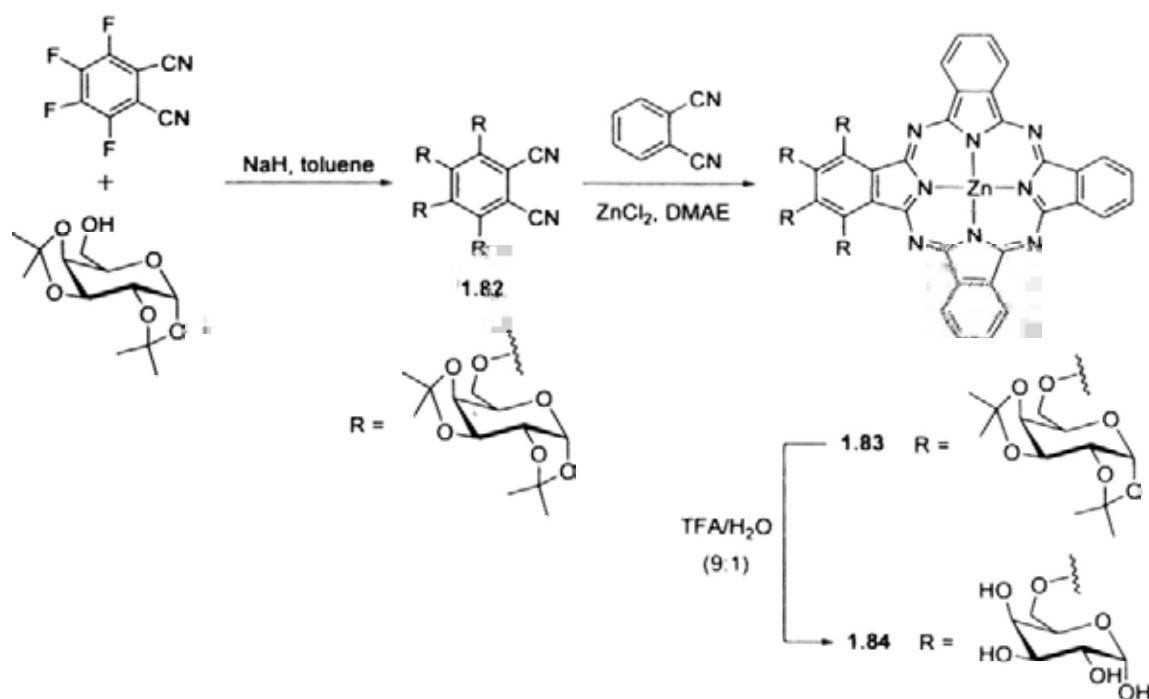


Figure 1.14. Structures of glucoconjugated silicon(IV) phthalocyanines **1.80** and **1.81**.

An unsymmetrical glycosylated zinc(II) phthalocyanine has also been prepared recently via a statistical cross-condensation method.⁸⁹ Phthalonitrile **1.82**, which can be obtained by aromatic nucleophilic substitution of the four fluoro groups of tetrafluorophthalonitrile by four 1,2:3,4-di-O-isopropylidene- α -D-galactopyranose units, reacts with an excess of unsubstituted phthalonitrile in the presence of zinc chloride in DMAE to give phthalocyanine **1.83**. Removal of the carbohydrate protecting groups in compound **1.83** with aqueous TFA at room temperature leads to the formation of phthalocyanine **1.84**. Again, the photobiological properties of these compounds were not studied.



Scheme 1.15. Synthesis of the unsymmetrical glycosylated zinc(II) phthalocyanine 1.84.

1.2 Boron Dipyrromethenes (BODIPYs)

1.2.1 General

Boron dipyrromethenes (BODIPYs) (Figure 1.15) have gained special attention as one of the most versatile classes of fluorophores, and these dyes have steadily increased in popularity over the past two decades.⁹⁰ They were firstly discovered by Treibs and Kreuzer in 1968.⁹¹ although people paid little attention to the discovery until the end of 1980s.⁹² Then, the potential use of these dyes for biological labeling was recognized⁹³ and several new BODIPY-based dyes⁹⁴ were designed and commercialized as labeling reagents for biomolecules. As a consequence, BODIPYs came to be known as photostable substitutes for fluorescein by the biochemists and biologists. In parallel, more fundamental studies on the chemical reactivity and the photophysical properties of these dyes began to emerge.⁹⁰ BODIPYs have many

attractive spectral characteristics, such as large absorption coefficient, high fluorescence quantum yield, and long-wavelength emission.⁹⁰ Other useful properties of BODIPYs include their low rates of intersystem crossing, good solubility, high chemical robustness, excellent thermal and photochemical stability, and insensitivity to changes in environment, such as the polarity, pH, and oxygen content of the media.⁹⁰

More importantly, the absorption and emission properties of these dyes can be tuned through rational modification of the BODIPY core.⁹⁰ The parent dye absorbs near 480 nm and emits around 490 nm. Alkylation or arylation at the *meso* position has almost no effect on the absorption and emission wavelengths even though this substitution position is structurally unique. While, generally, introduction of substituents on the pyrrole ring can slightly shift the absorption and emission position of BODIPY. When substituents that can extend the conjugation of the parent molecule are added, both the absorption and emission positions are shifted to longer wavelength. These properties make them excellent candidates in labeling of biomolecules,^{90a,95} ion sensing,^{90a,96} photodynamic therapy,⁹⁷ and light-harvesting systems,⁹⁸⁻¹⁰⁰ etc.

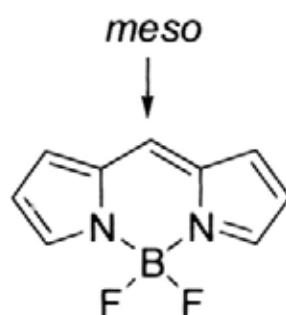


Figure 1.15. General structure of BODIPYs.

1.2.2 Light Harvesting Systems Based on BODIPYs

Light harvesting systems, which absorb light and funnel energy to the reaction center, play a very important role in natural photosynthesis.¹⁰¹ BODIPY dyes are well-known fluorophores having remarkable photophysical properties, which are ideal components of light harvesting systems. To date, many light harvesting molecules have been developed including BODIPYs as the core entity⁹⁸ and/or part of the antenna.^{99,100}

1.2.2.1 BODIPYs as the Core

Similar to many other organic fluorophores, BODIPY dyes possess small Stokes' shift, which hampers their optimum use in flow cytometry and fluorescence microscopy.^{90b} Synthetic strategies have been developed to circumvent this problem by covalent attachment of an ancillary pigment to the BODIPY core to form a cassette. In this way, all the photons absorbed by the secondary chromophore, which is usually an aromatic polycycle, can be channeled to the BODIPY emitter. As a consequence, there is a large position disparity in excitation and emission spectra and the full benefits of the BODIPY emitter are retained.^{90b}

Recently, the BODIPY-antracene conjugates **1.85-1.89** have been prepared by Burgess et al. via palladium-catalyzed cross-coupling reactions.^{98a} In these cassettes, Highly efficient photo-induced energy transfer occurred from antracene to BODIPY. The energy transfer efficiencies depend on the relative orientation of the two components and the structure of the linkers attaching them. All systems in which the donor is coupled to the long axis of the BODIPY acceptor (as in **1.87**) exhibit a significantly faster energy transfer than those with the donors attached to the short axis (as in **1.89**).

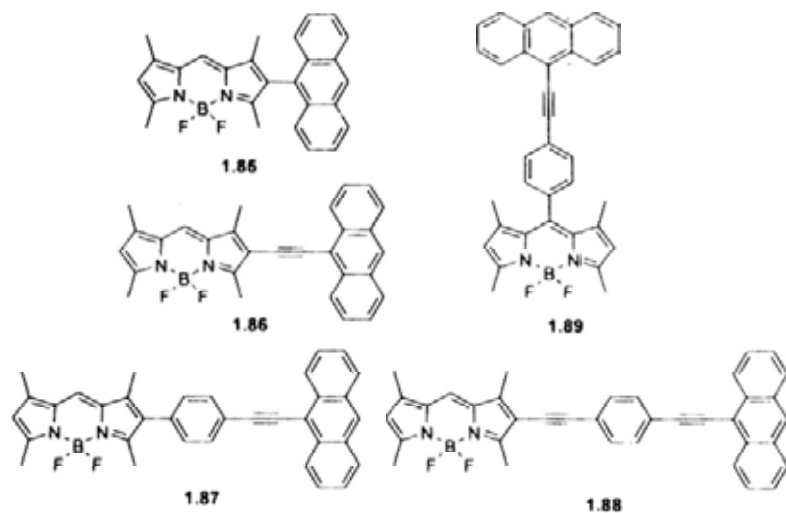


Figure 1.16. Structures of BODIPY-antracene conjugates **1.85-1.89**.

Highly fluorescent and soluble dual-dye probes **1.90-1.92** have also been synthesized.^{98b} The absorption spectra of these compounds indicate that the BODIPY and pyrene chromophores are spectrally isolated, thereby inducing a large “virtual” Stokes shift. The latter is realized by efficient intramolecular excitation energy transfer by the Förster dipole–dipole mechanism. For all the three systems, they exhibit efficient intramolecular excitation energy transfer from pyrene to BODIPY. The rate of energy transfer depends on the structure of the dual dye system and decreases as the center-to-center separation increases. The energy transfer efficiency, however, exceeds 90% in all systems. Linking the two pyrene residues by an ethyne group leads to a decrease in the energy-transfer efficiency, with the two polycycles acting as a single chromophore. The directly linked BODIPY–pyrene dyad **1.90** binds to DNA and functions as an efficient solar concentrator when dispersed in plastic.

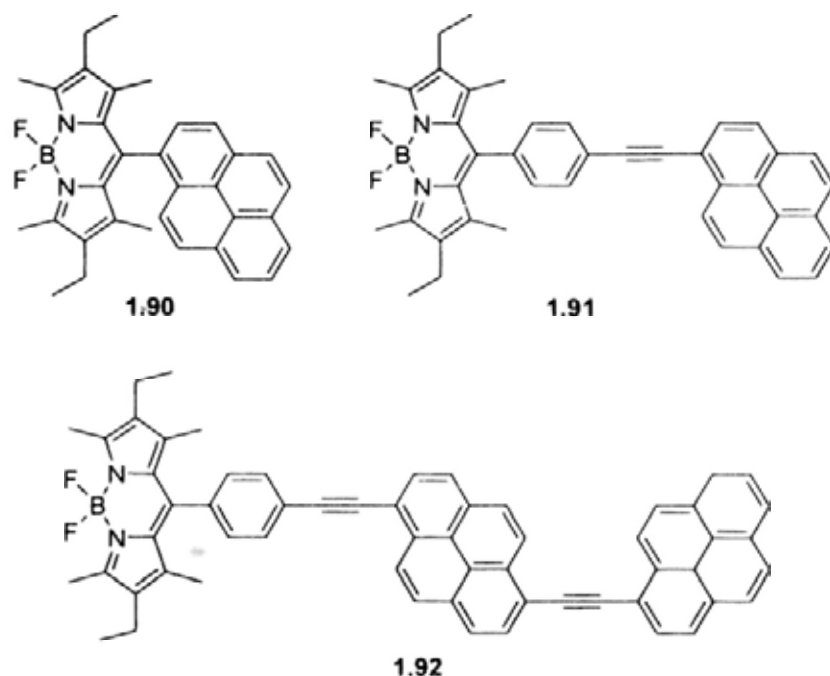


Figure 1.17. Structures of BODIPY-pyrene conjugates **1.90-1.92**.

Apart from these compounds, three related triads **1.93-1.95**, comprising a BODIPY core linked to two aromatic polycycles via the boron center, have also been prepared.^{98c} The polycyclic compounds are either pyrene or perylene, or a mixture of both. Whereas the absorption spectral profiles contain important contributions from each of the subunits, fluorescence occurs exclusively from the BODIPY fragment. Intramolecular excitation energy transfer is extremely efficient in each case, even though the spectral overlap integrals for the pyrene-based system are modest. The asymmetric derivative **1.94** is the most attractive dye since its absorption covers most of the accessible spectral range. This compound fluoresces strongly when dispersed in polymeric media and acts as a highly efficient solar concentrator. It also induces a large “virtual” Stokes’ shift and displays several clear absorption peaks that are useful as markers for chemical sensors.

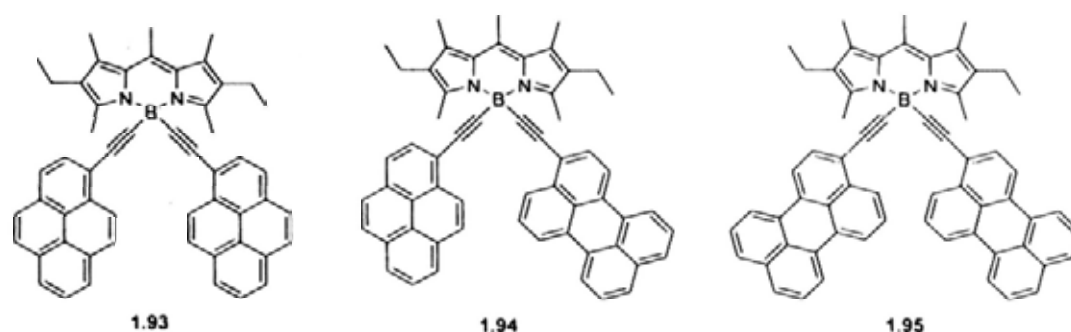


Figure 1.18. Structures of BODIPY-polycycle triads **1.93-1.95**.

1.2.2.2 BODIPYs as the Antenna

Porphyrin-based systems featuring BODIPY donors have been widely developed as models for natural photosynthesis to study the electron transfer and energy transfer processes. They are also promising energy cassettes for molecular photonic devices. For example, the pentad **1.96** was designed as a “linear molecular photonic wire” by Lindsey,^{99a} in which a BODIPY dye provides an optical input at one end, a linear array of three zinc(II) porphyrins as a signal transmission element, and a free base porphyrin serving as an optical output at the other end (Figure 1.19). This donor-acceptor pair is separated by 90 Å. When excited at 485 nm, highly efficient through bond energy transfer took place from the BODIPY to zinc(II) porphyrin (ZnP), and then to metal free porphyrin (H₂P). The overall signal transmission efficiency from input to output was found to be 76%. Systems **1.97** and **1.98** were described as “molecular optoelectronic linear- and T-gates”, respectively (Figure 1.19).^{99b} In these two systems, a magnesium(II) porphyrin was employed as a switcher which can turn on or off the emission of the acceptor. The oxidized state of this porphyrin quenched the fluorescence via intramolecular charge transfer (ICT).

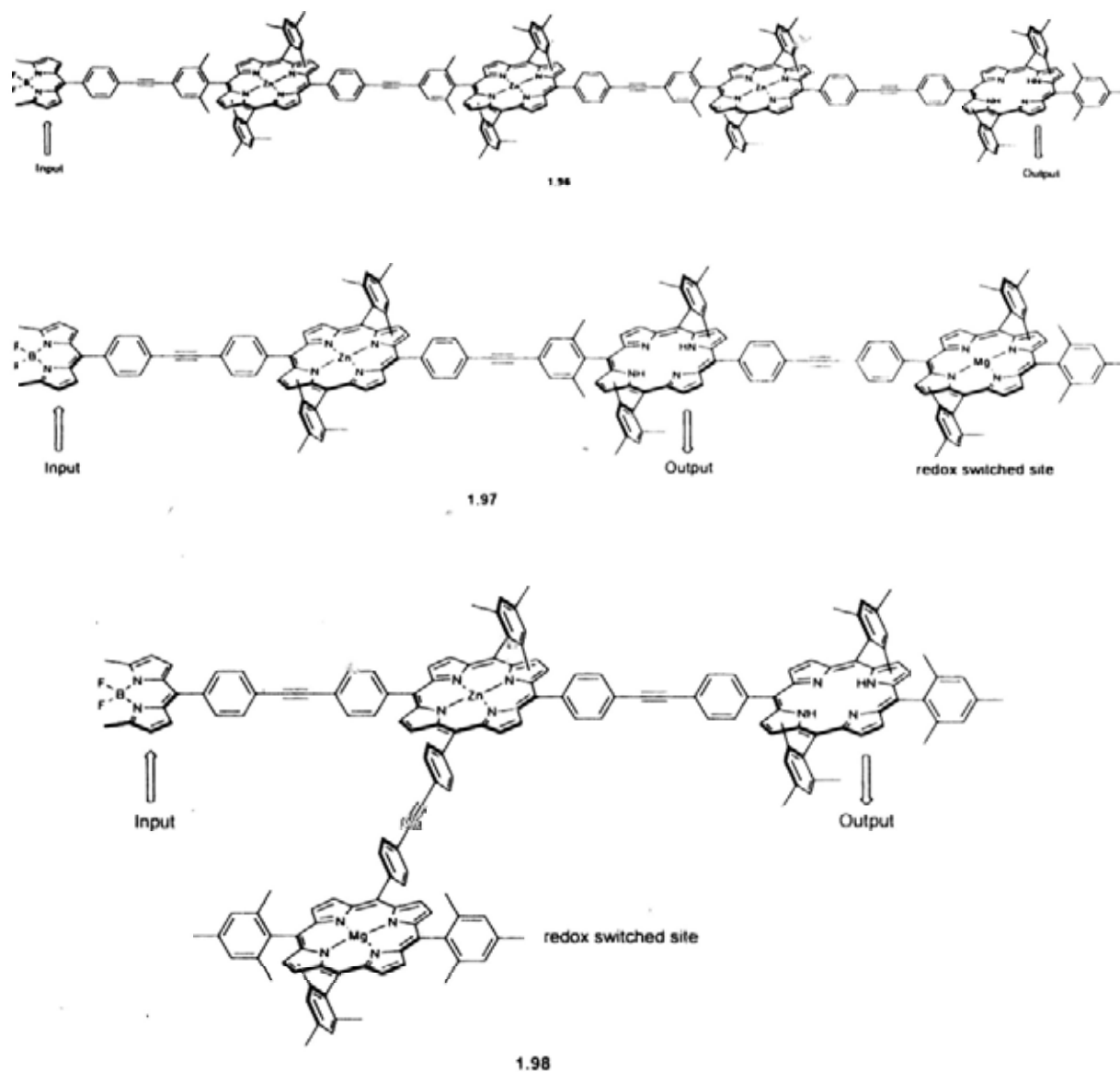


Figure 1.19. Molecular photonic wire **1.96** and molecular optoelectronic gates **1.97** and **1.98**.

The porphyrins **1.99-1.102** which are substituted with one, two, or eight BODIPY unit(s) have also been synthesized as light-harvesting arrays.^{99c} The blue-green BODIPY absorption complements the spectral coverage of the porphyrin chromophore, enhancing the light harvesting properties of the arrays and facilitating selective excitation of the accessory pigment for other applications. An efficient energy transfer (>85%) from the BODIPY pigment(s) to porphyrin has been observed for these conjugates.

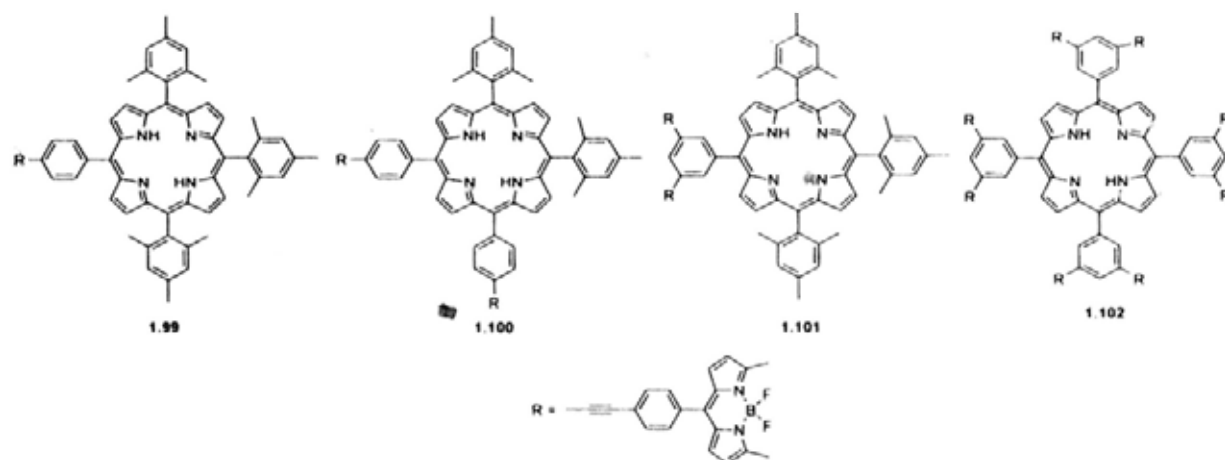


Figure 1.20. Structures of BODIPY-porphyrin conjugates **1.99-1.102**.

For the cassettes **1.103** and **1.104**, the emission from the BODIPY moieties virtually cannot be seen upon excitation of the BODIPY part at 485 nm. Instead, an emission corresponding to the thia or oxaporphyrin unit appears, suggesting the presence of an efficient energy transfer.^{99d,99e} It is difficult to directly compare the efficiency of energy transfer of these systems because the donor and acceptor fragments have different separation and orientations. Interestingly, the dithia analogous system **1.105**^{99f} gives a much lower energy transfer quantum yield (by ca. 11%) than **1.106**,^{99c} which has a normal porphyrin core ($\Phi_{\text{ENT}} = 97\%$).

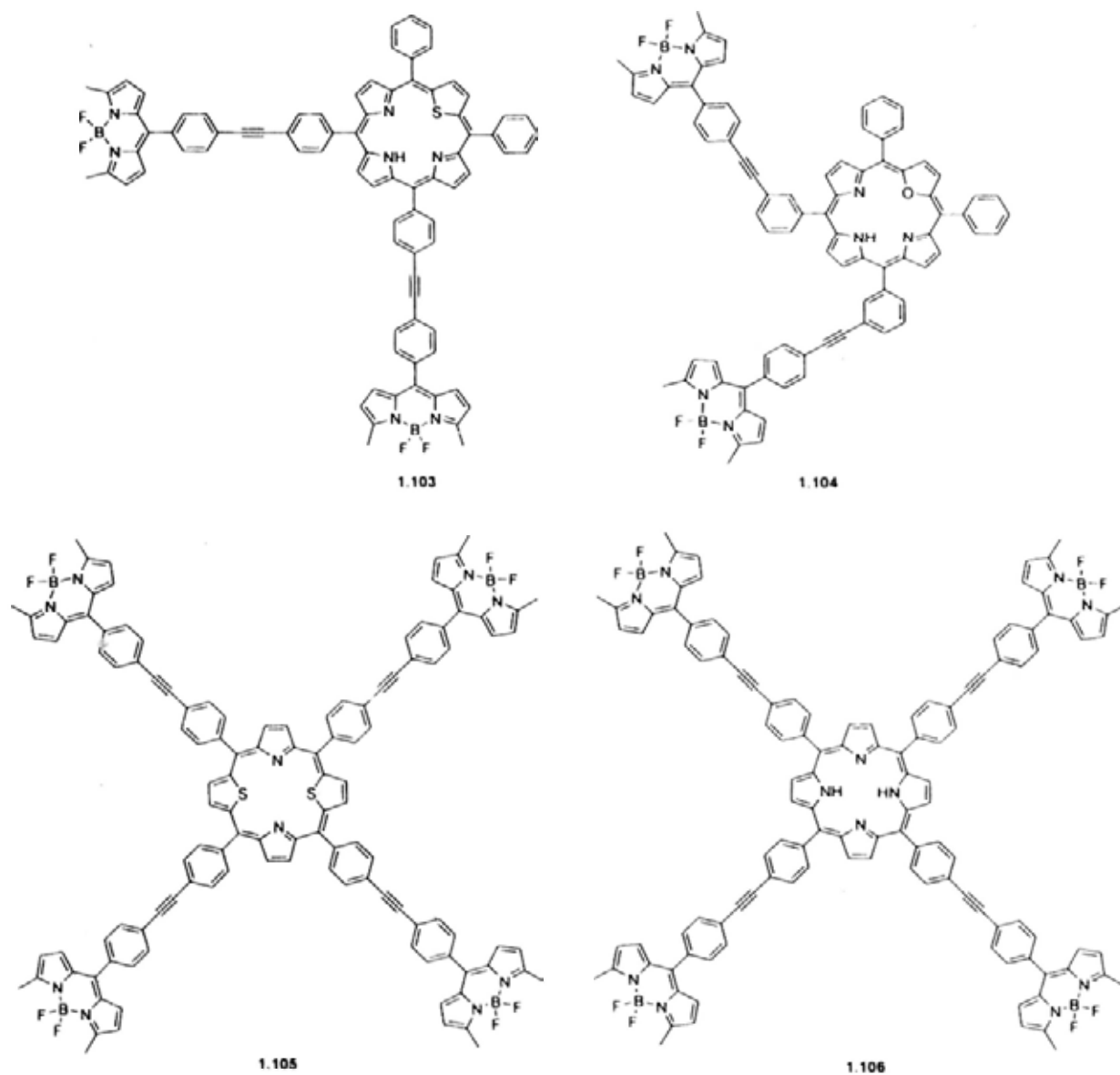


Figure 1.21. Structures of light harvesting arrays 1.103-1.106.

The supramolecular triad **1.107** was constructed by Weiss et al. It undergoes a stepwise energy transfer from the excited BODIPY to ZnP, and then to H_2P .^{99g} The efficiencies of these two energy transfer steps were calculated to be 80% and 85%, respectively.

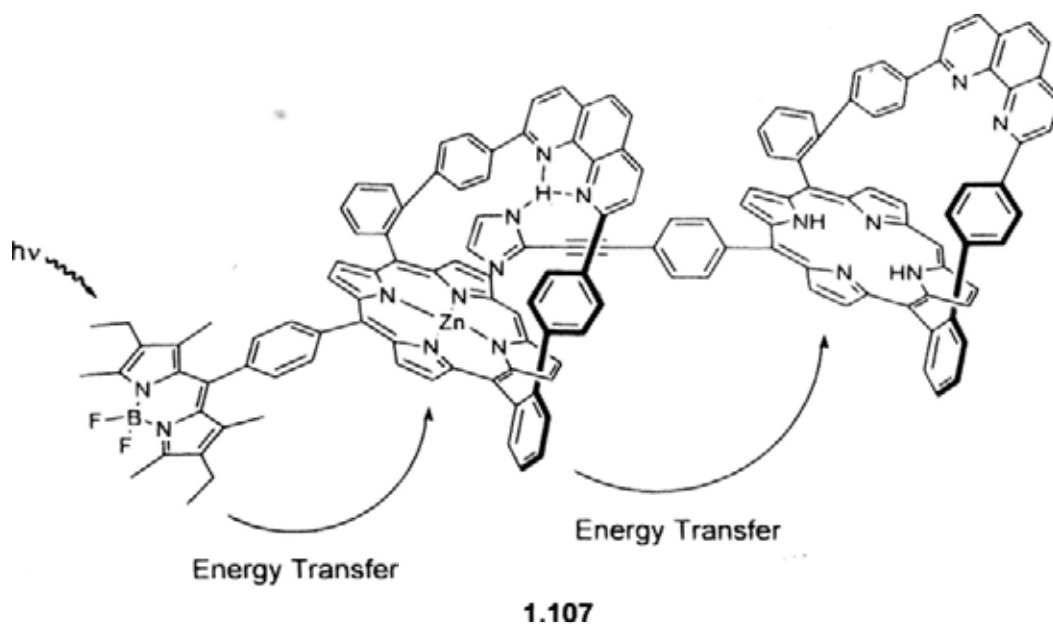


Figure 1.22. A stepwise energy transfer in the supramolecular triad **1.107**.

Energy transfer from the excited BODIPY axial ligands to the porphyrin core was also observed in **1.108-1.111** in non-polar solvents.^{99h} The efficiencies of energy transfer which are in the range of 13-40% increase as the length of the methylene bridge decreases. On the other hand, the emission of Sn(TPP) chromophores was quenched by BODIPY chromophores at rate constants of 10^8-10^9 s^{-1} , which are independent on the solvent polarity. Upon excitation of the BODIPY chromophore of **1.110**, the excited singlet state of the Sn(TPP) chromophore, generated by the energy transfer from the excited BODIPY chromophore, was quenched by the phenoxy ligand via a non-radiative electron transfer process. However, a rapid back electron-transfer may also occur because the absorption of the radical anion of Sn(TPP) was not observed by nanosecond laser photolysis.

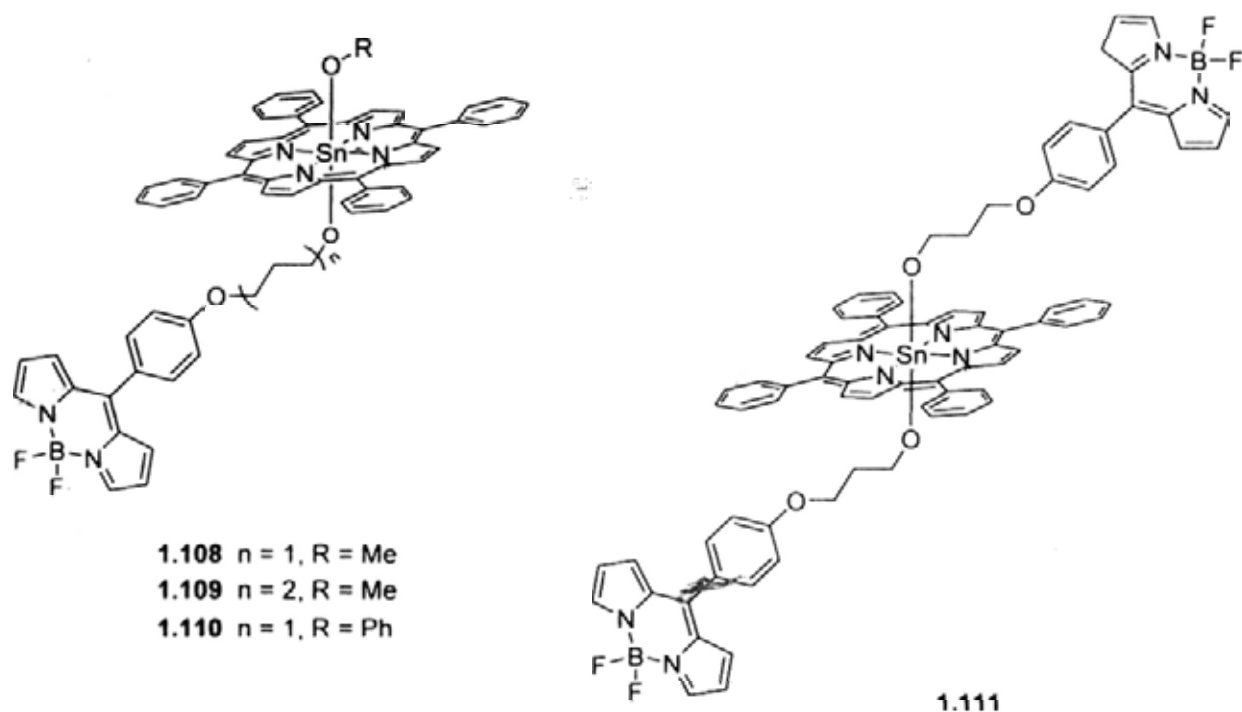


Figure 1.23. Structures of some tin(IV) porphyrins axially substituted BODIPY fluorophores.

Click chemistry was employed to prepare the light harvesting system **1.112** in which a perylene diimide (PDI) acceptor is linked to four BODIPY donors.⁹⁹ⁱ The electronic absorption spectrum of this conjugate is the same as the sum of the spectra of the donor and acceptor components, which indicates that the chromophoric components in this system do not have significant ground-state interactions. Upon excitation at 526 nm, very little residual emission corresponding to peripheral BODIPY was observed. Additionally, a very strong emission from PDI core evolved at 618 nm. This is due to a highly efficient energy transfer (99%) from the donor BODIPY to acceptor PDI.

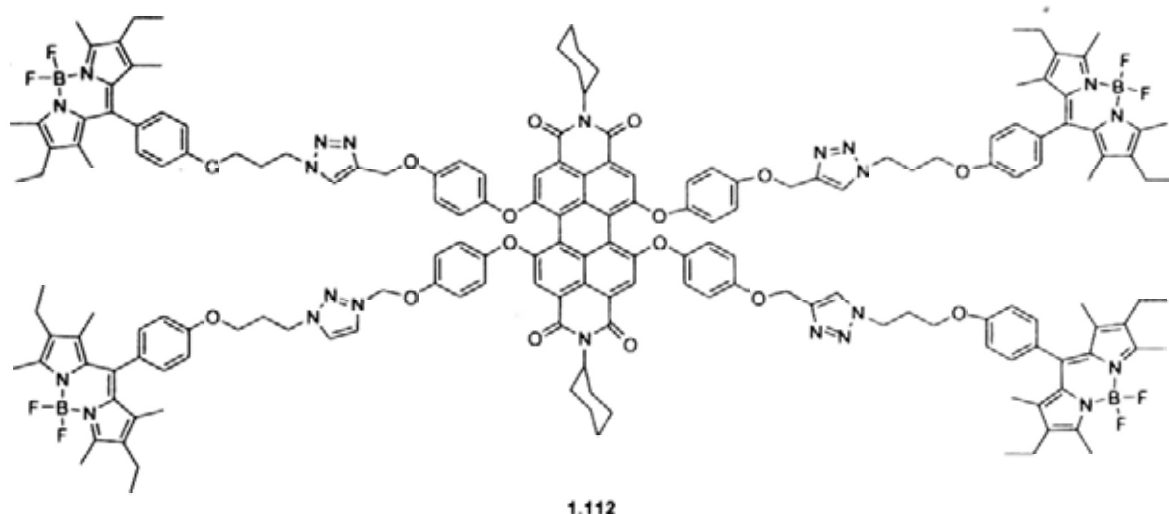


Figure 1.24. Structure of pentad **1.112** containing four BODIPY donors and a perylenediimide (PDI) acceptor.

A supramolecular approach was also employed to construct the artificial photosynthetic model **1.113**.^{99j} Upon selective excitation of the BODIPY unit in the dyad BODIPY-ZnP, an efficient energy transfer occurred from BODIPY to ZnP. Upon forming the supramolecular triad with C₆₀ derivative by axial coordination, the excited ZnP promoted electron transfer to the coordinated fullerene, resulting in a charge-separated state. The observed energy transfer followed by electron transfer in the present supramolecular triad mimics the events of natural photosynthesis. Here, the BODIPY acts as antenna chlorophyll that absorbs light energy and transports spatially to the photosynthetic reaction center, while the electron transfer from the excited zinc porphyrin to fullerene mimics the primary events of the reaction center where conversion of the electronic excitation energy to chemical energy in the form of charge separation takes place. The important feature of the present model system is its relative “simplicity” because of the use of supramolecular approach to mimic the rather complex “combined antenna-reaction center” events of photosynthesis.

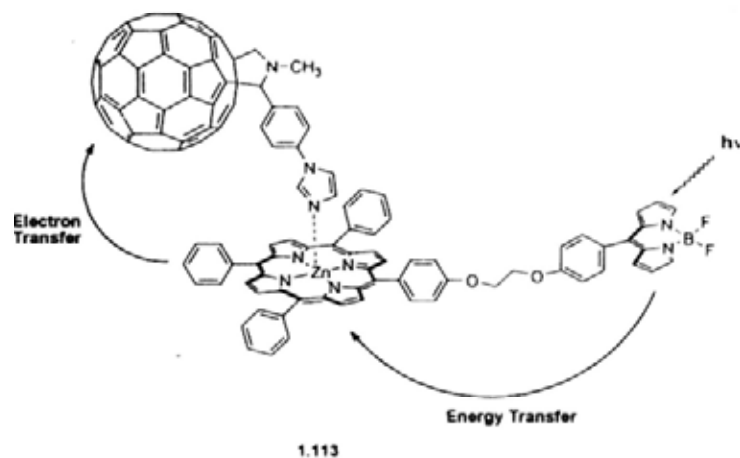


Figure 1.25. Energy transfer followed by electron transfer in the supramolecular triad **1.113**.

1.2.2.3 BODIPYs as Both the Core and Antenna

Fluorescence resonance energy transfer (FRET) cassettes **1.114** have also been prepared.^{100a} These cassettes are composed of two BODIPY chromophores which are linked via an acetylenic linker. Fluorescence spectroscopic studies of these compounds in very dilute CHCl₃ solution have showed that the FRET efficiency significantly decreased with increasing the length of the rigid spacer from about 98% ($n = 1$), to $\approx 85\%$ ($n = 3$), and to $\approx 35\%$ ($n = 6$).

Despite limited spectral overlap ($1.3 \times 10^{-14} \text{ mmol}^{-1} \text{ cm}^6$) and quite wide spatial separation distance (17.9 Å), an essentially quantitative excitation energy transfer occurs from the peripheral BODIPY units to the expanded BODIPY core in **1.115**.^{100b} The small degree of residual fluorescence from the normal BODIPY component is useful for ratiometric fluorescence spectroscopy.

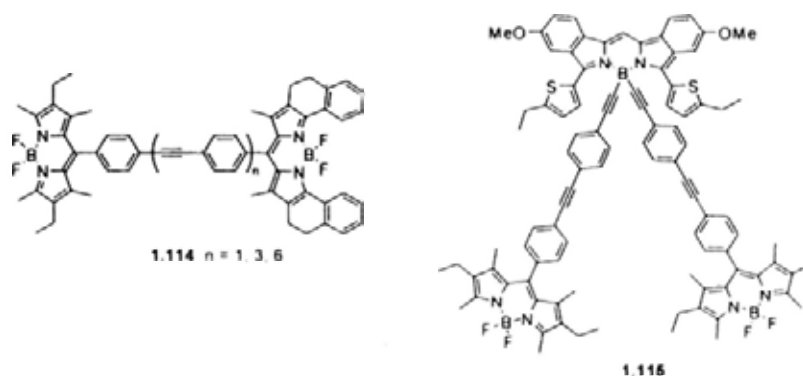


Figure 1.26. Structures of FRET cassettes **1.114** and **1.115** composed of two kinds of BODIPY fluorophores.

The energy transfer cassette **1.116**, which contains three kinds of BODIPY fluorophores has also been synthesized recently by Qian et al.^{100c} It exhibits a very strong absorption in the region from 300 to 700 nm covering most of the solar spectrum. Upon photoexcitation of this compound at 490 or 560 nm, a strong fluorescence emission of the central purple BODIPY dye at 660 nm has been observed. The emission is very weak for the yellow-green BODIPY at 520 nm and the pink BODIPY at 586 nm. These results suggest that a highly efficient energy transfer takes place from each donor to the acceptor in this system.

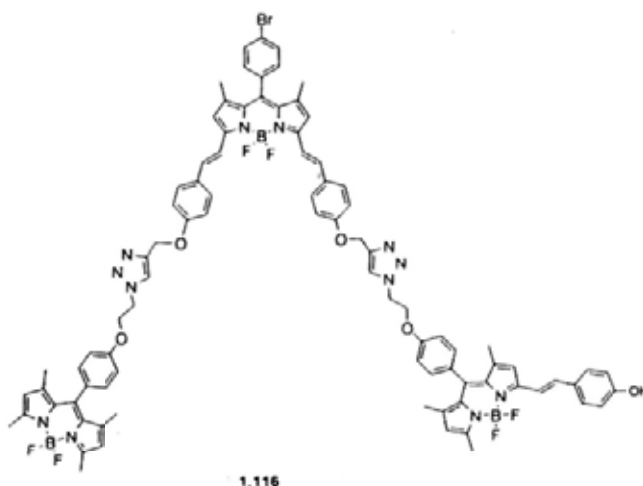


Figure 1.27. Structure of energy cassette **1.116** containing three kinds of BODIPY fluorophores.

Compound **1.117** was designed as a molecular switch.^{100a} Its UV-Vis spectrum displays three strong absorption bands assigned to the spacer (322 nm), the donor (529 nm), and the acceptor dyes (619 nm), respectively. It exists in a contracted conformation at room temperature. The donor-acceptor distance is separated by 7 Å. Upon excitation at 490 nm, intramolecular energy transfer occurred from the donor to acceptor. As a result, a strong emission at 630 nm from acceptor dye was observed. Addition of TFA or lowering the temperature to -60 °C switched the molecule to the expanded conformation, in which the donor-acceptor distance is enlarged by 70 Å. As a consequence, the emission from the acceptor disappeared completely, whereas fluorescence intensity of the donor doubles. These results indicated that no energy transfer occurred between the donor and acceptor in this case.

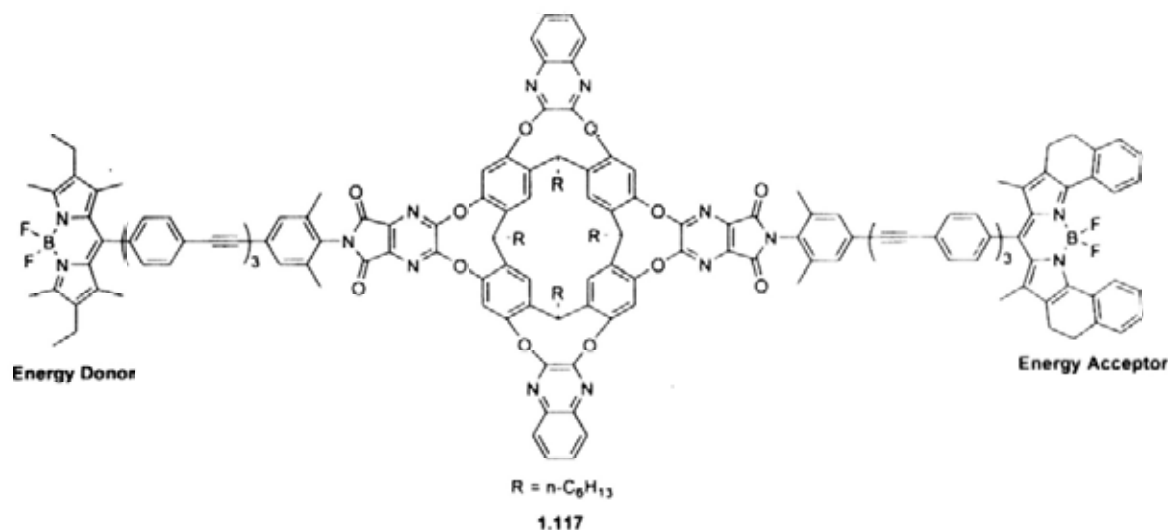


Figure 1.28. Structure of the molecular switch **1.117**.

1.3 References

- Braun, A.; Tcherniac, J. *Ber. Deut. Chem. Ges.* **1907**, *40*, 2709.
- (a) Linstead, R. P. *J. Am. Chem. Soc.* **1934**, *56*, 1016. (b) Linstead, R. P.; Lowe, A. R. *J. Am. Chem. Soc.* **1934**, *56*, 1022. (c) Linstead, R. P.; Lowe, A. R. *J. Am. Chem. Soc.* **1934**, *56*, 1031.

3. (a) *The Phthalocyanines - Properties*; Moser, F. H., Thomas, A. L., Eds.; CRC Press: Florida, **1983**, Vol. 1.
4. (a) *Phthalocyanines - Properties and Applications*; Leznoff, C. C., Lever, A. B. P., Eds.; VCH: New York, **1989**, Vol. 1; **1993**, Vols. 2 and 3; **1996**, Vol. 4. (b) *Phthalocyanine Materials: Synthesis, Structure and Function*; McKeown, N. B. Cambridge University Press: Cambridge, **1998**.
5. (a) Darwent, J. R.; Douglas, P.; Harriman, A.; Porter, G.; Richoux, M. C. *Coord. Chem. Rev.* **1982**, *44*, 83. (b) Ali, H.; van Lier, J. E. *Chem. Rev.* **1999**, *99*, 2379. (c) Wagner, J. R.; Ali, H.; Langlois, R.; Brasseur, N.; van Lier, J. E. *Photochem. Photobiol.* **1987**, *45*, 587.
6. (a) *Photosensitizing Compounds: Their Chemistry, Biology and Clinical Use*; Dougherty, T. J., Bock, G., Harnett, S., Eds.; Wiley: Chichester, **1989**, p 95. (b) Hur, E. B.; Siwecki, J. A.; Newman, H. C.; Crane, S. W.; Rosenthal, I. *Cancer Lett.* **1987**, *38*, 215.
7. Chan, W. S.; Marshall, J. F.; Svensen, R.; Philips, D; Hart, I. R. *Photochem. Photobiol.* **1987**, *45*, 757.
8. (a) Tolbin, A. Y.; Breusova, M. O.; Pushkarev, V. E.; Tomilova, L. G. *Russ. Chem. Bull.* **2005**, *54*, 2083. (b) Fukuzumi, S.; Ohkubo, K.; Ortiz, J.; Gutiérrez, A. M.; Fernández-Lazaro, F.; Sastre-Santos, A. *Chem. Commun.* **2005**, 3814. (c) Haas, M.; Liu, S.-X.; Kahnt, A.; Leiggenger, C.; Guldi, D. M.; Hauser, A.; Decurtins, S. *J. Org. Chem.* **2007**, *72*, 7533.
9. (a) Li, D.; Ratner, M. A.; Marks, T. J. *J. Am. Chem. Soc.* **1988**, *110*, 1707. (b) Torres, T.; de la Torre, G.; Garcia-Ruiz, J. *Eur. J. Org. Chem.* **1999**, 2323. (c) Rojo, G.; de la Torre, G.; Garcia-Ruiz, J.; Ledoux, I.; Torres, T.; Zyss, J.; Agullo-Lopez, F. *Chem. Phys.* **1999**, *245*, 27. (d) Maya, E. M.; Garcia, C.; Garcia-Frutos, E. M.; Vázquez, P.; Torres, T. *J. Org. Chem.* **2000**, *65*, 2733. (e) Maya, E. M.; Garcia-Frutos, E. M.; Vazquez, P.; Torres, T.; Martin, G.; Rojo, G.; Agullo-Lopez, F.; Gonzalez-Jonte, R. H.; Ferro, V. R.; Ledoux, I.; Zyss, J. *J. Phys. Chem. A* **2003**, *107*, 2110. (f) Reddy, P. Y.; Giribabu, L.; Lyness, C.; Snaith, H. J.; Vijaykumar, C.; Chandrasekharam, M.; Lakshmikantam, M.; Yum, J. H.; Kalyanasundaram, K.; Gratzel, M.; Nazeeruddin, M. K. *Angew. Chem. Int. Ed.* **2007**, *46*, 373.
10. (a) Ding, X.-M.; Shen, S.-Y.; Zhou, Q.-F.; Xu, H.-J. *Dyes Pigments* **1998**, *40*, 187. (b) Ding, X.; Xu, H. *Sensors Actuators B: Chem.* **2000**, *65*, 108.

11. (a) Michelsen, U.; Kliesch, H.; Schnurpfeil, G.; Sobbi, A. K.; Wöhrle, D. *Photochem. Photobiol.* **1996**, *64*, 694. (b) Hu, M.; Basseur, N.; Yildiz, S. Z.; van Lier, J. E.; Leznoff, C. C. *J. Med. Chem.* **1998**, *41*, 1789. (c) Giuntini, F.; Nistri, D.; Chiti, G.; Fantetti, L.; Jori, G.; Roncucci, G. *Tetrahedron Lett.* **2003**, *44*, 515. (d) Cosimelli, B.; Roncucci, G.; Dei, D.; Fantetti, L.; Ferroni, F.; Ricci, M.; Spinelli, D. *Tetrahedron* **2003**, *59*, 10025. (e) Bonneau, S.; Morlière, P.; Brault, D. *Biochem. Pharmacol.* **2004**, *68*, 1443. (f) Lo, P.-C.; Huang, J. D.; Cheng, D. Y. Y.; Chan, E. Y. M.; Fong, W. P.; Ko, W. H.; Ng, D. K. P. *Chem. Eur. J.* **2004**, *10*, 4831.
12. (a) Makhseed, S.; Bumajdad, A.; Ghanem, B.; Msayib, K.; McKeown, N. B. *Tetrahedron Lett.* **2004**, *45*, 4865. (b) Fatma, Y.; Devrim, A.; Vefa, A. *Polyhedron* **2007**, *26*, 4551.
13. (a) Engelkamp, H.; Middelbeek, S.; Nolte, R. J. M. *Science* **1999**, *284*, 785. (b) Martínez-Díaz, M. V.; Rodríguez-Morgade, M. S.; Feiters, M. C.; van Kan, P. J. M.; Nolte, J. M.; Stoddart, J. F.; Torres, T. *Org. Lett.* **2000**, *2*, 1057. (c) Charvet, R.; Jiang, D.; Aida, T. *Chem. Commun.* **2004**, 2664.
14. de la Torre, G.; Torre, T. in *The Porphyrin Handbook*; Kadish, K. M., Smith, K. M., Guilard, R., Eds.; Academic Press: San Diego, **2003**; Vol. 15, Ch. 99.
15. de la Torre, G.; Claessens, C. G.; Torres, T. *Eur. J. Org. Chem.* **2000**, 2821.
16. Fukuda, T.; Masuda, S.; Kobayashi, N. *J. Am. Chem. Soc.* **2007**, *129*, 5472.
17. Hammer, R. P.; Owens, C. V.; Hwang, S.-H.; Sayes, C. M.; Soper, S. A. *Bioconjugate Chem.* **2002**, *13*, 1244.
18. Torres, T. *J. Porphyrins Phthalocyanines* **2000**, *4*, 325.
19. (a) McKeown, N. B.; Chambrier, I.; Cook, M. J. *J. Chem. Soc., Perkin Trans. 1* **1990**, 1169. (b) Chambrier, I.; Cook, M. J.; Cracknell, S. J.; MacMurdo, J. *J. Mater. Chem.* **1993**, *3*, 841. (c) Chambrier, I.; Cook, M. J.; Russell, D. A. *Synthesis* **1995**, 1283.
20. (a) Clarkson, G. J.; McKeown, N. B.; Treacher, K. E. *J. Chem. Soc., Perkin Trans. 1* **1995**, 1817. (b) Treacher, K. E.; Clarkson, G. J.; McKeown, N. B. *Mol. Cryst., Liq. Cryst.* **1995**, *260*, 255. (c) Ali-Adib, Z.; Clarkson, G. J.; Cook, A.; McKeown, N. B. *Macromolecules* **1996**, *29*, 913.
21. Brewis, M.; Clarkson, G. J.; Holder, A. M.; McKeown, N. B. *Chem. Commun.* **1998**, 1979.
22. (a) Kobayashi, N.; Kondo, R.; Nakajima, S.-I.; Osa, T. *J. Am. Chem. Soc.* **1990**,

- 112, 9640. (b) Ando, M.; Mori, Y. *56th Annual Meeting, Chemical Society of Japan*, Tokyo, **1988**, Abstr. 3VA01. (c) Ando, M.; Mori, Y. (Tokyo Ink Mfg. Co., Ltd.), Jpn. Kokai Tokkyo Koho JP 02 09, 882 [90 09,882], **1990** [*Chem. Abstr.* **1990**, *113*, 25558c].
23. Geyer, M.; Plenzig, F.; Rauschnabel, J.; Hanack, M.; del Rey, B.; Sastre, A.; Torres, T. *Synthesis* **1996**, 1139.
24. Sharman, W. M.; van Lier, J. E. *J. Porphyrins Phthalocyanines* **2005**, *9*, 651.
25. (a) Weitemeyer, A.; Kliesch, H.; Wöhrle, D. *J. Org. Chem.* **1995**, *60*, 4900. (b) Sastre, A.; del Rey, B.; Torres, T. *J. Org. Chem.* **1996**, *61*, 8591. (c) Kobayashi, N.; Ishizaki, T.; Ishii, K.; Konami, H. *J. Am. Chem. Soc.* **1999**, *121*, 9096.
26. (a) Leznoff, C. C.; Hall, T. W. *Tetrahedron Lett.* **1982**, *23*, 3023. (b) Hall, T. W.; Greenberg, S.; McArthur, C. R.; Khouw, B.; Leznoff, C. C. *Nouv. J. Chim.* **1982**, *6*, 653. (c) Leznoff, C. C. *Can. J. Chem.* **2000**, *78*, 167. (d) Erdem, S. S.; Nesterova, I. V.; Soper, S. A.; Hammer, R. P. *J. Org. Chem.* **2008**, *73*, 5003.
27. Hirth, A.; Sobbi, A. K.; Wöhrle, D. *J. Porphyrins Phthalocyanines* **1997**, *1*, 275.
28. Hanack, M.; Stihler, P. *Eur. J. Org. Chem.* **2000**, 303.
29. Fukuda, T.; Kobayashi, N. *Chem. Lett.* **2002**, 866.
30. Idelson, E. M. U. S. Patent 4,061,654 **1977** [*Chem. Abstr.* **1977**, *88*, 171797m].
31. Young, J. G.; Onyebuagu, W. *J. Org. Chem.* **1990**, *55*, 2155.
32. Leznoff, C. C.; Greenberg, S.; Khouw, B.; Lever, A. B. P. *Can. J. Chem.* **1987**, *65*, 1705.
33. (a) Sakamoto, K.; Kato, T.; Ohno-Okumura, E.; Watanabe, M.; Cook, M. J. *Dyes Pigments* **2005**, *64*, 63.
34. Nolan, K. J. M.; Hu, M.; Leznoff, C. C. *Synlett.* **1997**, 593.
35. Oliver, S. W.; Smith, T. D. *J. Chem. Soc., Perkin Trans. 2* **1987**, 1579.
36. Kobayashi, N.; Kobayashi, Y.; Osa, T. *J. Am. Chem. Soc.* **1993**, *115*, 10994.
37. Daniell, M. D.; Hill, J. S. *Aust. NZ J. Surg.* **1991**, *61*, 340. (b) Ackroyd, R.; Kelty, C.; Brown, N.; Reed, M. *Photochem. Photobiol.* **2001**, *74*, 656.
38. Raab, O. *Zeitung Biol.* **1900**, *39*, 524.
39. von Tappeiner, H.; Jesionek, A. *Muench Med. Wochenschr.* **1903**, *47*, 2042.
40. For some recent reviews on PDT, see (a) MacDonald, I. J.; Dougherty, T. J. *J. Porphyrins Phthalocyanines* **2001**, *5*, 105. (b) Oleinick, N. L.; Morris, R. L.; Belichenko, I. *Photochem. Photobiol. Sci.* **2002**, *1*, 1. (c) Vrouenraets, M. B.; Visser, G. W. M.; Snow, G. B.; van Dongen, G. A. M. S. *Anticancer Res.* **2003**,

- 23, 505. (d) Dolmans, D. E. J. G. J.; Fukumura, D.; Jain, R. K. *Nature Rev. Cancer* **2003**, *3*, 380. (e) Brown, S. B.; Brown, E. A.; Walker, I. *Lancet Oncol.* **2004**, *5*, 497. (f) Detty, M. R.; Gibson, S. L.; Wagner, S. J. *J. Med. Chem.* **2004**, *47*, 3897. (g) Nyman, E. S.; Hynninen, P. H. *Photochem. Photobiol. B: Biol.* **2004**, *73*, 1.
41. Capella, M. A. M.; Capella, L. S. *J. Biomed. Sci.* **2003**, *10*, 361.
42. (a) Philips, D. *Prog. Reaction Kinetics* **1997**, *22*, 175. (b) Wöhrle, D.; Hirth, A.; Bogdahn-Rai, T.; Schnurpfeil, G.; Shopova, M. *Russ. Chem. Bull.* **1998**, *47*, 807.
43. (a) Sharman, W. M.; Allen, C. M.; van Lier, J. E. *Drug Discovery Today* **1999**, *4*, 507.
44. (a) Lukyanets, E. A. *J. Porphyrins Phthalocyanines* **1999**, *3*, 424. (b) Allen, C. M.; Shaman, W. M.; van Lier, J. E. *J. Porphyrins Phthalocyanines* **2001**, *5*, 161. (c) Tedesco, A. C.; Rotta, J. C. G.; Lunardi, C. N. *Curr. Org. Chem.* **2003**, *7*, 187.
45. He, J.; Larkin, H. E.; Li, Y. -S.; Rihter, B. D.; Zaidi, S. I. A.; Rodger, M. A. J.; Mukhtar, H.; Kenney, M. E.; Oleinick, N. L. *Photochem. Photobiol.* **1997**, *65*, 581.
46. Oleinick, N. L.; Antunez, A. R.; Clay, M. E.; Rihter, B. D.; Kenney, M. E. *Photochem. Photobiol.* **1993**, *57*, 242.
47. He, J.; Horng, M. -F.; Deahl, J. T.; Oleinick, N. L.; Evans, H. H. *Photochem. Photobiol.* **1998**, *67*, 720.
48. (a) Anderson, C.; Hrabovsky, S.; MicKinley, K.; Tubesing, K.; Tang, H. P.; Dunbar, R.; Mukhtar, H.; Elmets, C. A. *Photochem. Photobiol.* **1997**, *65*, 895. (b) Anderson, C. Y.; Freye, K.; Tubesing, K.; Li, Y. -S.; Kenney, M. E.; Mukhtar, H.; Elmets, C. A. *Photochem. Photobiol.* **1998**, *67*, 332.
49. Rywkin, S.; Ben-Hur, E.; Malik, Z.; Prince, A. M.; Li, Y.-S.; Kenney, M. E.; Oleinick, N. L. Horowitz, B. *Photochem. Photobiol.* **1994**, *60*, 165.
50. Colussi, V. C.; Feyes, D. K.; Mulvihill, J. W.; Li, Y.-S.; Kenney, M. E.; Elmets, C. A.; Oleinick, N. L.; Mukhtar, H. *Photochem. Photobiol.* **1999**, *69*, 236.
51. Soncin, M.; Buseti, A.; Biolo, R.; Jori, G.; Kwag, G.; Li, Y.-S.; Kenney, M. E.; Rodgers, M. A. J. *J. Photochem. Photobiol. B: Biol.* **1998**, *42*, 202.
52. Brasseur, N.; Ouellet, R.; La Madeleine, C.; van Lier, J. E. *Br. J. Cancer* **1999**, *80*, 1533.
53. Paquette, B.; Ali, H.; Langlois, R.; van Lier, J. E. *Photochem. Photobiol.* **1988**, *47*, 215.

54. Peng, Q.; Farrants, G. W.; Madslie, K.; Bommer, J. C.; Moan, J.; Danielsen, H. E.; Nesland, J. M. *Int. J. Cancer* **1991**, *49*, 290.
55. Peng, Q.; Moan, J.; Nesland, J. M. *Ultrastruct. Pathol.* **1996**, *20*, 106.
56. Korbelik, M. *J. Photochem. Photobiol. B.* **1993**, *20*, 173.
57. (a) Peng, Q.; Moan, J.; Nesland, J. M.; Rimmington, C. *Int. J. Cancer* **1990**, *46*, 719. (b) Chan, W.-S.; Brasseur, N.; La Madeleine, C.; van Lier, J. E. *Anticancer Res.* **1996**, *16*, 1887. (c) Chan, W.-S.; Brasseur, N.; La Madeleine, C.; Ouellet, R.; van Lier, J. E. *Eur. J. Cancer* **1997**, *33*, 1855. (d) Margaron, P.; Madarnas, P.; Ouellet, R.; van Lier, J. E. *Anticancer Res.* **1996**, *16*, 613.
58. Brasseur, N.; Ali, H.; Langlois, R.; van Lier, J. E. *Photochem. Photobiol.* **1987**, *46*, 739.
59. (a) Reddi, E.; LoCastro, G.; Biolo, R.; Jori, G. *Br. J. Cancer* **1987**, *56*, 597. (b) Reddi, E.; Zhou, C.; Biolo, R.; Menegaldo, E.; Jori, G. *Br. J. Cancer* **1990**, *61*, 407. (c) Larroque, C.; Pelegrin, A.; van Lier, J. E. *Br. J. Cancer* **1996**, *74*, 1886.
60. Ali, H.; Langlois, R.; Wagner, J. R.; Brasseur, N.; Paquette, B.; van Lier, J. E. *Photochem. Photobiol.* **1988**, *47*, 713.
61. Weber, J. H.; Busch, D. H. *Inorg. Chem.* **1965**, *4*, 469.
62. Li, Z.; van Lier, J. E.; Leznoff, C. C. *Can. J. Chem.* **1999**, *77*, 138.
63. Kudrevich, S.; Ali, H.; van Lier, J. E. *J. Chem. Soc., Perkin Trans. 1* **1994**, *19*, 2767.
64. Kudrevich, S. V.; Gilbert, S.; van Lier, J. E. *J. Org. Chem.* **1996**, *61*, 5706.
65. Brasseur, N.; Ali, H.; Autenrieth, D.; Langlois, R.; van Lier, J. E. *Photochem. Photobiol.* **1985**, *42*, 515.
66. Brasseur, N.; Ali, H.; Langlois, R.; van Lier, J. E. *Photochem. Photobiol.* **1988**, *47*, 705.
67. Brasseur, N.; Ali, H.; Langlois, R.; Wagner, J. R.; van Lier, J. E. *Photochem. Photobiol.* **1987**, *45*, 581.
68. Oda, K.; Ogura, S.; Okura, I. *J. Photochem. Photobiol. B: Biol.* **2000**, *59*, 20.
69. Sharman, W. M.; van Lier, J. E. *Bioconjugate Chem.* **2005**, *16*, 1166.
70. Valduga, G.; Reddi, E.; Jori, G. *J. Inorg. Biochem.* **1987**, *29*, 59.
71. For example, see: (a) Krasnykh, V.; Dmitriev, I.; Navarro, J.-G.; Belousova, N.; Kashentseva, E.; Xiang, J.; Douglas, J. T.; Curiel, D. T. *Cancer Res.* **2000**, *60*, 6784. (b) Wilderman, M. J.; Sun, J.; Jassar, A. S.; Kapoor, V.; Khan, M.; Vachani, A.; Suzuki, E.; Kinniry, P. A.; Serman, D. H.; Kaiser, L. R.; Albelda, S. M.

- Cancer Res.* **2005**, *65*, 8379. (c) Nakayama, K.; Pergolizzi, R. G.; Crystal, R. G. *Cancer Res.* **2005**, *65*, 254. (d) Guan, M.; Rodriguez-Madoz, J. R.; Alzuguren, P.; Gomar, C.; Kramer, M. G.; Kochanek, S.; Prieto, J.; Smerdou, C.; Qian, C. *Cancer Res.* **2006**, *66*, 1620.
72. For review, see (a) Wallberg-Henriksson, H.; Zierath, J. R. *Mol. Membr. Biol.* **2001**, *18*, 205. (b) Macheda, M.; Rogers, S.; Best, J. D. *J. Cell. Physiol.* **2005**, *202*, 654.
73. For example, see (a) Yamamoto, T.; Seino, Y.; Fukumoto, H.; Koh, G.; Yano, H.; Inagaki, N.; Yamada, Y.; Inoue, K.; Manabe, T.; Imura, H. *Biochem. Biophys. Res. Commun.* **1990**, *170*, 223. (b) Brown, R. S.; Wahl, R. L. *Cancer* **1993**, *72*, 2979. (c) Haber, R. S.; Rathan, A.; Weiser, K. R.; Pritsker, A.; Itzkowitz, S. H.; Bodian, C.; Slater, G.; Weiss, A.; Burstein, D. E. *Cancer* **1998**, *83*, 34. (d) Wang, B. Y.; Kalir, T.; Sabo, E.; Sherman, D. E.; Cohen, C.; Burstein, D. E. *Cancer* **2000**, *88*, 2774.
74. Carré, V.; Gaud, O.; Sylvain, I.; Bow-don, O.; Spiro, M.; Blais, J.; Granet, R.; Krausz, P.; Guilloton, M. *J. Photochem. Photobiol. B* **1999**, *48*, 57.
75. Mikata, Y.; Onchi, Y.; Shibata, M.; Kakuchi, T.; Ono, H.; Ogura, S.-i.; Okura, I.; Yanoa, S. *Bioorg. Med. Chem. Lett.* **1998**, *8*, 3543.
76. Mikata, Y.; Onchi, Y.; Tabata, K.; Ogura, S.-i.; Okura, I.; Ono, H.; Yanoa, S. *Tetrahedron Lett.* **1998**, *39*, 4505.
77. He, Y.-Y.; An, J.-Y.; Jiang, L. *J. Biochim. Biophys. Acta* **1999**, *1472*, 232.
78. Zheng, G.; Graham, A.; Shibata, M.; Missert, J. R.; Oseroff, A. R.; Dougherty, T. J.; Pandey, R. K. *J. Org. Chem.* **2001**, *66*, 8709.
79. Zhang, M.; Zhang, Z.; Blessington, D.; Li, H.; Busch, T. M.; Madrak, V.; Miles, J.; Chance, B.; Glickson, J. D.; Zheng, G.; *Bioconjugate Chem.* **2003**, *14*, 709.
80. Stasio, B. D.; Frochot, C.; Dumas, D.; Even, P.; Zwier, J.; Müller, A.; Didelon, J.; Guillemin, F.; Viriot, M.-L.; Barberi-Heyob, M. *Eur. J. Med. Chem.* **2005**, *40*, 1111.
81. Terasaki, M.; Song, J.; Wong, J. R.; Weiss, M. J.; Chen, L. B. *Cell* **1984**, *38*, 101.
82. Synytsyaa, A.; Krala, V.; Synytsyab, A.; Volkaa, K.; Sessler, J. L. *Biochimica et Biophysica Acta* **2003**, *1620*, 85.
83. Synytsya, A.; Král, V.; Blechová, M.; Volka, K. *J. Photochem. Photobiol. B* **2004**, *74*, 73.
84. Hirohara, S.; Obata, M.; Saito, A.; Ogata, S.-i.; Ohtsuki, C.; Higashida, S.; Ogura,

- S.-i.; Okura, I.; Sugai, Y.; Mikata, Y.; Tanihara, M.; Yano, S.; *Photochem. Photobiol.* **2004**, *80*, 301.
85. Ahmed, S.; Davoust, E.; Savoie, H.; Boa, A. N.; Boyle, R. W. *Tetrahedron Lett.* **2004**, *45*, 6045.
86. (a) Maillard, P.; Guerquin-Kern, J.-L.; Momenteau, M. *J. Am. Chem. Soc.* **1989**, *111*, 9125. (b) Alvarez, X.; Calvete, M. J. F.; Hanack, M.; Ziegler, T. *Tetrahedron Lett.* **2006**, *47*, 3283.
87. Lee, P. P. S.; Lo, P.-C.; Chan, E. Y. M.; Fong, W.-P.; Ko, W.-H.; Ng, D. K. P. *Tetrahedron Lett.* **2005**, *46*, 1551.
88. Lo, P.-C.; Chan, C. M. H.; Liu, J.-Y.; Fong, W.-P.; Ng, D. K. P. *J. Med. Chem.* **2007**, *50*, 2100.
89. Ribeiro, A. O.; Tomé, J. P. C.; Neves, M. G. P. M. S.; Tomé, A. C.; Cavaleiro, J. A. S.; Iamamoto, Y.; Torres, T. *Tetrahedron Lett.* **2006**, *47*, 9177.
90. (a) Loudet, A.; Burgess, K. *Chem. Rev.* **2007**, *107*, 4891. (b) Ulrich, G.; Ziesel, R.; Harriman, A. *Angew. Chem. Int. Ed.* **2008**, *47*, 1184.
91. Treibs, A.; Kreuzer, F.-H. *Justus Liebigs Ann. Chem.* **1968**, *718*, 208.
92. (a) Falk, H.; Hofer, O.; Lehner, H. *Monatsh. Chem.* **1974**, *105*, 169. (b) VosdeWael, E.; Pardoën, J. A.; Vankoevinge, J. A.; Lugtenburg, J. *Recl. Trav. Chim. Pays-Bas* **1977**, *96*, 306. (c) Worries, H. J.; Koek, J. H.; Lodder, G.; Lugtenburg, J.; Fokkens, R.; Driessen, O.; Mohn, G. R. *Recl. Trav. Chim. Pays-Bas* **1985**, *104*, 288.
93. (a) Haughland, R. P.; Kang, H. C. *US Patent US4774339* **1988**. (b) Monsma, F. J.; Barton, A. C.; Kang, H. C.; Brassard, D. L.; Haughland, R. P.; Sibley, D. R. *J. Neurochem.* **1989**, *52*, 1641.
94. Registered trademark of Molecular Probes; <http://probes.invitrogen.com>.
95. For example, see: (a) Boldyrev, I. A.; Zhai, X.-H.; Momsen, M. M.; Brockman, H. L.; Brown, R. E.; Molotkovsky, J. G. *J. Lipid Res.* **2007**, *48*, 1518. (b) Perronet, K.; Bouyer, P.; Westbrook, N.; Soler, N.; Fourmy, D.; Yoshizawa, S. *J. Lumin.* **2007**, *127*, 264. (c) Arnold, L. A.; Ranaivo, P.; Guy, R. K. *Bioorg. Med. Chem. Lett.* **2008**, *18*, 5867. (d) Marks, D. L.; Bittman, R.; Pagano, R. E. *Histochem. Cell Biol.* **2008**, *130*, 819. (e) Ikawa, Y.; Moriyama, S.; Furuta, H. *Anal. Biochem.* **2008**, *378*, 166.
96. For example, see: (a) Peng, X.-J.; Du, J.-J.; Fan, J.-l.; Wang, J.-Y.; Wu, Y.-K.; Zhao, J.-Z.; Sun, S.-G.; Xu, T. *J. Am. Chem. Soc.* **2007**, *129*, 1500. (b) Yuan, M.-

- J.; Li, Y.-L.; Li, J.-B.; Li, C.-H.; Liu, X.-F.; Lv, J.; Xu, J.-L.; Liu, H.-B.; Wang, S.; Zhu, D.-B. *Org. Lett.* **2007**, *9*, 2313. (c) Hudnall, T. W.; Gabbai, F. P. *Chem. Commun.* **2008**, 4596. (d) Ekmekci, Z.; Yilmaz, M. D.; Akkaya, E. U. *Org. Lett.* **2008**, *10*, 461. (e) Cheng, T.-Y.; Xu, Y.-F.; Zhang, S.-Y.; Zhu, W.-P.; Qian, X.-H.; Duan, L.-P. *J. Am. Chem. Soc.* **2008**, *130*, 16160. (f) Atilgan, S.; Ozdemir, T.; Akkaya, E. U. *Org. Lett.* **2008**, *10*, 4065.
97. Atilgan, S.; Ekmekci, Z.; Dogan, A. L.; Guc, D.; Akkaya, E. U. *Chem. Commun.* **2006**, 4398.
98. (a) Wan, C.-W.; Burghart, A.; Chen, J.; Bergström, F.; Johansson, L. B.-A.; Wolford, M. F.; Kim, T. G.; Topp, M. R.; Hochstrasser, R. M.; Burgess, K. *Chem. Eur. J.* **2003**, *9*, 4430. (b) Ziessel, R.; Goze, C.; Ulrich, G.; Césarío, M.; Retailleau, P.; Harriman, A.; Rostron, J. P. *Chem. Eur. J.* **2005**, *11*, 7366. (c) Harriman, A.; Izzet, G.; Ziessel, R. *J. Am. Chem. Soc.* **2006**, *128*, 10868.
99. (a) Wagner, R. W.; Lindsey, J. S. *J. Am. Chem. Soc.* **1994**, *116*, 9759. (b) Wagner, R. W.; Lindsey, J. S.; Seth, J.; Palaniappan, V.; Bocian, D. F. *J. Am. Chem. Soc.* **1996**, *118*, 3996. (c) Li, F.; Yang, S. I.; Ciringh, Y.; Seth, J.; Martin, C. H.; Singh, D. L.; Kim, D.; Birge, R. R.; Bocian, D. F.; Holten, D.; Lindsey, J. S. *J. Am. Chem. Soc.* **1998**, *120*, 10001. (d) Kumaresan, D.; Agarwal, N.; Gupta, I.; Ravikanth, M. *Tetrahedron* **2002**, *58*, 5347. (e) Kumaresan, D.; Gupta, I.; Ravikanth, M. *Tetrahedron Lett.* **2001**, *42*, 8547. (f) Ravikanth, M.; Agarwal, N.; Kumaresan, D. *Chem. Lett.* **2000**, 836. (g) Koepf, M.; Trabolsi, A.; Elhabiri, M.; Wytko, J. A.; Paul, D.; Albrecht-Gary, A. M.; Weiss, J. *Org. Lett.* **2005**, *7*, 1279. (h) Shiragami, T.; Tanaka, K.; Andou, Y.; Tsunami, S.-i.; Matsumoto, J.; Luo, H.; Araki, Y.; Ito, O.; Inoue, H.; Yasuda, M. *J. Photochem. Photobiol. A* **2005**, *170*, 287. (i) Yilmaz, M. D.; Bozdemir, O. A.; Akkaya, E. U. *Org. Lett.* **2006**, *8*, 2871. (j) D'Souza, F.; Smith, P. M.; Zandler, M. E.; McCarty, A. L.; Ito, M.; Araki, Y.; Ito, O. *J. Am. Chem. Soc.* **2004**, *126*, 7898.
100. (a) Azov, V. A.; Schlegel, A.; Diederich, F. *Angew. Chem. Int. Ed.* **2005**, *44*, 4635. (b) Harriman, A.; Mallon, L. J.; Goeb, S.; Ziessel, R. *Phys. Chem. Chem. Phys.* **2007**, *9*, 5199. (c) Zhang, X.-L.; Xiao, Y.; Qian, X.-H. *Org. Lett.* **2008**, *10*, 29.
101. Hu, X.; Damjanovic, A.; Ritz, T.; Schulten, K. *Proc. Natl. Acad. Sci. U.S.A.* **1998**, *95*, 5935.

Chapter 2

Synthesis, Characterization, and in vitro Photodynamic Activities of Novel Amphiphilic Zinc(II) Phthalocyanines Bearing Oxyethylene-Rich Substituents

2.1 Introduction

Photodynamic therapy (PDT) has emerged as a promising modality for the treatment of malignant tumors and wet age-related macular degeneration.¹ It is a binary therapy that involves the combination of visible light and a photosensitizer. Each component is harmless by itself, but in combination with molecular oxygen, they result in the generation of reactive oxygen species (ROS) causing oxidative cellular and tissue damage. This treatment has several potential advantages including its minimally invasive nature, tolerance of repeated doses, and high specificity that can be achieved through precise application of the light with modern fiber-optic systems and various types of endoscopy.^{1c} Currently, only a few porphyrin derivatives including porfimer sodium, temoporfin, and verteporfin are clinically approved for systemic administration. These compounds, though giving a positive response in a high percentage of patients, still have various deficiencies that demand a further development of better candidates.² Owing to the desirable electron absorption and photophysical properties, phthalocyanines are one of the most promising classes of candidates for this application.³ Over the last few years, our group has been interested

in rational modification of this class of functional dyes with the goal of enhancing their PDT efficiency. Several new series of silicon(IV) and zinc(II) phthalocyanines have been synthesized and evaluated for their photophysical and biological properties.⁴ As the amphiphilicity of photosensitizers is believed to have a beneficial effect on their photodynamic activity,⁵ amphiphilic phthalocyanines have been my targets. In this Chapter, I report the synthesis, photophysical properties, and in vitro photodynamic activity of three novel zinc(II) phthalocyanines bearing one or two 3,4,5-tris(3,6,9-trioxadecoxy)benzoxy substituent(s). Having three or six triethylene glycol methyl ether chains, these macrocycles are amphiphilic in nature, exhibiting a high in vitro photocytotoxicity.

2.2 Results and Discussion

2.2.1 Molecular Design and Chemical Synthesis

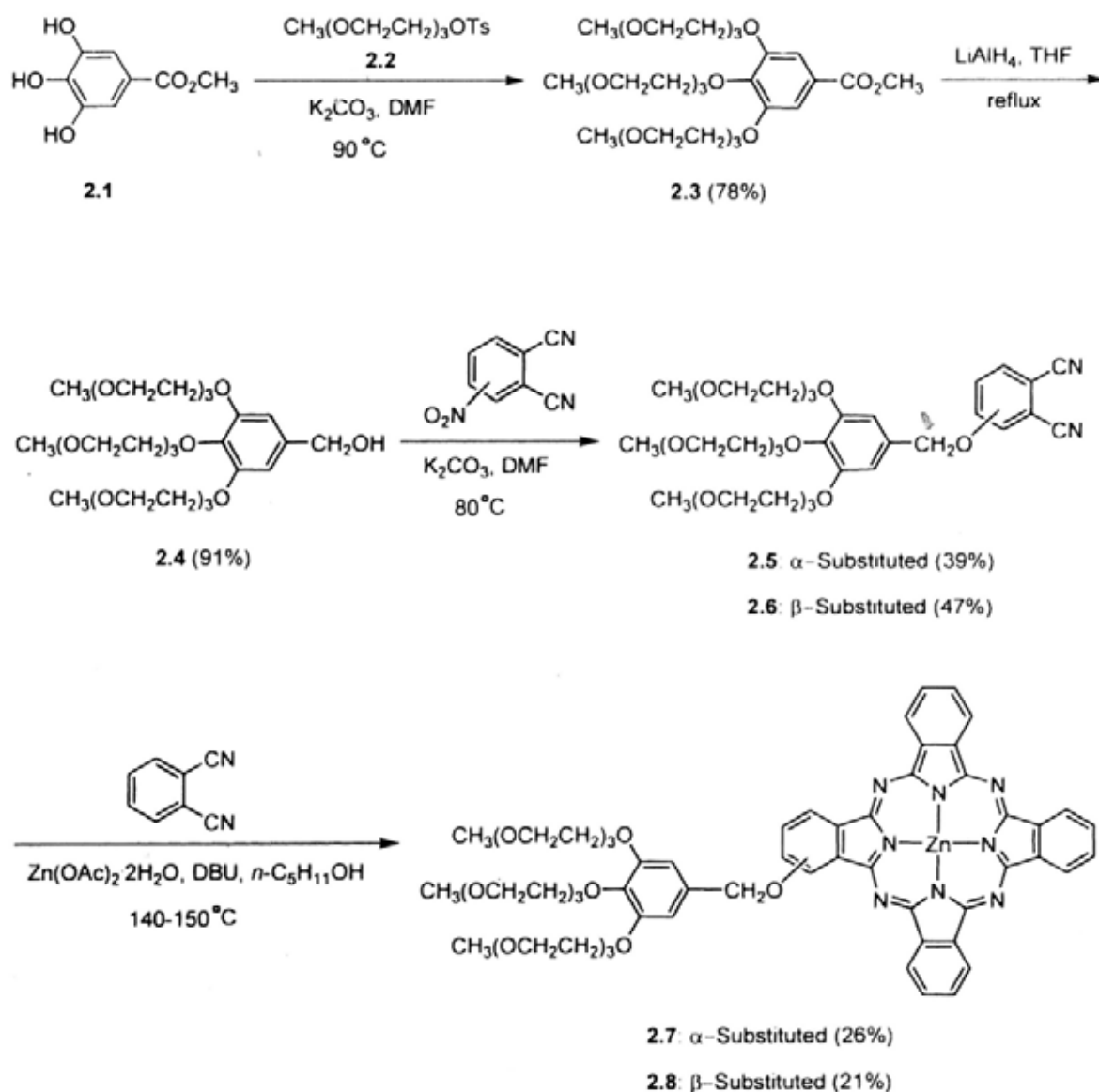
Zinc(II) phthalocyanines are good candidates for PDT application. In addition to their relatively high stability, the closed-shell zinc(II) center imparts desirable photophysical characteristics to the macrocycles.⁶ Introduction of substituents at the peripheral positions can also tailor the properties of the macrocycles such as their solubility in biological media, aggregation behavior, and targeting properties. As a result, zinc(II) phthalocyanines have received considerable attention as efficient photosensitizers.³ I describe herein three novel zinc(II) phthalocyanines (compounds **2.7**, **2.8**, and **2.11**) which contain the bulky and hydrophilic 3,4,5-tris(3,6,9-trioxadecoxy)benzoxy moiety. Having one or two of these

substituents, the π - π stacking tendency is reduced and the macrocycles become amphiphilic in nature. These properties should be advantageous for singlet oxygen generation and cellular uptake, by which the photodynamic activity can be enhanced. The relatively rare 1,4-disubstituted phthalocyanine **2.11** also has a longer Q-band maximum compared with the α - and β -monosubstituted counterparts, which is also an advantage that can increase the light penetration depth.⁷

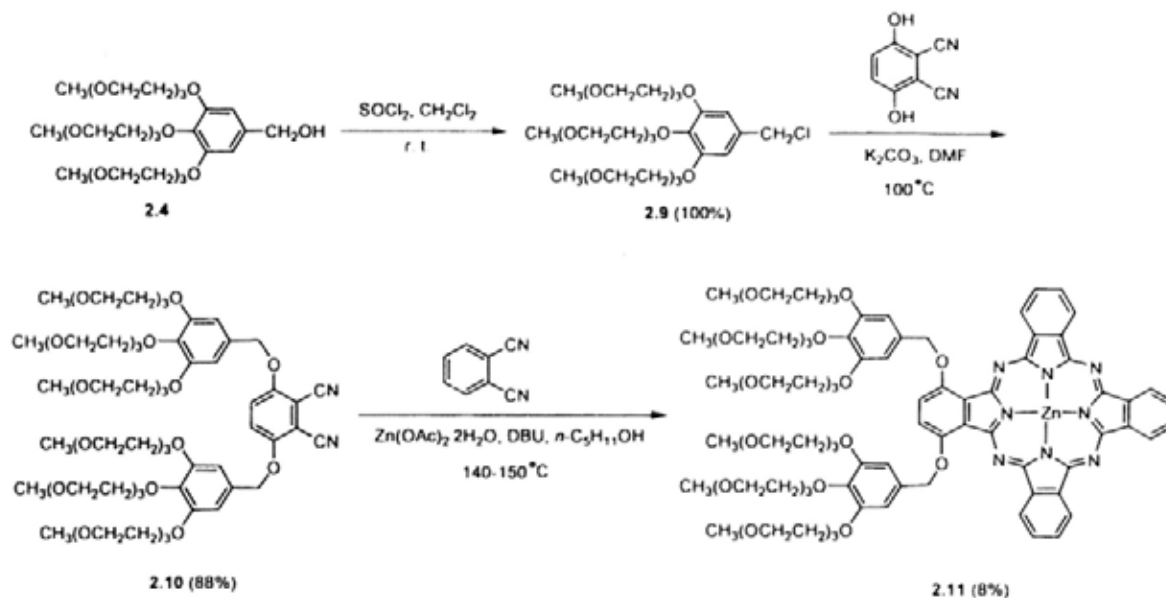
Scheme 2.1 shows the synthetic route used to prepare the monosubstituted phthalocyanines **2.7** and **2.8**. Treatment of methyl 3,4,5-trihydroxybenzoate (**2.1**) with triethylene glycol methyl ether tosylate (**2.2**) and K_2CO_3 led to trisubstitution giving **2.3**, which was then reduced with $LiAlH_4$ to afford benzyl alcohol **2.4**. This compound was then treated with 3- or 4-nitrophthalonitrile in the presence of K_2CO_3 in *N,N*-dimethylformamide (DMF) to give the substituted phthalonitrile **2.5** or **2.6**, respectively. These compounds then underwent a mixed cyclization with an excess of unsubstituted phthalonitrile (10 equiv.) in the presence of $Zn(OAc)_2 \cdot 2H_2O$ and 1,8-diazabicyclo[5.4.0]undec-7-ene (DBU) in *n*-pentanol to afford the corresponding “3+1” products **2.7** and **2.8**. These reactions also produced the unsubstituted zinc phthalocyanine (ZnPc) as a major side-product, which could be separated readily by filtration and chromatography as a result of its lower solubility and slower mobility in a silica gel column. During the chromatographic purification, a trace amount of some other blue products was also separated, but no attempt was made to characterize these minor side-products.

Similarly, treatment of 2,3-dicyanohydroquinone with benzyl chloride **2.9**,

prepared by chlorination of **2.4** with SOCl_2 , and K_2CO_3 afforded dinitrile **2.10**, which was then cyclized with the unsubstituted phthalonitrile in the presence of $\text{Zn}(\text{OAc})_2 \cdot 2\text{H}_2\text{O}$ and DBU to give **2.11** in 8% yield (Scheme 2.2). All of these zinc(II) phthalocyanines were soluble in common organic solvents and possessed high stability, which facilitated the purification by silica gel column chromatography, size exclusion chromatography, followed by recrystallization.



Scheme 2.1. Synthesis of phthalocyanines **2.7** and **2.8**.



Scheme 2.2. Synthesis of phthalocyanine 2.11.

2.2.2 Spectroscopic Characterization and Photophysical Properties

All the new compounds were fully characterized with various spectroscopic methods and the data are given in the Experimental Section. The NMR signals for the phthalocyanine ring protons of **2.7**, **2.8**, and **2.11** are very distinct in CDCl_3 (with a trace amount of pyridine- d_5 for the former two complexes to reduce their aggregation), which provide a useful means for characterization. As shown in Figure 2.1, the ^1H NMR spectrum of α -substituted phthalocyanine **2.7** shows a multiplet at δ 9.41-9.46 (5 H) and two doublets at δ 9.16 (1 H) and 9.13 (1 H) for the 7 phthalocyanine α protons. The 8 β protons resonate as a multiple at δ 8.07-8.15 (7 H) and a doublet at δ 7.69 (1 H). For the β -analogue **2.8**, a multiplet at δ 9.20-9.35 (6 H), a doublet at δ 9.05 (1 H), and a singlet at δ 8.66 (1 H) are seen for the 8 phthalocyanine α protons, while the signals for the 7 β protons appear as a multiplet at δ 8.06-8.12 (6 H) and a doublet at δ 7.62 (1 H). Phthalocyanine **2.11** has a C_{2v} symmetry. The doublet at δ

9.20 can be assigned to the two phthalocyanine α protons close to the benzoxy groups, while the multiplet at δ 9.43-9.47 is due to the remaining four α protons. The singlet at δ 7.68 can be readily assigned to the two β protons adjacent to the benzoxy groups, while the multiplet at δ 8.03-8.15 is attributed to the remaining six β protons.

The ^{13}C NMR data of these compounds were also in accord with the structures though some of the phthalocyanine ring carbon signals (for **2.7** and **2.8**) and the chain CH_2 signals were overlapped. For compound **2.11**, a total of 20 signals were observed in the aromatic region (δ 107.0-153.6) for the 16 phthalocyanine and 4 benzene ring carbons, which is consistent with the C_{2v} symmetry.

The ESI mass spectra of these phthalocyanines were also recorded. The molecular ion $[\text{M} + \text{Na}]^+$ isotopic cluster could be detected in all the cases. The isotopic distribution was in good agreement with the corresponding simulated pattern. The identity of these species was also confirmed by accurate mass measurements.

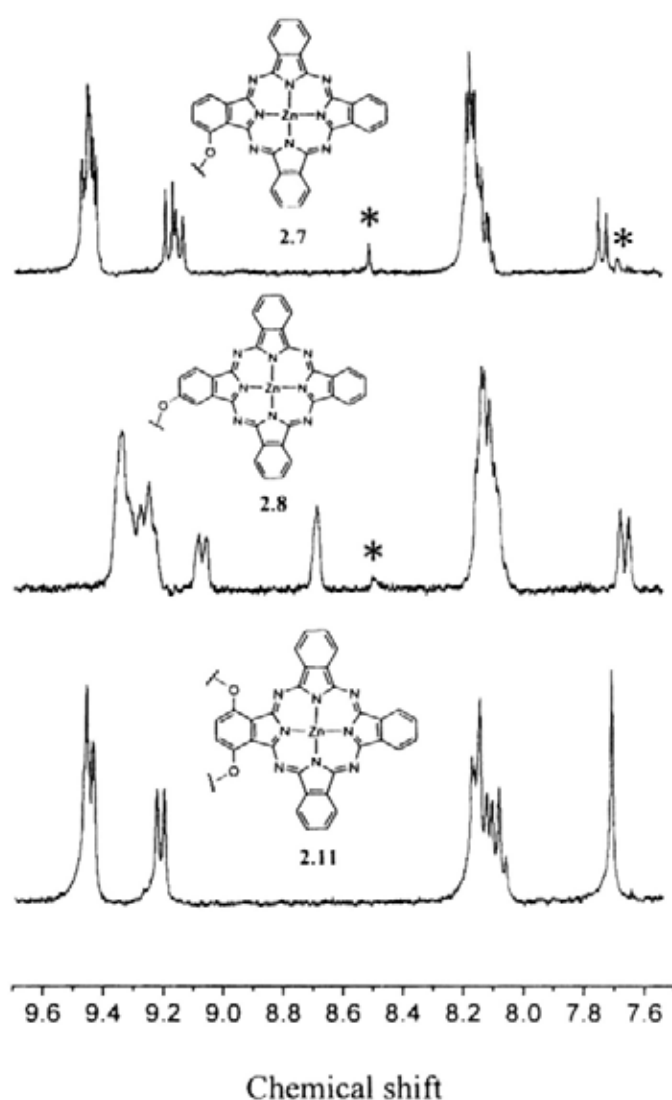


Figure 2.1. The aromatic region of the ^1H NMR spectra of **2.7**, **2.8**, and **2.11** in CDCl_3 ; * indicates the trace amount of pyridine- d_5 added for the former two complexes.

The electronic absorption and basic photophysical data of phthalocyanines **2.7**, **2.8**, and **2.11** were measured in DMF and are summarized in Table 2.1. All the three compounds gave very similar UV-Vis spectra, which are typical for nonaggregated phthalocyanines. The spectrum of compound **2.8**, for example, showed a B-band at 344 nm, a vibronic band at 606 nm, and an intense and sharp Q-band at 672 nm, which strictly followed the Lambert Beer's law (Figure 2.2). Upon excitation at 610

nm, the compound emitted at 677 nm with a fluorescence quantum yield of 0.19. Substitution at the α position (compound **2.7**) slightly shifted the Q-band and fluorescence emission to the red by 4-5 nm. Introduction of an additional α -substituent (compound **2.11**) further shifted the Q-band to 690 nm and the fluorescence emission to 696 nm.

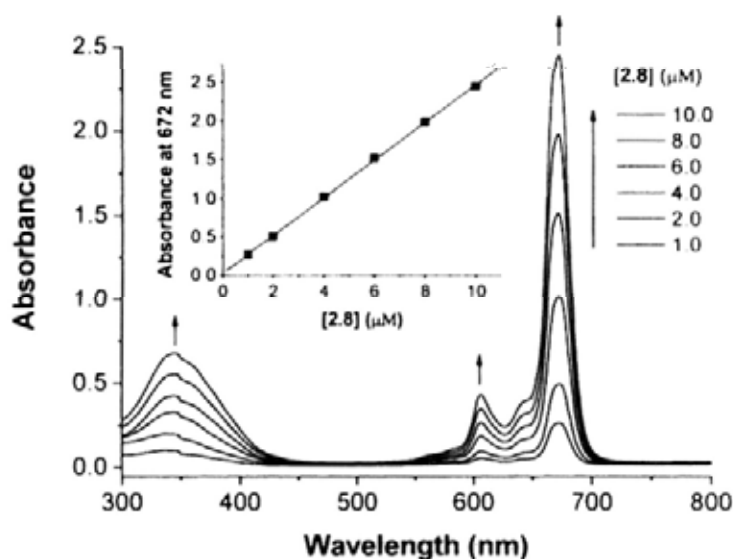


Figure 2.2. Electronic absorption spectra of **2.8** at different concentrations in DMF. The inset plots the Q-band absorbance versus the concentration of **2.8**.

Table 2.1. Electronic absorption and photophysical data for **2.7**, **2.8**, and **2.11** in DMF.

| Compound | λ_{\max} (nm) (log ϵ) | λ_{em} (nm) ^a | Φ_{F} ^b | Φ_{Δ} ^c |
|-------------|---|---|--------------------------------|------------------------------|
| 2.7 | 334 (4.69), 611 (4.58), 677 (5.40) | 681 | 0.20 | 0.60 |
| 2.8 | 344 (4.79), 606 (4.62), 672 (5.39) | 677 | 0.19 | 0.62 |
| 2.11 | 337 (4.73), 621 (4.55), 690 (5.31) | 696 | 0.14 | 0.84 |

^a Excited at 610 nm. ^b Using unsubstituted zinc(II) phthalocyanine (ZnPc) in DMF as the reference ($\Phi_{\text{F}} = 0.28$). ^c Using ZnPc as the reference ($\Phi_{\Delta} = 0.56$ in DMF).

The singlet oxygen quantum yields (Φ_{Δ}) of these compounds were also determined using 1,3-diphenylisobenzofuran (DPBF) as the scavenger. The concentration of the quencher was monitored spectroscopically at 411 nm along with time, from which the values of Φ_{Δ} could be determined by the method described previously.⁸ These data are also summarized in Table 2.1. Figure 2.3 compares the rates of decay of DPBF using these compounds and ZnPc as the photosensitizers. It can be seen that all these phthalocyanines are efficient singlet oxygen generators, particularly the 1,4-disubstituted analogue **2.11**, of which the value of Φ_{Δ} (0.84) is significantly higher than that of ZnPc (0.56), which was used as the reference.

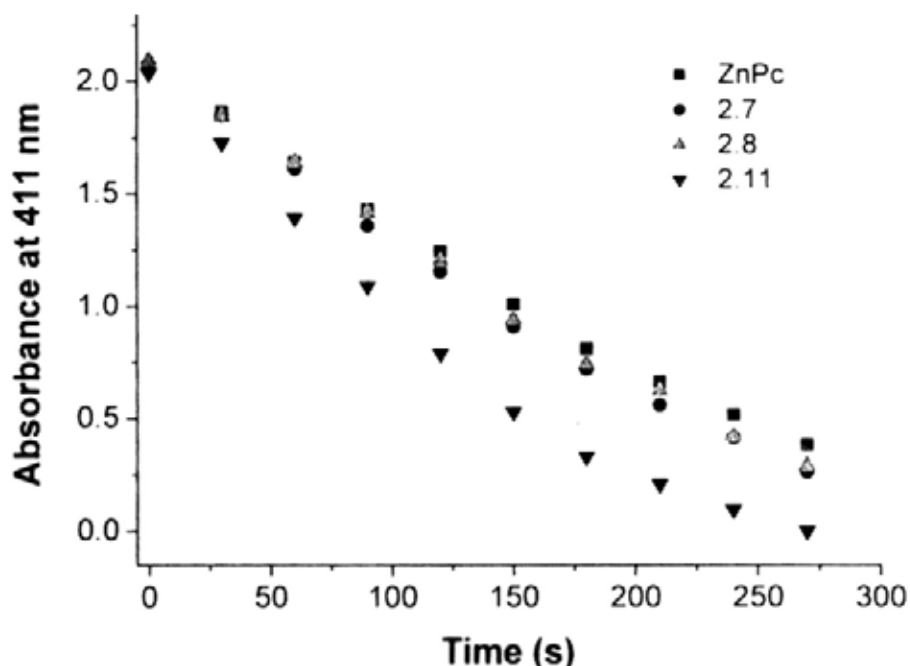


Figure 2.3. Comparison of the rates of decay of DPBF in DMF as monitored spectroscopically at 411 nm, using **2.7**, **2.8**, and **2.11** as the photosensitizers and ZnPc as the reference.

2.2.3 In vitro Photodynamic Activities

The in vitro photodynamic activity of photosensitizers **2.7**, **2.8**, and **2.11** in Cremophor EL emulsions was investigated against two different cell lines, namely HT29 human colorectal carcinoma and HepG2 human hepatocarcinoma cells. As shown in Figure 2.4, the three compounds are essentially noncytotoxic in the absence of light, but exhibit a very high photocytotoxicity. The corresponding IC_{50} values are summarized in Table 2.2. It can be seen that all these compounds are highly potent and the effects on HT29 are greater than those on HepG2. Phthalocyanine **2.7** is particularly potent with the IC_{50} values down to $0.02 \mu\text{M}$. About $1 \mu\text{M}$ of the dye is sufficient to kill 90% of the cells.

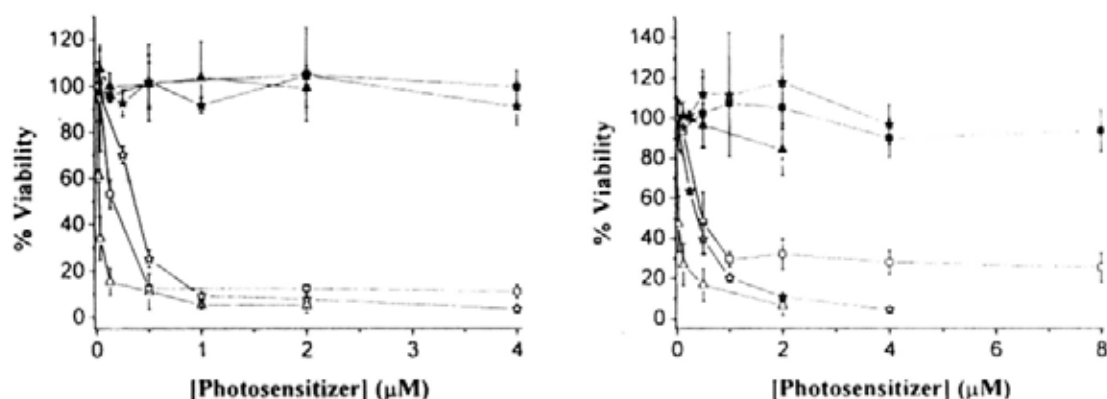


Figure 2.4. Effects of **2.7** (triangles), **2.8** (stars), and **2.11** (squares) on HT29 (left) and HepG2 (right) cells in the absence (closed symbols) and presence (open symbols) of light ($\lambda > 610 \text{ nm}$, 40 mW cm^{-2} , 48 J cm^{-2}). Data are expressed as mean values \pm S.E.M. of three independent experiments, each performed in quadruplicate.

Table 2.2. Comparison of the IC₅₀ values^a of phthalocyanines **2.7**, **2.8**, and **2.11** against HT29 and HepG2 cells.

| Compound | IC ₅₀ (μM) | |
|-------------|-----------------------|----------------|
| | For HT29 (μM) | For HepG2 (μM) |
| 2.7 | 0.02 | 0.03 |
| 2.8 | 0.36 | 0.39 |
| 2.11 | 0.15 | 0.49 |

^a Defined as the dye concentration required to kill 50% of the cells.

It is worth noting that although phthalocyanine **2.7** exhibits a relatively lower singlet oxygen quantum yield than the other two photosensitizers in DMF (Table 2.1), its photocytotoxicity is the highest among the three photosensitizers (Table 2.2). To account for the results, the absorption spectra of these compounds in the culture medium were recorded. As shown in Figure 2.5, the Q-band for compound **2.7** in the Dulbecco's modified Eagle's medium (DMEM) (for HT29) remains very sharp and intense, while those for **2.8** and **2.11** are weaker and broadened. Very similar results were obtained in the RPMI medium (for HepG2) (Figure 2.6). This is a strong indication that compound **2.7** is significantly less aggregated in these culture media, which should lead to a higher photosensitizing efficiency.

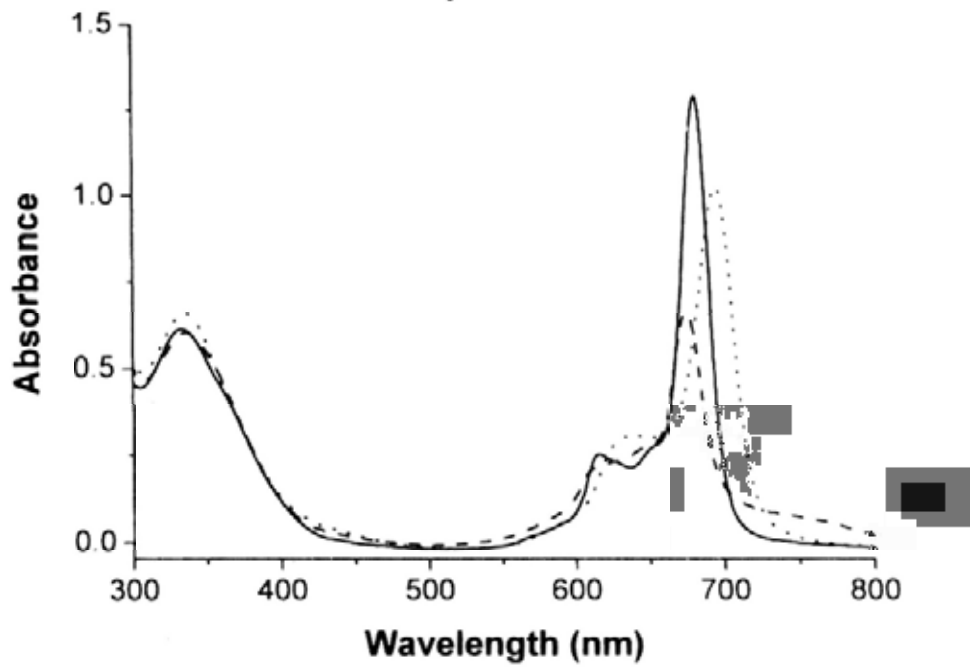


Figure 2.5. Electronic absorption spectra of 2.7 (—), 2.8 (---), and 2.11 (···), formulated with Cremophor EL, in the DMEM culture medium (all at 8 μ M).

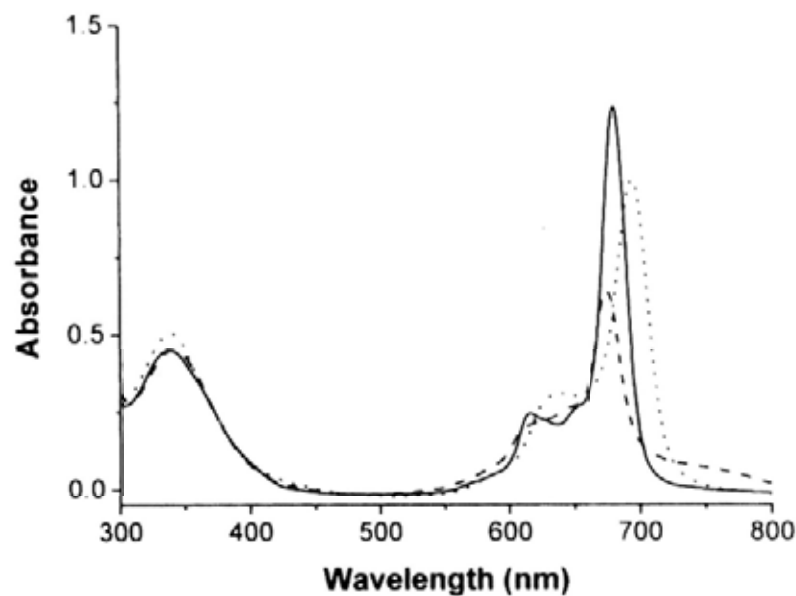


Figure 2.6. Electronic absorption spectra of 2.7 (—), 2.8 (---), and 2.11 (···), formulated with Cremophor EL, in the RPMI culture medium (all at 8 μ M).

To further explain the photocytotoxicity results, fluorescence microscopic studies were also carried out to shed light on the cellular uptake of photosensitizers 2.7, 2.8, and 2.11. After incubation with these compounds (formulated with Cremophor EL) for 2 hours and upon excitation at 630 nm, the HT29 cells showed intracellular fluorescence throughout the cytoplasm as shown in Figure 2.7, indicating that there was a substantial uptake of the dyes. The qualitative fluorescence intensity follows the order 2.7 > 2.8 > 2.11. Hence, the highest photocytotoxicity of 2.7 may be attributed to its lowest aggregation tendency in the biological media and/or highest cellular uptake.

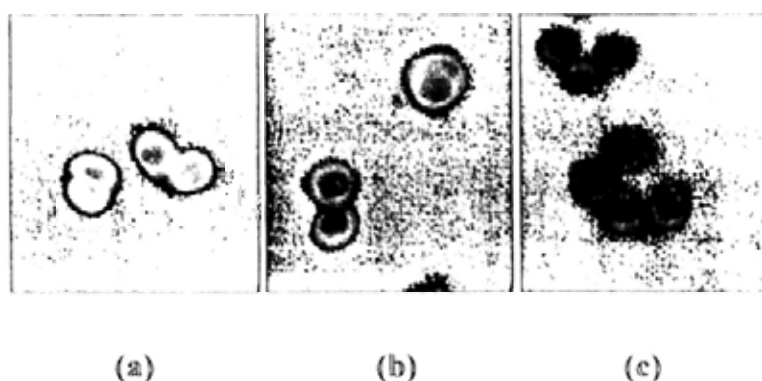


Figure 2.7. Fluorescence microscopic images of HT29 tumor cells being incubated with (a) 2.7, (b) 2.8, and (c) 2.11 at a concentration of 8 μM for 2 h.

2.3 Conclusion

In conclusion, I have prepared and characterized three novel “3+1” zinc(II) phthalocyanines substituted with one or two 3,4,5-tris(3,6,9-trioxadecoxy)benzoxy group(s). These compounds exhibit a high photocytotoxicity against HT29 and HepG2 cells with IC_{50} values down to 0.02 μM . The mono- α -substituted

phthalocyanine **2.7** is more potent than the other two analogues, which can be partly explained by its lower aggregation tendency in the culture media and higher cellular uptake as shown by absorption spectroscopy and fluorescence microscopy, respectively.

2.4 Experimental Section

2.4.1 General

All the reactions were performed under an atmosphere of nitrogen. Tetrahydrofuran (THF), toluene and *n*-pentanol, dichloromethane, pyridine, and DMF were distilled from sodium benzophenone ketyl, sodium, calcium hydride, potassium hydroxide, and barium oxide, respectively. Chromatographic purifications were performed on silica gel (Macherey-Nagel, 70-230 mesh) columns with the indicated eluents. Size exclusion chromatography was carried out on Bio-Rad Bio-Beads S-X1 beads (200-400 mesh). All other solvents and reagents were of reagent grade and used as received. Compound **2.2** was prepared as described.⁹

¹H and ¹³C{¹H} NMR spectra were recorded on a Bruker DPX 300 (¹H, 300; ¹³C, 75.4 MHz) or AVANCE II 400 (¹H, 400; ¹³C, 100.6 MHz) spectrometer in CDCl₃ or DMSO-d₆. Spectra were referenced internally using the residual solvent [¹H: CDCl₃ (δ 7.26); DMSO-d₆ (δ 2.50)] or solvent [¹³C: CDCl₃ (δ 77.0); DMSO-d₆ (δ 39.7)] resonances relative to SiMe₄. Electrospray ionization (ESI) mass spectra were measured on a Thermo Finnigan MAT 95 XL mass spectrometer. Matrix assisted laser desorption/ionization time-of-flight (MALDI-TOF) mass spectra were taken on a

Bruker Daltonics Autoflex MALDI-TOF mass spectrometer. Elemental analyses were performed by the Shanghai Institute of Organic Chemistry, Chinese Academy of Sciences.

2.4.2 Photophysical Studies

UV-Vis and steady-state fluorescence spectra were taken on a Cary 5G UV-Vis-NIR spectrophotometer and a Hitachi F-4500 spectrofluorometer, respectively. The fluorescence quantum yields were determined by the equation: $\Phi_{F(\text{sample})} = (F_{\text{sample}}/F_{\text{ref}})(A_{\text{ref}}/A_{\text{sample}})(n_{\text{sample}}^2/n_{\text{ref}}^2)\Phi_{F(\text{ref})}$,¹⁰ where F , A , and n are the measured fluorescence (area under the emission peak), the absorbance at the excitation position (610 nm), and the refractive index of the solvent, respectively. The unsubstituted zinc(II) phthalocyanine (ZnPc) in DMF was used as the reference [$\Phi_{F(\text{ref})} = 0.28$].¹¹ To minimize re-absorption of radiation by the ground-state species, the emission spectra were obtained in very dilute solutions where the absorbance at 610 nm was less than 0.03.

Singlet oxygen quantum yields (Φ_{Δ}) were measured by the method described by Wöhrle et al.⁸ with some modifications. A mixture of DPBF (370 μM , 1 mL) and the photosensitizer (absorbance of the Q band ≈ 1.0 , 1 mL) in DMF was illuminated with red light coming from a 100 W halogen lamp after passing through a water tank for cooling and a color glass filter (Newport, cu-on 610 nm). The decay of the DPBF absorption at 411 nm was monitored along with time. The quantum yield of the photoreaction Φ_{DPBF} was defined as: $\Phi_{\text{DPBF}} = -(V_{\text{R}}/I_{\text{abs}}) \cdot (c_{\text{I}} - c_0)/t$, where V_{R} is the

reaction volume and I_{abs} is related to the light intensity, which was not determined, c_0 and c_1 are the DPBF concentrations prior to and after irradiation, respectively, and t is the irradiation time in second. The value of $(I_{\text{abs}}/V_R) \cdot \Phi_{\text{DPBF}}$ was determined for each irradiation cycle using the extinction coefficient for DPBF ($\epsilon = 23,000 \text{ dm}^3 \text{ mol}^{-1} \text{ cm}^{-1}$ at 411 nm). The singlet oxygen quantum yield Φ_Δ is related to Φ_{DPBF} according to the equation: $1/\Phi_{\text{DPBF}} = 1/\Phi_\Delta + (1/\Phi_\Delta)(k_d/k_a)(1/[\text{DPBF}])$, where k_d is the decay rate constant of singlet oxygen and k_a is the rate constant of the reaction of DPBF with singlet oxygen. By comparing the slope or y-intercept of the plot $(V_R/I_{\text{abs}}) \cdot (1/\Phi_{\text{DPBF}})$ versus $1/[\text{DPBF}]$ with those derived from the experiment using the reference ZnPc as the sensitizer ($\Phi_\Delta = 0.56$ in DMF) under the same conditions, the Φ_Δ value of the sensitizer could be determined. The ratio of the slope or y-intercept should inversely proportional to their ratio of Φ_Δ .

2.4.3 Synthesis

3,4,5-Tris(2-(2-(2-methoxyethoxy)ethoxy)ethoxy)benzoate (2.3).¹² A mixture of methyl 3,4,5-trihydroxybenzoate (**2.1**) (2.96 g, 16 mmol), monotosylated triethylene glycol (**2.2**) (15.33 g, 48 mmol), and anhydrous potassium carbonate (19.95 g, 145 mmol) in DMF (30 mL) was stirred at 90 °C for 24 hours under a N_2 atmosphere. Then the volatiles were removed under vacuum. The resulting brown residue was mixed with water (100 mL), and extracted with CH_2Cl_2 (100 mL \times 3). The organic extracts were collected, dried over anhydrous MgSO_4 , filtered and evaporated to dryness under reduced pressure. The crude product was purified by

silica gel column chromatography using $\text{CHCl}_3/\text{CH}_3\text{OH}$ (100:1 v/v) as the eluent. Compound **2.3** was obtained as a slight yellow liquid (7.82 g, 78%). ^1H NMR (300 MHz, DMSO-d_6): δ 7.23 (s, 2 H, ArH), 4.09-4.18 (m, 6 H, CH_2), 3.83 (s, 3 H, COOCH_3), 3.75 (t, $J = 4.5$ Hz, 4 H, CH_2), 3.67 (t, $J = 4.5$ Hz, 2 H, CH_2), 3.45-3.62 (m, 18 H, CH_2), 3.38-3.45 (m, 6 H, CH_2), 3.22 (s, 9 H, OCH_3); $^{13}\text{C}\{^1\text{H}\}$ NMR (75.4 MHz, CDCl_3): δ 166.4, 152.2, 142.4, 124.8, 108.8, 72.3, 71.8, 70.7, 70.6, 70.4, 69.5, 68.7, 58.9, 52.0 (some of the CH_2 signals are overlapped).

(3,4,5-Tris(2-(2-(2-methoxyethoxy)ethoxy)ethoxy)phenyl)methanol (2.4).¹² To a well-stirred suspension of LiAlH_4 (1.16 g, 30.5 mmol) in THF (60 mL), a solution of compound **2.3** (12.63 g, 20.3 mmol) in THF (40 mL) was added dropwise using a dropping funnel at 0 °C under a N_2 atmosphere. The mixture was allowed to heat to reflux and stirred for overnight. The reaction was then quenched by dropwise addition of water (5 mL). The granular salts were separated using suction filtration, and rinsed thoroughly with THF. The filtrate was dried over anhydrous MgSO_4 , filtered, and evaporated to afford a pale yellow liquid (10.99 g, 91%). ^1H NMR (300 MHz, CDCl_3): δ 6.63 (s, 2 H, ArH), 4.58 (d, $J = 5.4$ Hz, 2 H, ArCH_2), 4.10-4.19 (m, 6 H, CH_2), 3.84 (t, $J = 5.1$ Hz, 4 H, CH_2), 3.78 (t, $J = 5.1$ Hz, 2 H, CH_2), 3.69-3.76 (m, 6 H, CH_2), 3.59-3.69 (m, 12 H, CH_2), 3.52-3.59 (m, 6 H, CH_2), 3.37 (s, 9 H, CH_3), 2.09 (t, $J = 5.4$ Hz, 1 H, OH); $^{13}\text{C}\{^1\text{H}\}$ NMR (75.4 MHz, CDCl_3): δ 152.5, 137.4, 136.7, 106.3, 72.1, 71.8, 70.6, 70.5, 70.3, 69.7, 68.6, 64.9, 58.9 (some of the CH_2 signals are overlapped).

3-[3,4,5-Tris(3,6,9-trioxadecoxy)benzoxy]phthalonitrile (2.5). To a mixture of 3-nitrophthalonitrile (1.73 g, 10 mmol) and compound **2.4** (2.97 g, 5 mmol) in DMF

(30 mL) was added anhydrous potassium carbonate (6.90 g, 50 mmol). The resulting mixture was stirred at 80 °C for 4 days. The solvent was then evaporated under reduced pressure and the residue was mixed with CHCl₃ (60 mL) and water (60 mL). The aqueous layer was separated and extracted with CHCl₃ (60 mL x 3). The combined organic fractions were dried over anhydrous MgSO₄, then filtered. The filtrate was collected and evaporated to dryness. The residue was purified by silica gel column chromatography using CHCl₃/MeOH (60:1 v/v) as the eluent to give compound **2.5** as a colorless liquid (1.41 g, 39%). ¹H NMR (300 MHz, CDCl₃): δ 7.61 (t, *J* = 8.7 Hz, 1 H, ArH), 7.37 (d, *J* = 7.5 Hz, 1 H, ArH), 7.25 (d, *J* = 7.5 Hz, 1 H, ArH), 6.66 (s, 2 H, ArH), 5.17 (s, 2 H, ArCH₂), 4.13-4.18 (m, 6 H, CH₂), 3.85 (t, *J* = 4.8 Hz, 4 H, CH₂), 3.79 (t, *J* = 5.1 Hz, 2 H, CH₂), 3.70-3.74 (m, 6 H, CH₂), 3.62-3.68 (m, 12 H, CH₂), 3.53-3.57 (m, 6 H, CH₂), 3.37 (two partially overlapping s, 9 H, CH₃), ¹³C{¹H} NMR (75.4 MHz, DMSO-d₆): δ 160.9, 152.4, 137.7, 136.0, 130.7, 126.2, 119.3, 116.0, 115.6, 113.9, 107.1, 103.6, 72.0, 71.5, 71.2, 70.2, 70.0, 69.9, 69.8, 69.1, 68.5, 58.2 (some of the CH₂ signals are overlapped); MS (ESI): isotopic clusters peaking at *m/z* 743 {100%, [M + Na]⁺}; HRMS (ESI): *m/z* calcd for C₃₆H₅₂N₂NaO₁₃ [M + Na]⁺: 743.3362, found 743.3365.

4-[3,4,5-Tris(3,6,9-trioxadecoxy)benzoxy]phthalonitrile (2.6). According to the above procedure using 4- instead of 3-nitrophthalonitrile as a starting material, compound **2.6** was obtained as a colorless liquid (1.71 g, 47%). ¹H NMR (300 MHz, CDCl₃): δ 7.73 (d, *J* = 8.7 Hz, 1 H, ArH), 7.34 (d, *J* = 2.4 Hz, 1 H, ArH), 7.25 (dd, *J* = 2.4, 8.7 Hz, 1 H, ArH), 6.63 (s, 2 H, ArH), 5.05 (s, 2 H, ArCH₂), 4.16 (t, *J* = 4.8 Hz, 6

H, CH₂), 3.85 (t, $J = 4.8$ Hz, 4 H, CH₂), 3.79 (t, $J = 5.1$ Hz, 2 H, CH₂), 3.68-3.75 (m, 6 H, CH₂), 3.59-3.68 (m, 12 H, CH₂), 3.51-3.59 (m, 6 H, CH₂), 3.37 (s, 9 H, CH₃); ¹³C{¹H} NMR (75.4 MHz, CDCl₃): δ 161.5, 152.9, 138.7, 135.2, 129.7, 120.0, 119.6, 117.3, 115.5, 115.1, 107.5, 107.2, 72.2, 71.8, 71.0, 70.7, 70.6, 70.4, 69.6, 68.9, 58.9 (some of the CH₂ signals are overlapped); MS (ESI): isotopic clusters peaking at m/z 743 {100%, [M + Na]⁺}; HRMS (ESI): m/z calcd for C₃₆H₅₂N₂NaO₁₃ [M + Na]⁺: 743.3362, found 743.3361.

Phthalocyanine 2.7. A mixture of phthalonitrile **2.5** (0.26 g, 0.36 mmol), unsubstituted phthalonitrile (0.46 g, 3.59 mmol), and Zn(OAc)₂·2H₂O (0.22 g, 1.00 mmol) in *n*-pentanol (15 mL) was heated to 100°C, then a small amount of DBU (0.5 mL) was added. The mixture stirred at 140-150°C for 24 hours. After a brief cooling, the volatiles were removed under reduced pressure. The residue was dissolved in CHCl₃ (120 mL), then filtered to remove part of the unsubstituted zinc(II) phthalocyanine formed. The filtrate was collected and evaporated to dryness in vacuo. The residue was purified by silica gel column chromatography using CHCl₃/CH₃OH (30:1 v/v) as the eluent, followed by size exclusion chromatography using THF as the eluent. The crude product was further purified by recrystallization from a mixture of THF and hexane (0.11 g, 26%). ¹H NMR (300 MHz, CDCl₃ with a trace amount of pyridine-d₅): δ 9.41-9.46 (m, 5 H, Pc-H_a), 9.16 (d, $J = 7.5$ Hz, 1 H, Pc-H_a), 9.13 (d, $J = 6.9$ Hz, 1 H, Pc-H_a), 8.07-8.15 (m, 7 H, Pc-H _{β}), 7.70 (d, $J = 7.8$ Hz, 1 H, Pc-H _{β}), 7.32 (s, 2 H, ArH), 5.81 (s, 2 H, ArCH₂), 4.32 (t, $J = 5.1$ Hz, 2 H, CH₂), 4.20 (t, $J = 5.1$ Hz, 4 H, CH₂), 3.92 (t, $J = 5.1$ Hz, 2 H, CH₂), 3.78-3.82 (m, 2 H, CH₂), 3.66-3.75

(m, 8 H, CH₂), 3.55-3.59 (m, 6 H, CH₂), 3.47-3.51 (m, 8 H, CH₂), 3.38-3.41 (m, 7 H, CH₂ and CH₃), 3.26 (s, 6 H, CH₃); ¹³C{¹H} NMR (75.4 MHz, DMSO-d₆): δ 155.6, 152.7, 152.6, 152.3, 152.2, 140.3, 138.4, 137.9, 137.7, 137.6, 133.5, 130.6, 129.1, 125.3, 122.5, 122.4, 122.1, 115.3, 114.0, 107.8, 72.3, 71.6, 71.5, 71.0, 70.2, 70.0, 69.9, 69.8, 69.3, 68.8, 58.3, 58.2 (some of signals are overlapped); MS (ESI): isotopic clusters peaking at *m/z* 1191 {100%, [M + Na]⁺}; HRMS (ESI): *m/z* calcd for C₆₀H₆₄N₈NaO₁₃Zn [M + Na]⁺: 1191.3777, found 1191.3783.

Phthalocyanine 2.8. According to the above procedure, phthalonitrile **2.6** (0.26 g, 0.36 mmol) was treated with unsubstituted phthalonitrile (0.46 g, 3.59 mmol) and Zn(OAc)₂·2H₂O (0.22 g, 1.00 mmol) to give phthalocyanine **2.8** as a blue solid (0.09 g, 21%). ¹H NMR (300 MHz, CDCl₃ with a trace amount of pyridine-d₅): δ 9.20-9.35 (m, 6 H, Pc-H_α), 9.05 (d, *J* = 7.8 Hz, 1 H, Pc-H_α), 8.66 (s, 1 H, Pc-H_α), 8.06-8.12 (m, 6 H, Pc-H_β), 7.62 (d, *J* = 8.4 Hz, 1 H, Pc-H_β), 6.99 (s, 2 H, ArH), 5.46 (s, 2 H, ArCH₂), 4.33 (t, *J* = 4.8 Hz, 4 H, CH₂), 4.24 (t, *J* = 5.1 Hz, 2 H, CH₂), 3.94 (t, *J* = 4.8 Hz, 4 H, CH₂), 3.86 (t, *J* = 4.8 Hz, 2 H, CH₂), 3.76-3.80 (m, 6 H, CH₂), 3.62-3.71 (m, 12 H, CH₂), 3.53-3.57 (m, 6 H, CH₂), 3.38 (s, 3 H, CH₃), 3.37 (s, 6 H, CH₃); ¹³C{¹H} NMR (75.4 MHz, DMSO-d₆): δ 159.9, 152.6, 152.4, 152.3, 152.2, 152.0, 151.7, 151.6, 139.5, 137.8, 137.5, 132.7, 130.7, 129.0, 128.9, 123.0, 122.2, 117.8, 107.2, 105.6, 72.1, 71.5, 70.3, 70.1, 70.0, 69.9, 69.4, 68.8, 58.3, 55.1 (some of signals are overlapped); MS (ESI): isotopic clusters peaking at *m/z* 1191 {100%, [M + Na]⁺}; HRMS (ESI): *m/z* calcd for C₆₀H₆₄N₈NaO₁₃Zn [M + Na]⁺: 1191.3777, found 1191.3771.

5-(Chloromethyl)-1,2,3-tris(2-(2-(2-methoxyethoxy)ethoxy)ethoxy)benzene

(2.9).¹² To a solution of compound 2.4 (2.00 g, 3.37 mmol) in dry CH₂Cl₂ (10 mL) and a small amount of DMF (0.2 mL), SOCl₂ (0.37 mL, 5.04 mmol) was added dropwise with vigorous stirring. After addition of SOCl₂ for 30 minutes, the reaction was essentially complete as indicated by TLC. The volatiles were evaporated in vacuo. The residue was mixed with water (20 mL), and extracted with CH₂Cl₂ (20 mL × 3). The combined organic fractions were collected, dried over anhydrous MgSO₄, filtered and evaporated in vacuo to give a pale yellow liquid (2.06 g, 100%).
¹H NMR (300 MHz, CDCl₃): δ 6.63 (s, 2 H, ArH), 4.49 (s, 2 H, ArCH₂), 4.11-4.19 (m, 6 H, CH₂), 3.85 (t, *J* = 4.8 Hz, 4 H, CH₂), 3.78 (t, *J* = 5.1 Hz, 2 H, CH₂), 3.69-3.76 (m, 6 H, CH₂), 3.60-3.69 (m, 12 H, CH₂), 3.51-3.59 (m, 6 H, CH₂), 3.38 (s, 9 H, OCH₃); ¹³C{¹H} NMR (75.4 MHz, CDCl₃): δ 152.6, 138.5, 132.7, 108.3, 72.3, 71.9, 70.8, 70.6, 70.5, 70.5, 69.7, 68.9, 59.0, 46.6 (some of the CH₂ signals are overlapped).

3,6-Bis[3,4,5-tris(3,6,9-trioxadecoxy)benzoxy]phthalonitrile (2.10). A mixture of compound 2.9 (2.06 g, 3.36 mmol), 2,3-dicyanohydroquinone (0.27 g, 1.69 mmol), and potassium carbonate (1.17 g, 8.47 mmol) in DMF (10 mL) was stirred at 100°C for 24 hours. The volatiles were then removed under reduced pressure. The residue was mixed with water (50 mL) and the mixture was extracted with CHCl₃ (50 mL × 3). The combined organic extracts were dried over anhydrous MgSO₄ and evaporated under reduced pressure. The residue was then purified by silica gel column chromatography using CHCl₃/MeOH (20:1 v/v) as the eluent to give the product as a pale yellow transparent liquid (1.95 g, 88%). ¹H NMR (300 MHz, CDCl₃): δ 7.15 (s, 2

H, ArH), 6.65 (s, 4 H, ArH), 5.08 (s, 4 H, ArCH₂), 4.12-4.20 (m, 12 H, CH₂), 3.85 (t, $J = 4.8$ Hz, 8 H, CH₂), 3.79 (t, $J = 5.1$ Hz, 4 H, CH₂), 3.69-3.76 (m, 12 H, CH₂), 3.62-3.69 (m, 24 H, CH₂), 3.51-3.59 (m, 12 H, CH₂), 3.37 (two partially overlapping s, 18 H, CH₃); ¹³C{¹H} NMR (75.4 MHz, CDCl₃): δ 154.7, 152.8, 138.2, 130.3, 119.4, 112.9, 106.4, 105.7, 72.2, 71.7, 71.6, 70.6, 70.5, 70.3, 69.5, 68.7, 58.8 (some of the CH₂ signals are overlapped); MS (ESI): isotopic clusters peaking at m/z 1336 {100%, [M + Na]⁺}; HRMS (ESI): m/z calcd for C₆₄H₁₀₀N₂NaO₂₆ [M + Na]⁺: 1335.6457, found 1335.6462.

Phthalocyanine 2.11. According to the procedure for 2.7 described above, phthalonitrile 2.10 (0.50 g, 0.38 mmol) was treated with unsubstituted phthalonitrile (0.49 g, 3.82 mmol) and Zn(OAc)₂·2H₂O (0.23 g, 1.05 mmol) to give phthalocyanine 2.11 as a blue solid (54 mg, 8%). ¹H NMR (300 MHz, CDCl₃): δ 9.43-9.47 (m, 4 H, Pc-H_a), 9.20 (d, $J = 7.5$ Hz, 2 H, Pc-H_a), 8.03-8.15 (m, 6 H, Pc-H_β), 7.68 (s, 2 H, Pc-H_β), 7.37 (s, 4 H, ArH), 5.90 (s, 4 H, ArCH₂), 4.05 (t, $J = 5.1$ Hz, 4 H, CH₂), 3.80 (t, $J = 5.1$ Hz, 8 H, CH₂), 3.70 (t, $J = 5.1$ Hz, 4 H, CH₂), 3.61-3.66 (m, 4 H, CH₂), 3.55-3.58 (m, 8 H, CH₂), 3.43-3.50 (m, 12 H, CH₂), 3.34-3.37 (m, 12 H, CH₂), 3.30 (s, 6 H, CH₃), 3.16-3.24 (m, 8 H, CH₂), 3.12 (s, 12 H, CH₂), 2.90 (s, 12 H, CH₃); ¹³C{¹H} NMR (75.4 MHz, CDCl₃): 153.6, 153.4, 153.3, 152.5, 152.2, 150.2, 138.6, 138.3, 138.1, 137.5, 133.6, 129.0, 128.8, 128.6, 128.5, 122.6, 122.3, 122.1, 116.5, 107.0, 72.3, 72.2, 71.8, 71.3, 70.5, 70.4, 69.9, 69.7, 69.2, 68.1, 58.8, 58.4 (some of the CH₂ signals are overlapped); MS (ESI): isotopic clusters peaking at m/z 1784 {100%, [M + Na]⁺}; HRMS (ESI): m/z calcd for C₈₈H₁₁₂N₈NaO₂₆Zn [M + Na]⁺: 1783.6871, found

1783.6862.

2.4.4 In vitro Studies

2.4.4.1 Cell lines and Culture Conditions

The HT29 human colorectal carcinoma cells (from ATCC, no. HTB-38) were maintained in DMEM (Invitrogen, cat no. 10313-021) supplemented with fetal calf serum (10%), penicillin-streptomycin ($100 \text{ units mL}^{-1}$ and 100 mg mL^{-1} , respectively), L-glutamine (2 mM), and transferrin (10 mg mL^{-1}). The HepG2 human hepatocarcinoma cells (from ATCC, no. HB-8065) were maintained in RPMI medium 1640 (Invitrogen, cat no. 23400-021) supplemented with fetal calf serum (10%) and penicillin-streptomycin ($100 \text{ units mL}^{-1}$ and 100 mg mL^{-1} , respectively). Approximately 3×10^4 (for HT29) or 4×10^4 (for HepG2) cells per well in these media were inoculated in 96-multiwell plates and incubated overnight at 37°C in a humidified 5% CO_2 atmosphere.

2.4.4.2 Photocytotoxicity Assay

Phthalocyanines **2.7**, **2.8**, and **2.11** were first dissolved in DMF to give 1.5 mM solutions, which were diluted to $80 \text{ }\mu\text{M}$ with an aqueous solution of Cremophor EL (Sigma, 4.7 g in 100 mL of water). The solutions were filtered with a $0.2 \text{ }\mu\text{m}$ filter, then diluted with the culture medium to appropriate concentrations (four-fold dilutions from $0.5 \text{ }\mu\text{M}$). The cells, after being rinsed with PBS, were incubated with $100 \text{ }\mu\text{L}$ of these phthalocyanine solutions for 2 h at 37°C under 5% CO_2 . The cells

were then rinsed again with PBS and re-fed with 100 μL of the culture medium before being illuminated at ambient temperature. The light source consisted of a 300 W halogen lamp, a water tank for cooling, and a color glass filter (Newport) cut-on 610 nm. The fluence rate ($\lambda > 610$ nm) was 40 mW cm^{-2} . An illumination of 20 min led to a total fluence of 48 J cm^{-2} .

Cell viability was determined by means of the colorimetric MTT assay¹³. After illumination, the cells were incubated at 37°C under 5% CO_2 overnight. An MTT (Sigma) solution in PBS (3 mg mL^{-1} , 50 μL) was added to each well followed by incubation for 2 hours under the same environment. A solution of sodium dodecyl sulfate (SDS, Sigma) (10% by weight, 50 μL) was then added to each well. The plate was incubated in an oven at 60 °C for 30 min, then 80 μL of *iso*-propanol was added to each well. The plate was agitated on a Bio-Rad microplate reader at ambient temperature for 10 sec before the absorbance at 540 nm at each well was taken. The average absorbance of the blank wells, which did not contain the cells, was subtracted from the readings of the other wells. The cell viability was then determined by the equation: % Viability = $[\Sigma(A_i/A_{\text{control}} \times 100)] / n$, where A_i is the absorbance of the i th data ($i = 1, 2, \dots, n$), A_{control} is the average absorbance of the control wells, in which the phthalocyanine was absent, and $n (= 4)$ is the number of the data points.

2.4.4.3 Fluorescence Microscopic Studies

For the detection of the intracellular fluorescence intensity of compounds **2.7**, **2.8**, and **2.11**, approximately 1.2×10^5 HT29 cells in the culture medium (2 mL) were

seeded on a coverslip and incubated overnight at 37°C under 5% CO₂. The medium was removed, then the cells were incubated with 2 mL of an 8 μM phthalocyanine dilution in the medium for 2 h under the same conditions. The cells were then rinsed with PBS and viewed with an Olympus IX 70 inverted microscope. The excitation light source (at 630 nm) was provided by a multi-wavelength illuminator (Polychrome IV, TILL Photonics). The emitted fluorescence (> 660 nm) was collected using a digital cooled CCD camera (Quantix, Photometrics). Images were digitized and analyzed using MetaFluor V.4.6 (Universal Imaging).

2.5 References

1. (a) Vrouenraets, M. B.; Visser, G. W. M.; Snow, G. B.; van Dongen, G. A. M. S. *Anticancer Res.* **2003**, *23*, 505. (b) Dolmans, D. E. J. G. J.; Fukumura, D.; Jain, R. K. *Nat. Rev. Cancer* **2003**, *3*, 380. (c) Brown, S. B.; Brown, E. A.; Walker, I. *Lancet Oncol.* **2004**, *5*, 497.
2. Detty, M. R.; Gibson, S. L.; Wagner, S. J. *J. Med. Chem.* **2004**, *47*, 3897.
3. Ali, H.; van Lier, J. E. *Chem. Rev.* **1999**, *99*, 2379.
4. (a) Huang, J.-D.; Fong, W.-P.; Chan, E. Y. M.; Choi, M. T. M.; Chan, W.-K.; Chan, M.-C.; Ng, D. K. P. *Tetrahedron Lett.* **2003**, *44*, 8029. (b) Huang, J.-D.; Wang, S.; Lo, P.-C.; Fong, W.-P.; Ko, W.-H.; Ng, D. K. P. *New J. Chem.* **2004**, *28*, 348. (c) Lo, P.-C.; Huang, J.-D.; Cheng, D. Y. Y.; Chan, E. Y. M.; Fong, W.-P.; Ko, W.-H.; Ng, D. K. P. *Chem. Eur. J.* **2004**, *10*, 4831. (d) Lee, P. P. S.; Lo, P.-C.; Chan, E. Y. M.; Fong, W.-P.; Ko, W.-H.; Ng, D. K. P. *Tetrahedron Lett.* **2005**, *46*, 1551. (e) Lai, J. C.; Lo, P.-C.; Ng, D. K. P.; Ko, W.-H.; Leung, S. C. H.; Fung, K.-P.; Fong, W.-P. *Cancer Biol. Ther.* **2006**, *5*, 413. (f) Choi, C.-F.; Tsang, P.-T.; Huang, J.-D.; Chan, E. Y. M.; Ko, W.-H.; Fong, W.-P.; Ng, D. K. P. *Chem. Commun.* **2004**, 2236. (g) Lo, P.-C.; Zhao, B.; Duan, W.; Fong, W.-P.; Ko,

- W.-H.; Ng, D. K. P. *Bioorg. Med. Chem. Lett.* **2007**, *17*, 1073. (h) Lo, P.-C.; Chan, C. M. H.; Liu, J.-Y.; Fong, W.-P.; Ng, D. K.-P. *J. Med. Chem.* **2007**, *50*, 2100. (i) Choi, C.-F.; Huang, J.-D.; Lo, P.-C.; Fong, W.-P.; Ng, D. K. P. *Org. Biomol. Chem.* **2008**, *6*, 2173. (j) Lo, P.-C.; Fong, W.-P.; Ng, D. K. P. *ChemMedChem* **2008**, *3*, 1110.
5. MacDonald, I. J.; Dougherty, T. J. *J. Porphyrins Phthalocyanines* **2001**, *5*, 105.
 6. Ishii, K.; Kobayashi, N. in *The Porphyrin Handbook*; Kadish, K. M., Smith, K. M., Guilard, R., Eds.; Academic Press: San Diego, **2003**, vol. 16, pp. 1-42.
 7. Jori, G. *J. Photochem. Photobiol. A: Chem.* **1992**, *62*, 371.
 8. Maree, M. D.; Kuznetsova, N.; Nyokong, T. *J. Photochem. Photobiol. A: Chem.* **2001**, *140*, 117.
 9. Snow, A. W.; Foos, E. E. *Synthesis* **2003**, *4*, 509.
 10. Eaton, D. F. *Pure Appl. Chem.* **1988**, *60*, 1107.
 11. Scalise, I.; Durantini, E. N. *Bioorg. Med. Chem.* **2005**, *13*, 3037.
 12. Oar, M. A.; Serin, J. M.; Dichtel, W. R.; Fréchet, J. M. J.; Ohulchanskyy, T. Y.; Prasad, P. N. *Chem. Mater.* **2005**, *17*, 2267.
 13. Tada, H.; Shiho, O.; Kuroshima, K.; Koyama, M.; Tsukamoto, K. *J. Immunol. Methods* **1986**, *93*, 157.

Chapter 3

Synthesis, Characterization, and in vitro Photodynamic Activities of Di- α -Substituted Zinc(II) Phthalocyanine Derivatives

3.1 Introduction

Phthalocyanines are promising second-generation photosensitizers which have received considerable attention over the last decade.¹ Various chemical modifications have been performed on the macrocyclic core with a view to improving their photophysical properties and enhancing their therapeutic outcome.²⁻³ In fact, it has been found that the position of substitution is also very important. For example, the Q bands for the α -substituted zinc(II) phthalocyanines are significantly red-shifted compared with those for the β -substituted counterparts. α -Substitution also leads to a weakening of fluorescence emission and enhancement of singlet oxygen generation ability.^{2d,4} In Chapter 2, I have reported that introduction of an additional α -substituent further shifts the Q-band to the red. In addition, the di- α -substituted analogue also exhibits a much higher singlet oxygen generation efficiency than the mono- α -substituted derivative. On this basis, in this Chapter, I describe a novel series of di- α -substituted zinc(II) phthalocyanine derivatives. The two substituents adding to the α positions of the macrocycles not only shift their Q band absorption further to the red (ca. 700 nm), allowing a deeper light penetration into tissues, but also reduce their

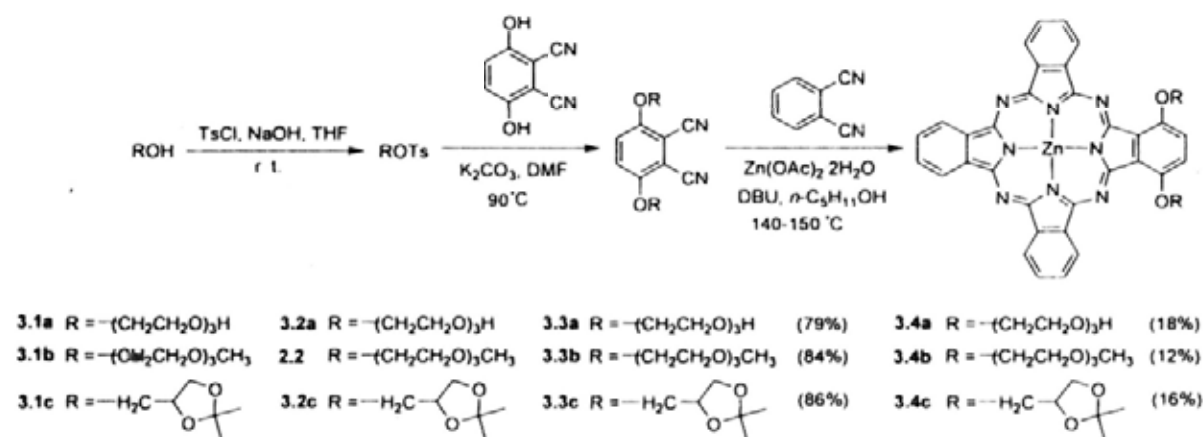
aggregation, thereby promoting the generation of singlet oxygen. To my knowledge, this class of disubstituted phthalocyanines remains relatively rare.^{2b,5} I report herein the synthesis, spectroscopic and photophysical characteristics, as well as the in vitro photodynamic activities of these compounds.

3.2 Results and Discussion

3.2.1 Synthesis and Characterization

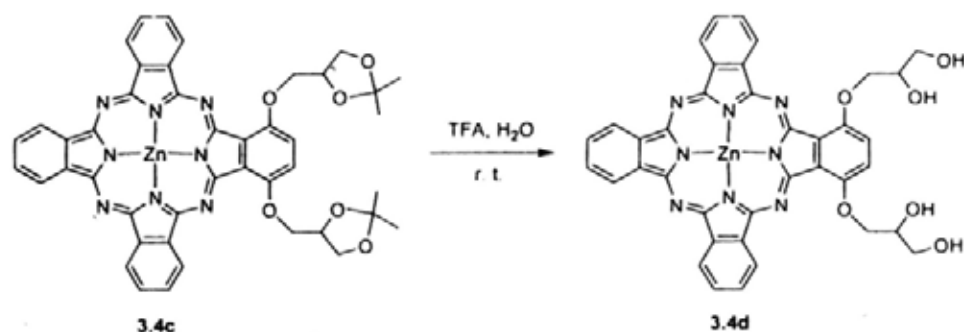
Scheme 3.1 shows the synthetic route used to prepare the 1,4-di- α -substituted phthalocyanines **3.4a-3.4c**. Firstly, the alcohols **3.1a-3.1c** were converted to the corresponding tosylates **3.2a**, **2.2**, and **3.2c**, which then underwent nucleophilic substitution with 2,3-dicyanohydroquinone to give the disubstituted phthalonitriles **3.3a-3.3c**. Mixed cyclization of these compounds with an excess of unsubstituted phthalonitrile (9 equiv.) in the presence of $\text{Zn}(\text{OAc})_2 \cdot 2\text{H}_2\text{O}$ and DBU in *n*-pentanol afforded the corresponding “3+1” cyclized products **3.4a-3.4c** as a blue solid. These oxygen-rich substituents were used to enhance the solubility and reduce the aggregation of these macrocycles, facilitating their separation from the other cyclized side products, particularly the insoluble unsubstituted ZnPc. Hence, these 1,4-di- α -substituted phthalocyanines **3.4a-3.4c** could be isolated readily by silica gel column chromatography followed by size exclusion chromatography in 12-18%. Polyethylene glycols are also known to be excellent pharmaceutical vehicles which can prolong circulating half-life, minimize nonspecific uptake, and enable specific tumor-targeting through the enhanced permeability and retention (EPR) effect.⁶ In

addition, these hydrophilic moieties adding to the hydrophobic core will make the molecules amphiphilic in character, which is a desirable characteristic for efficient photosensitizers.⁷



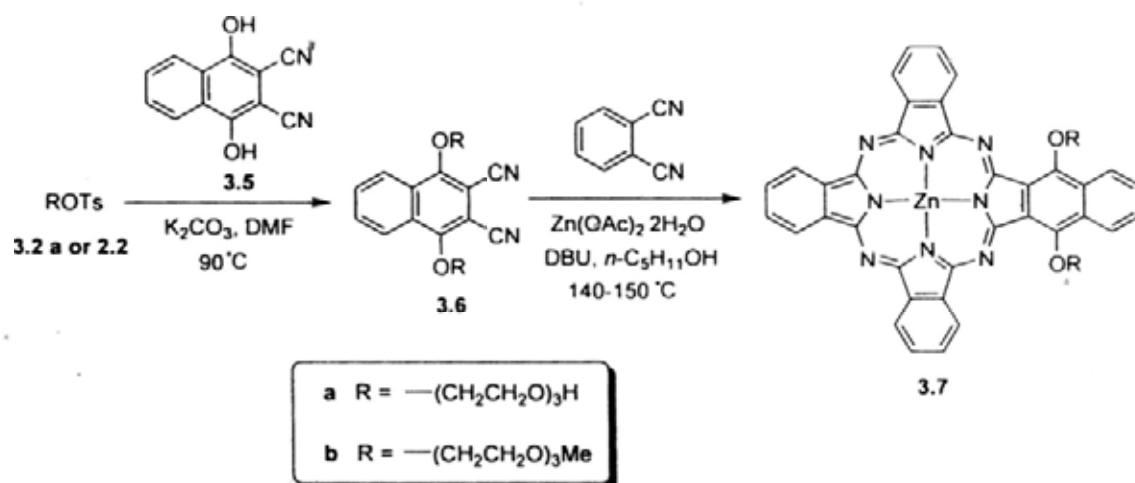
Scheme 3.1. Synthesis of 1,4-disubstituted zinc(II) phthalocyanines **3.4a-3.4c**.

The two isopropylidene groups of **3.4c** could be removed readily upon treatment with a mixture of trifluoroacetic acid (TFA) and H_2O (9:1 v/v) giving the tetrahydroxy phthalocyanine **3.4d** in 85% yield (Scheme 3.2). This compound has a very high polarity and could not be purified by column chromatography. It was simply isolated by precipitation. The sample was found to be essentially pure.



Scheme 3.2. Synthesis of tetrahydroxy zinc(II) phthalocyanine **3.4d**.

To further extend the Q-band absorption to the red, I also prepared the benzo-fused analogues **3.7a** and **3.7b** according to Scheme 3.3. The tosylates **3.2a** and **2.2** were treated with 1,4-dihydroxy-2,3-naphthalonitrile (**3.5**) and K_2CO_3 to give the disubstituted products **3.6a** and **3.6b**, respectively. Similarly, mixed cyclization of these naphthalonitriles with unsubstituted phthalonitrile (9 equiv.) in the presence of $Zn(OAc)_2 \cdot 2H_2O$ and DBU led to the formation of **3.7a** and **3.7b** as a green solid in 13-15% yield.



Scheme 3.3. Synthesis of benzo-fused zinc(II) phthalocyanines **3.7a** and **3.7b**.

All of the zinc(II) phthalocyanines are soluble in common organic solvents and possess a high general stability. They were fully characterized with various spectroscopic methods and elemental analysis. The NMR spectra were recorded in $CDCl_3$ with a trace amount of pyridine- d_5 , which can reduce the aggregation of these compounds. The only exception is the tetrahydroxy analogue **3.4d**, of which the spectra were recorded in $DMSO-d_6$. Figure 3.1 shows the 1H - 1H COSY spectrum of

3.4d to illustrate the general spectral features of these compounds. The signals for the six phthalocyanine α ring protons overlap as a multiplet at δ 9.32-9.41. For compounds **3.4a** and **3.4c**, a multiplet and a doublet (in 2:1 integration ratio) were observed instead for these protons. The phthalocyanine β ring protons of **3.4d** resonate as a multiplet (at δ 8.19-8.26, 6 H) and a singlet (at δ 7.77, 2 H). The doublet at δ 5.56 and triplet at δ 4.96 can easily be assigned to the secondary and primary hydroxy groups, respectively. The other signals can also be unambiguously assigned as shown in the Figure 3.1 with the aid of the connectivity revealed by the COSY experiment.

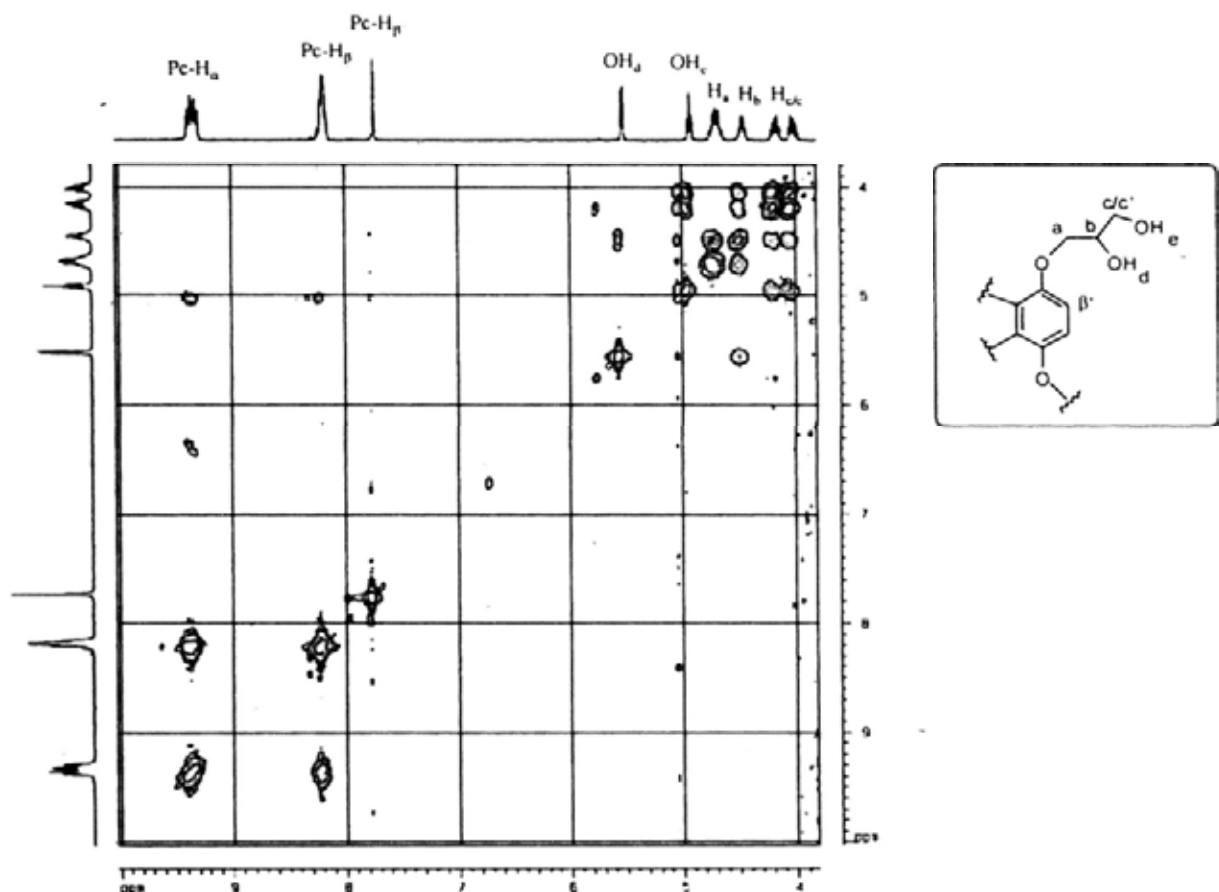


Figure 3.1. ^1H - ^1H COSY spectrum of **3.4d** in DMSO-d_6 .

For **3.7a** and **3.7b**, the signals for the naphthyl α and β ring protons were also seen adjacent to the respective phthalocyanine ring protons' signals. In the spectrum of **3.7b** (Figure 3.2), four well-resolved doublets of doublets (at δ 9.41, 9.37, 9.29, and 9.08) were observed for the four different sets of α ring protons. The remaining four different sets of β ring protons resonated as two overlapping doublets of doublets (at δ 8.09-8.15) and another two doublets of doublets (at δ 8.04 and 7.91). Six well-separated virtual triplets or multiplets (in the region δ 3.6-5.7) and a singlet (at δ 3.41) were also seen for the six sets of methylene protons and the methyl groups, respectively, of the chains.

The $^{13}\text{C}\{^1\text{H}\}$ NMR spectra of these phthalocyanines showed clearly the expected number of signals for the substituents, but for the phthalocyanine ring, some of the signals were overlapped. All of these compounds were further characterized with ESI mass spectrometry. The isotopic distribution as well as the exact mass for the $[\text{M} + \text{H}]^+$ or $[\text{M} + \text{Na}]^+$ species were in good agreement with the calculated ones.

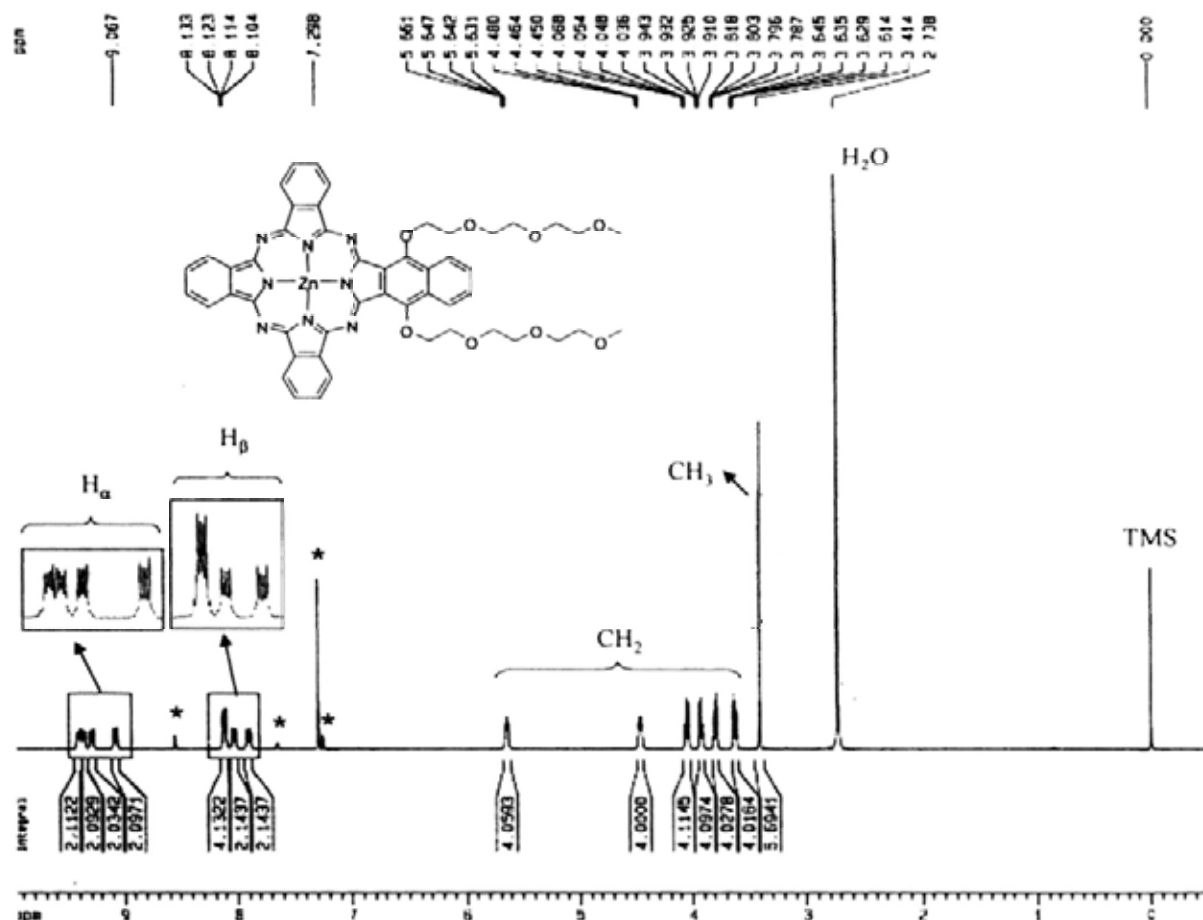


Figure 3.2. ^1H NMR spectrum of **3.7b** in CDCl_3 with a trace amount of pyridine- d_5 . Signals for the residual solvents are marked with asterisks.

3.2.2 Electronic Absorption and Photophysical Properties

The electronic absorption spectra of phthalocyanines **3.4a-3.4d** in DMF are very similar and are typical for nonaggregated phthalocyanines. Taking the spectrum of **3.4b** (Figure 3.3) as an example, it shows a broad Soret band peaking at 342 nm, an intense and sharp Q band at 689 nm, together with a vibronic band at 621 nm. The Q band strictly follows the Lambert Beer's law suggesting that aggregation of this compound is not significant. Compared with ZnPc, the mono- α -alkoxy analogues have a red-shifted Q band (from 670 to 672-679 nm).^{2d,8} The di- α -substitution in

3.4a-3.4d further shifts the Q band to the red (689-692 nm), but the positions are still not as far as those of the tetra- (696 nm) and octa- α -butoxy analogues (758 nm).⁴ It has been shown that attachment of an electron-releasing alkoxy group at the α position destabilizes the HOMO level more than the LUMO level.⁴ As a result, the HOMO-LUMO gap is reduced upon α -substitution, which can explain the red shift in this series of compounds. Introduction of an additional fused benzene ring in **3.7a-3.7b** extends the π -conjugated system, leading to a further red-shift of the Q band to 701 nm. These data are summarized in Table 3.1.

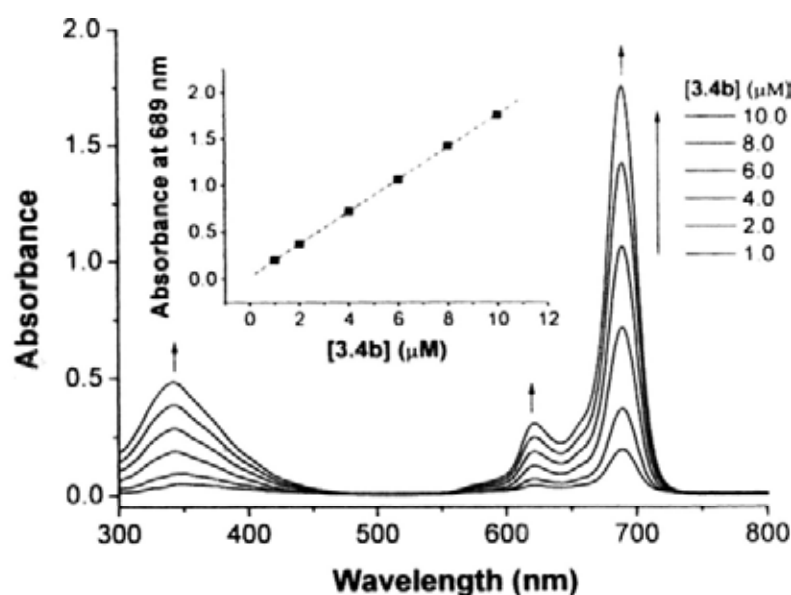


Figure 3.3. Electronic absorption spectra of **3.4b** in DMF at different concentrations. The inset plots the Q-band absorbance versus the concentration of **3.4b**.

Table 3.1. Electronic absorption and fluorescence data for **3.4a-3.4d** and **3.7a-3.7b** in DMF.

| Compound | λ_{\max} (nm) (log ϵ) | λ_{em} (nm) ^a | Φ_{F} ^b |
|-------------|---|---|--------------------------------|
| 3.4a | 341 (4.71), 621 (4.51), 689 (5.27) | 698 | 0.17 |
| 3.4b | 342 (4.69), 621 (4.47), 689 (5.24) | 698 | 0.19 |
| 3.4c | 341 (4.78), 621 (4.58), 689 (5.34) | 697 | 0.19 |
| 3.4d | 344 (4.77), 623 (4.57), 692 (5.32) | 699 | 0.18 |
| 3.7a | 343 (4.76), 632 (4.59), 701 (5.24) | 720 | 0.12 |
| 3.7b | 343 (4.78), 632 (4.60), 701 (5.25) | 720 | 0.14 |

^a Excited at 621 (for **3.4a-3.4d**) or 632 nm (for **3.7a-3.7b**). ^b Using ZnPc in DMF as the reference ($\Phi_{\text{F}} = 0.28$).

The fluorescence emission spectra of these compounds were also recorded in DMF. Upon excitation at 621 nm, compounds **3.4a-3.4d** showed a fluorescence emission at 697-699 nm with a quantum yield (Φ_{F}) of 0.17-0.19, which is substantially lower than that of ZnPc ($\Phi_{\text{F}} = 0.28$). For the benzo-fused analogues **3.7a-3.7b**, upon excitation at 632 nm, their fluorescence emission was red-shifted to 720 nm with an even lower Φ_{F} value (0.12-0.14) (Table 3.1). This is in accord with the general observation that the lower the energy of the Q band, the smaller the Φ_{F} value.⁴ It has been suggested that the excited state becomes unstable as the HOMO-LUMO gap decreases, probably due to the ease of electron transfer.

The efficiency of these compounds in generating singlet oxygen, as reflected by the rate of decay of the singlet oxygen quencher 1,3-diphenylisobenzofuran (DPBF), was also compared. As shown in Figure 3.4, all of these phthalocyanines can induce

the photo-bleaching of DPBF and the efficiency follows the order **3.7a-3.7b** > **3.4a-3.4d** > ZnPc. This suggests that as the HOMO-LUMO gap becomes smaller, the singlet excited state has a higher tendency to undergo intersystem crossing to generate singlet oxygen. This can also explain the opposite trend observed for the Φ_F values.

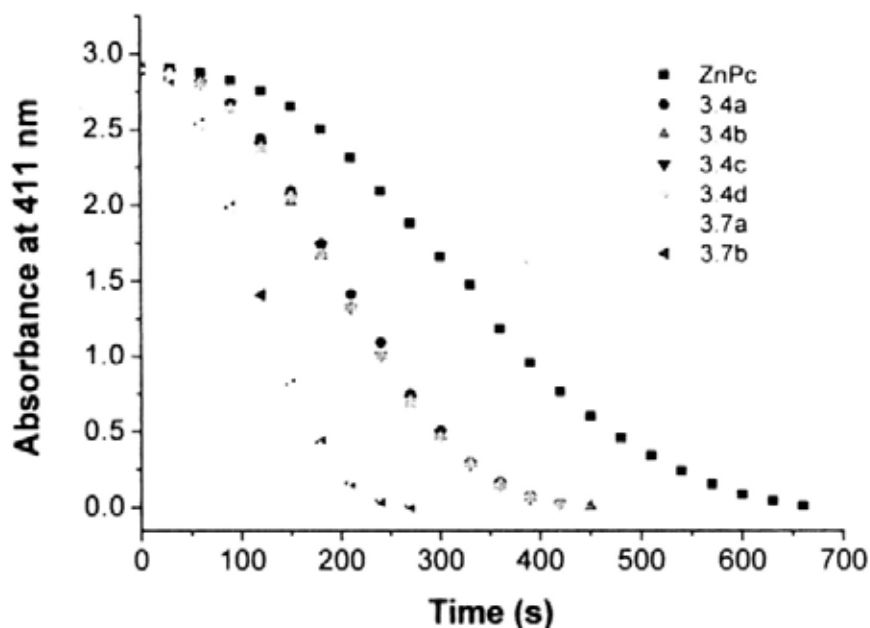


Figure 3.4. Comparison of the rates of decay of DPBF in DMF, as monitored spectroscopically at 411 nm, using phthalocyanines **3.4a-3.4d** and **3.7a-3.7b** as the photosensitizers and ZnPc as the reference.

3.2.3 In vitro Photodynamic Activities

The in vitro photodynamic activities of compounds **3.4a-3.4d** and **3.7a-3.7b** in Cremophor EL emulsions were investigated against HT29 and HepG2 cells. Figure 3.5 shows the dose-dependent survival curves for **3.4a** and **3.7a** toward these two cell lines. It can be seen that both compounds are essentially noncytotoxic in the absence of light (up to 4 and 8 μM , respectively). However, they become cytotoxic upon illumination with red light ($\lambda > 610 \text{ nm}$). Compound **3.4a** is significantly more potent

with an IC_{50} value of 0.41 or 0.16 μM (vs. 2.93 or 2.76 μM for **3.7a**). Only ca. 1 μM of dye is required to essentially kill all the cells (vs. $> 8 \mu\text{M}$ for **3.7a**). The photocytotoxicity of **3.4b-3.4d** is comparable with that of **3.4a**, which is significantly higher than that of **3.7a-3.7b**. The corresponding IC_{50} values are compiled in Table 3.2. Among these compounds, **3.4b** exhibits the highest photocytotoxicity with IC_{50} values down to 0.06 μM . This compound is among the most potent zinc(II) phthalocyanines prepared in our laboratory so far.^{2b,2d,8,9} Its in vitro photocytotoxicity almost reaches the level attained by some of the very potent silicon(IV) analogues.^{2a,2c,10} As shown by the IC_{50} values for **3.4c** and **3.4d** (Table 3.2), removing the isopropylidene protecting groups of **3.4c** does not exert a significant effect on the photocytotoxicity.

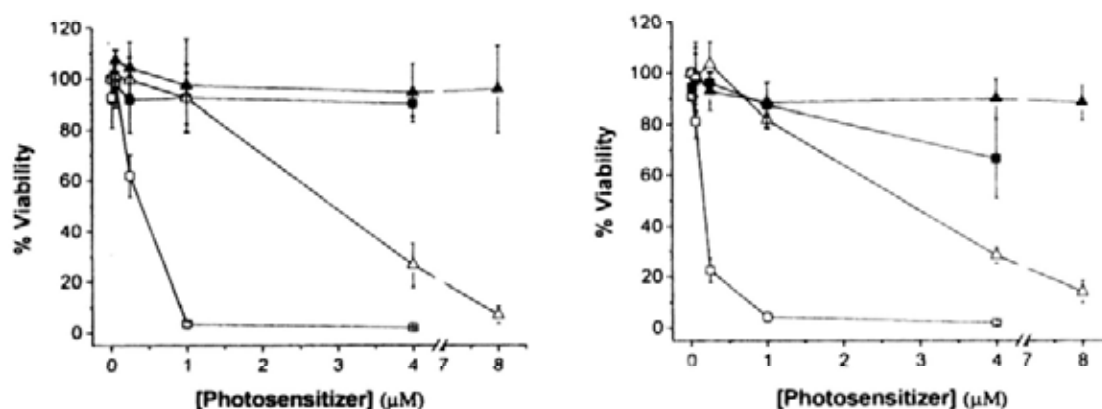


Figure 3.5. Effects of **3.4a** (squares) and **3.7a** (triangles) on HT29 (left) and HepG2 (right) cells in the absence (closed symbols) and presence (open symbols) of light ($\lambda > 610 \text{ nm}$, 40 mW cm^{-2} , 48 J cm^{-2}). Data are expressed as mean values \pm S.E.M. of three independent experiments, each performed in quadruplicate.

Table 3.2. IC₅₀ values of **3.4a-3.4d** and **3.7a-3.7b** against HT29 and HepG2 cells.

| Compound | IC ₅₀ (μM) | |
|-------------|-----------------------|-----------|
| | For HT29 | For HepG2 |
| 3.4a | 0.41 | 0.16 |
| 3.4b | 0.13 | 0.06 |
| 3.4c | 0.40 | 0.40 |
| 3.4d | 0.38 | 0.17 |
| 3.7a | 2.93 | 2.76 |
| 3.7b | 5.18 | 5.84 |

It is worth noting that although the benzo-fused phthalocyanines **3.7a-3.7b** exhibit a higher efficiency in generating singlet oxygen in DMF, their photocytotoxicity is significantly lower than that of **3.4a-3.4d**. To account for these results, the absorption spectra of these compounds in the culture media were examined. Figure 3.6 shows the spectra of **3.4a** and **3.7a** in the DMEM medium (used for HT29), which are typical for these two groups of compounds. It can be seen that the Q band for **3.4a** remains sharp and intense, while that for **3.7a** is significantly weaker and broadened. Similar results were observed in the RPMI medium (used for HepG2) (Figure 3.7). The results indicate that compound **3.7a** (as well as **3.7b**), having a larger π -conjugated system, is more aggregated than **3.4a** (as well as **3.4b-3.4d**) in the culture media, thereby reducing its photosensitizing efficiency.

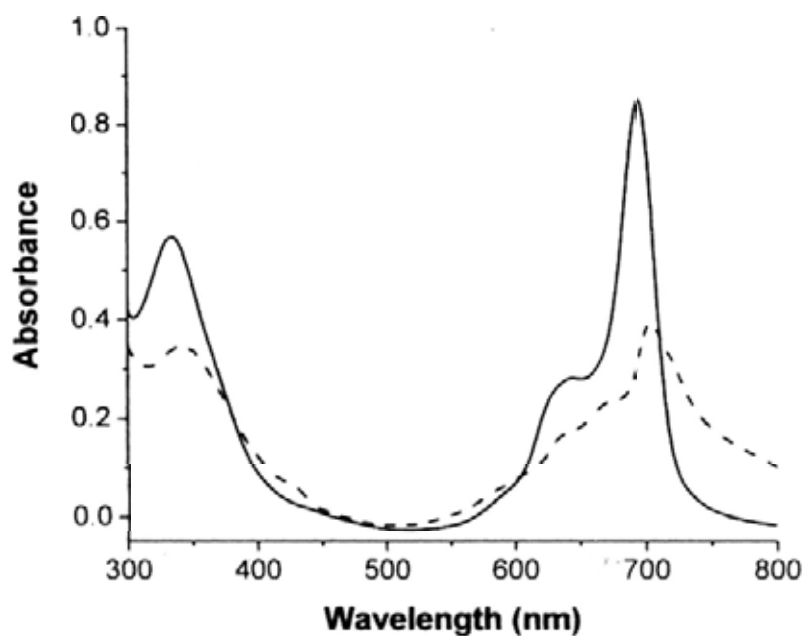


Figure 3.6. Electronic absorption spectra of **3.4a** (—) and **3.7a** (---), formulated with Cremophor EL, in the DMEM culture medium (both at 8 μ M).

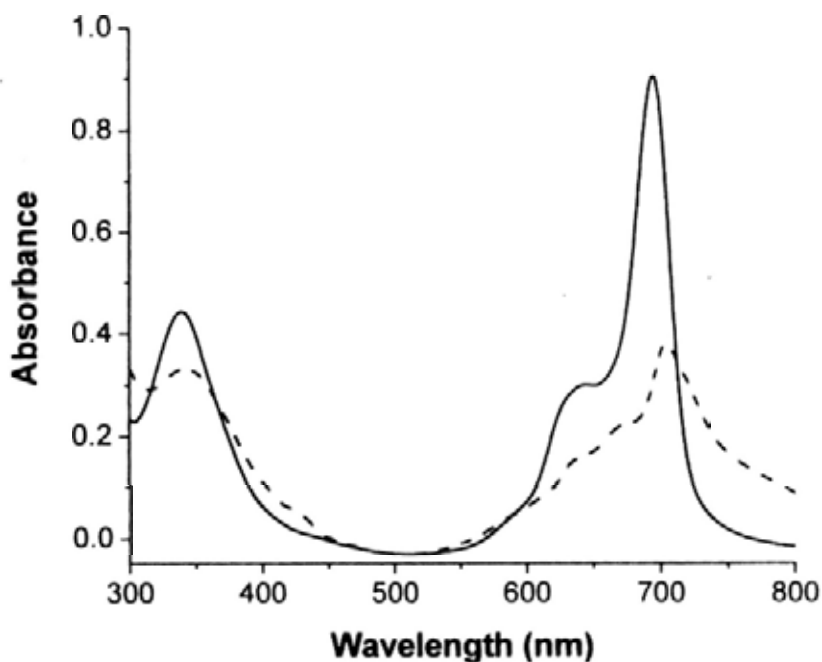


Figure 3.7. Electronic absorption spectra of **3.4a** (—) and **3.7a** (---), formulated with Cremophor EL, in the RPMI culture medium (both at 8 μ M).

The cellular uptake of these phthalocyanines was also investigated by fluorescence microscopy. After being incubated with the dyes **3.4a-3.4d** for 2 h and upon excitation, the HT29 cells showed a strong intracellular fluorescence image throughout the cytoplasm with similar brightness (Figure 3.8), indicating that there were substantial uptakes of these dyes. However, the intensity was much weaker when the dyes **3.7a-3.7b** were used. Hence, the lower photocytotoxicity of **3.7a-3.7b** may be attributed to their higher aggregation tendency in the biological media and/or lower cellular uptake.

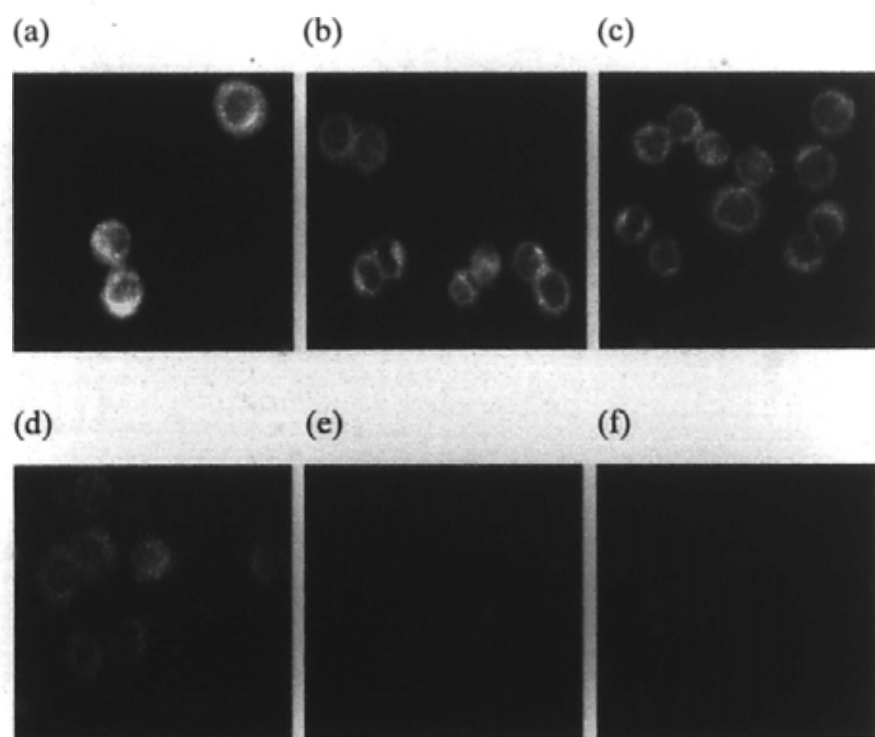


Figure 3.8. Visualization of intracellular fluorescences of HT29 after incubation with (a) **3.4a**, (b) **3.4b**, (c) **3.4c**, (d) **3.4d**, (e) **3.7a**, and (f) **3.7b** for 2 h.

3.3 Conclusion

In summary, I have prepared and characterized a new series of di- α -substituted zinc(II) phthalocyanine derivatives. These relatively rare substituted phthalocyanines possess a high solubility, low aggregation tendency, and high efficiency in generating singlet oxygen, rendering them to be useful as photosensitizers. The two substituents adding at the α positions also shift the Q-band absorption to the red, which is desirable for PDT application. Addition of a fused benzene ring, however, promotes aggregation of the macrocycles in biological media, resulting in a lower photocytotoxicity.

3.4 Experimental Section

3.4.1 General

Experimental details regarding the purification of solvents, instrumentation and in vitro studies were described in Section 2.4. The tosylates **3.2a**,¹¹ **2.2**,¹² and **3.2c**,¹³ and 1,4-dihydroxy-2,3-naphthalonitrile (**3.5**)¹⁴ were prepared as described.

3.4.2 Synthesis

3,6-Bis(8-hydroxy-3,6-dioxaoctoxy)phthalonitrile (3.3a). A mixture of 2,3-dicyanohydroquinone (2.40 g, 15.0 mmol), tosylate **3.2a** (9.12 g, 30.0 mmol), and K_2CO_3 (4.14 g, 30.0 mmol) in DMF (20 mL) was stirred at 90 °C under an atmosphere of nitrogen for 24 h. The volatiles were removed in vacuo. The residue was mixed with water (100 mL), then extracted with CH_2Cl_2 (80 mL \times 3). The

combined organic extracts were dried over anhydrous MgSO_4 and then evaporated to dryness under reduced pressure. The residue was chromatographed on a silica gel column using $\text{CHCl}_3/\text{CH}_3\text{OH}$ (100:1 v/v) as the eluent. The product was obtained as a white solid (5.02 g, 79%). M.p. 78.4-79.0 °C. ^1H NMR (300 MHz, DMSO-d_6): δ 7.64 (s, 2 H, ArH), 4.58 (t, $J = 5.4$ Hz, 2 H, OH), 4.30 (vt, $J = 4.5$ Hz, 4 H, CH_2), 3.77 (vt, $J = 4.5$ Hz, 4 H, CH_2), 3.59-3.62 (m, 4 H, CH_2), 3.51-3.54 (m, 4 H, CH_2), 3.46 (t, $J = 4.8$ Hz, 4 H, CH_2), 3.39-3.42 (m, 4 H, CH_2); $^{13}\text{C}\{^1\text{H}\}$ NMR (75.4 MHz, CDCl_3): δ 155.4, 119.4, 113.0, 105.4, 72.4, 71.1, 70.3, 70.1, 69.4, 61.6; MS (ESI): m/z 447 (100%, $[\text{M} + \text{Na}]^+$); HRMS (ESI) calcd for $\text{C}_{20}\text{H}_{28}\text{N}_2\text{NaO}_8$ $[\text{M} + \text{Na}]^+$ 447.1738, found: 447.1745. Anal. Calcd for $\text{C}_{21}\text{H}_{32}\text{N}_2\text{O}_9$ (**3.3a**· CH_3OH): C, 55.25; H, 7.07; N, 6.14. Found: C, 55.33; H, 6.73; N, 6.30.

3,6-Bis(3,6,9-trioxadecoxy)phthalonitrile (3.3b). According to the above procedure, 2,3-dicyanohydroquinone (1.60 g, 10.0 mmol) was treated with tosylate **2.2** (6.36 g, 20.0 mmol) and K_2CO_3 (2.76 g, 20.0 mmol) to give phthalonitrile **3.3b** as a white solid (3.81 g, 84%). M.p. 49.6-50.2 °C. ^1H NMR (300 MHz, CDCl_3): δ 7.25 (s, 2 H, ArH), 4.24 (t, $J = 4.8$ Hz, 4 H, CH_2), 3.90 (t, $J = 4.8$ Hz, 4 H, CH_2), 3.74-3.77 (m, 4 H, CH_2), 3.64-3.69 (m, 8 H, CH_2), 3.54-3.57 (m, 4 H, CH_2), 3.38 (s, 6 H, CH_3); $^{13}\text{C}\{^1\text{H}\}$ NMR (75.4 MHz, CDCl_3): δ 155.3, 119.2, 112.9, 105.5, 71.9, 71.0, 70.6, 70.5, 70.1, 69.4, 59.0; MS (ESI): m/z 475 (100%, $[\text{M} + \text{Na}]^+$); HRMS (ESI) calcd for $\text{C}_{22}\text{H}_{32}\text{N}_2\text{NaO}_8$ $[\text{M} + \text{Na}]^+$ 475.2051, found: 475.2046. Anal. Calcd for $\text{C}_{22}\text{H}_{32}\text{N}_2\text{O}_8$: C, 58.40; H, 7.13; N, 6.19. Found: C, 58.60; H, 7.06; N, 6.15.

3,6-Bis(2,2-dimethyl-1,3-dioxol-4-ylmethoxy)phthalonitrile (3.3c). According

to the above procedure, 2,3-dicyanohydroquinone (4.27 g, 26.7 mmol) was treated with tosylate **3.2c** (15.28 g, 53.4 mmol) and K_2CO_3 (7.45 g, 53.9 mmol) to give **3.3c** as a white solid (8.97 g, 86%). M.p. 174.5-175.4 °C. 1H NMR (300 MHz, $CDCl_3$): δ 7.24 (s, 2 H, ArH), 4.44-4.53 (m, 2 H, CH), 4.13-4.22 (m, 4 H, CH), 4.05-4.10 (m, 2 H, CH), 3.97-4.02 (m, 2 H, CH), 1.44 (s, 6 H, CH_3), 1.39 (s, 6 H, CH_3); $^{13}C\{^1H\}$ NMR (75.4 MHz, $CDCl_3$): δ 155.0, 118.9, 112.6, 110.0, 105.8, 73.5, 70.2, 66.4, 26.7, 25.2; MS (ESI): m/z 411 (100%, $[M + Na]^+$); HRMS (ESI) calcd for $C_{20}H_{24}N_2NaO_6$ $[M + Na]^+$ 411.1527, found: 411.1532. Anal. Calcd for $C_{20}H_{24}N_2O_6$: C, 61.85; H, 6.23; N, 7.21. Found: C, 61.80; H, 6.33; N, 6.96.

[1,4-Bis(8-hydroxy-3,6-dioxaoctoxy)phthalocyaninato]zinc(II) (**3.4a**). A mixture of phthalonitrile **3.3a** (0.50 g, 1.2 mmol), unsubstituted phthalonitrile (1.36 g, 10.6 mmol), and $Zn(OAc)_2 \cdot 2H_2O$ (0.65 g, 3.0 mmol) in *n*-pentanol (15 mL) was heated to 100 °C, then DBU (1 mL) was added. The mixture was stirred at 140-150 °C for 24 h. After a brief cooling, the volatiles were removed under reduced pressure. The residue was dissolved in $CHCl_3$ (150 mL), then filtered to remove the unsubstituted zinc(II)-phthalocyanine formed. The filtrate was collected and evaporated to dryness in vacuo. The residue was purified by silica gel column chromatography using $CHCl_3/MeOH$ (30:1 v/v) as the eluent, followed by size exclusion chromatography using THF as the eluent. The crude product was further purified by recrystallization from a mixture of THF and hexane to give phthalocyanine **3.4a** as a blue solid (0.19 g, 18%). 1H NMR (300 MHz, $CDCl_3$ with a trace amount of pyridine- d_5): δ 9.37-9.41 (m, 4 H, Pc- H_a), 9.25 (d, $J = 6.0$ Hz, 2 H,

Pc-H_α), 8.06-8.15 (m, 6 H, Pc-H_β), 7.39 (s, 2 H, Pc-H_β), 4.91 (t, $J = 4.8$ Hz, 4 H, CH₂), 4.49 (t, $J = 4.8$ Hz, 4 H, CH₂), 4.11-4.15 (m, 4 H, CH₂), 3.85-3.88 (m, 4 H, CH₂), 3.68-3.71 (m, 4 H, CH₂), 3.63-3.66 (m, 4 H, CH₂); ¹³C{¹H} NMR (75.4 MHz, CDCl₃ with a trace amount of pyridine-d₅): δ 153.8, 153.7, 153.5, 152.4, 150.2, 138.7, 138.4, 128.9, 128.8, 127.2, 122.6, 122.4, 114.9, 72.7, 71.0, 70.4, 69.1, 61.3 (some of the Pc and chain signals are overlapped); MS (ESI): an isotopic cluster peaking at m/z 873 (100%, [M + H]⁺); HRMS (ESI) calcd for C₄₄H₄₁N₈O₈Zn [M + H]⁺ 873.2333, found: 873.2342. Anal. Calcd for C₄₄H₄₀N₈O₈Zn: C, 60.45; H, 4.61; N, 12.82. Found: C, 60.49; H, 4.24; N, 12.83.

[1,4-Bis(3,6,9-trioxadecoxy)phthalocyaninato]zinc(II) (3.4b). According to the above procedure, phthalonitrile **3.3b** (0.50 g, 1.1 mmol) was treated with unsubstituted phthalonitrile (1.28 g, 10.0 mmol) and Zn(OAc)₂·2H₂O (0.61 g, 2.8 mmol) to give **3.4b** as a blue solid (0.12 g, 12%). ¹H NMR (300 MHz, CDCl₃ with a trace amount of pyridine-d₅): δ 9.41-9.49 (m, 6 H, Pc-H_α), ~~8.15-8.18~~ (m, 6 H, Pc-H_β), 7.58 (s, 2 H, Pc-H_β), 4.98 (t, $J = 5.1$ Hz, 4 H, CH₂), 4.56 (t, $J = 5.1$ Hz, 4 H, CH₂), 4.15-4.18 (m, 4 H, CH₂), 3.86-3.89 (m, 4 H, CH₂), 3.69-3.72 (m, 4 H, CH₂), 3.52-3.55 (m, 4 H, CH₂), 3.35 (s, 6 H, CH₃); ¹³C{¹H} NMR (75.4 MHz, CDCl₃ with a trace amount of pyridine-d₅): δ 153.5, 153.4, 153.3, 152.2, 150.0, 138.7, 138.3, 138.2, 128.7, 127.0, 122.5, 122.3, 114.6, 71.8, 71.0, 70.7, 70.5 70.4, 68.9, 58.9 (some of the Pc signals are overlapped); MS (ESI): an isotopic cluster peaking at m/z 901 (100%, [M + H]⁺); HRMS (ESI) calcd for C₄₆H₄₅N₈O₈Zn [M + H]⁺ 901.2646, found: 901.2645. Anal. Calcd for C₄₆H₄₄N₈O₈Zn: C, 61.23; H, 4.92; N, 12.42. Found: C,

61.21; H, 5.02; N, 12.04.

[1,4-Bis(2,2-dimethyl-1,3-dioxol-4-ylmethoxy)phthalocyaninato]zinc(II)

(3.4c). According to the above procedure, phthalonitrile **3.3c** (0.50 g, 1.3 mmol) was treated with unsubstituted phthalonitrile (1.49 g, 11.6 mmol) and $\text{Zn}(\text{OAc})_2 \cdot 2\text{H}_2\text{O}$ (0.71 g, 3.2 mmol) to give phthalocyanine **3.4c** as a blue solid (0.17 g, 16%). ^1H NMR (300 MHz, CDCl_3 with a trace amount of pyridine- d_5): δ 9.32-9.37 (m, 4 H, Pc- H_a), 9.13 (d, $J = 7.2$ Hz, 2 H, Pc- H_a), 8.00-8.13 (m, 6 H, Pc- H_β), 7.22 (d, $J = 8.1$ Hz, 2 H, Pc- H_β), 5.14-5.24 (m, 2 H, CH), 4.73-4.85 (m, 2 H, CH), 4.57-4.72 (m, 4 H, CH), 4.45-4.51 (m, 2 H, CH), 1.72 (s, 6 H, CH_3), 1.66 (s, 6 H, CH_3); $^{13}\text{C}\{^1\text{H}\}$ NMR (75.4 MHz, CDCl_3 with a trace amount of pyridine- d_5): δ 153.5, 153.4, 153.0, 151.7, 149.7, 138.7, 138.3, 128.7, 126.8, 122.4, 122.3, 122.2, 114.0, 113.9, 109.8, 74.8, 70.3, 67.3, 27.0, 25.6 (some of the Pc signals are overlapped); MS (ESI): an isotopic cluster peaking at m/z 837 (100%, $[\text{M} + \text{H}]^+$); HRMS (ESI) calcd for $\text{C}_{44}\text{H}_{37}\text{N}_8\text{O}_6\text{Zn}$ $[\text{M} + \text{H}]^+$ 837.2122, found: 837.2133. Anal. Calcd for $\text{C}_{44}\text{H}_{36}\text{N}_8\text{O}_6\text{Zn}$: C, 63.05; H, 4.33; N, 13.37. Found: C, 63.32; H, 4.49; N, 13.05.

[1,4-Bis(2,3-dihydroxypropoxy)phthalocyaninato]zinc(II) **(3.4d).** A

solution of phthalocyanine **3.4c** (60 mg, 0.07 mmol) in TFA/ H_2O (9:1 v/v) (4 mL) was stirred at room temperature for 30 min. The volatiles were then removed under reduced pressure. The residue was dissolved in a mixture of THF (2 mL) and methanol (4 mL), then hexane (8 mL) was added to induce precipitation. The mixture was filtered to give a blue solid which was dried in vacuo (46 mg, 85%). ^1H NMR (300 MHz, $\text{DMSO}-d_6$): δ 9.32-9.41 (m, 6 H, Pc- H_a), 8.19-8.26 (m, 6 H, Pc- H_β), 7.77

(s, 2 H, Pc-H β), 5.56 (d, $J = 4.5$ Hz, 2 H, OH), 4.96 (t, $J = 5.7$ Hz, 2 H, OH), 4.66-4.77 (m, 4 H, CH), 4.46-4.51 (m, 2 H, CH), 4.16-4.24 (m, 2 H, CH), 4.00-4.08 (m, 2 H, CH); $^{13}\text{C}\{^1\text{H}\}$ NMR (75.4 MHz, DMSO- d_6): δ 153.1, 152.9, 152.7, 150.6, 138.4, 138.1, 138.0, 129.5, 129.6, 129.7, 126.7, 123.1, 122.6, 116.5, 71.7, 70.9, 63.4 (some of the Pc signals are overlapped); MS (ESI): an isotopic cluster peaking at m/z 757 (100%, $[\text{M} + \text{H}]^+$); HRMS (ESI) calcd for $\text{C}_{38}\text{H}_{29}\text{N}_8\text{O}_6\text{Zn}$ $[\text{M} + \text{H}]^+$ 757.1496, found: 757.1480.

1,4-Bis(8-hydroxy-3,6-dioxaoctoxy)-2,3-naphthalonitrile (3.6a). A mixture of 1,4-dihydroxy-2,3-naphthalonitrile (**3.5**) (1.26 g, 6.0 mmol), tosylate **3.2a** (3.65 g, 12.0 mmol), and anhydrous K_2CO_3 (1.66 g, 12.0 mmol) in DMF (12 mL) was stirred vigorously at 90 °C for 24 h. The volatiles were then removed under reduced pressure. The residue was mixed with water (60 mL) and the mixture was extracted with chloroform (60 mL x 3). The combined organic extracts were dried over anhydrous MgSO_4 and evaporated to dryness under reduced pressure. The residue was subject to silica gel column chromatography using $\text{CHCl}_3/\text{CH}_3\text{OH}$ (60:1 v/v) as the eluent. Compound **3.6a** was obtained as a brown oil (2.53 g, 89%). ^1H NMR (300 MHz, CDCl_3): δ 8.38 (dd, $J = 3.3, 6.3$ Hz, 2 H, ArH), 7.79 (dd, $J = 3.3, 6.3$ Hz, 2 H, ArH), 4.57-4.60 (m, 4 H, CH_2), 3.96-3.99 (m, 4 H, CH_2), 3.68-3.77 (m, 12 H, CH_2), 3.58-3.61 (m, 4 H, CH_2), 2.49 (br s, 2 H, OH); $^{13}\text{C}\{^1\text{H}\}$ NMR (75.4 MHz, CDCl_3): δ 157.5, 130.7, 130.3, 123.9, 114.2, 99.6, 75.1, 72.4, 70.7, 70.2, 70.1, 61.6; MS (ESI): m/z 497 (100%, $[\text{M} + \text{Na}]^+$); HRMS (ESI) calcd for $\text{C}_{24}\text{H}_{30}\text{N}_2\text{NaO}_8$ $[\text{M} + \text{Na}]^+$ 497.1894, found: 497.1893.

1,4-Bis(3,6,9-trioxadecoxy)-2,3-naphthalonitrile (3.6b). According to the above procedure, 1,4-dihydroxy-2,3-naphthalonitrile (**3.5**) (0.63 g, 3.0 mmol) was treated with tosylate **2.2** (1.91 g, 6.0 mmol) and K_2CO_3 (0.83 g, 6.0 mmol) to give **3.6b** as a brown oil (1.31 g, 87%). 1H NMR (300 MHz, $CDCl_3$): δ 8.41 (dd, $J = 3.3, 6.3$ Hz, 2 H, ArH), 7.78 (dd, $J = 3.3, 6.3$ Hz, 2 H, ArH), 4.58 (vt, $J = 4.5$ Hz, 4 H, CH_2), 3.96 (vt, $J = 4.5$ Hz, 4 H, CH_2), 3.74-3.77 (m, 4 H, CH_2), 3.64-3.70 (m, 8 H, CH_2), 3.53-3.57 (m, 4 H, CH_2), 3.38 (s, 6 H, CH_3); $^{13}C\{^1H\}$ NMR (75.4 MHz, $CDCl_3$): δ 157.6, 130.6, 130.4, 124.1, 114.3, 99.6, 75.2, 71.9, 70.8, 70.6, 70.5, 70.1, 59.0; MS (ESI): m/z 525 (100%, $[M + Na]^+$); HRMS (ESI) calcd for $C_{26}H_{34}N_2NaO_8 [M + Na]^+$ 525.2207, found: 525.2210.

Benzo-fused phthalocyanine 3.7a. According to the procedure described for **3.4a**, naphthalonitrile **3.6a** (0.60 g, 1.3 mmol) was treated with unsubstituted phthalonitrile (1.46 g, 11.4 mmol) and $Zn(OAc)_2 \cdot 2H_2O$ (0.70 g, 3.2 mmol) to give **3.7a** as a green solid (0.17 g, 15%). 1H NMR (300 MHz, $CDCl_3$ with a trace amount of pyridine- d_5): δ 9.20-9.35 (m, 6 H, Pc- H_a), 9.02-9.06 (m, 2 H, Np- H_a), 7.98-8.09 (m, 6 H, Pc- H_b), 7.87-7.90 (m, 2 H, Np- H_b), 5.63 (vt, $J = 4.5$ Hz, 4 H, CH_2), 4.45 (vt, $J = 4.5$ Hz, 4 H, CH_2), 4.02-4.05 (m, 4 H, CH_2), 3.90-3.94 (m, 4 H, CH_2), 3.81-3.85 (m, 4 H, CH_2), 3.74-3.77 (m, 4 H, CH_2); $^{13}C\{^1H\}$ NMR (75.4 MHz, $CDCl_3$ with a trace amount of pyridine- d_5): δ 154.1, 154.0, 152.6, 152.3, 148.5, 138.3, 138.2, 137.9, 130.8, 129.0, 128.8, 128.5, 127.3, 125.6, 124.3, 122.5, 122.4, 122.2, 74.2, 72.8, 71.4, 71.0, 70.6, 61.6; MS (ESI): an isotopic cluster peaking at m/z 945 (100%, $[M + Na]^+$); HRMS (ESI) calcd for $C_{48}H_{42}N_8NaO_8Zn [M + Na]^+$ 945.2309, found: 945.2297. Anal.

Calcd for $C_{49}H_{46}N_8O_9Zn$ (**3.7a**·CH₃OH): C, 61.54; H, 4.85; N, 11.72. Found: C, 61.66; H, 4.80; N, 11.67.

Benzo-fused phthalocyanine 3.7b. According to the procedure described for **3.4a**, naphthalonitrile **3.6b** (0.44 g, 0.9 mmol) was treated with unsubstituted phthalonitrile (1.01 g, 7.9 mmol) and Zn(OAc)₂·2H₂O (0.48 g, 2.2 mmol) to give **3.7b** as a green solid (0.11 g, 13%). ¹H NMR (300 MHz, CDCl₃ with a trace amount of pyridine-d₅): δ 9.41 (dd, *J* = 2.7, 5.7 Hz, 2 H, Pc-H_a), 9.37 (dd, *J* = 2.7, 5.7 Hz, 2 H, Pc-H_a), 9.29 (dd, *J* = 3.0, 5.4 Hz, 2 H, Pc-H_a), 9.08 (dd, *J* = 3.3, 6.3 Hz, 2 H, Np-H_a), 8.09-8.15 (m, 4 H, Pc-H_β), 8.04 (dd, *J* = 2.7, 5.7 Hz, 2 H, Pc-H_β), 7.91 (dd, *J* = 3.3, 6.3 Hz, 2 H, Np-H_β), 5.64 (vt, *J* = 4.5 Hz, 4 H, CH₂), 4.46 (vt, *J* = 4.5 Hz, 4 H, CH₂), 4.04-4.07 (m, 4 H, CH₂), 3.91-3.94 (m, 4 H, CH₂), 3.79-3.82 (m, 4 H, CH₂), 3.61-3.65 (m, 4 H, CH₂), 3.41 (s, 6 H, CH₃); ¹³C{¹H} NMR (75.4 MHz, CDCl₃ with a trace amount of pyridine-d₅): δ 154.3, 154.2, 152.8, 152.4, 148.7, 138.4, 138.3, 137.9, 130.9, 129.0, 128.9, 128.6, 127.3, 125.7, 124.4, 122.6, 122.5, 122.2, 74.3, 71.9, 71.3, 71.0, 70.8, 70.6, 59.0; MS (ESI): an isotopic cluster peaking at *m/z* 951 (100%, [M + H]⁺); HRMS (ESI) calcd for C₅₀H₄₇N₈O₈Zn [M + H]⁺ 951.2803, found: 951.2805. Anal. Calcd for C₅₁H₅₀N₈O₉Zn (**3.7b**·CH₃OH): C, 62.23; H, 5.12; N, 11.38. Found: C, 61.69; H, 4.90; N, 11.44.

3.5 References

- (a) Ali, H.; van Lier, J. E. *Chem. Rev.* **1999**, *99*, 2379. (b) Lukyanets, E. A. *J. Porphyrins Phthalocyanines* **1999**, *3*, 424. (c) Allen, C. M.; Sharman, W. M.; van Lier, J. E. *J. Porphyrins Phthalocyanines* **2001**, *5*, 161. (d) Tedesco, A. C.; Rotta,

- J. C. G.; Lunardi, C. N. *Curr. Org. Chem.* **2003**, *7*, 187.
2. (a) Lo, P.-C.; Chan, C. M. H.; Liu, J.-Y.; Fong, W.-P.; Ng, D. K. P. *J. Med. Chem.* **2007**, *50*, 2100 and references cited therein. (b) Liu, J.-Y.; Jiang, X.-J.; Fong, W.-P.; Ng, D. K. P. *Metal-Based Drugs* **2008**, Article ID 284691. (c) Leung, S. C. H.; Lo, P.-C.; Ng, D. K. P.; Liu, W.-K.; Fung, K.-P.; Fong, W.-P. *Br. J. Pharm.* **2008**, *154*, 4. (d) Choi, C.-F.; Huang, J.-D.; Lo, P.-C.; Fong, W.-P.; Ng, D. K. P. *Org. Biomol. Chem.* **2008**, *6*, 2173. (e) Lo, P.-C.; Fong, W.-P.; Ng, D. K. P. *ChemMedChem* **2008**, *3*, 1110.
 3. See for example: (a) Nishiyama, N.; Iriyama, A.; Jang, W.-D.; Miyata, K.; Itaka, K.; Inoue, Y.; Takahashi, H.; Yanagi, Y.; Tamaki, Y.; Koyama, H.; Kataoka, K. *Nature Mater.* **2005**, *4*, 934. (b) Sharman, W. M.; van Lier, J. E. *Bioconjugate Chem.* **2005**, *16*, 1166. (c) Hofman, J.-W.; van Zeeland, F.; Turker, S.; Talsma, H.; Lambrechts, S. A. G.; Sakharov, D. V.; Hennink, W. E.; van Nostrum, C. F. *J. Med. Chem.* **2007**, *50*, 1485. (d) Sibrian-Vazquez, M.; Ortiz, J.; Nesterova, I. V.; Fernández-Lázaro, F.; Sastre-Santos, A.; Soper, S. A.; Vicente, M. G. H. *Bioconjugate Chem.* **2007**, *18*, 410. (e) Li, H.; Jensen, T. J.; Fronczek, F. R.; Vicente, M. G. H. *J. Med. Chem.* **2008**, *51*, 502.
 4. (a) Kobayashi, N.; Sasaki, N.; Higashi, Y.; Osa, T. *Inorg. Chem.* **1995**, *34*, 1636. (b) Kobayashi, N.; Ogata, H.; Nonaka, N.; Luk'yanets, E. A. *Chem. Eur. J.* **2003**, *9*, 5123.
 5. (a) Fukuda, T.; Homma, S.; Kobayashi, N. *Chem. Eur. J.* **2005**, *11*, 5205. (b) Maqanda, W.; Nyokong, T.; Maree, M. D. *J. Porphyrins Phthalocyanines* **2005**, *9*, 343. (c) Li, H.; Fronczek, F. R.; Vicente, M. G. H. *Tetrahedron Lett.* **2008**, *49*, 4828.
 6. (a) Stolnik, S.; Illum, L.; Davis, S. S. *Adv. Drug Deliv. Rev.* **1995**, *16*, 195. (b) Torchilin, V. P. *Pharm. Res.* **2007**, *24*, 1. (c) van Vlerken, L. E.; Vyas, T. K.; Amiji, M. M. *Pharm. Res.* **2007**, *24*, 1405.
 7. MacDonald, I. J.; Dougherty, T. J. *J. Porphyrins Phthalocyanines* **2001**, *5*, 105.
 8. Lo, P.-C.; Zhao, B.; Duan, W.; Fong, W.-P.; Ko, W.-H.; Ng, D. K. P. *Bioorg. Med. Chem. Lett.* **2007**, *17*, 1073.

9. Choi, C.-F.; Tsang, P.-T.; Huang, J.-D.; Chan, E. Y. M.; Ko, W.-H.; Fong, W.-P.; Ng, D. K. P. *Chem. Commun.* **2004**, 2236.
10. (a) Lo, P.-C.; Huang, J.-D.; Cheng, D. Y. Y.; Chan, E. Y. M.; Fong, W.-P.; Ko, W.-H.; Ng, D. K. P. *Chem. Eur. J.* **2004**, *10*, 4831. (b) Lo, P.-C.; Leung, S. C. H.; Chan, E. Y. M.; Fong, W.-P.; Ko, W.-H.; Ng, D. K. P. *Photodiag. Photodyn. Ther.* **2007**, *4*, 117.
11. Zhu, X.-Z.; Chen, C.-F. *J. Am. Chem. Soc.* **2005**, *127*, 13158.
12. Snow, A. W.; Foos, E. E. *Synthesis* **2003**, 509.
13. Bradshaw, J. S.; Huszthy, P.; McDaniel, C. W. *J. Org. Chem.* **1990**, *55*, 3129.
14. Reynolds, G. A.; Vanallan, J. A. *J. Org. Chem.* **1964**, *29*, 3591.

Chapter 4

Highly Photocytotoxic 1,4-Dipegylated Zinc(II) Phthalocyanines. Effects of the Chain Length on the in vitro Photodynamic Activities

4.1 Introduction

In Chapter 3, I describe the preparation and in vitro photodynamic activities of a novel series of di- α -substituted zinc(II) phthalocyanines. Compared with the unsubstituted zinc(II) phthalocyanine, these di- α -substituted analogues exhibit a red-shifted Q band, a relatively weaker fluorescence emission, and a higher efficiency to generate singlet oxygen. Upon illumination, these compounds are highly cytotoxic toward HT29 and HepG2 cells. As a continuing effort in this endeavour, I report herein a new series of zinc(II) phthalocyanines having two diethylene glycol to polyethylene glycol methyl ether chains at the 1,4-di- α -positions, including their synthesis, spectroscopic and photophysical properties, as well as the in vitro photodynamic activities. The effects of the chain length on these properties have also been examined.

4.2 Results and Discussion

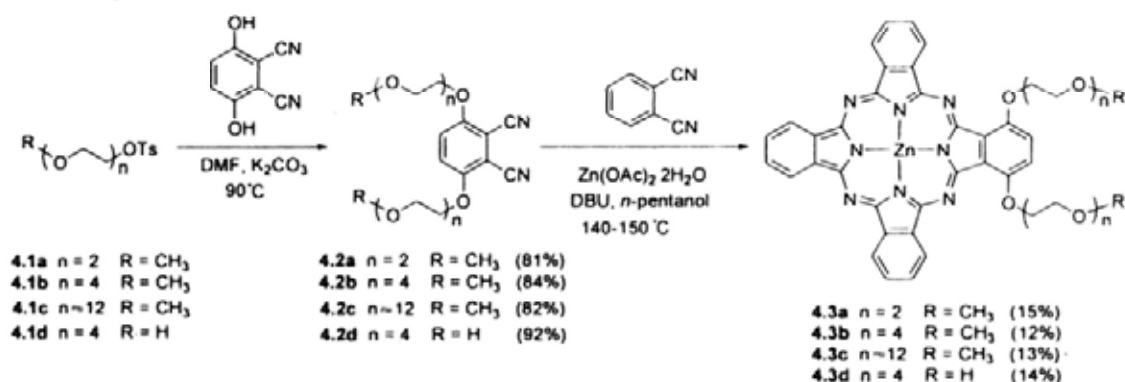
4.2.1 Molecular Design and Synthesis

Although a vast number of phthalocyanines have been reported, to my

knowledge, these 1,4-disubstituted analogues remain relatively rare.¹ Compared with the unsubstituted ZnPc, they exhibit a red-shifted Q band (at ca. 690 vs. 670 nm for ZnPc), which allows a deeper light penetration into tissues.² The two substituents added near the macrocyclic core can also effectively enhance the solubility and reduce the aggregation tendency of the macrocycles. This strategy is different from those reported in literatures such as the introduction of bulky substituents at the axial or peripheral positions,³ and the use of perfluorinated substituents.⁴ All of these characteristics are beneficial for PDT application. Zinc(II) ion was selected as the metal center because of the general robustness and the desirable photophysical properties of these metallo-phthalocyanines.⁵ Polyethylene glycols are also excellent pharmaceutical carriers which can prolong the drugs' circulating half-life, minimize their nonspecific uptake and enable specific tumor-targeting through the enhanced permeability and retention (EPR) effect.⁶ Addition of these hydrophilic chains to the hydrophobic macrocyclic core also imparts a high amphiphilicity to the photosensitizers. Hence, I believed that these specially designed molecules, which fulfill most of the criteria for superior photosensitizers,⁷ would behave ideally. Substituents having different numbers of oxyethylene units were introduced with a view to fine-tuning the photodynamic activities. It is worth noting that although various pegylated photosensitizers have been reported,⁸ the effects of the chain length on their photodynamic activities remain little studied.

Scheme 4.1 shows the synthetic pathway used to prepare phthalocyanines ZnPc[O(CH₂CH₂O)_nMe]₂ [n = 2 (**4.3a**), 4 (**4.3b**), ca. 12 (**4.3c**)], which contain

diethylene glycol to polyethylene glycol methyl ether chains at the 1,4-positions. The synthesis first involves the nucleophilic substitution reaction of tosylates **4.1a-4.1c** with 2,3-dicyanohydroquinone to afford the disubstituted phthalonitriles **4.2a-4.2c**. The tosylate **4.1c** was prepared from the commercially available polyethylene glycol methyl ether having an average molecular weight of 550. These phthalonitriles then underwent mixed cyclization with an excess of unsubstituted phthalonitrile (9 equiv.) in the presence of $\text{Zn}(\text{OAc})_2 \cdot 2\text{H}_2\text{O}$ and DBU in *n*-pentanol to give the respective phthalocyanines **4.3a-4.3c** in 12-15% yield. Although these reactions also afforded the other cyclized products, particularly ZnPc, the isolation of these disubstituted analogues by column chromatography followed by size exclusion chromatography was found to be readily as a result of their high solubility and low aggregation tendency in common organic solvents.

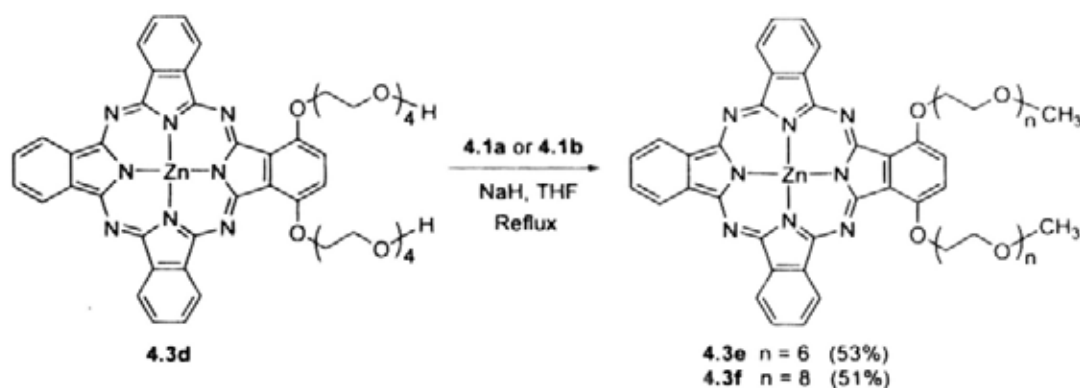


Scheme 4.1. Synthesis of phthalocyanines **4.3a-4.3d**.

This synthetic route can also be applied to prepare the non-methyl protected analogue **4.3d** (Scheme 4.1). Starting from the tetraethylene glycol monotosylate (**4.1d**) and following this reaction sequence, the dihydroxy phthalocyanine

ZnPc[O(CH₂CH₂O)₄H]₂ (**4.3d**) was obtained with comparable yield. The hydroxyl groups could tolerate the conditions for these substitution and cyclization reactions.

This compound was found to be an excellent precursor for other 1,4-disubstituted analogues through transformations of the terminal hydroxyl groups. Thus treatment of **4.3d** with tosylate **4.1a** or **4.1b** in the presence of NaH led to chain elongation giving ZnPc[O(CH₂CH₂O)_nMe]₂ [*n* = 6 (**4.3e**), 8 (**4.3f**)] in moderate yield (Scheme 4.2). With these two procedures, a series of 1,4-disubstituted zinc(II) phthalocyanines having diethylene glycol to polyethylene glycol methyl ether chains were prepared.



Scheme 4.2. Synthesis of phthalocyanines **4.3e** and **4.3f**.

All of the new compounds were fully characterized with various spectroscopic methods. The ¹H NMR spectra of phthalocyanines **4.3a-4.3f** were recorded in CDCl₃ with a trace amount of pyridine-d₅ added to reduce the aggregation of these compounds. Generally, the spectra showed one to two multiplet(s) at the most downfield position (at ca. δ 9.4) for the phthalocyanine α ring protons, and one multiplet (at ca. δ 8.2, 6 H) and a singlet (at ca. δ 7.6, 2 H) for the phthalocyanine β ring protons. For the chains' methylene protons near the phthalocyanine ring, the

signals mostly in a triplet form were shifted downfield significantly (up to ca. δ 5.0) by the ring current. As expected, the length of the chains did not exert a significant influence on the positions of these signals.

The FAB or ESI mass spectra of all of these compounds showed the molecular ion signals. Accurate mass measurements were also performed to confirm the identity of these compounds. In the ESI mass spectrum of **4.3c**, two major envelopes for the protonated $[M + H]^+$ and sodiated $[M + Na]^+$ molecular ions were observed. For both of them, the clusters are separated by 44 mass units corresponding to the molecular mass of the repeating unit of polyethylene glycol.

4.2.2 Electronic Absorption and Photophysical Properties

The electronic absorption spectra of $ZnPc[O(CH_2CH_2O)_nMe]_2$ ($n = 2, 4, 6, 8, ca. 12$) **4.3a-4.3c** and **4.3e-4.3f** were recorded in DMF. The spectra showed typical features of nonaggregated phthalocyanines. They displayed a Soret band at 340 nm, an intense and sharp Q band at 689 nm, together with a vibronic band at 621-622 nm. The data are collected in Table 4.1. To briefly examine the aggregation behavior, the absorption spectra of these compounds in DMF were recorded in different concentrations. Figure 4.1 shows the spectra of **4.3a** as an example. By plotting the Q-band absorbance versus the concentration, a straight line is obtained indicating that compound **4.3a** is essentially free from aggregation under these conditions.

For comparison, the absorption spectra of **4.3a** and **4.3f** in thin solid films were also recorded (Figure 4.2). The Q bands were significantly broadened with a shoulder

at ca. 650 nm. However, the absorption maxima (at ca. 700 nm) were not significantly shifted compared with those in DMF (689 nm). It suggested that the two α -substituents can somewhat reduce the stacking tendency of these compounds even in the solid state.

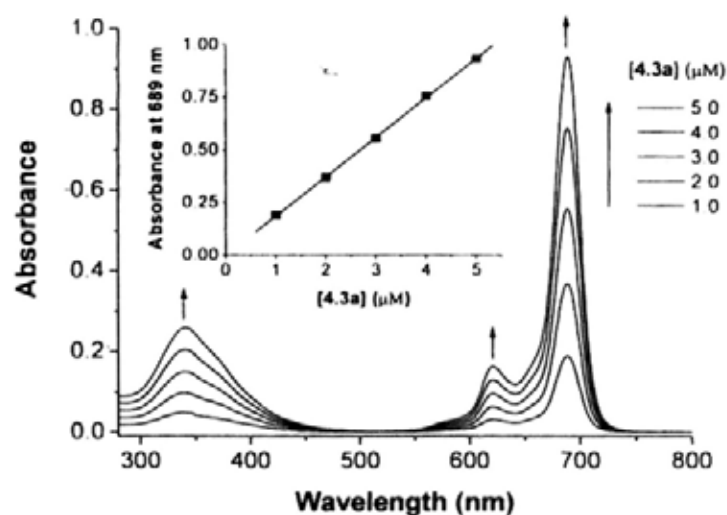


Figure 4.1. Electronic absorption spectra of **4.3a** at different concentrations in DMF. The insert plots the Q-band absorbance at 689 nm versus the concentration of **4.3a**.

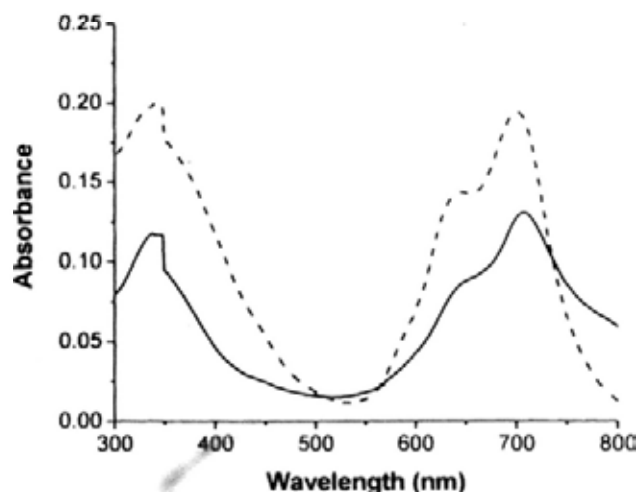


Figure 4.2. Electronic absorption spectra of **4.3a** (—) and **4.3f** (---) in thin solid films.

Upon excitation at 621 nm, these compounds showed a fluorescence emission at 698 nm with a quantum yield of 0.18-0.19 in DMF.

One of the key parameters relating to the photosensitizing efficiency is the singlet oxygen quantum yield. The values for these compounds were determined by steady-state method using 1,3-diphenylisobenzofuran (DPBF) as the scavenger. By plotting its concentration spectroscopically at 411 nm along with time, the values of Φ_{Δ} could be determined as described previously.⁹ Figure 4.3 compares the rates of decay of DPBF using **4.3a-4.3c**, **4.3e-4.3f**, and ZnPc as the photosensitizers. The values of Φ_{Δ} are also compiled in Table 4.1. It can be seen that all of these di- α -substituted phthalocyanines are highly efficient singlet oxygen generators having comparable quantum yields ($\Phi_{\Delta} = 0.81-0.83$). Their efficiency is significantly higher than that of ZnPc, which was used as the reference.

As shown in Table 4.1, this series of compounds have very similar absorption maxima, Φ_F , and Φ_{Δ} showing that the length of the chains does not affect significantly the electronic absorption and photophysical properties of these marocycles in DMF.

Table 4.1. Electronic absorption and photophysical data for phthalocyanines **4.3a-4.3c** and **4.3e-4.3f**.

| Compound | λ_{\max} (nm) (log ϵ) | λ_{em} (nm) ^a | Φ_{F} ^b | Φ_{Δ} ^c |
|---|---|---|--------------------------------|------------------------------|
| ZnPc[O(CH ₂ CH ₂ O) ₂ Me] ₂ (4.3a) | 340 (4.73), 621 (4.52), 689 (5.27) | 698 | 0.18 | 0.83 |
| ZnPc[O(CH ₂ CH ₂ O) ₄ Me] ₂ (4.3b) | 340 (4.77), 621 (4.58), 689 (5.33) | 698 | 0.18 | 0.83 |
| ZnPc[O(CH ₂ CH ₂ O) ₆ Me] ₂ (4.3e) | 340 (4.77), 622 (4.57), 689 (5.31) | 698 | 0.18 | 0.83 |
| ZnPc[O(CH ₂ CH ₂ O) ₈ Me] ₂ (4.3f) | 340 (4.73), 621 (4.53), 689 (5.28) | 698 | 0.18 | 0.82 |
| ZnPc[O(CH ₂ CH ₂ O) _n Me] ₂ (n = ca. 12) (4.3c) | 340 (4.71), 622 (4.48), 689 (5.23) | 698 | 0.19 | 0.81 |

^a Excited at 621 nm. ^b Relative to ZnPc ($\Phi_{\text{F}} = 0.28$ in DMF). ^c Relative to ZnPc ($\Phi_{\Delta} = 0.56$ in DMF).

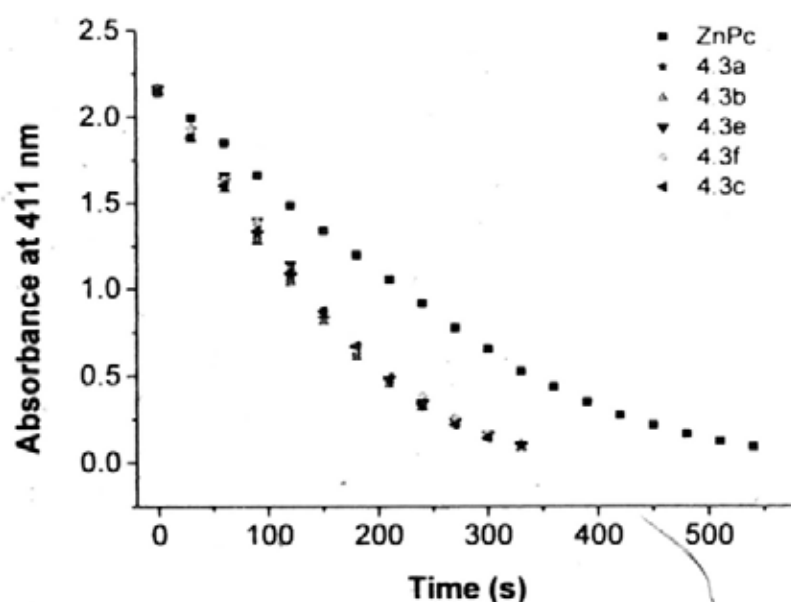


Figure 4.3. Comparison of the rates of decay of DPBF in DMF, as monitored spectroscopically at 411 nm, using phthalocyanines **4.3a-4.3c** and **4.3e-4.3f** as the photosensitizers and ZnPc as the reference.

4.2.3 In vitro Photodynamic Activities

The in vitro photodynamic activities of these phthalocyanines in Cremophor EL emulsions were investigated against HT29 and HepG2 cells. Figure 4.4 compares the effects of these compounds on the two cell lines both in the absence and presence of light. It can be seen that all of these compounds are essentially noncytotoxic in dark, but upon illumination, they exhibit a substantial cytotoxicity. The corresponding IC_{50} values are summarized in Table 4.2. For both of the cell lines, the photocytotoxicity of these compounds depends on the length of the substituents. Figure 4.5 depicts the variation of the IC_{50} values with the number of oxyethylene unit in the chains. For HepG2, the dyes with shorter chains ($n = 2, 4, 6$) are generally more potent than the analogues with longer substituents ($n = 8, ca. 12$). For HT29, compound **4.3e** (with $n = 6$) shows the highest photocytotoxicity. A further increase in the chain length results in a substantial increase in the IC_{50} value. The in vitro photocytotoxicity attained by **4.3e** ($IC_{50} = 0.02 \mu\text{M}$ for HT29) is in fact very high compared with that of the classical photosensitizer porfimer sodium ($IC_{50} = 7.5 \mu\text{g mL}^{-1}$ vs. 23.3 ng mL^{-1} for **4.3e**),¹⁰ pheophorbide α ($IC_{50} = 0.5 \mu\text{M}$),¹⁰ and other mono- and tetrasubstituted zinc(II) phthalocyanines prepared by us recently.^{1,11,12} It is believed that the high potency of **4.3e** is also related to its unique 1,4-di- α -substitution pattern.

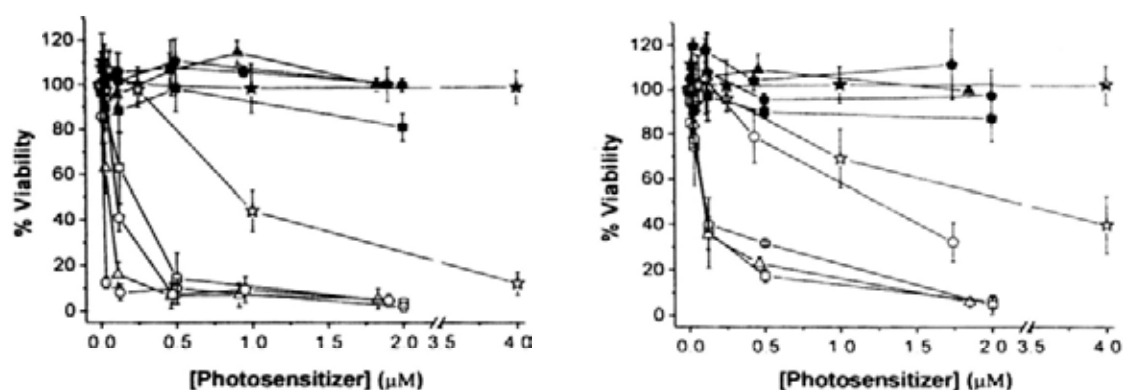


Figure 4.4. Effects of **4.3a** (squares), **4.3b** (triangles), **4.3c** (stars), **4.3e** (circles), and **4.3f** (pentagons) on HT29 (left) and HepG2 (right) cells in the absence (closed symbols) and presence (open symbols) of light ($\lambda > 610$ nm, 40 mW cm^{-2} , 48 J cm^{-2}). Data are expressed as mean values \pm S.E.M. of three independent experiments, each performed in quadruplicate.

Table 4.2. Comparison of the IC_{50} values of phthalocyanines **4.3a-4.3c** and **4.3e-4.3f** against HT29 and HepG2 cells.

| Photosensitizer | IC_{50} (μM) | |
|--|------------------------------------|-------------------------|
| | For HT29 (μM) | HepG2 (μM) |
| ZnPc[O(CH ₂ CH ₂ O) ₂ Me] ₂ (4.3a) | 0.22 | 0.09 |
| ZnPc[O(CH ₂ CH ₂ O) ₄ Me] ₂ (4.3b) | 0.05 | 0.09 |
| ZnPc[O(CH ₂ CH ₂ O) ₆ Me] ₂ (4.3e) | 0.02 | 0.10 |
| ZnPc[O(CH ₂ CH ₂ O) ₈ Me] ₂ (4.3f) | 0.11 | 1.24 |
| ZnPc[O(CH ₂ CH ₂ O) _n Me] ₂ ($n = \text{ca. } 12$) (4.3c) | 0.92 | 2.98 |

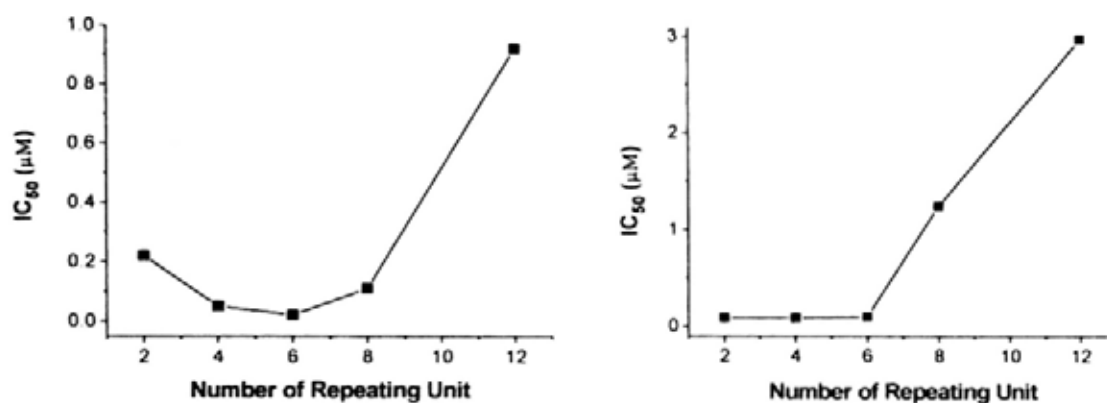


Figure 4.5. The effects of chain length on the photocytotoxicity of phthalocyanines **4.3a-4.3c** and **4.3e-4.3f** for HT29 (left) and HepG2 (right) cells.

To account for the different photodynamic activities of these compounds, their aggregation behavior in the culture media was examined by absorption spectroscopy. Figure 4.6 shows the electronic absorption spectra of these compounds in the DMEM medium used for HT29 cells. It can be seen that the Q bands of $\text{ZnPc}[\text{O}(\text{CH}_2\text{CH}_2\text{O})_4\text{Me}]_2$ (**4.3b**) and $\text{ZnPc}[\text{O}(\text{CH}_2\text{CH}_2\text{O})_6\text{Me}]_2$ (**4.3e**) remain sharp and intense, indicating that these compounds are not significantly aggregated in the medium. The spectrum of $\text{ZnPc}[\text{O}(\text{CH}_2\text{CH}_2\text{O})_2\text{Me}]_2$ (**4.3a**) also has similar spectral features, but the intensity of the Q band is substantially weaker due to its lower solubility in this medium. In fact, precipitation occurred after leaving the solution for ca. 2 h. For $\text{ZnPc}[\text{O}(\text{CH}_2\text{CH}_2\text{O})_8\text{Me}]_2$ (**4.3f**) and $\text{ZnPc}[\text{O}(\text{CH}_2\text{CH}_2\text{O})_n\text{Me}]_2$ ($n = \text{ca. } 12$) (**4.3c**), in addition to the Q band at ca. 700 nm, the blue-shifted Q band at ca. 650 nm attributable to the H-aggregates¹³ becomes more prominent. Hence, for this series of compounds, when the number of oxyethylene unit is larger than 6, the compounds tend to aggregate in the culture medium, probably due to the stronger dipole-dipole

interactions among the side chains. Aggregation provides an efficient nonradiative relaxation pathway thereby reducing the population of triplet state and the singlet oxygen generation efficiency.¹⁴ The different solubility and aggregation tendency of this series of compounds in DMEM can well explain the observed trend of photocytotoxicity (Table 4.2 and Figure 4.5), despite these compounds have virtually the same singlet oxygen quantum yield in DMF (Table 4.1). Similar results were observed in the RPMI medium used for HepG2 (Figure 4.7).

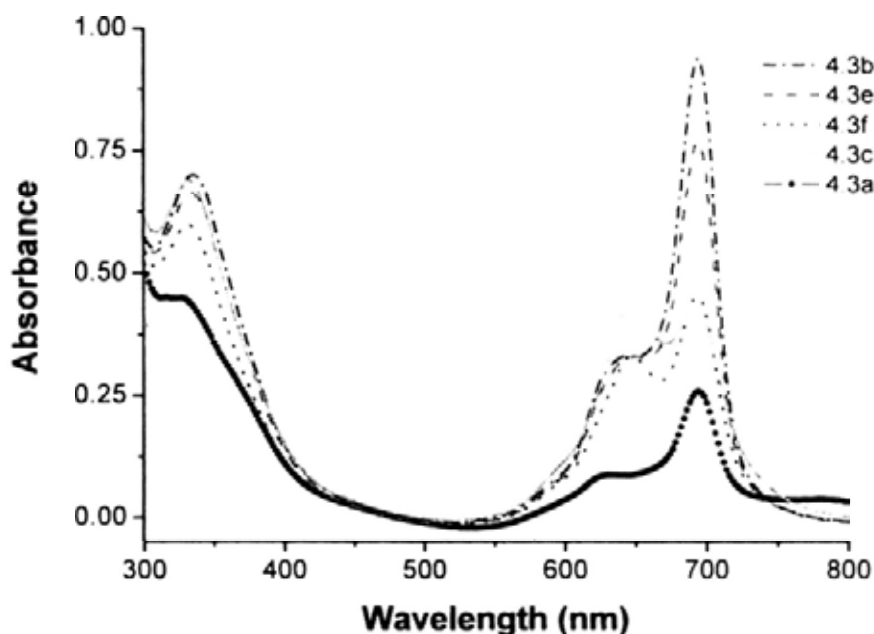


Figure 4.6. Electronic absorption spectra of ZnPc[O(CH₂CH₂O)_nMe]₂ [*n* = 2 (**4.3a**), 4 (**4.3b**), 6 (**4.3e**), 8 (**4.3f**), and ca. 12 (**4.3c**)], formulated with Cremophor EL, in the DMEM culture medium (all at 8 μM).

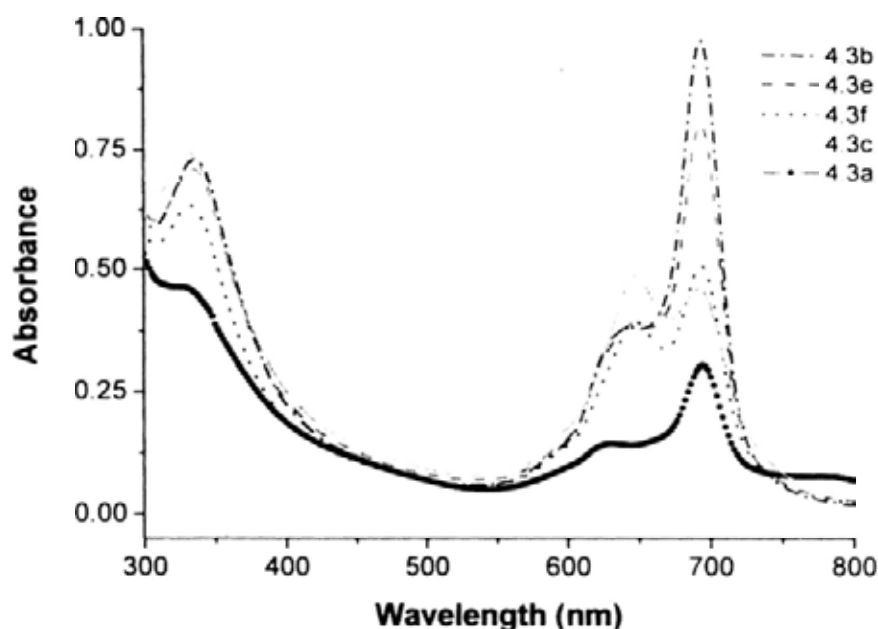


Figure 4.7. Electronic absorption spectra of ZnPc[O(CH₂CH₂O)_nMe]₂ [*n* = 2 (**4.3a**), 4 (**4.3b**), 6 (**4.3e**), 8 (**4.3f**), and ca. 12 (**4.3c**)], formulated with Cremophor EL, in the RPMI culture medium (all at 8 μM).

In addition to the cell viability studies, I also employed confocal microscopy to investigate the uptake of these photosensitizers by HT29 cells. After incubation with these compounds (formulated with Cremophor EL) for 2 h and upon excitation at 630 nm, the HT29 cells showed intracellular fluorescence throughout the cytoplasm as shown in Figure 4.8, indicating that there was a substantial uptake of the dyes. The intensity generally decreases as the length of the substituent increases, i.e. **4.3a** > **4.3b** > **4.3e** > **4.3f** > **4.3c**. The results suggest that as the length of the substituent increases, the compounds show a lower cellular uptake and/or higher aggregation tendency, both of which are undesirable for photosensitization. This can also explain the trend of photocytotoxicity observed for this series of compounds (Table 4.2).

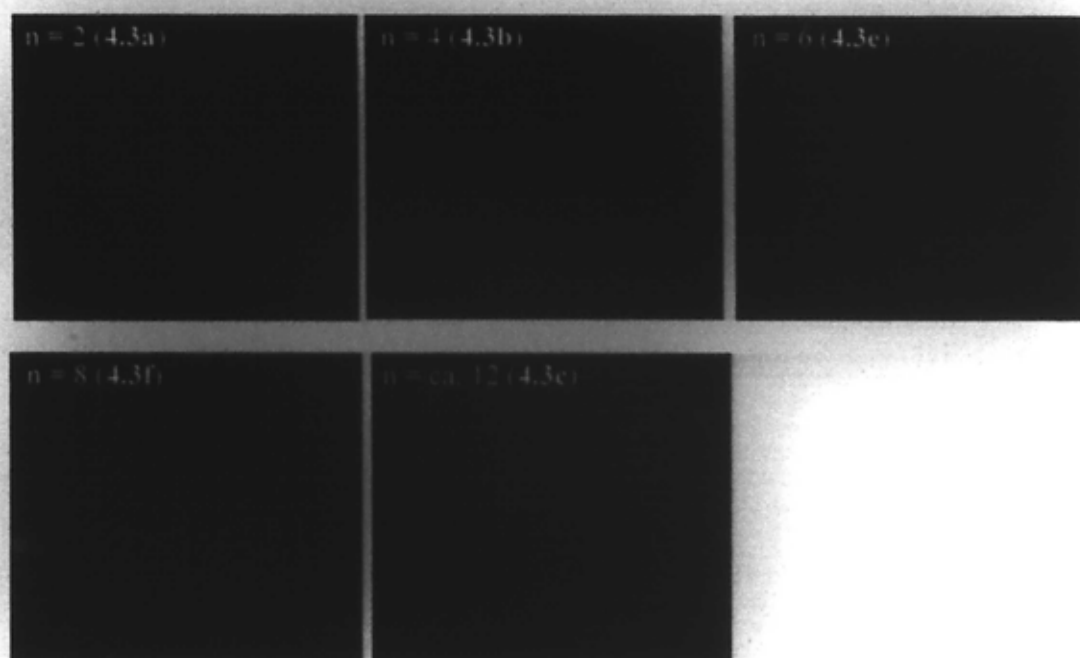


Figure 4.8. Fluorescence microscopic images of HT29 cells after incubation with $\text{ZnPc}[\text{O}(\text{CH}_2\text{CH}_2\text{O})_n\text{Me}]_2$ (**4.3a-4.3c** and **4.3e-4.3f**) at a concentration of $8 \mu\text{M}$ for 2 h.

4.3 Conclusion

In summary, we have prepared and characterized a new series of zinc(II) phthalocyanines with two diethylene glycol to polyethylene glycol methyl ether chains at the 1,4-di- α -positions. This unique substitution pattern shifts the Q-band absorption to the red and reduces the aggregation of the macrocycles. All of these compounds are photocytotoxic against HT29 and HepG2 cells. The solubility and aggregation behavior in the culture media, cellular uptake, and eventually the potency of these compounds greatly depend on the chain length. Optimal results can be achieved for compounds **4.3b** and **4.3e**, which respectively have two tetra- and hexaethylene glycol methyl ether chains.

4.4 Experimental Section

4.4.1 General

Experimental details regarding the purification of solvents, instrumentation and in vitro studies are described in Section 2.4. Tosylates **4.1a**,¹⁵ **4.1b**,¹⁵ **4.1c**¹⁶ and **4.1d**¹⁷ were prepared as described.

4.4.2 Synthesis

General procedure for the preparation of phthalonitriles **4.2a-4.2d**

A mixture of 2,3-dicyanohydroquinone (1 equiv.), tosylates **4.1a-4.1d** (2 equiv.), and K₂CO₃ (2 equiv.) in DMF (20-30 mL) was stirred at 90 °C under an atmosphere of nitrogen for 24 h. The volatiles were removed in vacuo, then the residue was mixed with water (100 mL) and extracted with CH₂Cl₂ (80 mL × 3). The combined organic extracts were dried over anhydrous MgSO₄. After evaporation under reduced pressure, the residue was purified by silica gel column chromatography using CHCl₃/CH₃OH (100:1 v/v) as the eluent.

Phthalonitrile 4.2a. According to the general procedure, 2,3-dicyanohydroquinone (2.40 g, 15.0 mmol) was treated with tosylate **4.1a** (8.22 g, 30.0 mmol) and K₂CO₃ (4.14 g, 30.0 mmol) to give **4.2a** as a pale white solid (4.42 g, 81%). M.p. 84.4-85.2 °C. ¹H NMR (300 MHz, CDCl₃): δ 7.23 (s, 2 H, ArH), 4.25 (t, *J* = 4.8 Hz, 4 H, CH₂), 3.90 (t, *J* = 4.8 Hz, 4 H, CH₂), 3.73-3.76 (m, 4 H, CH₂), 3.55-3.58 (m, 4 H, CH₂), 3.39 (s, 6 H, CH₃); ¹³C{¹H} NMR (75.4 MHz, CDCl₃): δ 155.4, 119.1, 112.9, 105.6, 71.9, 71.1, 70.1, 69.4, 59.0; MS (ESI): *m/z* 387 {100%, [M

+ Na]⁺}; HRMS (ESI) calcd for C₁₈H₂₄N₂NaO₆ [M + Na]⁺ 387.1527, found: 387.1535; Anal. Calcd for C₁₈H₂₄N₂O₆: C, 59.33; H, 6.64; N, 7.69. Found: C, 59.50; H, 6.82; N, 7.55.

Phthalonitrile 4.2b. According to the general procedure, 2,3-dicyanohydroquinone (0.48 g, 3.0 mmol) was treated with tosylate **4.1b** (2.17 g, 6.0 mmol) and K₂CO₃ (0.83 g, 6.0 mmol) to give **4.2b** as a pale white solid (1.36 g, 84%). M.p. 83.3-83.9 °C. ¹H NMR (300 MHz, CDCl₃): δ 7.27 (s, 2 H, ArH), 4.25 (t, *J* = 4.2 Hz, 4 H, CH₂), 3.90 (t, *J* = 4.2 Hz, 4 H, CH₂), 3.71-3.76 (m, 4 H, CH₂), 3.63-3.68 (m, 16 H, CH₂), 3.53-3.58 (m, 4 H, CH₂), 3.37 (s, 6 H, CH₃); ¹³C {¹H} NMR (75.4 MHz, CDCl₃): δ 155.3, 119.2, 112.9, 105.3, 71.8, 71.0, 70.5 (three overlapping signals), 70.4, 70.0, 69.3, 58.9; MS (FAB): *m/z* 541 {100%, [M + H]⁺}; HRMS (FAB) calcd for C₂₆H₄₁N₂O₁₀ [M + H]⁺ 541.2756, found: 541.2742.

Phthalonitrile 4.2c. According to the general procedure, 2,3-dicyanohydroquinone (2.00 g, 12.5 mmol) was treated with tosylate **4.1c** (18.51 g, 26.3 mmol) and K₂CO₃ (3.63 g, 26.3 mmol) to give **4.2c** as a pale yellow oil (12.57 g, 82%). ¹H NMR (300 MHz, CDCl₃): δ 7.26 (s, 2 H, ArH), 4.24 (t, *J* = 4.5 Hz, 4 H, CH₂), 3.90 (t, *J* = 4.5 Hz, 4 H, CH₂), 3.61-3.76 (m, ca. 84 H, CH₂), 3.53-3.56 (m, 4 H, CH₂), 3.38 (s, 6 H, CH₃); MS (ESI): *m/z* 1267 {52%, [M + Na]⁺ for n = 12}.

Phthalonitrile 4.2d. According to the general procedure, 2,3-dicyanohydroquinone (1.91 g, 11.9 mmol) was treated with tosylate **4.1d** (8.28 g, 23.8 mmol) and K₂CO₃ (3.28 g, 23.7 mmol) to afford **4.2d** as a pale white solid (5.62 g, 92%). M.p. 26.8-27.5 °C. ¹H NMR (300 MHz, CDCl₃): δ 7.29 (s, 2 H, ArH), 4.26

(t, $J = 4.5$ Hz, 4 H, CH₂), 3.89 (t, $J = 4.5$ Hz, 4 H, CH₂), 3.73-3.77 (m, 4 H, CH₂), 3.64-3.71 (m, 16 H, CH₂), 3.59-3.62 (m, 4 H, CH₂), 2.86 (br s, 2 H, OH); ¹³C{¹H} NMR (75.4 MHz, CDCl₃): δ 155.3, 119.3, 113.0, 105.2, 72.4, 70.9, 70.5, 70.4, 70.1, 70.0, 69.3, 61.5; MS (ESI): m/z 535 {100%, [M + Na]⁺}; HRMS (ESI) calcd for C₂₄H₃₆N₂NaO₁₀ [M + Na]⁺ 535.2262, found: 535.2255.

General procedure for the preparation of phthalocyanines 4.3a-4.3d

A mixture of phthalonitriles **4.2a-4.2d** (1 equiv.), unsubstituted phthalonitrile (9 equiv.), and Zn(OAc)₂·2H₂O (2.5 equiv.) in *n*-pentanol (25 mL) was heated to 100 °C, then a small amount of DBU (1 mL) was added. The mixture was stirred at 140-150 °C for 24 h. After a brief cooling, the volatiles were removed under reduced pressure. The residue was dissolved in CHCl₃ (200 mL), then the solution was filtered to remove ZnPc formed. The filtrate was collected and evaporated to dryness in vacuo. The residue was purified by silica gel column chromatography using CHCl₃/CH₃OH (30:1 v/v) as the eluent, followed by size exclusion chromatography using THF as the eluent. The crude product was further purified by recrystallization from a mixture of THF and hexane to give the product as a blue solid or oil.

ZnPc[O(CH₂CH₂O)₂Me]₂ (4.3a). According to the general procedure, phthalonitrile **4.2a** (0.73 g, 2.0 mmol) was treated with unsubstituted phthalonitrile (2.31 g, 18.0 mmol) and Zn(OAc)₂·2H₂O (1.10 g, 5.0 mmol) to give **4.3a** as a blue solid (0.24 g, 15%). ¹H NMR (300 MHz, CDCl₃ with a trace amount of pyridine-*d*₅): δ 9.41-9.49 (m, 6 H, Pc-H _{α}), 8.14-8.19 (m, 6 H, Pc-H _{β}), 7.57 (s, 2 H, Pc-H _{β}), 4.99 (t,

$J = 5.1$ Hz, 4 H, CH₂), 4.57 (t, $J = 5.1$ Hz, 4 H, CH₂), 4.15 (t, $J = 4.8$ Hz, 4 H, CH₂), 3.76 (t, $J = 4.8$ Hz, 4 H, CH₂), 3.44 (s, 6 H, CH₃); ¹³C{¹H} NMR (75.4 MHz, DMSO-d₆): δ 152.6, 152.5, 152.4, 151.9, 149.8, 138.3, 138.0, 137.9, 129.3, 129.2, 126.2, 122.5, 122.3, 115.4, 71.8, 70.4, 70.3, 69.1, 58.4 (some of the Pc signals are overlapped); MS (ESI): an isotopic cluster peaking at m/z 813 {100%, [M + H]⁺}; HRMS (ESI) calcd for C₄₂H₃₇N₈O₆Zn [M + H]⁺ 813.2122, found: 813.2121; Anal. Calcd for C₄₂H₃₆N₈O₆Zn: C, 61.96; H, 4.46; N, 13.76. Found: C, 62.45; H, 4.83; N, 13.47.

ZnPc[O(CH₂CH₂O)₄Me]₂ (4.3b). According to the general procedure, phthalonitrile **4.2b** (0.54 g, 1.0 mmol) was treated with unsubstituted phthalonitrile (1.15 g, 9.0 mmol) and Zn(OAc)₂·2H₂O (0.55 g, 2.5 mmol) to give **4.3b** as a blue solid (0.12 g, 12%). ¹H NMR (300 MHz, CDCl₃ with a trace amount of pyridine-d₅): δ 9.34-9.40 (m, 4 H, Pc-H _{α}), 9.25-9.27 (m, 2 H, Pc-H _{α}), 8.07-8.15 (m, 6 H, Pc-H _{β}), 7.42 (s, 2 H, Pc-H _{β}), 4.92 (t, $J = 5.1$ Hz, 4 H, CH₂), 4.52 (t, $J = 5.1$ Hz, 4 H, CH₂), 4.15 (t, $J = 4.8$ Hz, 4 H, CH₂), 3.87 (t, $J = 4.8$ Hz, 4 H, CH₂), 3.72-3.75 (m, 4 H, CH₂), 3.60-3.67 (m, 8 H, CH₂), 3.49-3.52 (m, 4 H, CH₂), 3.33 (s, 6 H, CH₃); ¹³C{¹H} NMR (75.4 MHz, CDCl₃ with a trace amount of pyridine-d₅): δ 153.9, 153.8, 153.6, 152.6, 150.4, 138.9, 138.5, 129.0, 127.4, 122.7, 122.5, 115.0, 71.8, 71.1, 70.8, 70.6, 70.5 (two overlapping signals), 70.4, 69.2, 58.9 (some of the Pc signals are overlapped); MS (FAB): an isotopic cluster peaking at m/z 989 {100%, [M + H]⁺}; HRMS (FAB) calcd for C₅₀H₅₃N₈O₁₀Zn [M + H]⁺ 989.3171, found: 989.3149.

ZnPc[O(CH₂CH₂O) _{n} Me]₂ ($n = \text{ca. } 12$) (4.3c). According to the general

procedure, phthalonitrile **4.2c** (0.57 g, 0.47 mmol) was treated with unsubstituted phthalonitrile (0.53 g, 4.14 mmol) and $\text{Zn}(\text{OAc})_2 \cdot 2\text{H}_2\text{O}$ (0.25 g, 1.14 mmol) to give **4.3c** as a blue oil (0.10 g, 13%). ^1H NMR (300 MHz, CDCl_3 with a trace amount of pyridine- d_5): δ 9.41-9.49 (m, 6 H, Pc- H_α), 8.15-8.18 (m, 6 H, Pc- H_β), 7.58 (s, 2 H, Pc- H_β), 4.97 (t, $J = 5.1$ Hz, 4 H, CH_2), 4.56 (t, $J = 5.1$ Hz, 4 H, CH_2), 4.16 (t, $J = 4.8$ Hz, 4 H, CH_2), 3.87 (t, $J = 4.8$ Hz, 4 H, CH_2), 3.69-3.72 (m, 4 H, CH_2), 3.57-3.68 (m, ca. 72 H, CH_2), 3.51-3.56 (m, 4 H, CH_2), 3.35-3.38 (m, 6 H, CH_3); MS (ESI): an isotopic cluster peaking at m/z 1715 {13%, $[\text{M} + \text{Na}]^+$ for $n = 12$ }.

ZnPc[O(CH₂CH₂O)₄H]₂ (**4.3d**). According to the general procedure, phthalonitrile **4.2d** (0.50 g, 0.98 mmol) was treated with unsubstituted phthalonitrile (1.13 g, 8.82 mmol) and $\text{Zn}(\text{OAc})_2 \cdot 2\text{H}_2\text{O}$ (0.54 g, 2.46 mmol) to give **4.3d** as a blue solid (0.13 g, 14%). ^1H NMR (300 MHz, CDCl_3 with a trace amount of pyridine- d_5): δ 9.43-9.49 (m, 4 H, Pc- H_α), 9.39-9.41 (m, 2 H, Pc- H_α), 8.12-8.18 (m, 6 H, Pc- H_β), 7.58 (s, 2 H, Pc- H_β), 4.97 (t, $J = 4.8$ Hz, 4 H, CH_2), 4.54 (t, $J = 4.8$ Hz, 4 H, CH_2), 4.14 (t, $J = 4.5$ Hz, 4 H, CH_2), 3.84 (t, $J = 4.5$ Hz, 4 H, CH_2), 3.58-3.68 (m, 12 H, CH_2), 3.51 (t, $J = 4.5$ Hz, 4 H, CH_2); $^{13}\text{C}\{^1\text{H}\}$ NMR (75.4 MHz, CDCl_3): δ 153.0, 152.8, 152.7, 150.9, 148.4, 138.4, 138.3, 138.2, 128.5, 128.3, 128.2, 125.1, 123.0, 122.3, 121.9, 112.3, 70.8, 70.6, 70.2 (two overlapping signals), 70.0, 69.1, 67.9, 59.4; UV-Vis (DMF) [λ_{max} (nm), (log ϵ): 341 (4.72), 621 (4.53), 689 (5.28)]; MS (ESI): an isotopic cluster peaking at m/z 961 {100%, $[\text{M} + \text{H}]^+$ }; HRMS (ESI) calcd for $\text{C}_{48}\text{H}_{49}\text{N}_8\text{O}_{10}\text{Zn}$ $[\text{M} + \text{H}]^+$ 961.2858, found: 961.2848; Anal. Calcd for $\text{C}_{48}\text{H}_{48}\text{N}_8\text{O}_{10}\text{Zn}$: C, 59.91; H, 5.03; N, 11.64. Found: C, 59.49; H, 5.17; N, 11.16.

ZnPc[O(CH₂CH₂O)₆Me]₂ (4.3e). Phthalocyanine **4.3d** (96 mg, 0.10 mmol) was added to a suspension of NaH (60% in mineral oil, 40 mg, 1.00 mmol) in THF (8 mL). After the evolution of gas bubbles had ceased, a solution of the monotosylate **4.1a** (110 mg, 0.40 mmol) in THF (2 mL) was added slowly. The resulting mixture was refluxed overnight. A few drops of water were then added to quench the reaction. The volatiles were removed under reduced pressure. The residue was mixed with water (20 mL) and the mixture was extracted with CHCl₃ (20 mL x 3). The combined organic extracts were dried over anhydrous MgSO₄ and evaporated under reduced pressure. The residue was chromatographed on a silica gel column using CHCl₃/CH₃OH (20:1 v/v) as the eluent. The product was obtained as a blue solid (62 mg, 53%). ¹H NMR (300 MHz, CDCl₃ with a trace amount of pyridine-d₅): δ 9.40-9.51 (m, 6 H, Pc-H_α), 8.12-8.20 (m, 6 H, Pc-H_β), 7.58 (s, 2 H, Pc-H_β), 4.97 (t, *J* = 4.8 Hz, 4 H, CH₂), 4.56 (t, *J* = 4.8 Hz, 4 H, CH₂), 4.15 (t, *J* = 4.8 Hz, 4 H, CH₂), 3.87 (t, *J* = 4.8 Hz, 4 H, CH₂), 3.69-3.73 (m, 4 H, CH₂), 3.57-3.65 (m, 24 H, CH₂), 3.47-3.52 (m, 4 H, CH₂), 3.32 (s, 6 H, CH₃); ¹³C{¹H} NMR (75.4 MHz, CDCl₃ with a trace amount of pyridine-d₅): δ 154.0, 153.8, 153.7, 152.7, 150.4, 138.9, 138.5, 129.0, 127.4, 122.7, 122.5, 115.0, 71.8, 71.1, 70.7, 70.6, 70.5, 69.2, 58.9 (some of the signals are overlapped); MS (ESI): an isotopic cluster peaking at *m/z* 1165 {98%, [M + H]⁺}; HRMS (ESI) calcd for C₅₈H₆₉N₈O₁₄Zn [M + H]⁺ 1165.4219, found: 1165.4209.

ZnPc[O(CH₂CH₂O)₈Me]₂ (4.3f). According to the above procedure, treatment of phthalocyanine **4.3d** (96 mg, 0.10 mmol) with tosylate **4.1b** (145 mg, 0.40 mmol) and NaH (60% in mineral oil, 40 mg, 1.00 mmol) afforded **4.3f** as a blue solid (68 mg,

51%). ^1H NMR (300 MHz, CDCl_3 with a trace amount of pyridine- d_5): δ 9.43-9.47 (m, 4 H, Pc-H $_{\alpha}$), 9.37-9.40 (m, 2 H, Pc-H $_{\alpha}$), 8.11-8.16 (m, 6 H, Pc-H $_{\beta}$), 7.53 (s, 2 H, Pc-H $_{\beta}$), 4.96 (t, $J = 5.1$ Hz, 4 H, CH $_2$), 4.55 (t, $J = 5.1$ Hz, 4 H, CH $_2$), 4.16 (t, $J = 4.8$ Hz, 4 H, CH $_2$), 3.87 (t, $J = 4.8$ Hz, 4 H, CH $_2$), 3.70-3.73 (m, 4 H, CH $_2$), 3.59-3.66 (m, 40 H, CH $_2$), 3.50-3.53 (m, 4 H, CH $_2$), 3.35 (s, 6 H, CH $_3$); $^{13}\text{C}\{^1\text{H}\}$ NMR (75.4 MHz, CDCl_3 with a trace amount of pyridine- d_5): δ 153.5, 153.3, 153.2, 152.2, 150.0, 138.7, 138.3, 138.2, 128.7, 126.9, 122.5, 122.3, 114.5, 71.8, 71.0, 70.7, 70.5, 70.4, 68.9, 58.9 (some of the signals are overlapped); MS (FAB): an isotopic cluster peaking at m/z 1342 {100%, $[\text{M} + \text{H}]^+$ }. HRMS (FAB) calcd for $\text{C}_{66}\text{H}_{85}\text{N}_8\text{O}_{18}\text{Zn}$ $[\text{M} + \text{H}]^+$ 1341.5268, found: 1341.5282.

4.5 References

1. (a) Fukuda, T.; Homma, S.; Kobayashi, N. *Chem. Eur. J.* **2005**, *11*, 5205. (b) Maqanda, W.; Nyokong, T.; Marce, M. D. *J. Porphyrins Phthalocyanines* **2005**, *9*, 343. (c) Li, H.; Fronczek, F. R.; Vicente, M. G. H. *Tetrahedron Lett.* **2008**, *49*, 4828. (d) Liu, J.-Y.; Jiang, X.-J.; Fong, W.-P.; Ng, D. K. P. *Metal-Based Drugs* **2008**, Article ID 284691.
2. (a) Jori, G. *J. Photochem. Photobiol. A: Chem.* **1992**, *62*, 371. (b) Lane, N. *Sci. Am.* **2003**, *288(1)*, 38.
3. See for example: (a) Shirk, J. S.; Pong, R. G. S.; Flom, S. R.; Heckmann, H.; Hanack, M. *J. Phys. Chem. A* **2000**, *104*, 1438. (b) Ng, D. K. P. *C. R. Chim.* **2003**, *6*, 903. (c) Chen, Y.; El-Khouly, M. E.; Sasaki, M.; Araki, Y.; Ito, O. *Org. Lett.* **2005**, *7*, 1613. (d) Makhseed, S.; Ibrahim, F.; Samuel, J.; Helliwell, M.; Warren, J. E.; Bezzu, C. G.; McKeown, N. B. *Chem. Eur. J.* **2008**, *14*, 4810.
4. Yoshiyama, H.; Shibata, N.; Sato, T.; Nakamura, S.; Toru, T. *Chem. Commun.* **2008**, 1977.

5. Ishii, K.; Kobayashi, N. in *The Porphyrin Handbook*; Kadish, K. M., Smith, K. M., Guillard, R., Eds; Academic Press, San Diego, **2003**; Vol. 16, ch. 102.
6. Stolnik, S.; Illum, L.; Davis, S. S. *Adv. Drug Deliv. Rev.* **1995**, *16*, 195. (b) Torchilin, V. P. *Pharm. Res.* **2007**, *24*, 1. (c) van Vlerken, L. E.; Vyas, T. K.; Amiji, M. M. *Pharm. Res.* **2007**, *24*, 1405.
7. Bonnett, R. *Chem. Soc. Rev.* **1995**, 19.
8. (a) Ris, H.-B.; Krueger, T.; Giger, A.; Lim, C. K.; Stewart, J. C. M.; Althaus, U.; Altermatt, H. J. *Br. J. Cancer* **1999**, *79*, 1061. (b) Brasseur, N.; Ouellet, R.; La Madeleine, C.; van Lier, J. E. *Br. J. Cancer* **1999**, *80*, 1533. (c) Huang, J.-D.; Wang, S.; Lo, P.-C.; Fong, W.-P.; Ko, W.-H.; Ng, D. K. P. *New J. Chem.* **2004**, *28*, 348. (d) Sibrian-Vazquez, M.; Jensen, T. J.; Vicente, M. G. H. *J. Photochem. Photobiol. B: Biol.* **2007**, *86*, 9.
9. (a) Spiller, W.; Kliesch, H.; Wöhrle, D.; Hackbarth, S.; Röder, B.; Schnurpfeil, G. *J. Porphyrins Phthalocyanines* **1998**, *2*, 145. (b) Maree, M. D.; Kuznetsova, N.; Nyokong, T. *J. Photochem. Photobiol. A: Chem.* **2001**, *140*, 117.
10. Hajri, A.; Wack, S.; Meyer, C.; Smith, M. K.; Leberquier, C.; Kedinger, M.; Aprahamian, M. *Photochem. Photobiol.* **2002**, *75*, 140.
11. Choi, C.-F.; Huang, J.-D.; Lo, P.-C.; Fong, W.-P.; Ng, D. K. P. *Org. Biomol. Chem.* **2008**, *6*, 2173.
12. (a) Choi, C.-F.; Tsang, P.-T.; Huang, J.-D.; Chan, E. Y. M.; Ko, W.-H.; Fong, W.-P.; Ng, D. K. P. *Chem. Commun.* **2004**, 2236. (b) Lo, P.-C.; Zhao, B.; Duan, W.; Fong, W.-P.; Ko, W.-H.; Ng, D. K. P. *Bioorg. Med. Chem. Lett.* **2007**, *17*, 1073.
13. (a) Schutte, W. J.; Sluyters-Rehbach, M.; Sluyters, J. H. *J. Phys. Chem.* **1993**, *97*, 6069. (b) Li, X.; Sinks, L. E.; Rybtchinski, B.; Wasielewski, M. R. *J. Am. Chem. Soc.* **2004**, *126*, 10810. (c) Qiu, Y.; Chen, P.; Liu, M. *Langmuir* **2008**, *24*, 7200.
14. (a) Spikes, D. *J. Photochem. Photobiol.* **1986**, *43*, 691. (b) Dhimi, S.; Phillips, D. *J. Photochem. Photobiol. A: Chem.* **1996**, *100*, 77. (c) Howe, L.; Zhang, J. Z. *J. Phys. Chem. A* **1997**, *101*, 3207. (d) Suchetti, C. A.; Durantini, E. N. *Dyes Pigments* **2007**, *74*, 630.

15. Snow, A. W.; Foos, E. E. *Synthesis* **2003**, 509.
16. Rivera, E.; Belletete, M.; Natansohn, A.; Durocher, G. *Can. J. Chem.* **2003**, *81*, 1076.
17. Kishimoto, K.; Suzawa, T.; Yokota, T.; Mukai, T.; Ohno, H.; Kato, T. *J. Am. Chem. Soc.* **2005**, *127*, 15618.

Chapter 5

Effects of the Number and Position of the Substituents on the *in vitro* Photodynamic Activities of Glucosylated Zinc(II) Phthalocyanines

5.1 Introduction

Owing to the strong absorption in the red visible region, high efficiency at generating singlet oxygen, and extraordinary stability, phthalocyanines have emerged as a promising class of photosensitizers for photodynamic therapy (PDT).¹ In addition to some classical phthalocyanine-based photosensitizers such as liposomal zinc(II) phthalocyanine, sulfonated zinc(II) and aluminum(III) phthalocyanines, and the silicon(IV) phthalocyanine Pc4 developed by Kenney et al., a substantial number of other phthalocyanine derivatives have been studied over the past few years with a view to improving the therapeutic outcomes and gaining insight about the structure-activity relationships.² Recently, a considerable effort has been devoted to enhance their selectivity toward malignant tissues. To this end, various tumor-specific vectors such as antibodies, synthetic peptides, epidermal growth factor, and adenoviruses have been conjugated to these photosensitizers.³ Unfortunately, only a limited target specificity has been achieved so far.

On the basis that cancer cells have increased levels of glucose uptake and glycolysis to provide sufficient metabolic energy to sustain their proliferation,⁴

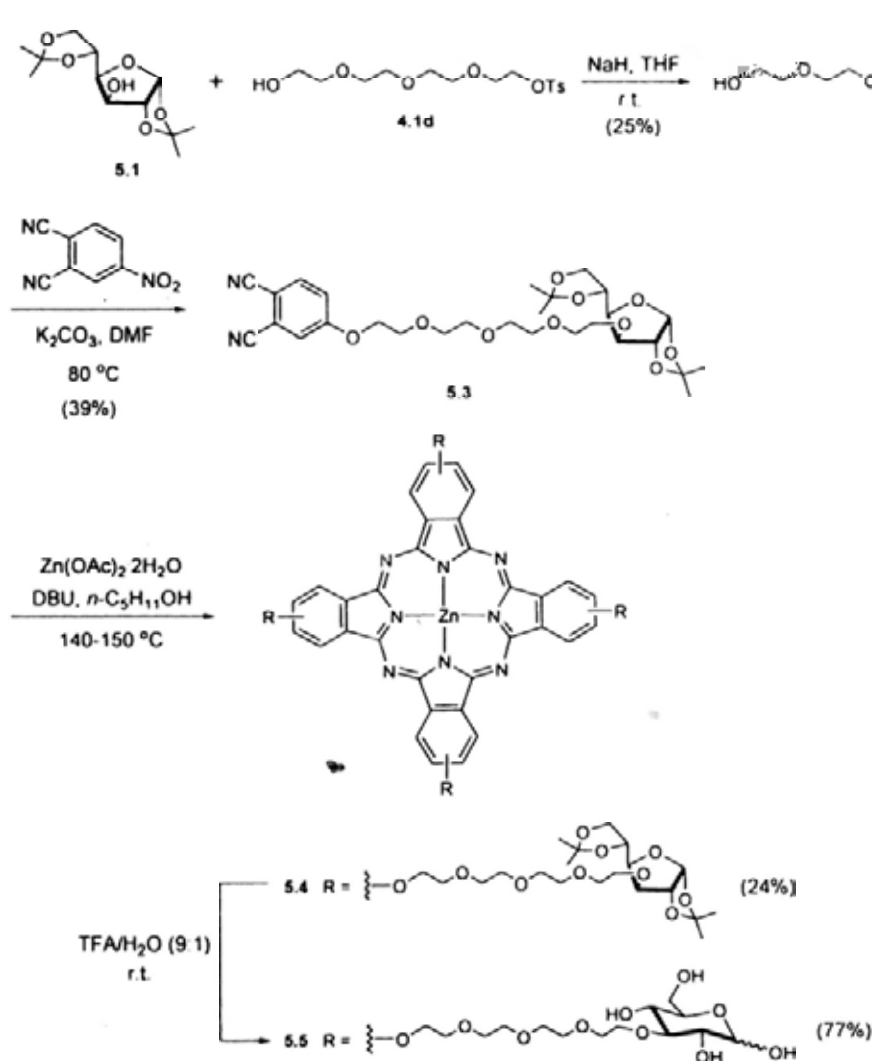
glucoconjugation may promote the uptake of photosensitizers through the glucose transporter proteins, which are over-expressed in a variety of human carcinomas.⁵ The hydrophilic glucose moieties connected to the hydrophobic core of the photosensitizers can also tune the amphiphilicity of the resulting conjugates, which is an important parameter for cellular uptake.⁶ This strategy has been employed for various photosensitizers such as porphyrins,⁷ chlorins,⁸ pyropheophorbides,⁹ and hypocrellins.¹⁰ Recently, our group has extended the studies to phthalocyanines. A series of glycosylated silicon(IV)¹¹ and zinc(II)¹² phthalocyanines have been synthesized and evaluated for their in vitro photodynamic activities. These compounds, particularly the silicon(IV) analogues, are highly potent having IC₅₀ values as low as 6 nM. In this Chapter, I report the synthesis, characterization, photophysical properties, and in vitro photocytotoxicity of a new series of zinc(II) phthalocyanines substituted with 1, 2 or 4 tetraethylene-glycol-linked glucose unit(s) at the α - or β -position(s). By studying this series of structurally related compounds, I aim to reveal the effects of the number and position of this substituent on the photodynamic activities of this novel series of glycoconjugated photosensitizers.

5.2 Results and Discussion

5.2.1 Synthesis and Characterization

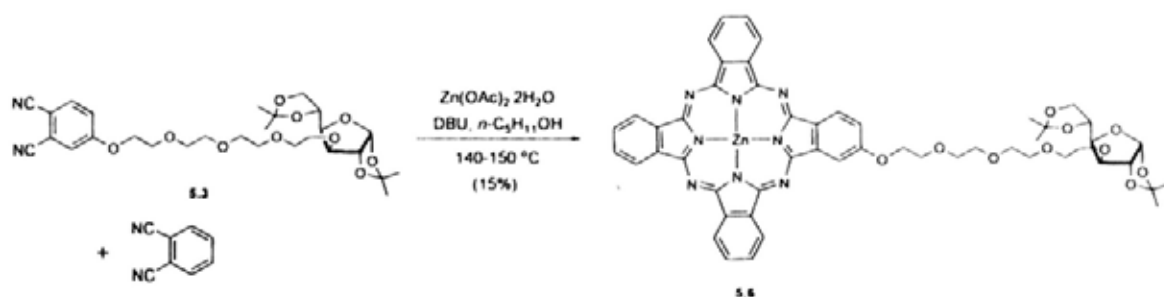
Scheme 5.1 shows the synthetic route for the tetra- β -glucosylated phthalocyanines 5.4 and 5.5. Reaction of 1,2:5,6-di-*O*-isopropylidene- α -D-glucofuranose (5.1) with tetraethylene glycol

mono(*p*-toluenesulfonate) (**4.1d**) and NaH gave product **5.2**. Treatment of this compound with 4-nitrophthalonitrile in the presence of K_2CO_3 in DMF led to nucleophilic aromatic substitution giving the corresponding glucosylated phthalonitrile **5.3**. This compound then underwent self-cyclization in the presence $Zn(OAc)_2 \cdot 2H_2O$ and DBU to afford $ZnPc(\beta\text{-PGlu})_4$ (**5.4**) as a mixture of structural isomers. Upon treatment with trifluoroacetic acid (TFA) and water (9:1 v/v), the isopropylidene groups of **5.4** were removed giving the deprotected glucosylated analogue $ZnPc(\beta\text{-Glu})_4$ (**5.5**).



Scheme 5.1. Synthesis of tetra- β -glucosylated phthalocyanines **5.4** and **5.5**.

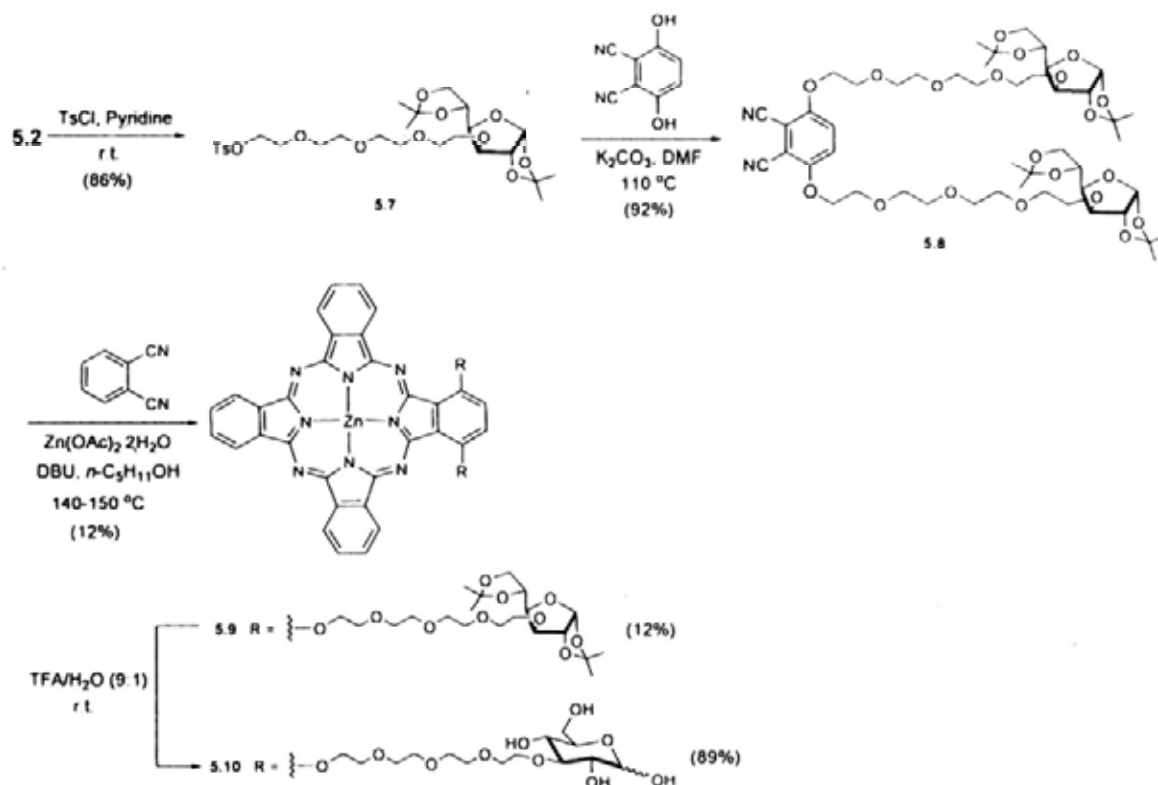
To enhance the amphiphilicity of the molecules, which is generally believed to be an advantageous character of photosensitizers,⁶ I also prepared the mono- and di-glucosylated derivatives. As shown in Scheme 5.2, mixed cyclization of the glucose-appended phthalonitrile **5.3** with an excess of unsubstituted phthalonitrile (9 equiv.) in the presence $Zn(OAc)_2 \cdot 2H_2O$ and DBU afforded the mono- β -glucosylated phthalocyanine $ZnPc(\beta\text{-PGlu})$ (**5.6**). This compound could be isolated readily from the reaction mixture (in 15% yield) by silica gel column chromatography followed by size exclusion chromatography.



Scheme 5.2. Synthesis of mono- β -glucosylated phthalocyanine **5.6**.

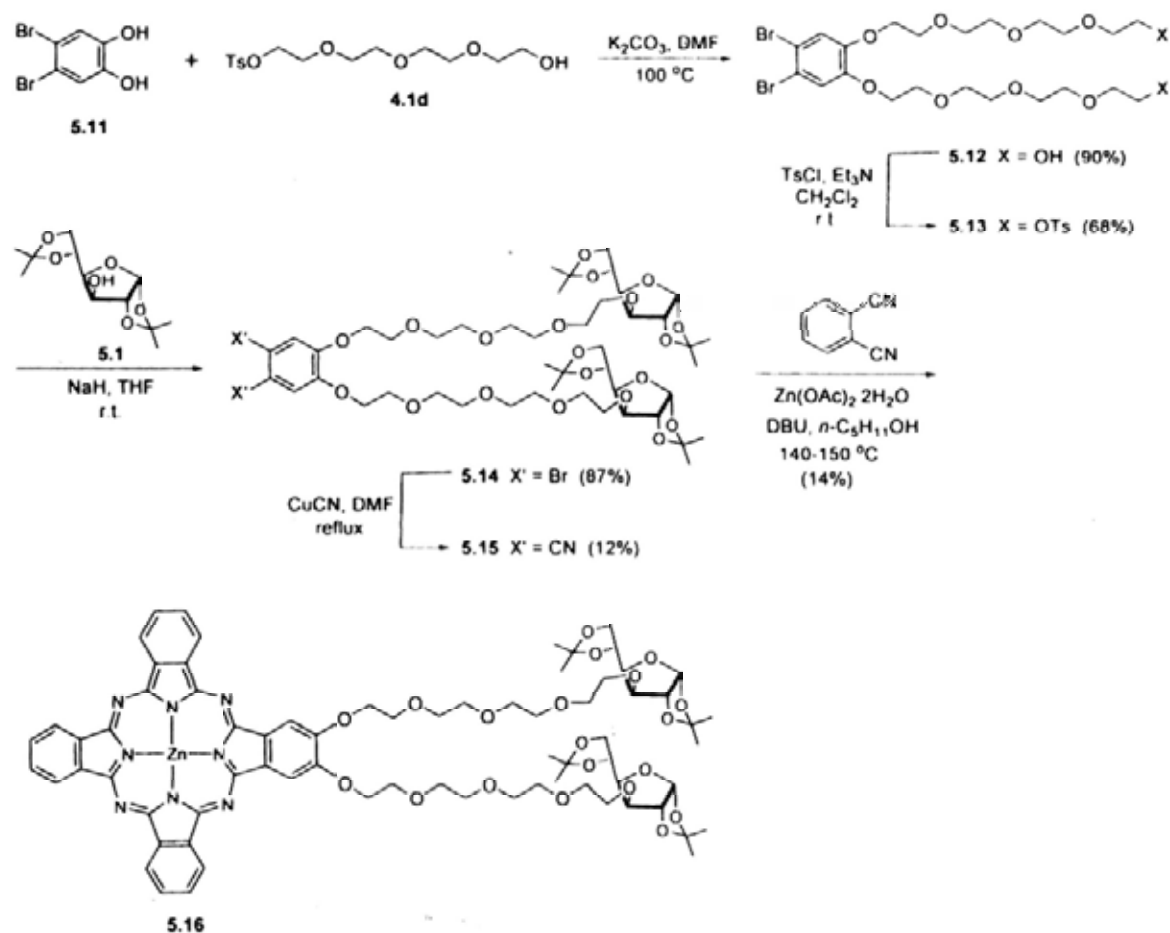
Scheme 5.3 shows the pathway used to prepare the di- α -substituted derivatives. Treatment of tosylate **5.7**, prepared from **5.2** in 86% yield, with 2,3-dicyanohydroquinone and K_2CO_3 resulted in disubstitution giving phthalonitrile **5.8**. This compound then underwent a typical mixed cyclization reaction with unsubstituted phthalonitrile to afford the di- α -glucosylated phthalocyanine $ZnPc(\alpha\text{-PGlu})_2$ (**5.9**) in 12% yield. This kind of 1,4-disubstituted phthalocyanines remains relatively rare,¹³ but has recently been shown to possess desirable characteristics for PDT application.^{2g,14} For this compound, deprotection was also

performed, again with TFA and water (9:1 v/v), to give the deprotected derivative ZnPc(α -Glu)₂ (**5.10**) in excellent yield.



Scheme 5.3. Synthesis of di- α -glucosylated phthalocyanines **5.9** and **5.10**.

The di- β -glucosylated analogue ZnPc(β -PGlu)₂ (**5.16**) was prepared according to Scheme 5.4. Firstly, 4,5-dibromocatechol (**5.11**) was treated with tetraethylene glycol mono(*p*-toluenesulfonate) (**4.1d**) to afford the disubstituted product **5.12**, which was then converted to the ditosylate **5.13**. This compound then underwent nucleophilic substitution with 1,2:5,6-di-*O*-isopropylidene- α -D-glucofuranose (**5.1**) to give **5.14**. Reaction of this compound with CuCN led to the formation of phthalonitrile **5.15**, which was then converted to **5.16** by typical mixed cyclization with unsubstituted phthalonitrile.



Scheme 5.4. Synthesis of di- β -glucosylated phthalocyanine **5.16**.

All of the new compounds were fully characterized with various spectroscopic methods. For the tetra- β -glucosylated phthalocyanine $\text{ZnPc}(\beta\text{-PGlu})_4$ (**5.4**), although it exists as a mixture of structural isomers, the ^1H NMR spectrum recorded in CDCl_3 in the presence of a trace amount of pyridine- d_5 is simpler than expected. Three well-separated multiplets in the region δ 7.7-9.3 were observed for the three sets of phthalocyanine ring protons. The signals for the sugar and tetraethylene glycol protons could also be partially assigned with the aid of 2D COSY spectroscopy. The spectra for the other substituted analogues also showed distinct ^1H NMR patterns for the phthalocyanine ring protons, and the signals could be assigned unambiguously (see the

Experimental Section).

For the two deprotected analogues $\text{ZnPc}(\beta\text{-Glu})_4$ (**5.5**) and $\text{ZnPc}(\alpha\text{-Glu})_2$ (**5.10**), the spectra still showed downfield signals which could be assigned to the phthalocyanine ring protons. However, the signals for the sugar and tetraethylene glycol protons were significantly broadened and overlapped. Assignment of these signals was found to be difficult. It is likely that the deprotected sugar moieties promote the aggregation of the macrocycles through hydrogen bonding formation. This possible phenomenon, together with the anomerization of the sugar moieties, hinders the assignment of signals. Nevertheless, the purity of these compounds was confirmed by HPLC (Figure 5.1). The relatively broad signal for $\text{ZnPc}(\beta\text{-Glu})_4$ (**5.5**) can be attributed to the fact that it exists as a mixture of structural isomers.

The ESI mass spectra of all these phthalocyanines were also recorded. The protonated $[\text{M} + \text{H}]^+$ and/or sodiated $[\text{M} + \text{Na}]^+$ molecular ion signal(s) could be detected in all the cases. The isotopic distribution was in good agreement with the corresponding simulated pattern. The identity of these species was also confirmed by accurate mass measurements.

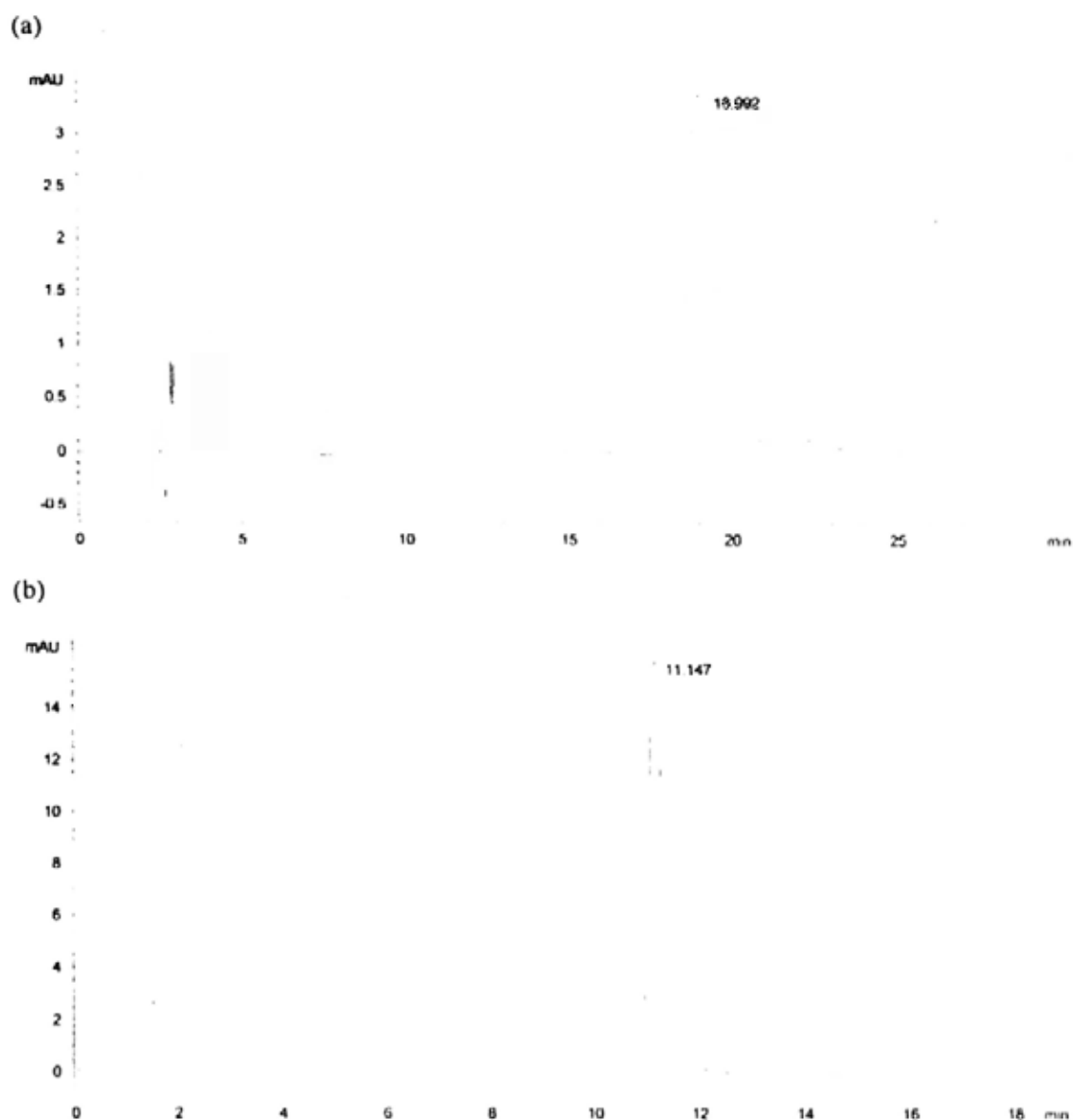


Figure 5.1. HPLC analysis of the purified (a) ZnPc(β -Glu)₄ (5.5) and (b) ZnPc(α -Glu)₂ (5.10). The mobile phase was CH₃OH/H₂O (4:1 v/v) and CH₃OH/H₂O (2:3 v/v) respectively.

5.2.2 Electronic Absorption and Photophysical Properties

The electronic absorption and basic photophysical data of all these phthalocyanines were measured in DMF and are summarized in Table 5.1. All of these compounds gave typical UV-Vis spectra for nonaggregated phthalocyanines, showing an intense and sharp Q band in the red visible region. Figure 5.2 shows the

spectrum of $\text{ZnPc}(\alpha\text{-PGlu})_2$ (**5.9**) as an example. The Q band for this di- α -substituted phthalocyanine was significantly red-shifted (by 19 nm) compared with that for the di- β -substituted counterpart **5.16** (Table 5.1). α -Glucosylation also led to weakening and red shift of the fluorescence emission. These results are in accord with the observations and theoretical calculations reported previously for a series of metal-free and zinc(II) phthalocyanines.¹⁵ The effects of sugar moieties are insignificant both on the absorption and fluorescence emission properties.

The singlet oxygen quantum yields (Φ_{Δ}) of these glucosylated phthalocyanines were also determined in DMF using 1,3-diphenylisobenzofuran (DPBF) as the scavenger.¹⁶ These data are also compiled in Table 5.1. It can be seen that all of these phthalocyanines are efficient singlet oxygen generators, particularly the di- α -substituted zinc(II) analogues **5.9** and **5.10**, of which the values of Φ_{Δ} (0.86 and 0.78 respectively) are significantly higher than that of ZnPc ($\Phi_{\Delta} = 0.56$), which was used as the reference.¹⁷

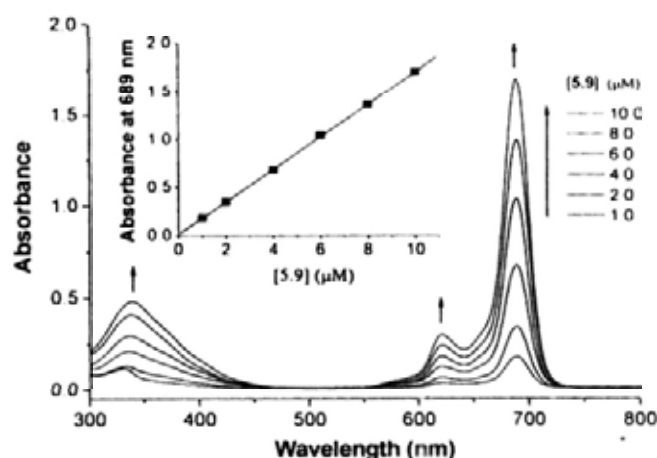


Figure 5.2. Electronic absorption spectra of $\text{ZnPc}(\alpha\text{-PGlu})_2$ (**5.9**) at different concentrations in DMF.

Table 5.1. Electronic absorption and photophysical data for all the glucosylated phthalocyanines in DMF.

| Compound | λ_{\max} (nm) ($\log \epsilon$) | λ_{em} (nm) ^a | Φ_F ^b | Φ_Δ ^c |
|---|---|----------------------------------|-----------------------|----------------------------|
| ZnPc(β -PGlu) ₄ (5.4) | 355 (4.97), 611 (4.60), 679 (5.31) | 684 | 0.33 | 0.49 |
| ZnPc(β -Glu) ₄ (5.5) | 353 (4.85), 612 (4.49), 679 (5.16) | 686 | 0.23 | 0.58 |
| ZnPc(β -PGlu) (5.6) | 346 (4.66), 606 (4.44), 672 (5.21) | 676 | 0.32 | 0.43 |
| ZnPc(α -PGlu) ₂ (5.9) | 334 (4.62), 621 (4.46), 689 (5.23) | 698 | 0.15 | 0.86 |
| ZnPc(α -Glu) ₂ (5.10) | 335 (4.47), 621 (4.36), 688 (5.13) | 697 | 0.18 | 0.78 |
| ZnPc(β -PGlu) ₂ (5.16) | 340 (4.73), 605 (4.54), 670 (5.35) | 676 | 0.31 | 0.51 |

^a Excited at 610 nm. ^b Relative to ZnPc in DMF ($\Phi_F = 0.28$).¹⁸ ^c Relative to ZnPc in DMF ($\Phi_\Delta = 0.56$).

5.2.3 In vitro Photodynamic Activities

The photodynamic activities of all these glucosylated zinc(II) phthalocyanines in Cremophor EL emulsions were investigated against HT29 and HepG2 cells. In the absence of light, all of these compounds were essentially nontoxic to the cells. Upon illumination, these compounds exhibited different degrees of photocytotoxicities. The tetra- β -glucosylated phthalocyanines ZnPc(β -PGlu)₄ (**5.4**) and ZnPc(β -Glu)₄ (**5.5**) were least cytotoxic. The cell viability dropped by less than 20% upon incubation with up to 8 μ M of these dyes. Figure 5.3 shows the dose response curves for the other glucosylated phthalocyanines against the two cell lines. The corresponding IC₅₀ values are compiled in Table 5.2. It can be seen that the photocytotoxicity follows the order ZnPc(α -PGlu)₂ (**5.9**) > ZnPc(β -PGlu)₂ (**5.16**) > ZnPc(β -PGlu) (**5.6**) > ZnPc(α -Glu)₂ (**5.10**). The di- α -substituted derivative **5.9** obviously has a much higher

potency, while the deprotected counterpart **5.10** shows the lowest photocytotoxicity. The potency of these compounds is significantly higher than that of the classical photosensitizer porfimer sodium, of which the IC_{50} values were found to be ca. $4.5 \mu\text{g mL}^{-1}$ for both the cell lines under the same conditions (*versus* ca. 50 ng mL^{-1} for the most potent **5.9**). The mono- β -substituted derivative $\text{ZnPc}(\beta\text{-PGlu})$ (**5.6**) is slightly more photocytotoxic compared with the non-tetraethylene-glycol-linked analogue ($IC_{50} = 1.8\text{-}2.0 \mu\text{M}$),¹² which may be due to the advantageous properties of the linker such as the high hydrophilicity and ability to reduce aggregation of the phthalocyanine core. Compared with the non-glucosylated analogue $\text{ZnPc}[\alpha\text{-O}(\text{CH}_2\text{CH}_2\text{O})_4\text{Me}]_2$ ($IC_{50} = 0.05\text{-}0.09 \mu\text{M}$),¹⁴ the photocytotoxicity of the most potent compound $\text{ZnPc}(\alpha\text{-PGlu})_2$ (**5.9**) is also marginally higher, but the small difference suggests that the sugar moieties do not play a functional role in the uptake process.

Table 5.2. Comparison of the IC_{50} values of phthalocyanines **5.6**, **5.9**, **5.10**, and **5.16** against HT29 and HepG2 cells.

| Compound | IC_{50} (μM) | |
|--|-----------------------------|-----------|
| | For HT29 | For HepG2 |
| $\text{ZnPc}(\beta\text{-PGlu})$ (5.6) | 1.38 | 1.52 |
| $\text{ZnPc}(\alpha\text{-PGlu})_2$ (5.9) | 0.03 | 0.04 |
| $\text{ZnPc}(\alpha\text{-Glu})_2$ (5.10) | 2.97 | 2.48 |
| $\text{ZnPc}(\beta\text{-PGlu})_2$ (5.16) | 0.26 | 0.28 |

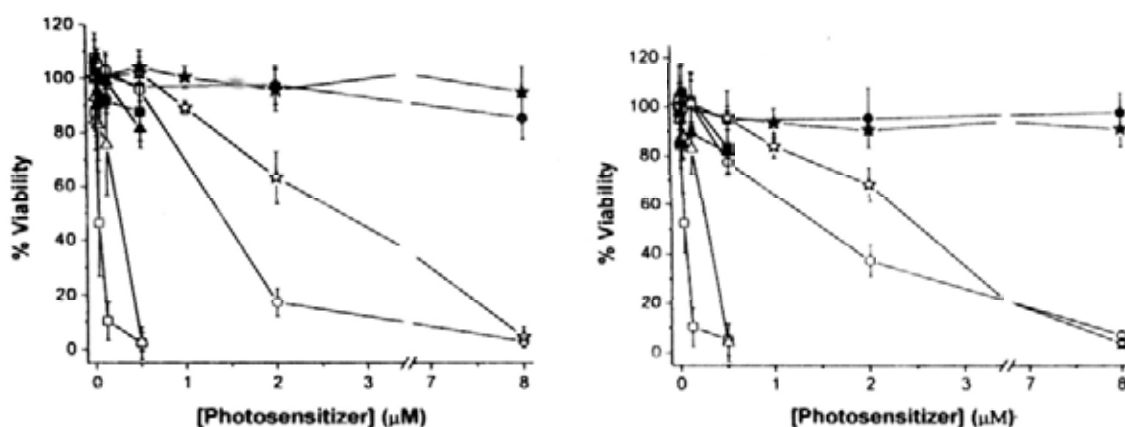


Figure 5.3. Effects of **5.6** (circles), **5.9** (squares), **5.10** (stars), and **5.16** (triangles) on HT29 (left) and HepG2 (right) cells in the absence (closed symbols) and presence (open symbols) of light ($\lambda > 610$ nm, 40 mW cm^{-2} , 48 J cm^{-2}). Data are expressed as mean values \pm standard error of the mean of three independent experiments, each performed in quadruplicate.

To account for the different photodynamic activities of these compounds, their aggregation behavior in the culture media was examined by absorption and fluorescence spectroscopic methods. Figure 5.4 shows the UV-Vis spectra of all the glucosylated phthalocyanines in the DMEM used for HT29 cells. It can be seen that a Q band can be observed readily for the mono- and di-substituted analogues **5.6**, **5.9**, **5.10**, and **5.16**. The Q band of **5.9** is relatively sharp and intense. These observations indicate that these compounds, particularly **5.9**, are not extensively aggregated in the culture medium. By contrast, for the tetra- β -substituted analogues **5.4** and **5.5**, the Q bands are much broadened and shifted to the blue, showing that these two compounds are highly aggregated in the medium. These conclusions were also supported by their different fluorescence spectra. As shown in Figure 5.5, a fluorescence emission can be observed for the mono- and di-substituted derivatives **5.6**, **5.9**, **5.10**, and **5.16**, while

the tetra- β -substituted analogues **5.4** and **5.5** are not fluorescent in the medium. The weaker and red-shifted emission of **5.9** and **5.10** is related to their di- α -substitution pattern.¹⁵ Similar results were obtained in the RPMI medium used for HepG2 cells (see the absorption and fluorescence spectra given in Figures 5.6 and 5.7). As molecular aggregation provides an efficient nonradiative relaxation pathway for the singlet excited state of the dyes, the fluorescence intensity as well as efficiency at generating singlet oxygen will be reduced as the aggregation tendency increases.¹⁹ Thus, these results can explain that even though **5.4** and **5.5** have a reasonably high singlet oxygen quantum yield in DMF (Table 5.1), they are virtually nonphotocytotoxic. The very high potency of **5.9** is related to its low aggregation tendency in the media.

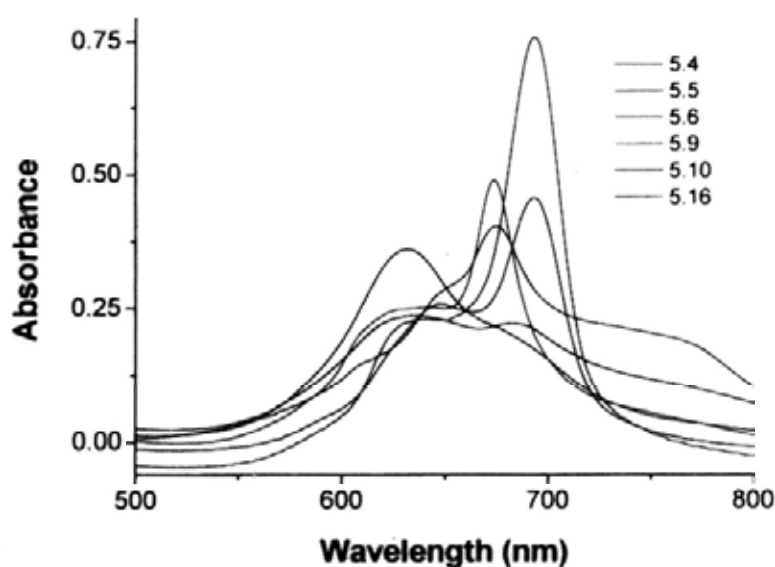


Figure 5.4. Electronic absorption spectra of all the glucosylated phthalocyanines, formulated with Cremophor EL, in the DMEM culture medium. The concentrations of the phthalocyanines were fixed at 8 μ M.

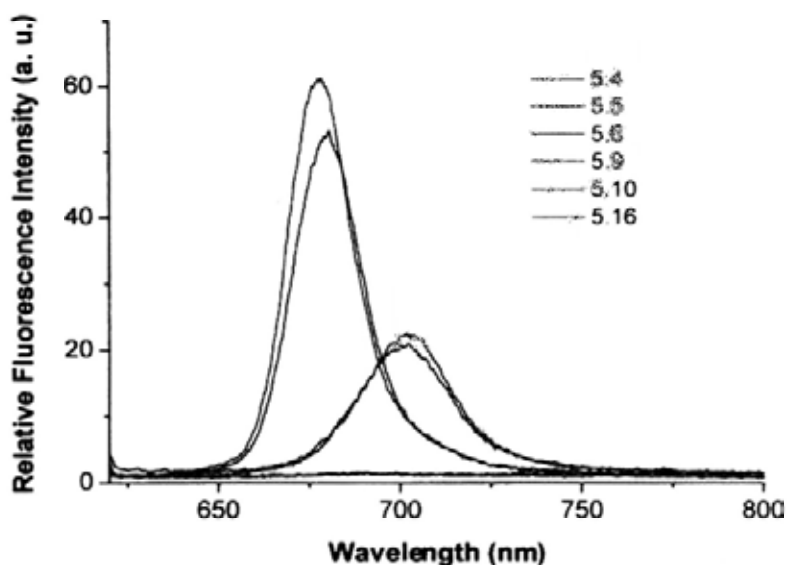


Figure 5.5. Fluorescence spectra of all the glucosylated phthalocyanines, formulated with Cremophor EL, in the DMEM culture medium. The concentrations of the phthalocyanines were fixed at 8 μ M.

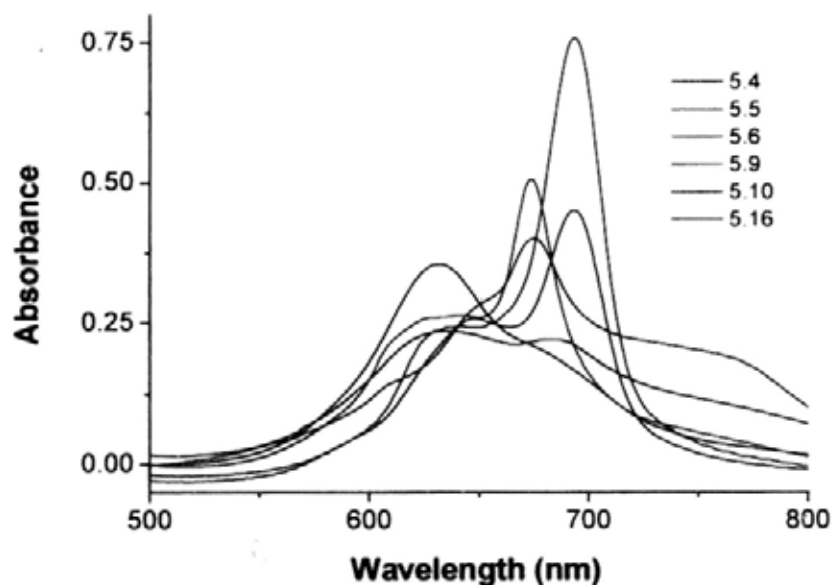


Figure 5.6. Electronic absorption spectra of all the glucosylated phthalocyanines, formulated with Cremophor EL, in the RPMI culture medium. The concentrations of the phthalocyanines were fixed at 8 μ M.

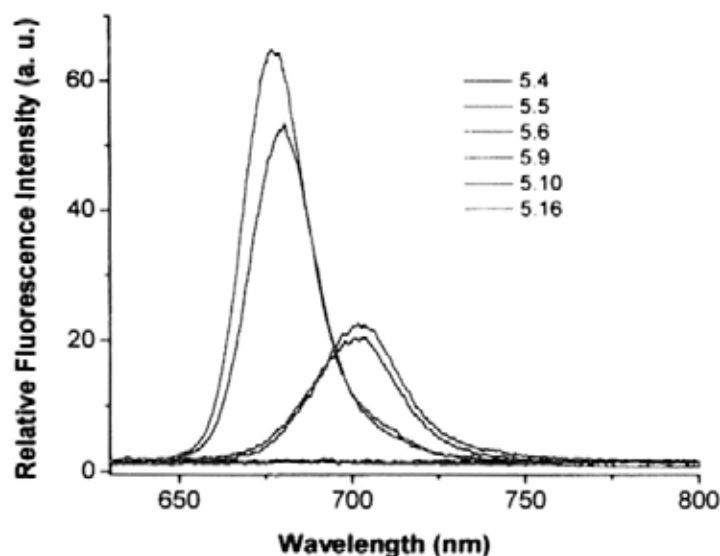


Figure 5.7. Fluorescence spectra of all the glucosylated phthalocyanines, formulated with Cremophor EL, in the RPMI culture medium. The concentrations of the phthalocyanines were fixed at 8 μM .

To further explain the photocytotoxicity results, fluorescence microscopic studies were also carried out to shed light on the cellular uptake of these compounds. HT29 cells were incubated respectively with all of these glucosylated phthalocyanines (8 μM) for 2 h. Upon excitation at 630 nm, the fluorescence images of the cells were then taken (Figure 5.8). It was found that for the tetra- β -substituted analogues **5.4** and **5.5**, no fluorescence could be observed. This indicated that the cellular uptake is negligible for these compounds and/or they are highly aggregated within the cells, both of which disfavour the photodynamic action. Hence, these compounds are not photocytotoxic. By contrast, the mono- and di-substituted derivatives **5.6**, **5.9**, **5.10**, and **5.16** showed intracellular fluorescence throughout the cytoplasm. The apparent intensity, which reflects the extent of cellular uptake and aggregation of the dyes, follows the order: **5.9** > **5.16** > **5.6** > **5.10**, which is in good agreement with the trend

in photocytotoxicity. For the deprotected derivative **5.10**, since it does not seem to have a high aggregation tendency in the media, the weak intracellular fluorescence intensity may be due to its low cellular uptake, which can explain its relatively low photocytotoxicity.

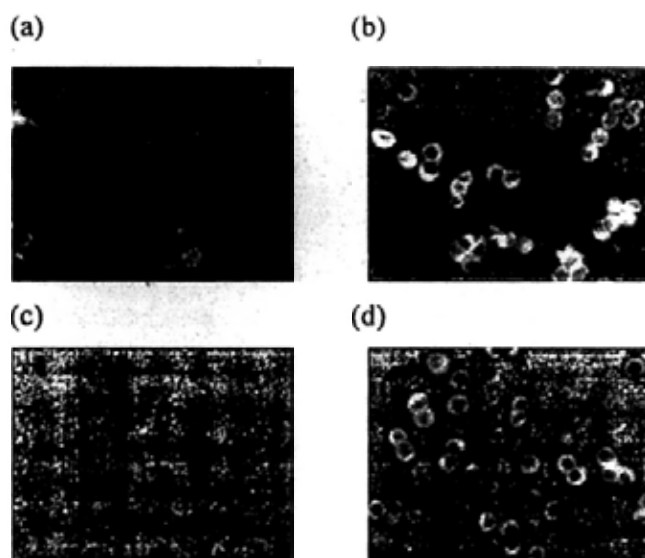


Figure 5.8. Fluorescence microscopic images of HT29 cells after being incubated with (a) **5.6**, (b) **5.9**, (c) **5.10**, and (d) **5.16** (all at $8 \mu\text{M}$) for 2 h.

5.3. Conclusion

In summary, I have prepared and characterized a new series of tetraethylene-glycol-linked glucosylated zinc(II) phthalocyanines. Their *in vitro* photodynamic activities have also been evaluated and compared. It has been found that both the number and position of the substituents have a great influence on their *in vitro* photocytotoxicity, which follows the order: di- α -substituted > di- β -substituted > mono- α -substituted > tetra- β -substituted derivatives. Removal of the isopropylidene protecting groups leads to an adverse effect on the photocytotoxicity. The different

photodynamic activities of these compounds can be well explained by their different extent of cellular uptake and aggregation tendency. The di- α -substituted analogue **5.9** is particularly potent having IC_{50} values as low as $0.03 \mu\text{M}$, and is thus a very promising photosensitizer.

According to the results reported in Chapter 2 to 5, some insight can be gained about the structure-activity relationship of phthalocyanine-based photosensitizers. Generally, amphiphilic di- α -substituted analogues appear to be more efficient as a result of their longer-wavelength absorption, lower aggregation behavior, higher singlet oxygen generation efficiency, and higher cellular uptake. Introduction of oligoethylene glycol chains usually further enhance the efficiency. Among these photosensitizers, the 1,4-di-pegylated analogues $\text{ZnPc}[\alpha\text{-O}(\text{CH}_2\text{CH}_2\text{O})_n\text{Me}]_2$ ($n = 3, 4, 6$) are among the most potent photosensitizers in vitro, and therefore can be used as the parent compounds for further modification. For example, the terminal of the chains can be linked up to some tumor specific moieties to enhance the selectivity of the photosensitizers. The resulting conjugates may be useful for targeted photodynamic therapy.

5.4 Experimental Section

5.4.1 General

Experimental details regarding the purification of solvents, instrumentation and in vitro studies were described in Section 2.4. The protected glucose **5.1**,¹⁰ tosylate **4.1d**,¹¹ and 4,5-dibromocatechol **5.11**¹² were prepared as described.

5.4.2 Synthesis

3-*O*-(11-Hydroxy-3,6,9-trioxaundecyl)-1,2:5,6-di-*O*-isopropylidene- α -D-glucopyranose (5.2). The protected glucose **5.1** (6.0 g, 23.1 mmol) was added to a suspension of NaH (60% in mineral oil, 0.92 g, 23.0 mmol) in THF (50 mL). After the evolution of gas bubbles had ceased, a solution of the monotosylate **4.1d** (4.0 g, 11.5 mmol) in THF (30 mL) was added slowly. The mixture was stirred vigorously at room temperature for 24 h. A few drops of water were then added to quench the reaction, then the volatiles were removed under reduced pressure. The residue was mixed in water (120 mL) and the mixture was extracted with chloroform (100 mL x 3). The combined organic extracts were dried over anhydrous MgSO₄ and evaporated under reduced pressure. The residue was subjected to silica gel column chromatography using ethyl acetate as the eluent. The product was obtained as a colorless transparent liquid (1.25 g, 25% yield). ¹H NMR (300 MHz, CDCl₃): δ 5.88 (d, J = 3.6 Hz, 1 H, H1), 4.58 (d, J = 3.6 Hz, 1 H, H2), 4.28-4.36 (m, 1 H, H5), 4.07-4.15 (m, 2 H, H6), 3.98-4.01 (m, 1 H, H4), 3.91 (d, J = 3.0 Hz, 1 H, H3), 3.58-3.77 (m, 16 H, CH₂), 2.88 (t, J = 7.5 Hz, 1 H, OH), 1.48 (s, 3 H, Me), 1.41 (s, 3 H, Me), 1.34 (s, 3 H, Me), 1.30 (s, 3 H, Me); ¹³C{¹H} NMR (300 MHz, CDCl₃): δ 111.7, 108.9, 105.2, 82.6, 81.1, 72.5, 70.6 (several overlapping signals), 70.4, 70.3, 70.1, 67.1, 61.7, 26.8 (two overlapping signals), 26.2, 25.4; MS (ESI): an isotopic cluster peaking at m/z 459 {100%, [M + Na]⁺}; HRMS (ESI): m/z calcd for C₂₀H₃₆NaO₁₀ [M + Na]⁺ 459.2201, found 459.2204.

Glucosylated phthalonitrile 5.3. To a solution of **5.2** (1.11 g, 2.54 mmol) and 4-nitrophthalonitrile (0.66 g, 3.81 mmol) in DMF (8 mL) was added anhydrous K_2CO_3 (1.57 g, 11.36 mmol). The mixture was stirred at 80 °C for 48 h, then the volatiles were removed in vacuo. The residue was mixed with water (80 mL) and the mixture was extracted with $CHCl_3$ (80 mL x 3). The combined organic fractions were dried over anhydrous $MgSO_4$, then evaporated to dryness under reduced pressure. The crude product was purified by silica gel column chromatography using ethyl acetate/hexane (1:1 v/v) as the eluent. The product was obtained as a colorless liquid (0.56 g, 39%). 1H NMR (300 MHz, $CDCl_3$): δ 7.71 (d, $J = 8.7$ Hz, 1 H, ArH), 7.32 (d, $J = 2.7$ Hz, 1 H, ArH), 7.23 (dd, $J = 2.7, 8.7$ Hz, 1 H, ArH), 5.87 (d, $J = 3.6$ Hz, 1 H, H1), 4.57 (d, $J = 3.6$ Hz, 1 H, H2), 4.28-4.34 (m, 1 H, H5), 4.23 (virtual t, $J = 4.5$ Hz, 2 H, $ArOCH_2$), 4.06-4.14 (m, 2 H, H6), 3.96-4.02 (m, 1 H, H4), 3.92 (d, $J = 3.0$ Hz, 1 H, H3), 3.89 (virtual t, $J = 4.5$ Hz, 2 H, CH_2), 3.61-3.77 (m, 12 H, CH_2), 1.49 (s, 3 H, CH_3), 1.42 (s, 3 H, CH_3), 1.35 (s, 3 H, CH_3), 1.31 (s, 3 H, CH_3). $^{13}C\{^1H\}$ NMR (75.4 MHz, $CDCl_3$): δ 162.0, 135.1, 119.8, 119.5, 117.4, 115.6, 115.2, 111.7, 108.9, 107.4, 105.2, 82.7, 82.6, 81.1, 72.5, 70.9, 70.6 (three overlapping CH_2 signals), 70.4, 70.1, 69.2, 68.6, 67.1, 26.8, 26.7, 26.2, 25.4. MS (ESI): an isotopic cluster peaking at m/z 585 (100%, $[M + Na]^+$). HRMS (ESI): m/z calcd for $C_{28}H_{38}N_2NaO_{10}$ $[M + Na]^+$ 585.2419, found 585.2417.

ZnPc(β -PGlu) $_4$ (5.4). A mixture of phthalonitrile **5.3** (0.56 g, 1.0 mmol) and $Zn(OAc)_2 \cdot 2H_2O$ (55 mg, 0.25 mmol) in *n*-pentanol (10 mL) was heated to 100 °C, then a small amount of DBU (0.8 mL) was added. The mixture was stirred at 140-150

$^{\circ}\text{C}$ for 24 h. After a brief cooling, the volatiles were removed under reduced pressure. The residue was purified by silica gel column chromatography using THF/hexane (3:2 v/v) as the eluent, followed by size exclusion chromatography using THF as the eluent. The crude product was further purified by recrystallization from a mixture of THF and hexane (0.14 g, 24%). ^1H NMR (300 MHz, CDCl_3 with a trace amount of pyridine- d_5): δ 9.21-9.28 (m, 4 H, Pc- H_a), 8.82 (virtual s, 4 H, Pc- H_a), 7.69-7.75 (m, 4 H, Pc- H_β), 5.89-5.90 (m, 4 H, H1), 4.70 (br s, 8 H, PcOCH_2), 4.59-4.61 (m, 4 H, H2), 4.32-4.39 (m, 4 H, H5), 3.98-4.21 (m, 20 H, CH_2 , H4 and H6), 3.92-3.96 (m, 12 H, CH_2 and H3), 3.83 (virtual t, $J = 4.5$ Hz, 8 H, CH_2), 3.69-3.78 (m, 24 H, CH_2), 3.66 (t, $J = 4.2$ Hz, 8 H, CH_2), 1.47 (s, 12 H, CH_3), 1.42 (s, 12 H, CH_3), 1.36 (s, 12 H, CH_3), 1.29 (s, 12 H, CH_3). MS (ESI): an isotopic cluster peaking at m/z 2316 {100%, $[\text{M} + \text{H}]^+$ }. HRMS (ESI): m/z calcd for $\text{C}_{112}\text{H}_{153}\text{N}_8\text{O}_{40}\text{Zn}$ $[\text{M} + \text{H}]^+$: 2314.9504, found 2314.9502.

ZnPc(β -Glu) $_4$ (5.5). A mixture of phthalocyanine **5.4** (70 mg, 0.03 mmol) in TFA/water (9:1 v/v) (2 mL) was stirred at room temperature for 30 min. The volatiles were then removed under reduced pressure. The residue was dissolved in water (2 mL), then CH_3OH (ca. 10 mL) was added to induce precipitation. The product was collected by filtration as a blue solid which was then dried in vacuo (46 mg, 77%). ^1H NMR (300 MHz, CDCl_3 with a trace amount of pyridine- d_5): δ 9.25 (br s, 4 H, Pc- H_a), 8.84 (br s, 4 H, Pc- H_a), 7.71 (br s, 4 H, Pc- H_β), 3.6-5.9 (several multiplets). MS (ESI): an isotopic cluster peaking at m/z 1995 {100%, $[\text{M} + \text{H}]^+$ }. HRMS (ESI): m/z calcd for $\text{C}_{88}\text{H}_{121}\text{N}_8\text{O}_{40}\text{Zn}$ $[\text{M} + \text{H}]^+$: 1993.6966, found 1993.6934.

ZnPc(β -PGlu) (5.6). A mixture of phthalonitrile **5.3** (0.56 g, 1.0 mmol), unsubstituted phthalonitrile (1.15 g, 9.0 mmol), and Zn(OAc)₂·2H₂O (0.55 g, 2.5 mmol) in *n*-pentanol (15 mL) was heated to 100 °C, then a small amount of DBU (1 mL) was added. The mixture was stirred at 140-150 °C for 24 h. After a brief cooling, the volatiles were removed under reduced pressure. The residue was dissolved in CHCl₃ (150 mL), then filtered to remove part of the unsubstituted zinc(II) phthalocyanine formed. The filtrate was collected and evaporated to dryness in vacuo. The residue was purified by silica gel column chromatography using CHCl₃/CH₃OH (30:1 v/v) as the eluent, followed by size exclusion chromatography using THF as the eluent. The product was further purified by recrystallization from a mixture of THF and hexane (0.15 g, 15%). ¹H NMR (300 MHz, CDCl₃ with a trace amount of pyridine-d₅): δ 9.31-9.39 (m, 6 H, Pc-H_a), 9.14 (d, J = 8.4 Hz, 1 H, Pc-H_a), 8.71 (s, 1 H, Pc-H_a), 8.06-8.15 (m, 6 H, Pc-H _{β}), 7.62-7.69 (m, 1 H, Pc-H _{β}), 5.89 (d, J = 3.6 Hz, 1 H, H1), 4.68 (virtual t, J = 4.5 Hz, 2 H, PcOCH₂), 4.60 (d, J = 3.6 Hz, 1 H, H2), 4.31-4.38 (m, 1 H, H5), 4.08-4.20 (m, 4 H, CH₂ and H6), 3.92-4.03 (m, 4 H, CH₂, H3 and H4), 3.82-3.86 (m, 2 H, CH₂), 3.72-3.79 (m, 6 H, CH₂), 3.67 (t, J = 4.5 Hz, 2 H, CH₂), 1.48 (s, 3 H, CH₃), 1.43 (s, 3 H, CH₃), 1.36 (s, 3 H, CH₃), 1.30 (s, 3 H, CH₃). ¹³C{¹H} NMR (100.6 MHz, CDCl₃ with a trace amount of pyridine-d₅): δ 160.3, 153.4, 153.3, 153.2, 153.0, 152.7, 152.6, 152.5, 140.1, 138.3, 138.2, 138.1, 137.9, 131.5, 128.8, 128.7, 128.6, 123.3, 122.4, 122.2, 118.2, 111.6, 108.8, 105.2, 82.6, 82.5, 81.0, 72.5, 71.0, 70.7 (two overlapping signals), 70.6, 70.4, 70.1, 69.9, 68.0, 67.1, 26.7 (two overlapping signals), 26.2, 25.4 (some of the Pc signals are

overlapped). MS (ESI): an isotopic cluster peaking at m/z 1011 {100%, $[M + H]^+$ }.

HRMS (ESI): m/z calcd for $C_{52}H_{51}N_8O_{10}Zn$ $[M + H]^+$: 1011.3014, found 1011.3023.

Glucosylated tosylate 5.7. To a solution of *p*-toluenesulfonyl chloride (345 mg, 1.81 mmol) in pyridine (2 mL) was added the glucose-substituted tetraethylene glycol **5.2** (280 mg, 0.64 mmol). The mixture was stirred at room temperature for 24 h, then water (5 mL) was added to quench the reaction. The mixture was then extracted with CH_2Cl_2 (20 mL x 3). The combined organic fractions were dried over anhydrous $MgSO_4$ and rotary-evaporated to dryness. The residue was chromatographed using ethyl acetate as the eluent to give the product as a colorless liquid (325 mg, 86%). 1H NMR (300 MHz, $CDCl_3$): δ 7.80 (d, $J = 8.1$ Hz, 2 H, ArH), 7.34 (d, $J = 8.1$ Hz, 2 H, ArH), 5.86 (d, $J = 3.6$ Hz, 1 H, H1), 4.57 (d, $J = 3.6$ Hz, 1 H, H2), 4.26-4.32 (m, 1 H, H5), 4.05-4.18 (m, 4 H, CH_2 and H6), 3.96-4.02 (m, 1 H, H4), 3.92 (d, $J = 2.7$ Hz, 1 H, H3), 3.71-3.77 (m, 2 H, CH_2), 3.69 (t, $J = 4.8$ Hz, 2 H, CH_2), 3.58-3.63 (m, 10 H, CH_2), 2.45 (s, 3 H, CH_3), 1.49 (s, 3 H, CH_3), 1.42 (s, 3 H, CH_3), 1.34 (s, 3 H, CH_3), 1.31 (s, 3 H, CH_3). $^{13}C\{^1H\}$ NMR (75.4 MHz, $CDCl_3$): δ 144.8, 133.0, 129.8, 127.9, 111.7, 108.8, 105.2, 82.7, 82.6, 81.1, 72.5, 70.7, 70.6 (two overlapping signals), 70.5, 70.4, 70.1, 69.2, 68.7, 67.1, 26.8, 26.7, 26.2, 25.4, 21.6. MS (ESI): an isotopic cluster peaking at m/z 613 {100%, $[M + Na]^+$ }. HRMS (ESI): m/z calcd for $C_{27}H_{42}NaO_{12}S$ $[M + Na]^+$ 613.2289, found 613.2282.

Bis(glucosylated) phthalonitrile 5.8. To a mixture of tosylate **5.7** (2.70 g, 4.57 mmol) and 2,3-dicyanohydroquinone (0.37 g, 2.31 mmol) in DMF (10 mL) was added anhydrous K_2CO_3 (1.26 g, 9.12 mmol). The mixture was stirred at 110 °C for 24 h,

then the solvent was removed at ca. 60 °C in vacuo. The residue was mixed with water (100 mL) and the mixture was extracted with CH₂Cl₂ (100 mL x 3). The combined organic fractions were dried over anhydrous MgSO₄ and rotary-evaporated to dryness. The crude product was purified by silica gel column chromatography using ethyl acetate/CHCl₃ (1:5 v/v) as the eluent. The product was isolated as a colorless oil (2.10 g, 92%). ¹H NMR (300 MHz, CDCl₃): δ 7.23 (s, 2 H, ArH), 5.87 (d, *J* = 3.6 Hz, 2 H, H1), 4.58 (d, *J* = 3.6 Hz, 2 H, H2), 4.28-4.33 (m, 2 H, H5), 4.23 (virtual t, *J* = 4.8 Hz, 4 H, ArOCH₂), 4.06-4.14 (m, 4 H, H6), 3.96-4.02 (m, 2 H, H4), 3.88-3.93 (m, 6 H, CH₂ and H3), 3.72-3.78 (m, 8 H, CH₂), 3.61-3.69 (m, 16 H, CH₂), 1.49 (s, 6 H, CH₃), 1.42 (s, 6 H, CH₃), 1.35 (s, 6 H, CH₃), 1.31 (s, 6 H, CH₃). ¹³C {¹H} NMR (75.4 MHz, CDCl₃): δ 155.3, 119.1, 112.9, 111.7, 108.8, 105.2, 82.6, 82.5, 81.0, 72.5, 71.1, 70.6, 70.4, 70.1, 70.0, 69.3, 67.1, 26.8, 26.7, 26.2, 25.4 (some of the signals are overlapped). MS (ESI): an isotopic cluster peaking at *m/z* 1020 {100%, [M + Na]⁺}. HRMS (ESI): *m/z* calcd for C₄₈H₇₂N₂NaO₂₀ [M + Na]⁺ 1019.4572, found 1019.4573.

ZnPc(α-PGlu)₂ (5.9). According to the procedure described for **5.6**, phthalonitrile **5.8** (0.50 g, 0.50 mmol) was treated with unsubstituted phthalonitrile (0.58 g, 4.51 mmol) and Zn(OAc)₂·2H₂O (0.28 g, 1.25 mmol) to give **5.9** as a blue-green solid (87 mg, 12%). ¹H NMR (300 MHz, CDCl₃ with a trace amount of pyridine-*d*₅): δ 9.37-9.43 (m, 4 H, Pc-H_a), 9.30 (d, *J* = 6.0 Hz, 2 H, Pc-H_a), 8.08-8.17 (m, 6 H, Pc-H_β), 7.45 (s, 2 H, Pc-H_β), 5.87 (d, *J* = 3.6 Hz, 2 H, H1), 4.93 (t, *J* = 5.1 Hz, 4 H, PcOCH₂), 4.56 (d, *J* = 3.6 Hz, 2 H, H2), 4.53 (t, *J* = 5.1 Hz, 4 H, CH₂), 4.28-4.35

(m, 2 H, H5), 4.06-4.17 (m, 8 H, CH₂ and H6), 3.97-4.01 (m, 2 H, H4), 3.86-3.91 (m, 6 H, CH₂ and H3), 3.58-3.75 (m, 16 H, CH₂), 1.47 (s, 6 H, CH₃), 1.41 (s, 6 H, CH₃), 1.34 (s, 6 H, CH₃), 1.28 (s, 6 H, CH₃). ¹³C{¹H} NMR (75.4 MHz, CDCl₃ with a trace amount of pyridine-d₅): δ 153.9, 153.8, 153.6, 152.6, 150.4, 138.9, 138.5, 129.0, 127.4, 122.6, 122.5, 115.0, 111.6, 108.8, 105.2, 82.6, 82.5, 81.0, 72.5, 71.1, 70.8, 70.7, 70.6, 70.5, 70.4, 70.0, 69.2, 67.1, 26.7 (two overlapping signals), 26.2, 25.4 (some of the Pc signals are overlapped). MS (ESI): an isotopic cluster peaking at *m/z* 1468 {100%, [M + Na]⁺}. HRMS (ESI): *m/z* calcd for C₇₂H₈₄N₈NaO₂₀Zn [M + Na]⁺: 1467.4986, found 1467.4976.

ZnPc(α-Glu)₂ (5.10). Phthalocyanine **5.9** (60 mg, 0.04 mmol) was dissolved in TFA/water (9:1 v/v) (2 mL). The mixture was stirred at room temperature for 30 min, then the volatiles were removed in vacuo. The residue was dissolved in water (2 mL), then CH₃OH (ca. 10 mL) was added to induce precipitation. The product was collected by filtration as a blue solid which was then dried in vacuo (47 mg, 89%). ¹H NMR (300 MHz, CDCl₃ with a trace amount of pyridine-d₅): δ 9.24 (br s, 4 H, Pc-H_α), 9.15 (br s, 2 H, Pc-H_α), 7.90-8.00 (m, 6 H, Pc-H_β), 7.36 (s, 2 H, Pc-H_β), 3.1-5.4 (several multiplets). MS (ESI): an isotopic cluster peaking at *m/z* 1307 {100%, [M + Na]⁺}. HRMS (ESI): *m/z* calcd for C₆₀H₆₈N₈NaO₂₀Zn [M + Na]⁺: 1307.3734, found 1307.3734.

Diol 5.12. A mixture of 4,5-dibromocatechol (**5.11**) (3.1 g, 11.6 mmol), tosylate **4.1d** (16.0 g, 45.9 mmol), and K₂CO₃ (21.1 g, 0.15 mol) in DMF (80 mL) was stirred at 100 °C for ca. 60 h. The mixture was allowed to cool down to room temperature,

then it was poured into water (160 mL). The organic layer was extracted with CH_2Cl_2 (120 mL x 3), washed with water (90 mL x 4), and dried over anhydrous MgSO_4 . The crude product was purified by silica gel column chromatography using $\text{CH}_2\text{Cl}_2/\text{CH}_3\text{OH}$ (8:1 v/v) as the eluent to give the product as a colorless liquid (6.4 g, 90%). ^1H NMR (300 MHz, CDCl_3): δ 7.13 (s, 2 H, ArH), 4.13 (t, $J = 4.8$ Hz, 4 H, CH_2), 3.85 (t, $J = 4.8$ Hz, 4 H, CH_2), 3.65–3.75 (m, 20 H, CH_2), 3.57–3.61 (m, 4 H, CH_2), 3.07 (t, $J = 5.4$ Hz, 2 H, OH). $^{13}\text{C}\{^1\text{H}\}$ NMR (75.4 MHz, CDCl_3): δ 148.5, 118.5, 115.1, 72.5, 70.6, 70.4, 70.3, 70.0, 69.3, 69.0, 61.4. MS (ESI): several isotopic clusters peaking at m/z 485 {100%, $[\text{M} + \text{Na} - 2 \text{Br}]^+$ }, 565 {29%, $[\text{M} + \text{Na} - \text{Br}]^+$ } and 643 {56%, $[\text{M} + \text{Na}]^+$ }. HRMS (ESI): m/z calcd for $\text{C}_{22}\text{H}_{36}\text{Br}_2\text{NaO}_{10}$ $[\text{M} + \text{Na}]^+$: 643.0547, found 643.0545.

Ditosylate 5.13. A mixture of the diol **5.12** (4.80 g, 7.7 mmol), tosyl chloride (5.72 g, 30.0 mmol) and triethylamine (2.6 mL, 18.6 mmol) in CH_2Cl_2 (60 mL) was stirred at room temperature for 24 h. The mixture was poured into 2 N hydrochloric acid (60 mL), then extracted with CH_2Cl_2 (180 mL). The organic layer was washed with water (100 mL x 3) and dried over anhydrous MgSO_4 . After evaporation, the residue was chromatographed on a silica gel column using ethyl acetate/hexane (1:1 v/v) followed by ethyl acetate as the eluents. The product was isolated as a colorless oil (4.88 g, 68%). ^1H NMR (300 MHz, CDCl_3): δ 7.79 (d, $J = 8.4$ Hz, 4 H, ArH), 7.34 (d, $J = 8.4$ Hz, 4 H, ArH), 7.13 (s, 2 H, ArH), 4.10–4.17 (m, 8 H, CH_2), 3.83 (virtual t, $J = 5.1$ Hz, 4 H, CH_2), 3.58–3.71 (m, 20 H, CH_2), 2.44 (s, 6 H, CH_3). $^{13}\text{C}\{^1\text{H}\}$ NMR (75.4 MHz, CDCl_3): δ 148.8, 144.7, 132.9, 129.8, 127.9, 119.0, 115.2, 70.8, 70.7, 70.6,

70.5, 69.5, 69.2 (two overlapping signals), 68.6, 21.6. MS (ESI): several isotopic clusters peaking at m/z 793 {64%, $[M + Na - 2 Br]^+$ }, 873 {42%, $[M + Na - Br]^+$ } and 951 {100%, $[M + Na]^+$ }. HRMS (ESI): m/z calcd for $C_{36}H_{48}Br_2NaO_{14}S_2 [M + Na]^+$: 951.0724, found 951.0723.

Bis(glucosylated) dibromobenzene 5.14. Ditosylate **5.13** (5.85 g, 6.3 mmol) was added into a mixture of 1,2:5,6-di-*O*-isopropylidene- α -D-glucufuranose (**5.1**) (3.28 g, 12.6 mmol) and NaH (60% in mineral oil, 0.50 g, 12.5 mmol) in THF (60 mL). The mixture was stirred at room temperature overnight, then evaporated in vacuo. The residue was mixed with water (120 mL) and the mixture was extracted with CH_2Cl_2 (120 mL x 3). The combined organic fractions were dried over anhydrous $MgSO_4$. After evaporation, the residue was chromatographed on a silica gel column using ethyl acetate as the eluent (6.05 g, 87%). 1H NMR (300 MHz, $CDCl_3$): δ 7.15 (s, 2 H, ArH), 5.87 (d, $J = 3.6$ Hz, 2 H, H1), 4.57 (d, $J = 3.6$ Hz, 2 H, H2), 4.27-4.33 (m, 2 H, H5), 4.05-4.15 (m, 8 H, CH_2 and H6), 3.97-4.02 (m, 2 H, H4), 3.92 (d, $J = 3.0$ Hz, 2 H, H3), 3.83 (t, $J = 5.1$ Hz, 4 H, CH_2), 3.60-3.76 (m, 24 H, CH_2), 1.49 (s, 6 H, CH_3), 1.42 (s, 6 H, CH_3), 1.34 (s, 6 H, CH_3), 1.31 (s, 6 H, CH_3). $^{13}C\{^1H\}$ NMR (75.4 MHz, $CDCl_3$): δ 148.8, 119.1, 115.3, 111.7, 108.9, 105.2, 82.7, 82.6, 81.1, 72.5, 70.9, 70.7 (three overlapping signals), 70.4, 70.1, 69.6, 69.2, 67.1, 26.8, 26.7, 26.2, 25.4. MS (ESI): an isotopic cluster peaking at m/z 1127 {100%, $[M + Na]^+$ }. HRMS (ESI): m/z calcd for $C_{46}H_{72}Br_2NaO_{20} [M + Na]^+$: 1127.2855, found 1127.2857.

Bis(glucosylated) phthalonitrile 5.15. A mixture of **5.14** (1.62 g, 1.47 mmol) and CuCN (0.39 g, 4.35 mmol) in DMF (15 mL) was refluxed for 12 h. The mixture

was allowed to cool down to room temperature, then poured into 30% aqueous ammonia (25 mL). The blue solution was bubbled with air for 2 h, then filtered. The filtrate was extracted with CH₂Cl₂ (200 mL) and the organic portion was washed with water (90 mL x 3). After evaporation, the residue was chromatographed on a silica gel column using ethyl acetate as the eluent to give the product as a colorless oil (0.18 g, 12%). ¹H NMR (300 MHz, CDCl₃): δ 7.34 (s, 2 H, ArH), 5.87 (d, *J* = 3.6 Hz, 2 H, H1), 4.57 (d, *J* = 3.6 Hz, 2 H, H2), 4.20-4.33 (m, 6 H, CH₂ and H5), 4.05-4.14 (m, 4 H, H6), 3.97-4.02 (m, 2 H, H4), 3.87-3.92 (m, 6 H, CH₂ and H3), 3.60-3.77 (m, 24 H, CH₂), 1.49 (s, 6 H, CH₃), 1.42 (s, 6 H, CH₃), 1.35 (s, 6 H, CH₃), 1.31 (s, 6 H, CH₃). ¹³C{¹H} NMR (75.4 MHz, CDCl₃): δ 152.3, 117.1, 115.7, 113.5, 111.7, 108.9, 105.2, 82.7, 82.6, 81.1, 72.5, 70.6, 70.4, 70.1, 69.4, 69.3, 67.1, 26.8, 26.7, 26.2, 25.4 (some of the signals are overlapped). MS (ESI): an isotopic cluster peaking at *m/z* 1019 {100%, [M + Na]⁺}. HRMS (ESI): *m/z* calcd for C₄₈H₇₂N₂NaO₂₀ [M + Na]⁺: 1019.4571, found 1019.4579.

ZnPc(β-PGlu)₂ (5.16). According to the procedure described for **5.6**, phthalonitrile **5.15** (218 mg, 0.22 mmol) was treated with unsubstituted phthalonitrile (281 mg, 2.19 mmol) and Zn(OAc)₂·2H₂O (132 mg, 0.60 mmol) to give **5.16** as a blue solid (45 mg, 14%). ¹H NMR (300 MHz, CDCl₃ with a trace amount of pyridine-d₅): δ 9.23-9.35 (m, 6 H, Pc-H_a), 8.58 (s, 2 H, Pc-H_a), 8.06-8.14 (m, 6 H, Pc-H_β), 5.88 (d, *J* = 3.6 Hz, 2 H, H1), 4.72 (t, *J* = 4.8 Hz, 4 H, PcOCH₂), 4.59 (d, *J* = 3.6 Hz, 2 H, H2), 4.30-4.37 (m, 2 H, H5), 4.24 (virtual t, *J* = 4.8 Hz, 4 H, CH₂), 4.08-4.15 (m, 4 H, H6), 3.98-4.02 (m, 6 H, CH₂ and H4), 3.94 (d, *J* = 3.0 Hz, 2 H, H3), 3.85-3.88 (m, 4 H,

CH₂); 3.72-3.82 (m, 12 H, CH₂), 3.65-3.68 (m, 4 H, CH₂), 1.48 (s, 6 H, CH₃), 1.42 (s, 6 H, CH₃), 1.35 (s, 6 H, CH₃), 1.30 (s, 6 H, CH₃). ¹³C{¹H} NMR (75.4 MHz, CDCl₃ with a trace amount of pyridine-d₅): δ 153.1, 153.0, 152.8, 150.7, 138.3, 138.1, 132.1, 128.7, 122.4, 111.6, 108.8, 105.6, 105.2, 82.6 (two overlapping signals), 81.0, 72.5, 71.0, 70.8, 70.7, 70.6, 70.4, 70.0, 69.8, 68.9, 67.0, 26.7 (two overlapping signals), 26.1, 25.4 (some of the Pc signals are overlapped). MS (ESI): an isotopic cluster peaking at *m/z* 1468 {100%, [M + Na]⁺}. HRMS (ESI): *m/z* calcd for C₇₂H₈₄N₈NaO₂₀Zn [M + Na]⁺: 1467.4986, found 1467.4981.

5.5. References

- 1 (a) Ali, H.; van Lier, J. E. *Chem. Rev.* **1999**, *99*, 2379. (b) Lukyanets, E. A. *J. Porphyrins Phthalocyanines* **1999**, *3*, 424. (c) Allen, C. M.; Sharman, W. M.; van Lier, J. E. *J. Porphyrins Phthalocyanines* **2001**, *5*, 161. (d) Ogura, S.; Tabata, K.; Fukushima, K.; Kamachi, T.; Okura, I. *J. Porphyrins Phthalocyanines* **2006**, *10*, 1116.
- 2 See for example: (a) Lo, P.-C.; Huang, J.-D.; Cheng, D. Y. Y.; Chan, E. Y. M.; Fong, W.-P.; Ko, W.-H.; Ng, D. K. P. *Chem. Eur. J.* **2004**, *10*, 4831. (b) Nishiyama, N.; Iriyama, A.; Jang, W.-D.; Miyata, K.; Itaka, K.; Inoue, Y.; Takahashi, H.; Yanagi, Y.; Tamaki, Y.; Koyama, H.; Kataoka, K. *Nature Mater.* **2005**, *4*, 934. (c) Sharman, W. M.; van Lier, J. E. *Bioconjugate Chem.* **2005**, *16*, 1166. (d) Hofman, J.-W.; van Zeeland, F.; Turker, S.; Talsma, H.; Lambrechts, S. A. G.; Sakharov, D. V.; Hennink, W. E.; van Nostrum, C. F. *J. Med. Chem.* **2007**, *50*, 1485. (e) Sibrian-Vazquez, M.; Ortiz, J.; Nesterova, I. V.; Fernández-Lázaro, F.; Sastre-Santos, A.; Soper, S. A.; Vicente, M. G. H. *Bioconjugate Chem.* **2007**, *18*, 410. (f) Li, H.; Jensen, T. J.; Fronczek, F. R.; Vicente, M. G. H. *J. Med. Chem.* **2008**, *51*, 502. (g) Liu, J.-Y.; Jiang, X.-J.; Fong, W.-P.; Ng, D. K. P. *Metal-Based*

- Drugs* **2008**, Article ID 284691. (h) Leung, S. C. H.; Lo, P.-C.; Ng, D. K. P.; Liu, W.-K.; Fung, K.-P.; Fong, W.-P. *Br. J. Pharm.* **2008**, *154*, 4.
- 3 Taquet, J.-P.; Frochot, C.; Manneville, V.; Barberi-Heyob, M. *Curr. Med. Chem.* **2007**, *14*, 1673.
- 4 Warburg, O. *Science* **1956**, *123*, 309.
- 5 Airley, R. E.; Mobasheri, A. *Chemotherapy* **2007**, *53*, 233.
- 6 MacDonald, I. J.; Dougherty, T. J. *J. Porphyrins Phthalocyanines* **2001**, *5*, 105.
- 7 (a) Aksenova, A. A.; Sebyakin, Yu. L.; Mironov, A. F. *Russ. J. Bioorg. Chem.* **2003**, *29*, 210. (b) Chen, X.; Drain, C. M. *Drug Design Rev. - Online* **2004**, *1*, 215. (c) Chen, X.; Hui, L.; Foster, D. A.; Drain, C. M. *Biochemistry* **2004**, *43*, 10918. (d) Laville, I.; Pigaglio, S.; Blais, J.-C.; Doz, F.; Loock, B.; Maillard, P.; Grierson, D. S.; Blais, J. *J. Med. Chem.* **2006**, *49*, 2558. (e) Obata, M.; Hirohara, S.; Sharyo, K.; Alitomo, H.; Kajiwara, K.; Ogata, S.-i.; Tanihara, M.; Ohtsuki, C.; Yano, S. *Biochim. Biophys. Acta* **2007**, *1770*, 1204.
- 8 (a) Laville, I.; Figueiredo, T.; Loock, B.; Pigaglio, S.; Maillard, Ph.; Grierson, D. S.; Carrez, D.; Croisy, A.; Blais, J. *Bioorg. Med. Chem.* **2003**, *11*, 1643. (b) Hirohara, S.; Obata, M.; Ogata, S.-i.; Kajiwara, K.; Ohtsuki, C.; Tanihara, M.; Yano, S. *J. Photochem. Photobiol. B: Biol.* **2006**, *84*, 56. (c) Pandey, S. K.; Zheng, X.; Morgan, J.; Missert, J. R.; Liu, T.-H.; Shibata, M.; Bellnier, D. A.; Oseroff, A. R.; Henderson, B. W.; Dougherty, T. J.; Pandey, R. K. *Mol. Pharm.* **2007**, *4*, 448.
- 9 Zhang, M.; Zhang, Z.; Blessington, D.; Li, H.; Busch, T. M.; Madrak, V.; Miles, J.; Chance, B.; Glickson, J. D.; Zheng, G. *Bioconjugate Chem.* **2003**, *14*, 709.
- 10 (a) He, Y.-Y.; An, J.-Y.; Jiang, L.-J. *Biochim. Biophys. Acta* **1999**, *1472*, 232. (b) Jiang, L.-J.; He, Y.-Y. *Chin. Sci. Bull.* **2001**, *46*, 6.
- 11 (a) Lee, P. P. S.; Lo, P.-C.; Chan, E. Y. M.; Fong, W.-P.; Ko, W.-H.; Ng, D. K. P. *Tetrahedron Lett.* **2005**, *46*, 1551. (b) Lo, P.-C.; Chan, C. M. H.; Liu, J.-Y.; Fong, W.-P.; Ng, D. K. P. *J. Med. Chem.* **2007**, *50*, 2100. (c) Lo, P.-C.; Leung, S. C. H.; Chan, E. Y. M.; Fong, W.-P.; Ko, W.-H.; Ng, D. K. P. *Photodiagn. Photodyn. Ther.* **2007**, *4*, 117. (d) Lo, P.-C.; Fong, W.-P.; Ng, D. K. P. *ChemMedChem* **2008**, *3*, 1110.

- 12 Choi, C.-F.; Huang, J.-D.; Lo, P.-C.; Fong, W.-P.; Ng, D. K. P. *Org. Biomol. Chem.* **2008**, *6*, 2173.
- 13 (a) Fukuda, T.; Homma, S.; Kobayashi, N. *Chem. Eur. J.* **2005**, *11*, 5205. (b) Maqanda, W.; Nyokong, T.; Maree, M. D. *J. Porphyrins Phthalocyanines* **2005**, *9*, 343. (c) Li, H.; Fronczek, F. R.; Vicente, M. G. H. *Tetrahedron Lett.* **2008**, *49*, 4828.
- 14 Liu, J.-Y.; Jiang, X.-J.; Fong, W.-P.; Ng, D. K. P. *Org. Biomol. Chem.* **2008**, *6*, 4560.
- 15 (a) Kobayashi, N.; Sasaki, N.; Higashi, Y.; Osa, T. *Inorg. Chem.* **1995**, *34*, 1636. (b) Kobayashi, N.; Ogata, H.; Nonaka, N.; Luk'yanets, E. A. *Chem. Eur. J.* **2003**, *9*, 5123.
- 16 Maree, M. D.; Kuznetsova, N.; Nyokong, T. *J. Photochem. Photobiol. A: Chem.* **2001**, *140*, 117.
- 17 Spiller, W.; Kliesch, H.; Wöhrle, D.; Hackbarth, S.; Röder, B.; Schnurpfeil, G. *J. Porphyrins Phthalocyanines* **1998**, *2*, 145.
- 18 Scalise, I.; Durantini, E. N. *Bioorg. Med. Chem.* **2005**, *13*, 3037.
- 19 (a) Spikes, D. *J. Photochem. Photobiol.* **1986**, *43*, 691. (b) Dhami, S.; Phillips, D. *J. Photochem. Photobiol. A: Chem.* **1996**, *100*, 77. (c) Howe, L.; Zhang, J. Z. *J. Phys. Chem. A* **1997**, *101*, 3207. (d) Suchetti, C. A.; Durantini, E. N. *Dyes Pigments* **2007**, *74*, 630.
- 20 Li, Z. Y.; Lieberman, M. *Inorg. Chem.* **2001**, *40*, 932.
- 21 Bauer, H.; Stier, F.; Petry, C.; Knorr, A.; Stadler, C.; Staab, H. A. *Eur. J. Org. Chem.* **2001**, 3255.
- 22 Schmidt, O. T. in *Methods in Carbohydrate Chemistry*; eds. Whistler, R. L., Wolfrom, M. L., eds.; Academic Press, New York, 1963; vol. II, pp 318-325.

Chapter 6

Highly Efficient Energy Transfer in Subphthalocyanine-BODIPY Conjugates

6.1 Introduction

Excitation energy transfer (EET) is a vital process in nature. Photosynthetic organisms, for example, make use of chromophore-rich antenna proteins to funnel the captured light energy to the reaction center where it initiates a multistep electron-transfer reaction, leading eventually to the oxidation of water to oxygen and the fixation of carbon dioxide.¹ Energy transfer also plays an important role in many artificial processes such as photochemical conversion of solar energy by artificial photosynthetic systems,^{1,2} information processing with a variety of molecular devices and machines,³ and detection of analytes with molecular based sensors.⁴ Numerous artificial antenna systems with different combinations of chromophores have been studied with a view to enhancing the energy transfer efficiency and facilitating their use in different forms.^{1,2a,5} Among the different chromophores, boron dipyrromethene (BODIPY) dyes are of particular interest because of their large extinction coefficients, high fluorescence quantum yields, reasonably long excited singlet-state lifetimes, and good solubility and stability in many solvent systems.⁶ More importantly, the BODIPY core can be modified readily to tailor their absorption and emission properties. Light-harvesting BODIPY derivatives conjugated with energy donors such

as pyrenes and anthracenes,⁷ and energy acceptors such as porphyrins,^{3a,8} perylenediimides,⁹ and extended BODIPY¹⁰ have been reported. I report in this Chapter the preparation and energy transfer properties of the first BODIPY derivatives linked to a subphthalocyanine unit. Subphthalocyanines are lower homologues of phthalocyanines, and they are also versatile functional dyes with remarkable photophysical and photochemical properties.¹¹ Several subphthalocyanine-C₆₀¹² and subphthalocyanine-phthalocyanine¹³ dyads have been reported which exhibit an efficient singlet-singlet energy transfer process. The major absorption and fluorescence emission positions of subphthalocyanines (ca. 560-570 nm) are complementary with those of BODIPY (ca. 500-520 nm) and distyryl BODIPY (ca. 630-680 nm). Therefore, the resulting conjugates should absorb over a broad range in the visible region and have a good spectral overlap between the donor emission and the acceptor absorption. Both of these features are desirable for efficient light-harvesting systems.

In this Chapter, two novel subphthalocyanines substituted axially with a BODIPY or distyryl BODIPY moiety have been synthesized. Both systems exhibit a highly efficient photoinduced energy transfer process, either from the excited BODIPY to the subphthalocyanine core (for the former) or from the excited subphthalocyanine to the distyryl BODIPY unit (for the latter) as shown in Figure 6.1.

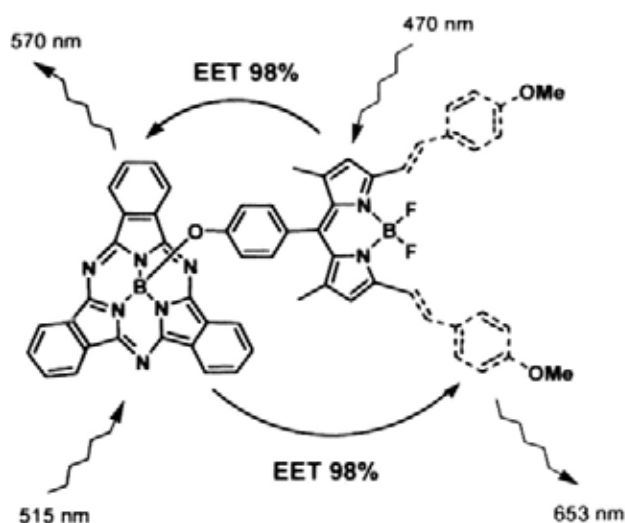


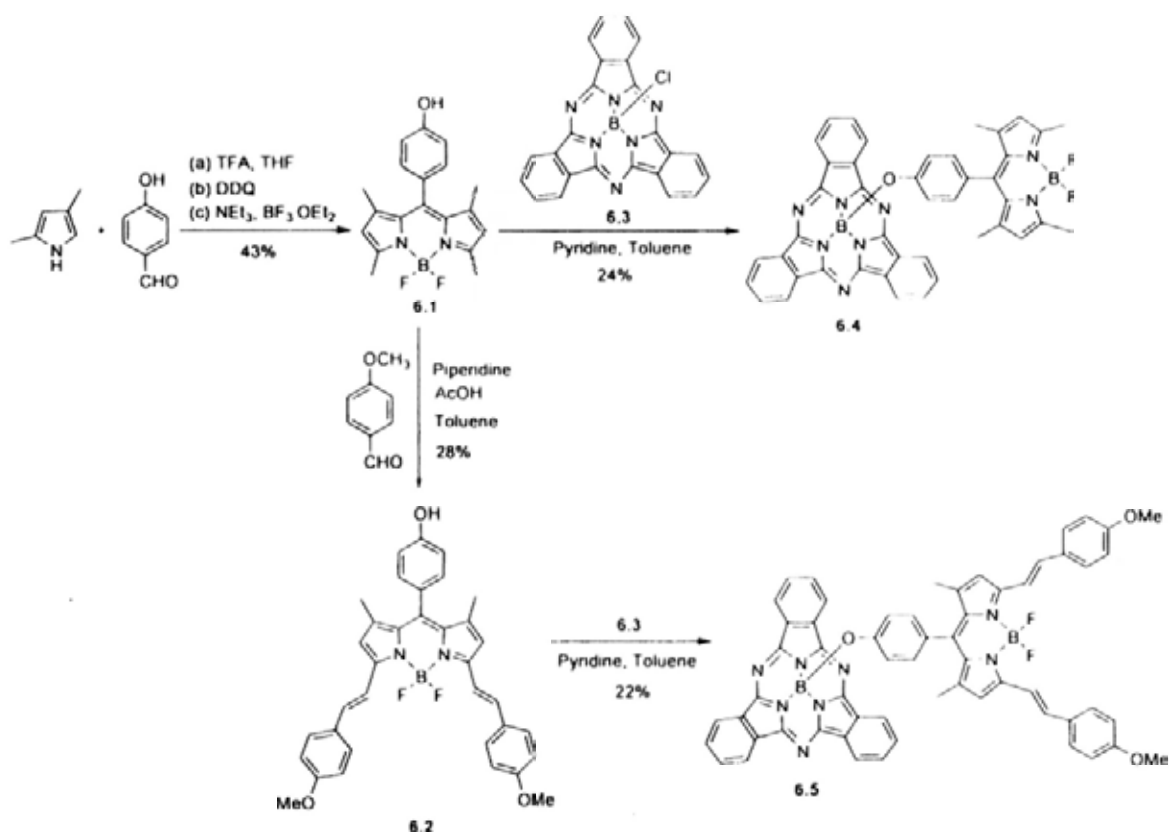
Figure 6.1. Energy transfer processes in subphthalocyanine-BODIPY conjugates.

6.2 Results and Discussion

6.2.1 Preparation and Characterization

Two subphthalocyanine-BODIPY derivatives **6.4** and **6.5** were prepared according to Scheme 6.1. The phenol-containing BODIPY **6.1** was first prepared by treating 2,4-dimethylpyrrole with 4-hydroxybenzaldehyde via sequential condensation, oxidation, and complexation reactions. The preparation of this compound had been reported previously,¹⁴ but by following this procedure, only a tiny amount of product could be obtained in our hands. After several attempts, we found that by changing the solvent from CH_2Cl_2 to THF (which can better solublize the reagents) and using 2,3-dichloro-5,6-dicyano-*p*-benzoquinone (DDQ) instead of tetrachlorobenzoquinone as the oxidizing agent, compound **6.1** could be obtained in 43% yield. This compound then underwent condensation reaction with 4-methoxybenzaldehyde in the presence of piperidine to give the distyryl BODIPY **6.2** in 28% yield. Both **6.1** and **6.2** were then treated with the commercially available boron(III) subphthalocyanine chloride (**6.3**) in

the presence of pyridine in toluene to afford the substituted products **6.4** and **6.5**, respectively. The yields of these products are relatively low probably due to the low reactivity of the BODIPY-appended phenols **6.1** and **6.2**. Both conjugates possess good solubility in common organic solvents and could be purified readily by column chromatography followed by size exclusion chromatography and recrystallization.



Scheme 6.1. Synthesis of conjugates **6.4** and **6.5**.

All of the new BODIPY derivatives **6.2**, **6.4**, and **6.5** were characterized with various spectroscopic methods and X-ray diffraction analyses. The ^1H NMR signals for the meso-*p*-phenylene protons of **6.4** and **6.5** are significantly upfield-shifted compared with those of their respective precursors **6.1** and **6.2** (both by 0.5 and 1.4

ppm for the two doublets), as a result of the shielding effect by the subphthalocyanine ring current. The high-resolution ESI mass spectrum of **6.5** showed two major envelopes peaking at m/z 970 and 951, which are due to the ions $[M]^+$ and $[M - F]^+$, respectively. The isotopic distribution was in good agreement with the simulated pattern as shown in Figure 6.2. Accurate mass measurements also gave very satisfactory results.

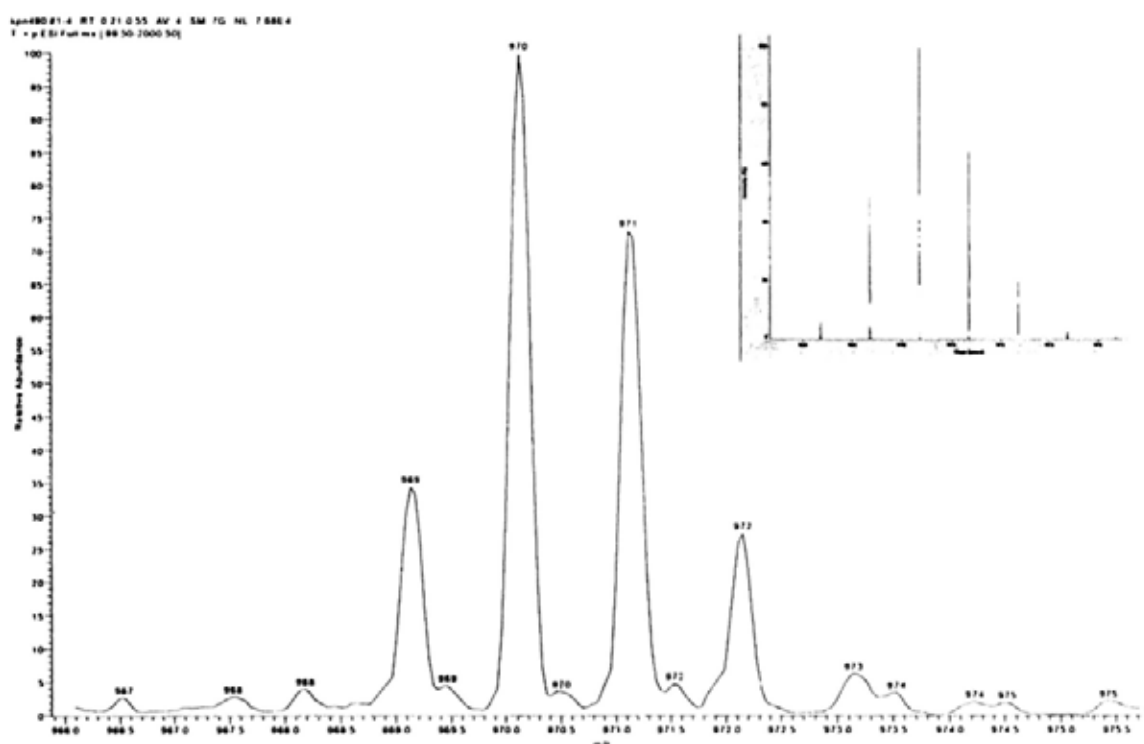


Figure 6.2. The enlarged high-resolution ESI mass spectrum of **6.5** showing the $[M]^+$ ion peak. The inset shows the simulated isotopic pattern.

Single crystals of all these compounds were grown by layering hexane onto their CH_2Cl_2 solutions. The distyryl BODIPY **6.2** crystallizes in the monoclinic system with a Cc space group. Its molecular structure (Figure 6.3) shows typical structural features of BODIPYs¹⁵ with two extended styryl groups. The

subphthalocyanine-BODIPY dyad **6.4** crystallizes with a water molecule in the monoclinic system with a $P2_1/c$ space group, while the dyad **6.5** crystallizes in the triclinic system with a $P1(\bar{bar})$ space group containing a CH_2Cl_2 solvent molecule. Their molecular structures are shown in Figures 6.4 and 6.5, which clearly show that the cone-shaped subphthalocyanine unit is axially bound to BODIPY **6.1** or **6.2** via the phenoxy group. The B-O bond distances [1.435(5) and 1.440(8) Å for **6.4** and **6.5**, respectively] and the average B-N bond distances of the subphthalocyanine core are very similar with those in the subphthalocyanine analogue having an axial 4-(3,6-dioxaheptoxy)phenoxy group [1.440(4) and 1.496(5) Å, respectively].¹⁶ The structural parameters of **6.2** are not significantly changed upon conjugation to the subphthalocyanine unit.

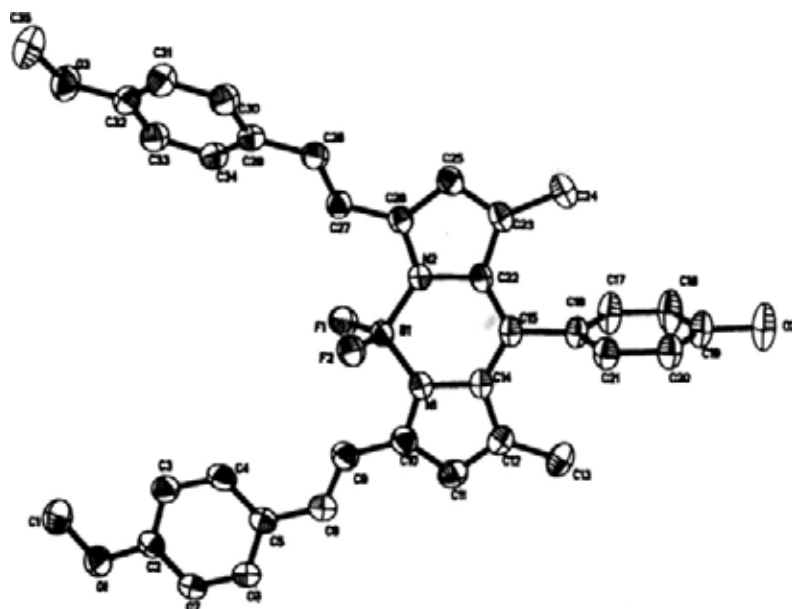


Figure 6.3. Molecular structure of **6.2** showing the 30% probability thermal ellipsoids for all non-hydrogen atoms.

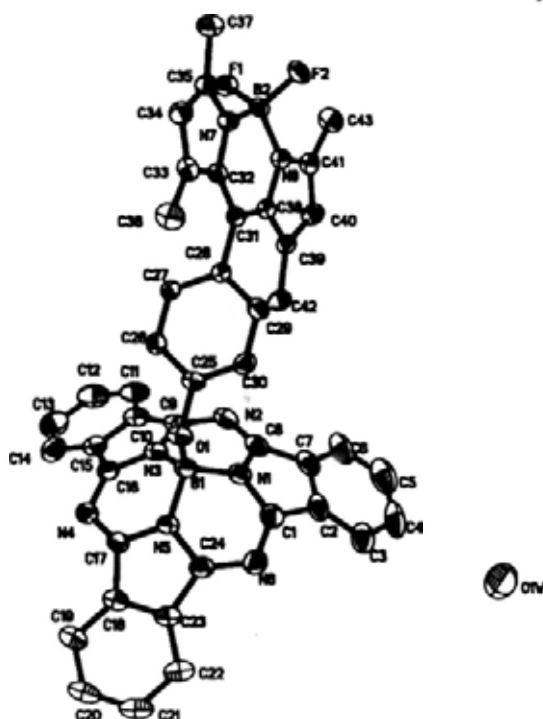


Figure 6.4. Molecular structure of 6.4 showing the 30% probability thermal ellipsoids for all non-hydrogen atoms.

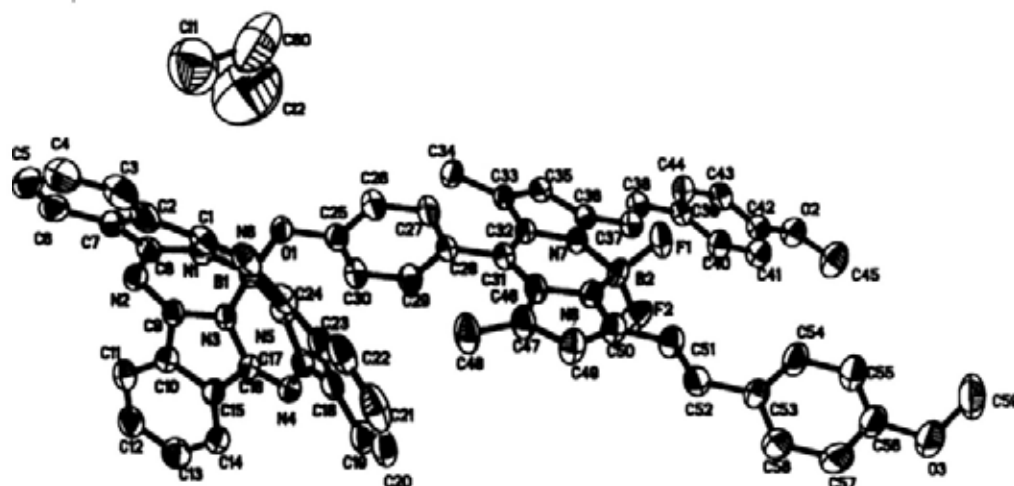
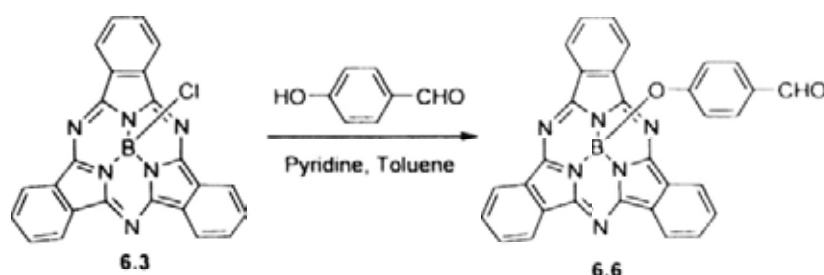


Figure 6.5. Molecular structure of 6.5 showing the 30% probability thermal ellipsoids for all non-hydrogen atoms.

6.2.2 Electronic Absorption and Photophysical Properties

Figure 6.6 shows the normalized absorption spectra of the dyad **6.4**, BODIPY **6.1**, and the subphthalocyanine with an axial 4-methanoylphenoxy group (compound **6.6**), which was prepared by the substitution reaction of **6.3** with 4-hydroxybenzaldehyde (Scheme 6.2).¹⁷ The latter two compounds were used as the references. The dyad **6.4** shows two major absorption bands at 502 and 563 nm, which are virtually unshifted compared with those of **6.1** and **6.6**. Similarly, the electronic absorption spectrum of the dyad **6.5** is essentially the same as the sum of the spectra of the two reference compounds **6.2** and **6.6** (Figure 6.7). These observations indicate that the two chromophores in **6.4** and **6.5** do not have significant ground-state interactions.



Scheme 6.2. Synthesis of subphthalocyanine **6.6** as a reference compound.

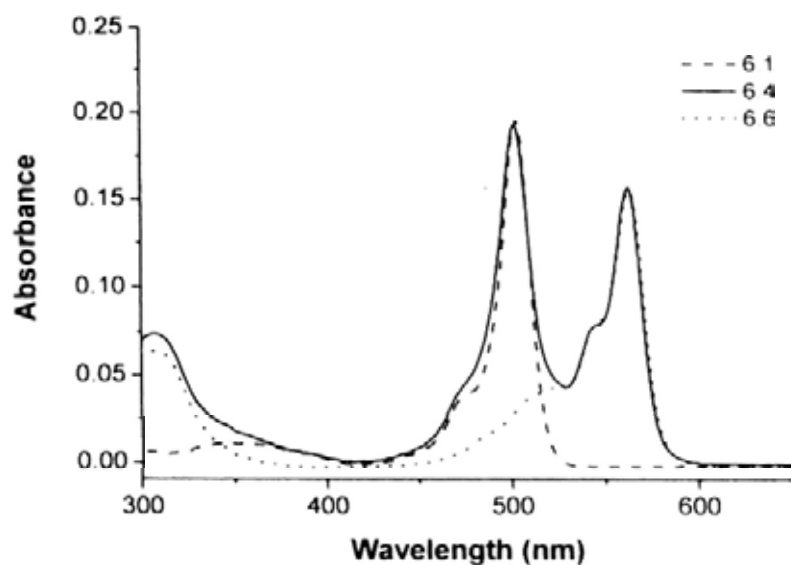


Figure 6.6. Normalized absorption spectra of compounds **6.1**, **6.4**, and **6.6** in toluene. The spectra of **6.1** and **6.4** were normalized at 502 nm, while those of **6.4** and **6.6** were normalized at 563 nm.

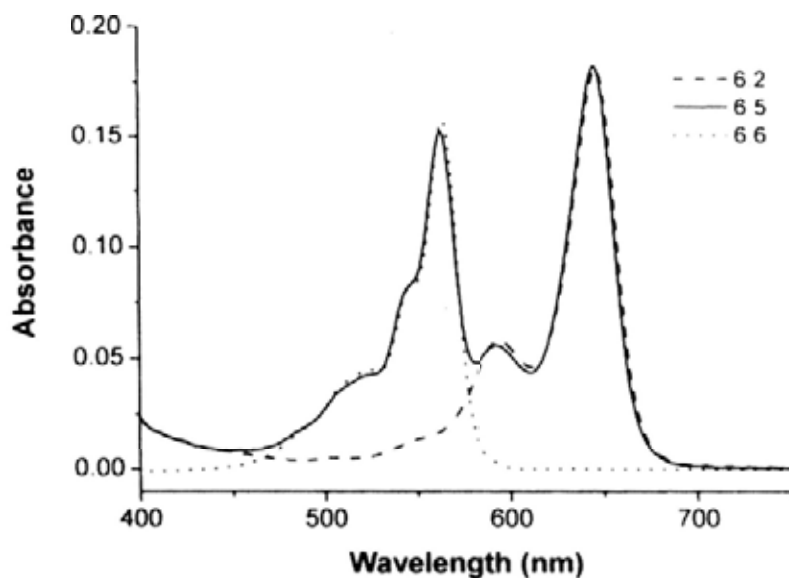


Figure 6.7. Normalized absorption spectra of compounds **6.2**, **6.5**, and **6.6** in toluene. The spectra of **6.5** and **6.6** were normalized at 563 nm, while those of **6.2** and **6.5** were normalized at 647 nm.

Efficient energy transfer via a Förster mechanism requires a good spectral overlap between the energy donor (D) emission and the energy acceptor (A) absorption.¹⁸ BODIPY-subphthalocyanine and subphthalocyanine-distyryl BODIPY are excellent donor-acceptor pairs which fulfill this requirement. This can be clearly seen in Figure 6.8 showing the overlap between the fluorescence spectrum of BODIPY **6.1** and the absorption spectrum of subphthalocyanine **6.6**, and Figure 6.9 showing the fluorescence spectrum of subphthalocyanine **6.6** and the absorption spectrum of distyryl BODIPY **6.2**. As a result, it is expected that both the dyads **6.4** and **6.5** should exhibit an efficient through-space energy transfer.

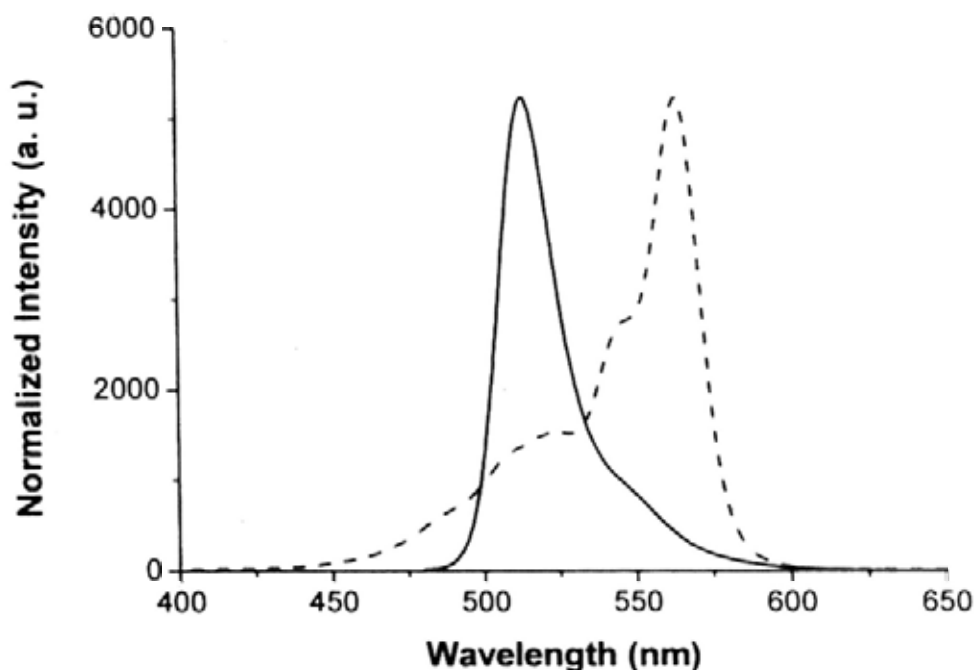


Figure 6.8. Overlap between the fluorescence spectrum of BODIPY **6.1** (—) and the absorption spectrum of subphthalocyanine **6.6** (---) in toluene.

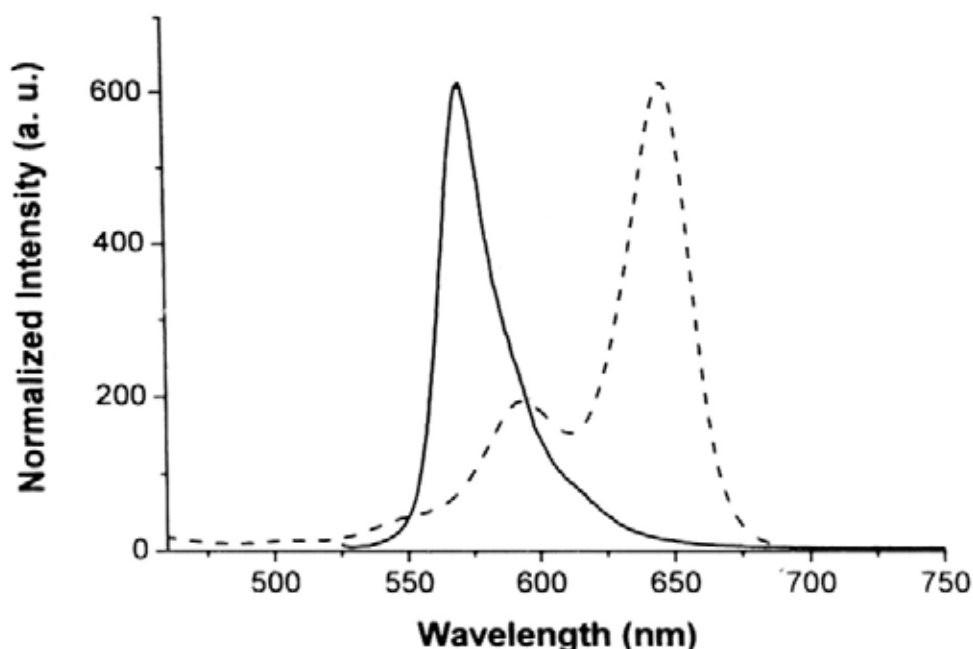


Figure 6.9. Overlap between the fluorescence spectrum of subphthalocyanine **6.6** (—) and the absorption spectrum of distyryl BODIPY **6.2** (---) in toluene.

The energy transfer process of **6.4** and **6.5** in toluene was studied by steady-state and time-resolved fluorescence spectroscopy. Table 6.1 compiles the fluorescence as well as the electronic absorption data of these dyads and the reference compounds in toluene. As shown in Figure 6.10, excitation of BODIPY **6.1** at 470 nm gives a strong fluorescence emission at 514 nm. However, this signal virtually cannot be seen upon excitation of the dyad **6.4** at the same position. Instead, an emission at 570 nm appears, which is due to the subphthalocyanine unit of **6.4**. The intensity is stronger than that caused by **6.6** at a similar concentration (Figure 6.10). These observations indicate the presence of an efficient singlet-singlet energy transfer process in **6.4**, from the excited BODIPY part to the subphthalocyanine unit. This was confirmed by the excitation spectrum monitored at 570 nm, which resembles the absorption spectrum of **6.4**

(Figure 6.11). In toluene, both the reference compounds **6.1** and **6.6** revealed monoexponential decay. The calculated lifetimes were found to be 4.26 and 2.31 respectively (Table 6.1). In the dyad **6.4**, the monoexponential decay of the excited BODIPY moiety was very fast ($\tau_F < 50$ ps). This decay is due to the energy transfer process. The fluorescence quantum yield (Φ_F) of **6.1** in toluene is 0.94, while that of the BODIPY part of **6.4** is greatly reduced to 0.015 (Table 6.1). According to the equation: $\Phi_{ENT} = 1 - \Phi_{F(dyad)} / \Phi_{F(donor)}$,¹⁹ where Φ_{ENT} is the energy transfer quantum yield, $\Phi_{F(dyad)}$ and $\Phi_{F(donor)}$ are the fluorescence quantum yields of the dyad (the donor part) and the donor without connecting to the acceptor, respectively, the value of Φ_{ENT} was estimated to be 0.98, showing that this is a very efficient process in **6.4**.

Table 6.1. Absorption and fluorescence data for the dyads **6.4** and **6.5**, and the reference compounds **6.1**, **6.2**, and **6.6** in toluene.

| Compound | $\lambda_{max} / \text{nm}$ ($\log \epsilon$) | λ_{em} / nm | Φ_F^a | τ_F / ns |
|------------|---|----------------------------|--------------------|---------------------------------------|
| 6.4 | 502 (5.06), 563 (4.96) | 570 ^b | 0.015 ^c | 2.41 ^{d,e} |
| 6.5 | 562 (5.02), 645 (5.10) | 653 ^f | 0.013 ^c | 0.06 ^c , 4.03 ^d |
| 6.1 | 503 (4.99) | 514 ^b | 0.94 | 4.26 |
| 6.2 | 647 (5.11) | 653 ^f | 0.73 | 3.90 |
| 6.6 | 564 (4.99) | 571 ^f | 0.75 | 2.31 |

^a Using *N,N'*-di-*n*-hexyl-1,7-bis(4-*tert*-butylphenoxy)-3,4,9,10-perylenetetracarboxylic diimide in CHCl_3 as the reference ($\Phi_F = 1$). ^b Excited at 470 nm. ^c Due to the donor part. ^d Due to the acceptor part. ^e The lifetime for the donor part is too short to be determined. ^f Excited at 515 nm.

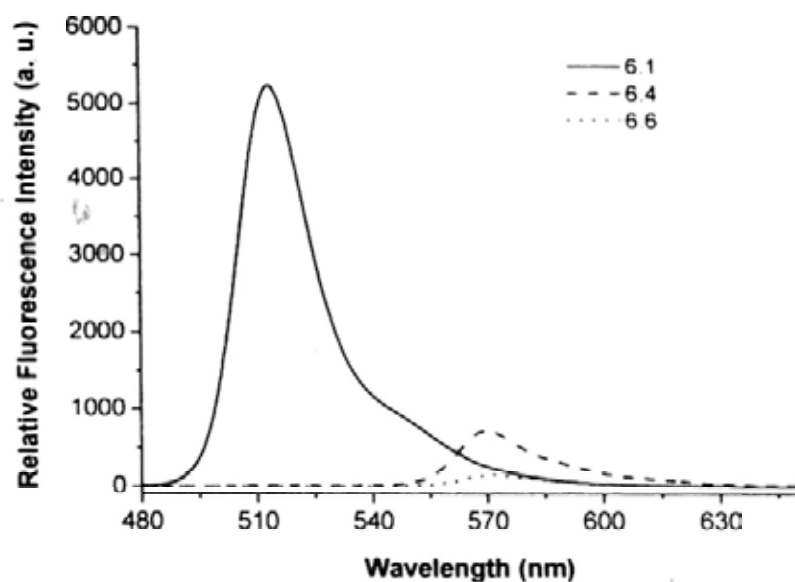


Figure 6.10. Fluorescence spectra of **6.1**, **6.4**, and **6.6** (in toluene) at equal absorbance at 470 nm for **6.1** and **6.4**, and at 563 nm for **6.4** and **6.6**. All of the compounds were excited at 470 nm.

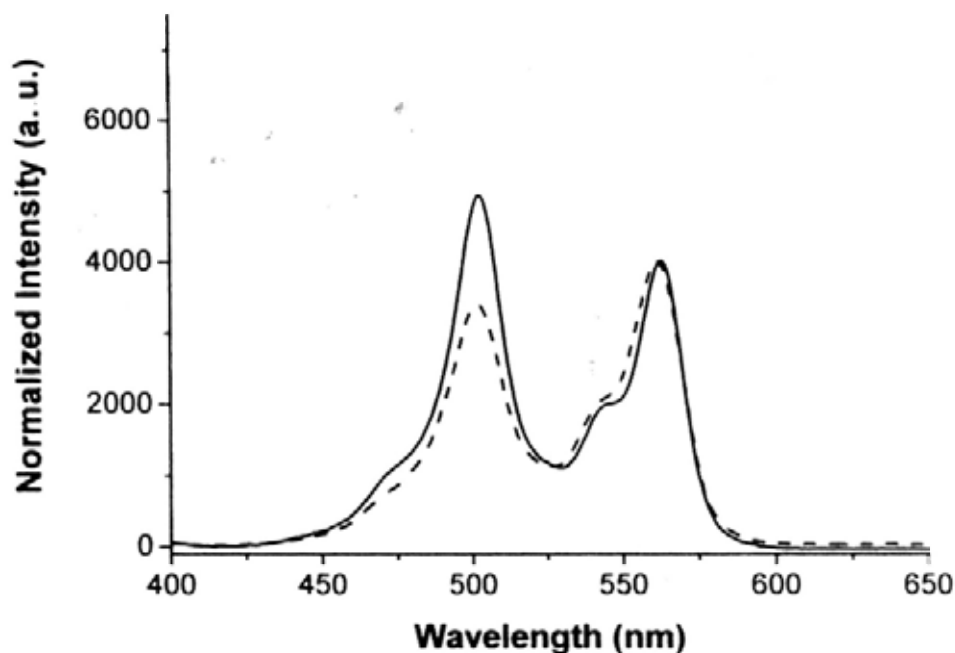


Figure 6.11. Normalized (at 563 nm) absorption (—) and excitation (---) (monitored at 570 nm) spectra of **6.4** in toluene.

For the dyad **6.5**, similar results were obtained, but the energy donor is now switched to the subphthalocyanine unit. As shown in Figure 6.12, excitation of **6.5** at 515 nm only shows a very weak emission at ca. 570 nm assignable to the subphthalocyanine emission, together with a rather strong emission at 653 nm, which is due to the distyryl BODIPY moiety. The excitation spectrum of **6.5** monitored at 653 nm also resembles its absorption spectrum (Figure 6.13). In toluene, the subphthalocyanine part in **6.5** revealed monoexponential decay, which is attributed to the energy transfer process. Its fluorescence lifetime (0.06 ns) is much shorter than that of **6.6** (2.31 ns), showing the presence of a very efficient competition pathway. By taking the fluorescence quantum yields of **6.6** (0.75) and **6.5** (0.013 for the donor part), the value of Φ_{ENT} was also found to be 0.98. Hence, photo-induced singlet-singlet energy transfer is also a very efficient process for this dyad.

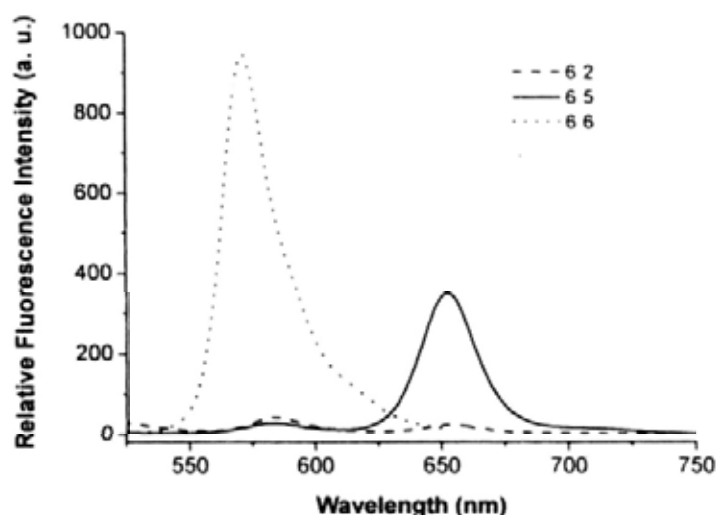


Figure 6.12. Fluorescence spectra of **6.2**, **6.5**, and **6.6** (in toluene) at equal absorbance at 515 nm for **6.5** and **6.6**, and at 647 nm for **6.2** and **6.5**. All of the compounds were excited at 515 nm.

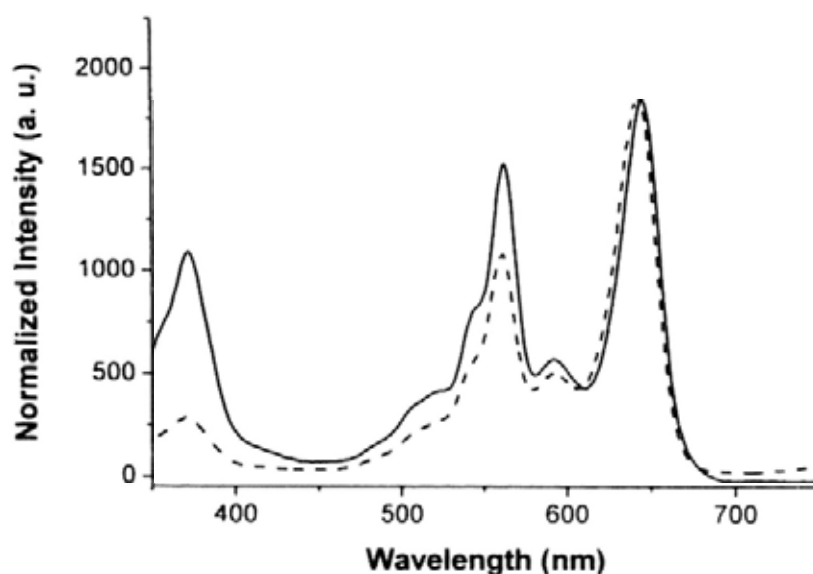


Figure 6.13. Normalized (at 647 nm) absorption (—) and excitation (---) (monitored at 653 nm) spectra of **6.5** in toluene.

6.3 Conclusion

In conclusion, I have synthesized and characterized two novel conjugates of subphthalocyanines and BODIPY derivatives. Due to the good spectral overlap between the energy donor emission and the energy acceptor absorption, these dyads exhibit a highly efficient photoinduced energy transfer process with an energy transfer quantum yield of 98%.

6.4 Experimental section

6.4.1 General

The general procedure for solvent purification and details for instrumental analysis have been described in Section 2.4.1.

6.4.2 Photophysical Studies

The fluorescence quantum yields were determined by using *N,N'*-Di-*n*-hexyl-1,7-bis(4-*tert*-butylphenoxy)-3,4,9,10-perylenetetracarboxylic diimide in CHCl₃ as the reference [$\Phi_{F(ref)} = 1$].²⁰ The fluorescence lifetimes were measured with a multifrequency phase modulation method with a scattering sample as standard.

6.4.3 Synthesis

Phenol-containing BODIPY 6.1. To a solution of 4-hydroxybenzaldehyde (0.37 g, 3.0 mmol) and 2,4-dimethylpyrrole (0.63 g, 6.6 mmol) in THF (90 mL) was added several drops of trifluoroacetic acid. The mixture was stirred at ambient temperature overnight, then a solution of 2,3-dichloro-5,6-dicyano-*p*-benzoquinone (0.68 g, 3.0 mmol) in THF (120 mL) was added. The mixture was stirred continuously for another 4 h. After the addition of triethylamine (18 mL, 0.13 mol), BF₃·OEt₂ (18 mL, 0.15 mol) was added dropwise to the mixture, which was cooled in an ice-water bath. The mixture was kept stirring at ambient temperature overnight, then filtered through a celite pad. The residue was washed with CH₂Cl₂ (ca. 50 mL), then the combined filtrate was rotary evaporated to dryness. The residue was redissolved in CH₂Cl₂ (100 mL) and the solution was washed with 5% aqueous NaHCO₃ solution (100 mL) followed with water (100 mL × 2). The organic portion was dried over anhydrous MgSO₄, then evaporated in vacuo. The crude product was purified by silica gel column chromatography using CH₂Cl₂ as the eluent to give **6.1** as an orange-yellow

solid (0.44 g, 43%). ^1H NMR (300 MHz, CDCl_3): δ 7.13 (d, $J = 8.4$ Hz, 2 H, ArH), 6.95 (d, $J = 8.4$ Hz, 2 H, ArH), 5.98 (s, 2 H, pyrrole-H), 5.12 (s, 1 H, OH), 2.55 (s, 6 H, CH_3), 1.45 (s, 6 H, CH_3); $^{13}\text{C}\{^1\text{H}\}$ NMR (75.4 MHz, CDCl_3): δ 156.3, 155.3, 143.2, 141.8, 131.8, 129.4, 127.1, 121.1, 116.1, 14.5 (two overlapping signals).

Distyryl BODIPY 6.2. A mixture of the phenol-containing BODIPY **6.1** (0.34 g, 1.0 mmol), 4-methoxybenzaldehyde (0.33 g, 2.4 mmol), glacial acetic acid (2.0 mL, 34.9 mmol), piperidine (2.4 mL, 24.3 mmol), and a small amount of $\text{Mg}(\text{ClO}_4)_2$ in toluene (60 mL) was refluxed for 24 h. The water formed during the reaction was removed azeotropically with a Dean-Stark apparatus. The mixture was concentrated under reduced pressure, then the residue was purified by silica gel column chromatography using ethyl acetate/hexane (1:2 v/v) as the eluent. The blue colored fraction was collected and rotary evaporated to yield the desired product **6.2** (0.16 g, 28%). ^1H NMR (300 MHz, CDCl_3): δ 7.61 (d, $J = 16.2$ Hz, 2 H, $\text{CH}=\text{CH}$), 7.58 (d, $J = 8.7$ Hz, 4 H, ArH), 7.21 (d, $J = 16.2$ Hz, 2 H, $\text{CH}=\text{CH}$), 7.18 (d, $J = 8.7$ Hz, 2 H, ArH), 6.96 (d, $J = 8.7$ Hz, 2 H, ArH), 6.93 (d, $J = 8.7$ Hz, 4 H, ArH), 6.61 (s, 2 H, pyrrole-H), 5.14 (s, 1 H, OH), 3.86 (s, 6 H, OCH_3), 1.51 (s, 6 H, CH_3); $^{13}\text{C}\{^1\text{H}\}$ NMR (75.4 MHz, CDCl_3): δ 160.3, 156.3, 152.6, 141.8, 138.1, 135.6, 133.5, 129.9, 129.6, 129.0, 127.4, 117.4, 117.2, 116.0, 114.2, 55.4, 14.8; MS (ESI): isotopic clusters peaking at m/z 542 {100%, $[\text{M} - \text{F} - \text{CH}_3]^+$ }, 557 {43%, $[\text{M} - \text{F}]^+$ }, and 599 {62%, $[\text{M} + \text{Na}]^+$ }; HRMS (ESI): m/z calcd for $\text{C}_{35}\text{H}_{31}\text{BF}_2\text{N}_2\text{NaO}_3$ $[\text{M} + \text{Na}]^+$: 599.2288, found 599.2290. Anal. Calcd for $\text{C}_{35}\text{H}_{31}\text{BF}_2\text{N}_2\text{O}_3$: C, 72.93; H, 5.42; N, 4.86. Found: C, 73.64; H, 5.51; N, 4.93.

Subphthalocyanine-BODIPY conjugate 6.4. A mixture of the phenol-containing BODIPY **6.1** (136 mg, 0.4 mmol), boron(III) subphthalocyanine chloride (**6.3**) (90%, 96 mg, 0.2 mmol), and pyridine (0.5 mL, 6.2 mmol) in toluene (15 mL) was heated under reflux for 48 h. The mixture was then rotary evaporated to dryness. The residue was chromatographed on a silica gel column using CH₂Cl₂ as the eluent until the orange band containing the unreacted compound **6.1** had been eluted out. The eluent was then changed to CH₂Cl₂/methanol (100:1 v/v) to develop a red band, which was collected and evaporated in vacuo. The crude product was further purified by size exclusion chromatography using THF as the eluent, followed by recrystallization from a mixture of CH₂Cl₂ and hexane to give dyad **6.4** as a red solid (35 mg, 24%). ¹H NMR (300 MHz, CDCl₃): δ 8.85-8.88 (m, 6 H, SubPc-H_α), 7.92-7.95 (m, 6 H, SubPc-H_β), 6.64 (d, *J* = 8.1 Hz, 2 H, ArH), 5.91 (s, 2 H, pyrrole-H), 5.55 (d, *J* = 8.1 Hz, 2 H, ArH), 2.50 (s, 6 H, CH₃), 1.18 (s, 6 H, CH₃); ¹³C{¹H} NMR (75.4 MHz, CDCl₃): δ 155.1, 153.5, 151.1, 143.1, 141.6, 131.5, 130.9, 129.9, 128.4, 122.2, 121.0, 120.8, 14.5, 14.3 (two of the signals are overlapped); MS (ESI): isotopic clusters peaking at *m/z* 735 {100%, [M + H]⁺} and 715 {77%, [M - F]⁺}; HRMS (ESI): *m/z* calcd for C₄₃H₃₁B₂F₂N₈O [M + H]⁺: 735.2770, found 735.2773. Anal. Calcd for C₄₃H₃₀B₂F₂N₈O: C, 70.33; H, 4.12; N, 15.26. Found: C, 70.25; H, 4.75; N, 15.05.

Subphthalocyanine-BODIPY conjugate 6.5. According to the above procedure, subphthalocyanine **6.3** (90%, 68 mg, 0.14 mmol) was treated with the distyryl BODIPY **6.2** (161 mg, 0.28 mmol) to give conjugate **6.5** as a purple solid (30 mg,

22%). ^1H NMR (300 MHz, CDCl_3): δ 8.84-8.88 (m, 6 H, SubPc- H_α), 7.91-7.95 (m, 6 H, SubPc- H_β), 7.53-7.60 (m, 6 H, ArH + CH=CH), 7.17 (d, $J = 16.2$ Hz, 2 H, CH=CH), 6.91 (d, $J = 8.7$ Hz, 4 H, ArH), 6.69 (d, $J = 8.4$ Hz, 2 H, ArH), 6.55 (s, 2 H, pyrrole-H), 5.57 (d, $J = 8.4$ Hz, 2 H, ArH), 3.84 (s, 6 H, OCH_3), 1.24 (s, 6 H, CH_3); $^{13}\text{C}\{^1\text{H}\}$ NMR (75.4 MHz, CDCl_3): δ 160.3, 153.5, 152.5, 151.1, 141.8, 138.1, 135.5, 133.2, 131.0, 129.9, 129.6, 129.0, 128.7, 122.3, 120.7, 117.3, 114.2, 55.4, 14.6 (some of the signals are overlapped); MS (ESI): isotopic clusters peaking at m/z 970 {100%, $[\text{M}]^+$ } and 951 {31%, $[\text{M} - \text{F}]^+$ }; HRMS (ESI): m/z calcd for $\text{C}_{59}\text{H}_{42}\text{B}_2\text{F}_2\text{N}_8\text{O}_3$ $[\text{M}]^+$: 970.3529, found 970.3534. Anal. Calcd for $\text{C}_{59.5}\text{H}_{43}\text{B}_2\text{ClF}_2\text{N}_8\text{O}_3$ ($2 \cdot 0.5\text{CH}_2\text{Cl}_2$): C, 70.54; H, 4.28; N, 11.06. Found: C, 70.33; H, 4.59; N, 10.70.

Subphthalocyanine 6.6. A mixture of subphthalocyanine **6.3** (90%, 144 mg, 0.3 mmol) and 4-hydroxybenzaldehyde (184 mg, 1.5 mmol) in toluene (3 mL) was refluxed overnight. After a brief cooling, the mixture was evaporated. The residue was washed with methanol/water (4:1 v/v), then chromatographed on a silica gel column using dichloromethane/hexane (1:2 v/v) as eluent. The product was isolated as a red solid (139 mg, 90%). ^1H NMR (300 MHz, CDCl_3): δ 9.62 (s, 1 H, CHO), 8.86-8.89 (m, 6 H, Pc- H_α), 7.92-7.95 (m, 6 H, Pc- H_β), 7.31 (d, $J = 8.4$ Hz, 2 H, ArH), 5.45 (d, $J = 8.4$ Hz, 2 H, ArH); $^{13}\text{C}\{^1\text{H}\}$ NMR (75.4 MHz, CDCl_3): δ 190.7, 158.6, 151.4, 131.3, 130.9, 130.0, 122.3, 118.9; MS (ESI): isotopic clusters peaking at m/z 412 {100%, $[\text{M} - \text{PhCHO} + \text{H}]^+$ }, 395 {44%, $[\text{M} - \text{OPhCHO}]^+$ }, and 539 {21%, $[\text{M} + \text{Na}]^+$ }; HRMS (ESI): m/z calcd for $\text{C}_{31}\text{H}_{17}\text{BN}_6\text{NaO}_2$ $[\text{M} + \text{Na}]^+$: 539.1398, found 539.1410.

6.4.4 X-ray Crystallographic Analysis of 6.2, 6.4·H₂O, and 6.5·CH₂Cl₂.

Crystal data and details of data collection and structure refinement are given in Table 6.2. Data were collected on a Bruker SMART CCD diffractometer with an MoKa sealed tube ($\lambda = 0.71073 \text{ \AA}$) at 293 K, using a ω scan mode with an increment of 0.3° . Preliminary unit cell parameters were obtained from 45 frames. Final unit cell parameters were obtained by global refinements of reflections obtained from integration of all the frame data. The collected frames were integrated using the preliminary cell-orientation matrix. SMART software was used for collecting frames of data, indexing reflections and determination of lattice constants; SAINT-PLUS for integration of intensity of reflections and scaling;²¹ SADABS for absorption correction;²² and SHELXL for space group and structure determination, refinements, graphics and structure reporting.²³

Table 6.2. Crystallographic data for **6.2**, **6.4·H₂O**, and **6.5·CH₂Cl₂**.

| | 6.2 | 6.4·H₂O | 6.5·CH₂Cl₂ |
|---|---|---|---|
| formula | C ₃₅ H ₃₁ BF ₂ N ₂ O ₃ | C ₄₃ H ₃₂ B ₂ F ₂ N ₈ O ₂ | C ₆₀ H ₄₄ B ₂ Cl ₂ F ₂ N ₈ O ₃ |
| <i>M_r</i> | 576.43 | 752.39 | 1055.55 |
| crystal size [mm ³] | 0.40 × 0.30 × 0.20 | 0.30 × 0.20 × 0.20 | 0.50 × 0.40 × 0.30 |
| crystal system | monoclinic | monoclinic | triclinic |
| space group | Cc | P2 ₁ /c | P ₁ (bar) |
| <i>a</i> [Å] | 13.149(2) | 23.538(3) | 12.271(4) |
| <i>b</i> [Å] | 14.113(2) | 12.339(1) | 14.939(5) |
| <i>c</i> [Å] | 16.121(3) | 12.841(2) | 16.667(6) |
| <i>α</i> [°] | 90 | 90 | 65.534(6) |
| <i>β</i> [°] | 94.354(3) | 104.603(3) | 70.060(6) |
| <i>γ</i> [°] | 90 | 90 | 86.605(6) |
| <i>V</i> [Å ³] | 2982.9(8) | 3608.9(7) | 2602.3(15) |
| <i>Z</i> | 4 | 4 | 2 |
| <i>F</i> (000) | 1208 | 1560 | 1092 |
| <i>ρ</i> _{calcd} [mg m ⁻³] | 1.284 | 1.385 | 1.347 |
| <i>μ</i> [mm ⁻¹] | 0.090 | 0.094 | 0.188 |
| <i>θ</i> range [°] | 2.12 to 28.05 | 0.89 to 28.03 | 1.43 to 25.00 |
| reflections collected | 10051 | 24264 | 14197 |
| independent reflections | 5738 (R _{int} = 0.0406) | 8717 (R _{int} = 0.0855) | 9131 (R _{int} = 0.0478) |
| parameters | 388 | 514 | 694 |
| <i>R</i> 1 [<i>I</i> > 2σ(<i>I</i>)] | 0.0449 | 0.0592 | 0.1017 |
| w <i>R</i> 2 [<i>I</i> > 2σ(<i>I</i>)] | 0.1060 | 0.1500 | 0.2936 |
| goodness of fit | 0.995 | 0.999 | 1.026 |

6.5 References

1. Balzani, V.; Credi, A.; Venturi, M. *ChemSusChem* **2008**, *1*, 26.
2. (a) Wasielewski, M. R. *J. Org. Chem.* **2006**, *71*, 5051. (b) Fukuzumi, S. *Phys. Chem. Chem. Phys.* **2008**, *10*, 2283.
3. (a) Holten, D.; Bocian, D. F.; Lindsey, J. S. *Acc. Chem. Res.* **2002**, *35*, 57. (b) Saha, S.; Stoddart, J. F. *Chem. Soc. Rev.* **2007**, *36*, 77. (c) Balzani, V.; Credi, A.; Venturi, M. *Chem. Eur. J.* **2008**, *14*, 26.
4. Kikuchi, K.; Takakusa, H.; Nagano, T. *Trends Anal. Chem.* **2004**, *23*, 407.
5. See for example: (a) Peng, Z.; Melinger, J. S.; Kleiman, V. *Photosyn. Res.* **2006**, *87*, 115. (b) Satake, A.; Kobuke, Y. *Org. Biomol. Chem.* **2007**, *5*, 1679. (c) Nakamura, Y.; Aratani, N.; Osuka, A. *Chem. Soc. Rev.* **2007**, *36*, 831.
6. (a) Loudet, A.; Burgess, K. *Chem. Rev.* **2007**, *107*, 4891. (b) Ulrich, G.; Ziessel, R.; Harriman, A. *Angew. Chem. Int. Ed.* **2008**, *47*, 1184.
7. (a) Goze, C.; Ulrich, G.; Ziessel, R. *Org. Lett.* **2006**, *8*, 4445. (b) Ziessel, R.; Ulrich, G.; Harriman, A. *New J. Chem.* **2007**, *31*, 496. (c) Bonaradi, L.; Ulrich, G.; Ziessel, R. *Org. Lett.* **2008**, *10*, 2183.
8. (a) D'Souza, F.; Smith, P. M.; Zandler, M. E.; McCarty, A. L.; Itou, M.; Araki, Y.; Ito, O. *J. Am. Chem. Soc.* **2004**, *126*, 7898. (b) Koepf, M.; Trabolsi, A.; Elhabiri, M.; Wytko, J. A.; Paul, D.; Albrecht-Gary, A. M.; Weiss, J. *Org. Lett.* **2005**, *7*, 1279.
9. Yilmaz, M. D.; Bozdemir, O. A.; Akkaya, E. U. *Org. Lett.* **2006**, *8*, 2871.
10. (a) Azov, V. A.; Schlegel, A.; Diederich, F. *Angew. Chem. Int. Ed.* **2005**, *44*, 4635. (b) Zhang, X.; Xiao, Y.; Qian, X. *Org. Lett.* **2008**, *10*, 29.
11. Claessens, C. G.; González-Rodríguez, D.; Torres, T. *Chem. Rev.* **2002**, *102*, 835.
12. González-Rodríguez, D.; Torres, T.; Guldi, D. M.; Rivera, J.; Herranz, M. Á.; Echegoyen, L. *J. Am. Chem. Soc.* **2004**, *126*, 6301.
13. González-Rodríguez, D.; Claessens, C. G.; Torres, T.; Liu, S.; Echegoyen, L.; Vila, N.; Nonell, S. *Chem. Eur. J.* **2005**, *11*, 3881.
14. Coskun, A.; Deniz, E.; Akkaya, E. U. *Org. Lett.* **2005**, *7*, 5187.

15. (a) Zheng, Q.; Xu, G.; Prasad, P. N. *Chem. Eur. J.* **2008**, *14*, 5812. (b) Deniz, E.; Isabasar, G. C.; Bozdemir, Ö. A.; Yildirim, L. T.; Siemiarczuk, A.; Akkaya, E. U. *Org. Lett.* **2008**, *10*, 3401.
16. Xu, H.; Jiang, X.-J.; Chan, E. Y. M.; Fong, W.-P.; Ng, D. K. P. *Org. Biomol. Chem.* **2007**, *5*, 3987.
17. Claessens, C. G.; González-Rodríguez, D.; del Rey, B.; Torres, T.; Mark, G.; Schuchmann, H.-P.; von Sonntag, C.; MacDonald, J. G.; Nohr, R. S. *Eur. J. Org. Chem.* **2003**, 2547.
18. Turro, N. J. *Modern Molecular Photochemistry*; University Science Books: Sausalito, 1991; Chapter 9.
19. (a) Jensen, K. K.; Van Berlekom, B. S.; Kajanus, J.; Martensson, J.; Albinsson, B. *J. Phys. Chem. A* **1997**, *101*, 2218. (b) Kilsa, K.; Kajanus, J.; Martensson, J.; Albinsson, B. *J. Phys. Chem. B* **1999**, *103*, 7329.
20. Xu, W.; Chen, H.; Wang, Y.; Zhao, C.; Li, X.; Wang, S.; Weng, Y. *ChemPhysChem* **2008**, *9*, 1409.
21. *SMART and SAINT for Windows NT Software Reference Manuals*, Version 5.0, Bruker Analytical X-ray Systems, Madison, WI, 1997.
22. Sheldrick, G. M. *SADABS - A Software for Empirical Absorption Correction*, University of Göttingen, Germany, 1997.
23. *SHELXL Reference Manual*, Version 5.1, Bruker Analytical X-ray Systems, Madison, WI, 1997.

Chapter 7

Switching the Photo-induced Energy and Electron Transfer Processes in BODIPY-Phthalocyanine Conjugates

7.1 Introduction

Development of bioinspired artificial photosynthetic systems is of much current interest.¹ It involves careful selection of photo and redox-active building blocks arranged in an appropriate manner to mimic the primary events of natural photosynthesis, including light harvesting, photo-induced multi-step electron transfer and catalysis. The studies are important not only for the photochemical conversion of solar energy into fuels,² but also for the construction of various optoelectronic devices.³

Phthalocyanines⁴ and boron dipyrromethenes (BODIPYs)⁵ are two versatile classes of functional dyes. The former are structural analogues of natural porphyrins, showing strong absorptions in the UV-Vis region (at ca. 350 and 670 nm), and desirable photochemical and photophysical properties. BODIPYs also exhibit large extinction coefficients (at ca. 500 nm), high fluorescence quantum yields, reasonably long excited singlet-state lifetimes, and good solubility and stability in many solvent systems. The absorption and emission properties of these compounds can also be tuned readily through chemical modification of the BODIPY core. As a result, these two classes of compounds are excellent

candidates for the aforementioned applications.⁶ Conjugation of these compounds can extend the absorption region well covering the solar spectrum, and combine the advantageous characteristics of individual components. We therefore initiated a study on the mixed arrays of phthalocyanines and BODIPYs. In this Chapter, we report the preparation and photophysical properties of two novel silicon(IV) phthalocyanines substituted axially with two BODIPY or mono-styryl BODIPY moieties. Depending on the axial substituents, these conjugates exhibit predominantly a photo-induced energy or electron transfer process in toluene (Figure 7.1). While a substantial number of conjugates of these functional dyes with other photo and redox-active units such as porphyrins, fullerenes, carotenoids, anthraquinones, perylene diimides, and ruthenium polypyridine complexes have been studied extensively,⁴⁻⁶ to our knowledge, mixed BODIPY-phthalocyanine arrays have not been reported so far.

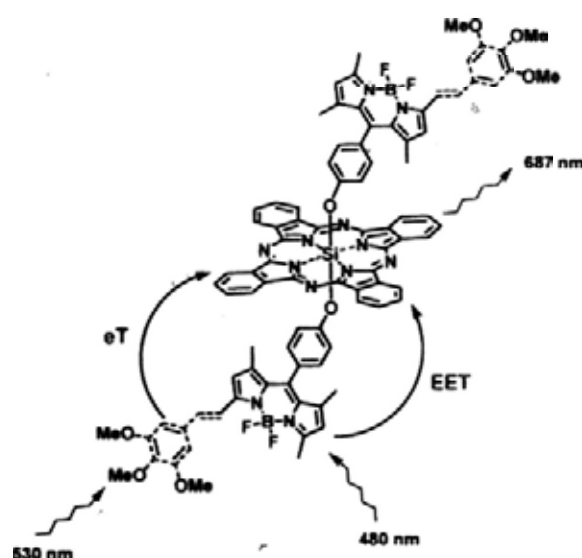
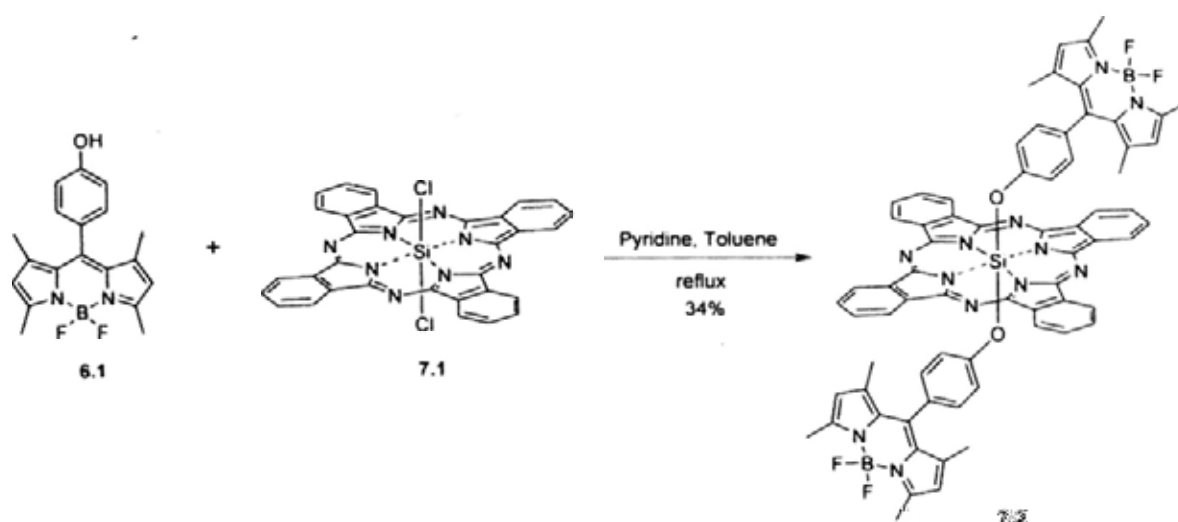


Figure 7.1. Photo-induced energy or electron transfer process in BODIPY-phthalocyanine conjugates.

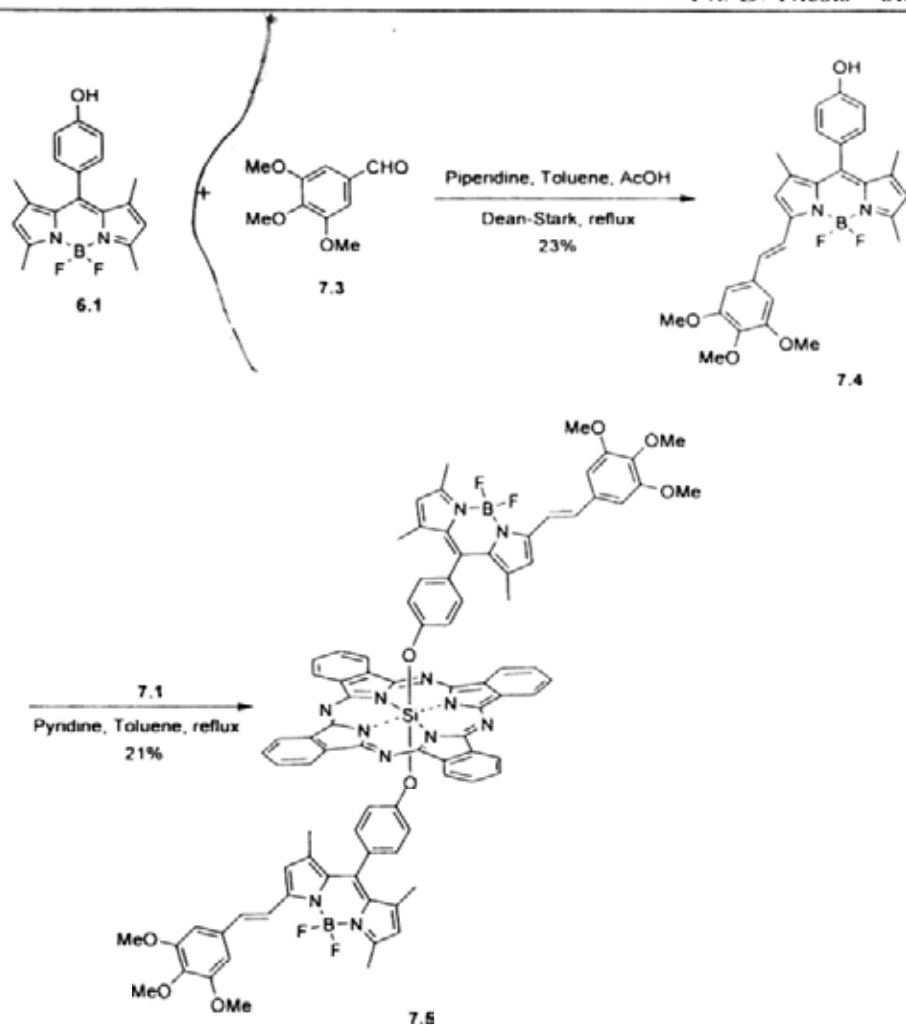
7.2 Results and Discussion

7.2.1 Preparation and Characterization

Scheme 7.1 shows the synthetic route to one of the target conjugates. Treatment of the BODIPY-appended phenol **6.1**⁷ with the commercially available silicon(IV) phthalocyanine dichloride (SiPcCl₂) (**7.1**) in the presence of pyridine gave the bis(BODIPY) substituted phthalocyanine **7.2** in 34% yield. The mono-styryl BODIPY analogue **7.5** was synthesized in a similar manner using phenol **7.4** as a starting material, which was prepared by Knoevenagel condensation of **6.1** with 3,4,5-trimethoxybenzaldehyde (**7.3**) (Scheme 7.2) according to a previously described procedure.⁸



Scheme 7.1. Synthesis of bis(BODIPY) substituted phthalocyanine **7.2**.



Scheme 2. Synthesis of bis(mono-styryl BODIPY) substituted phthalocyanine 7.5.

All the new compounds were fully characterized with various spectroscopic methods. For BODIPY-phthalocyanine 7.2, the ^1H NMR signals for the *p*-phenylene protons appeared as two doublets at δ 5.50 and 2.60, which are significantly shifted upfield compared with those of 6.1 (δ 7.05 and 6.87)⁹ due to the phthalocyanine ring current. A similar upfield shift was also observed for 7.5 [from δ 7.16 and 6.97 (for 7.4) to δ 5.53 and 2.63 (for 7.5) respectively]. The results provided a strong evidence of axial coordination of phthalocyanine with these BODIPY moieties. The experimental details including full characterization data are given in Experimental Section.

Figure 7.2 shows the high resolution ESI mass spectrum of **7.5**. The isotopic clusters peaking at m/z 1057 and 1598 are due to $[M - (\text{mono-styryl BODIPY})]^+$ and $[M + \text{Na}]^+$ species, respectively. As shown in the inset, the isotopic pattern of these signals is in good agreement with the simulated pattern.

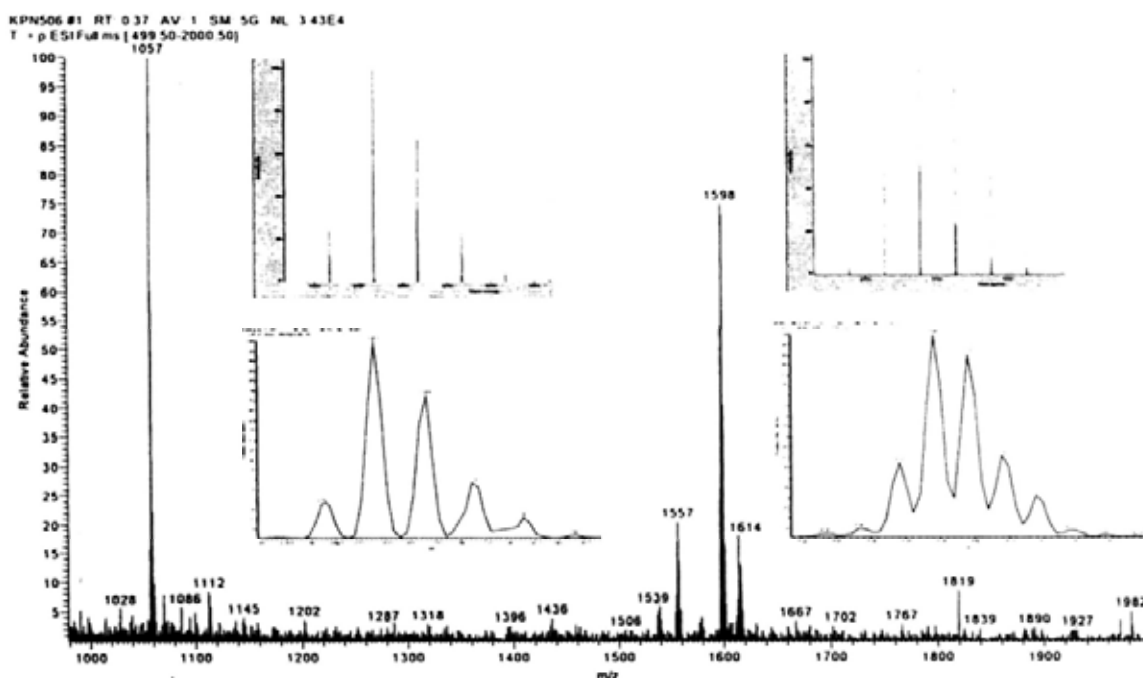
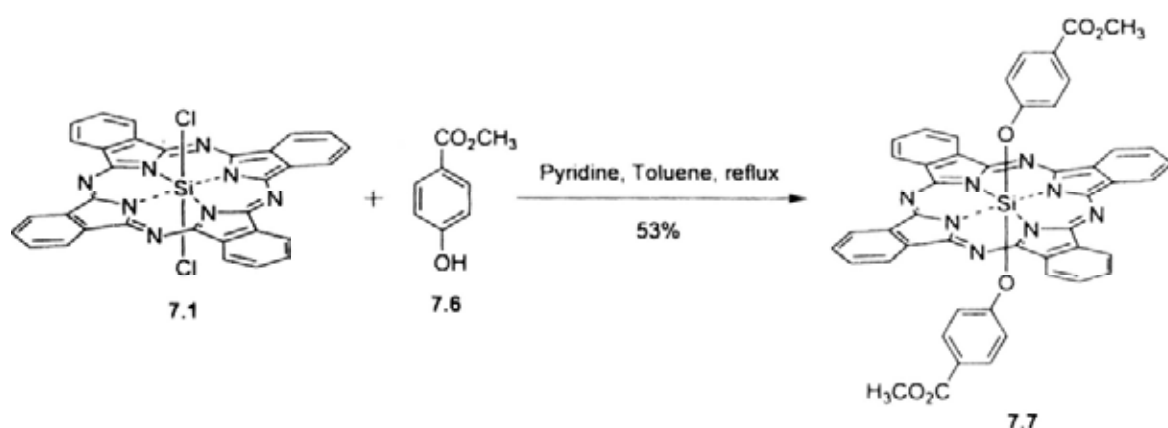


Figure 7.2. ESI-Mass spectrum of compound **7.5**. The inset shows the enlarged spectrum in the $[M - (\text{mono-styryl BODIPY})]$ and molecular ion region and the corresponding simulated isotopic pattern.

7.2.2 Electronic Absorption and Photophysical Properties

Figure 7.3 shows the normalized absorption spectra of the triad **7.2** together with the reference compounds **6.1** and $\text{SiPc}(\text{OC}_6\text{H}_4\text{CO}_2\text{CH}_3)_2$ (**7.7**), which was prepared by treating SiPcCl_2 (**7.1**) with methyl 4-hydroxybenzoate (**7.6**) in the presence of pyridine (Scheme 7.3). In toluene, the triad **7.2** showed two major absorption bands at 502 and 683 nm, which were virtually unshifted compared

with those of **6.1** and **7.7**. Similarly, the electronic absorption spectrum of the mono-styryl analogue **7.5** was essentially the same as the sum of the spectra of the two reference compounds **7.4** and **7.7** (Figure 7.4). These observations indicated that the chromophoric components in **7.2** and **7.5** do not have significant ground-state interactions.



Scheme 7.3. Synthesis of phthalocyanine **7.7** as a reference compound.

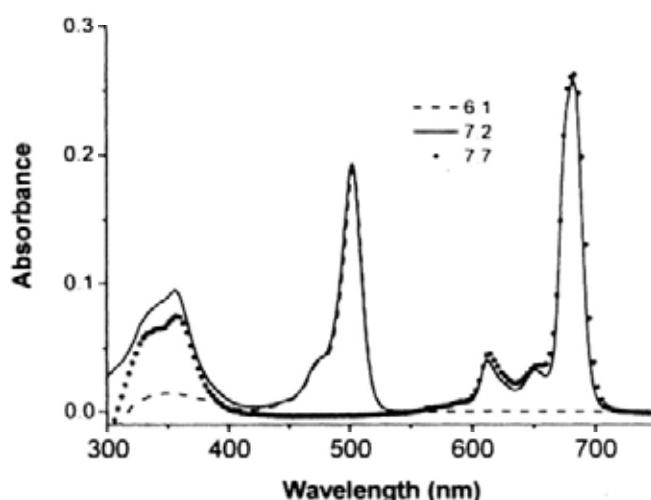


Figure 7.3. Normalized absorption spectra of **6.1**, **7.2**, and **7.7** in toluene. The spectra of **6.1** and **7.2** were normalized at 502 nm, while those of **7.2** and **7.7** were normalized at 683 nm.

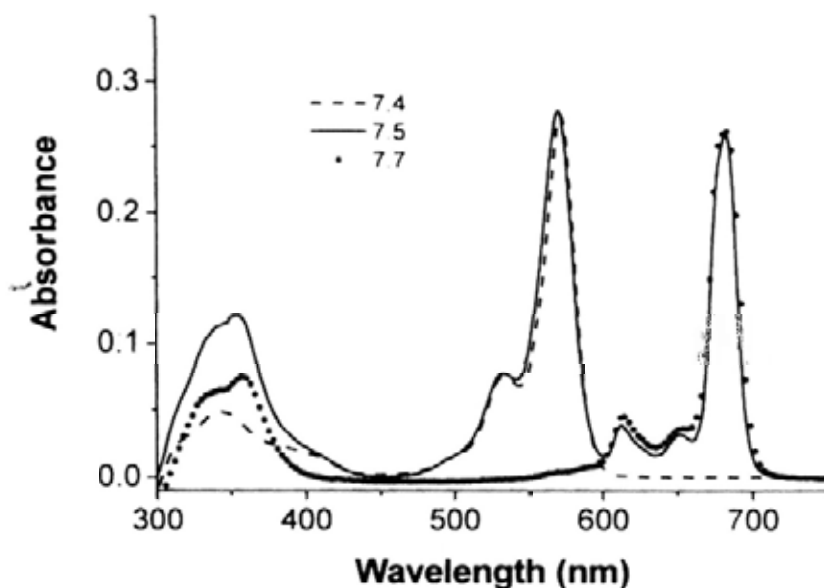


Figure 7.4. Normalized absorption spectra of 7.4, 7.5, and 7.7 in toluene. The spectra of 7.4 and 7.5 were normalized at 573 nm, while those of 7.5 and 7.7 were normalized at 683 nm.

The steady-state fluorescence spectra of compounds **6.1**, **7.2**, and **7.7** in toluene are shown in Figure 7.5. Upon excitation at 480 nm, where only the BODIPY moieties have an absorption, the triad **7.2** gave an emission band at 687 nm due to the phthalocyanine core. The BODIPY emission at ca. 510 nm (as shown in the spectrum of **6.1**) was not observed. Excitation of the reference compound **7.7** at the same position did not give the emission band at 687 nm. These observations clearly indicated the occurrence of an efficient photo-induced energy transfer from the excited BODIPY units to the phthalocyanine core in **7.2**. This was corroborated with the much larger Förster radius R_0 calculated (33 Å) compared with the estimated center-to-center distance between the donor and acceptor (6 Å, by HyperChem 5.0 programme package).

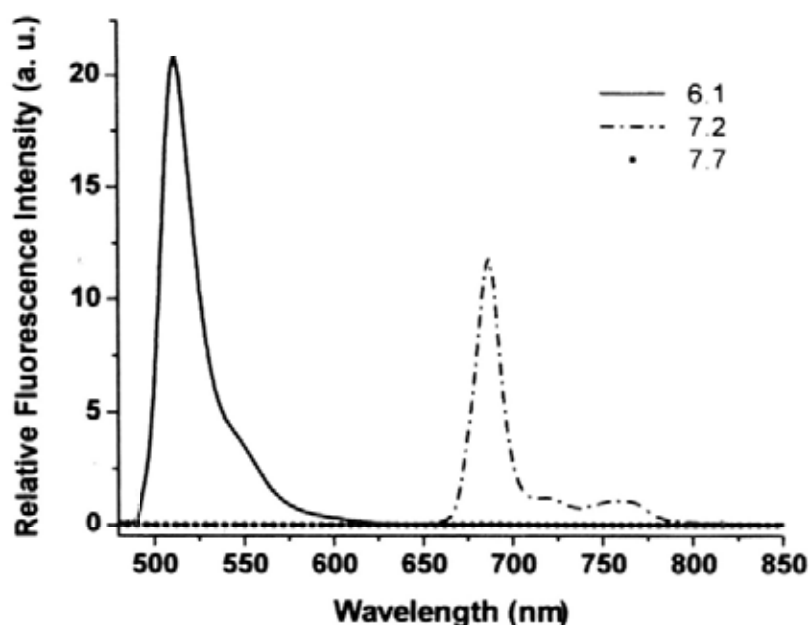


Figure 7.5. Fluorescence spectra of **6.1**, **7.2**, and **7.7** in toluene at equal absorbance at 480 nm for **6.1** and **7.2**, and at 683 nm for **7.2** and **7.7**. All of the compounds were excited at 480 nm.

The excitation spectrum of **7.2** was also recorded by monitoring the phthalocyanine emission at 687 nm. As shown in Figure 7.6, the spectrum closely resembled the absorption spectrum. The corresponding spectra for **7.7** and an equimolar mixture of **6.1** and **7.7** showed only the band due to phthalocyanine at ca. 680 nm, but not the band attributable to BODIPY at ca. 500 nm. These results provided further evidence for the energy transfer process in **7.2**. By comparing the normalized absorption and excitation spectra at the BODIPY region (430-540 nm), the energy transfer quantum yield (Φ_{ENT}) was estimated to be 57%.

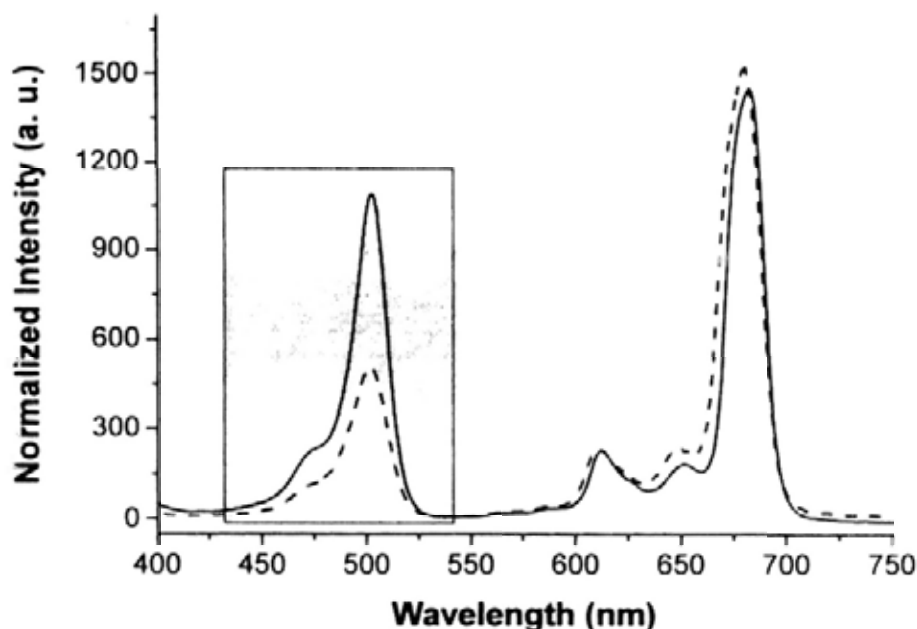


Figure 7.6. Normalized (at 613 nm) absorption (—) and excitation (---) (monitored at 687 nm) spectra of **7.2** in toluene.

The energy transfer process was also studied by time-resolved fluorescence spectroscopy. In toluene, the singlet excited states of both the reference compounds **6.1** and **7.7** decayed mono-exponentially with a lifetime of 3.03 ± 0.01 and 5.07 ± 0.01 ns respectively. For the triad **7.2**, upon BODIPY-part excitation, the fluorescence decay of phthalocyanine was detected, which also followed a mono-exponential manner with a lifetime of 5.20 ± 0.01 ns. The value is very close to that of **7.7**. In fact, upon direct excitation of the phthalocyanine core of **7.2** at 615 nm, a strong emission band at 686 nm was also observed, of which the intensity (Figure 7.7) and lifetime (5.20 ± 0.01 ns) were virtually the same as those of **7.7**. The results suggested that electron transfer was not taken place to quench the excited phthalocyanine in **7.2**. However, it was noted that

when the BODIPY moieties were excited, the fluorescence quantum yield (Φ_F) of the phthalocyanine emission was significantly lower than that obtained by direct excitation of the phthalocyanine core [$\Phi_F = 0.35$ vs. 0.60 with reference to *meso*-tetraphenylporphyrin (H_2TPP) in DMF ($\Phi_F = 0.11$)].¹⁰ Thus, in addition to energy transfer, electron transfer is also a plausible pathway to quench the excited BODIPY in 7.2.

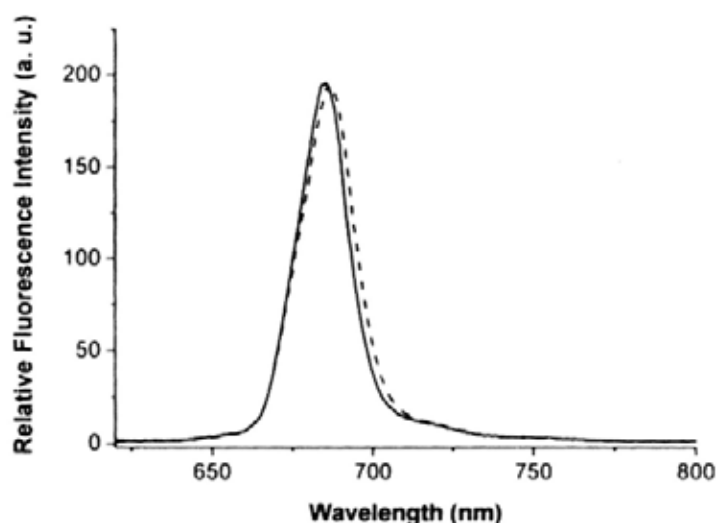


Figure 7.7. Fluorescence spectra of 7.2 (—) and 7.7 (---) at equal absorbance at 615 nm in toluene ($\lambda_{ex} = 615$ nm).

Having two extended mono-styryl BODIPY substituents, the triad 7.5 behaved remarkably different. Table 7.1 summarizes the absorption and fluorescence data for 7.2, 7.5, and all the reference compounds. It was found that upon excitation of the mono-styryl BODIPY moieties in 7.5 at 530 nm, the BODIPY emission at ca. 580 nm was greatly reduced compared with that for 7.4 (Figure 7.8). The fluorescence quantum yield dropped from 0.78 (for 7.4) to 0.003

(for 7.5) [with reference to rhodamine 6G in ethanol ($\Phi = 0.95$)].^{11a} A very weak emission band at 686 nm due to the phthalocyanine core was also observed, which was stronger than that of 7.7 being excited at the same position. These results showed that excitation energy transfer occurred from the initially excited mono-styryl BODIPY moieties to the phthalocyanine core in 7.5, but the fluorescence emission was largely quenched probably by an efficient electron transfer process.

Table 7.1. Absorption and fluorescence data for the triads 7.2 and 7.5, and the reference compounds 6.1, 7.4, and 7.7 in toluene.

| Compd | λ_{\max} (nm) (log ϵ) | λ_{em} (nm) | | Φ_f^a | |
|-------|---|------------------------------------|--------------------|--|--------------------|
| | | BODIPY-part excitation | Pc-part excitation | BODIPY-part excitation | Pc-part excitation |
| 7.2 | 356 (5.00), 502 (5.31), 683 (5.44) | 687 ^b | 687 | 0.35 ^b | 0.60 |
| 7.5 | 355 (5.05), 571 (5.40), 683 (5.37) | 588, ^c 686 ^b | 686 | 0.003, ^c 0.002 ^b | 0.003 |
| 6.1 | 503 (4.99) | 512 | — | 0.55 | — |
| 7.4 | 573 (5.08) | 583 | — | 0.78 | — |
| 7.7 | 357 (4.87), 683 (5.37) | — | 688 | — | 0.60 |

^a With reference to rhodamine 110 in ethanol ($\Phi_F = 0.94$)^{11b} (for BODIPY-part emission of 6.1 and 7.2), rhodamine 6G in ethanol ($\Phi_F = 0.95$)^{11a} (for BODIPY-part emission of 7.4 and 7.5) or H₂TPP in DMF ($\Phi_F = 0.11$)¹⁰ (for Pc-part emission). ^b Pc-part emission. ^c BODIPY-part emission.

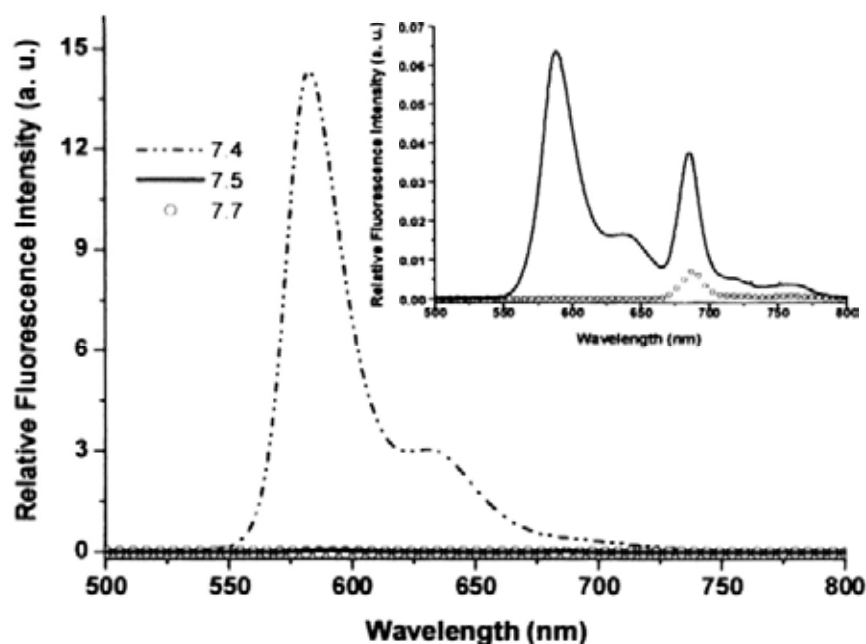


Figure 7.8. Fluorescence spectra of 7.4, 7.5, and 7.7 in toluene at equal absorbance at 530 nm for 7.4 and 7.5, and at 683 nm for 7.5 and 7.7. All of the compounds were excited at 530 nm. The inset shows the enlarged spectra of 7.5 and 7.7.

In fact, upon excitation of the phthalocyanine core in 7.5 at 615 nm, its fluorescence (at 686 nm) was also greatly reduced compared with that of 7.7 (Figure 7.9), and the fluorescence quantum yield decreased from 0.60 (for 7.7) to 0.003 (for 7.5) (Table 7.1). Based on the absorption positions, the energies of $S_1 \rightarrow S_0$ transition for the phthalocyanine part and $S_0 \rightarrow S_1$ transition for the mono-styryl BODIPY part of **6** were estimated to be 1.81 and 2.16 eV respectively. So photo-induced excitation energy transfer from the initially excited phthalocyanine to the mono-styryl BODIPY unit is energetically unfavorable, the quenching should be mainly due to an electron transfer process.

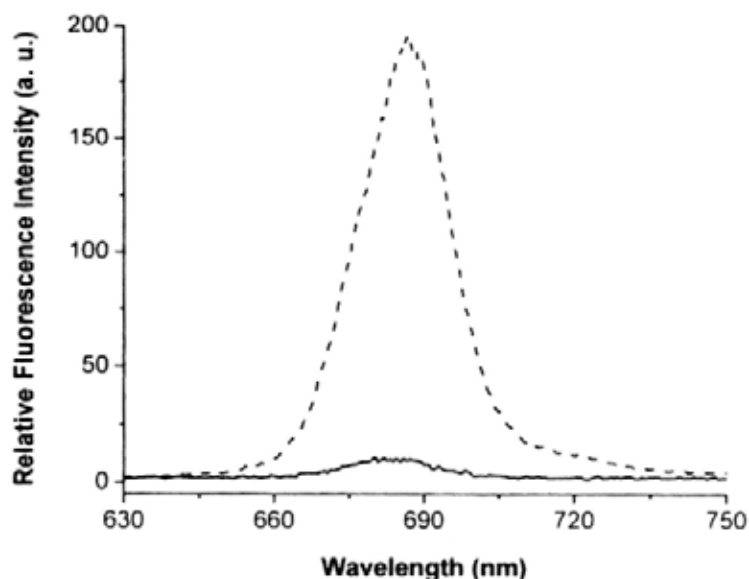


Figure 7.9. Fluorescence spectra of 7.5 (—) and 7.7 (---) at equal absorbance at 615 nm in toluene ($\lambda_{\text{ex}} = 615$ nm).

The transient absorption spectra of 7.5 in toluene were also recorded with excitation at 530 (for the BODIPY-part) and 615 nm (for the Pc-part) (Figure 7.10). Both spectra were very similar showing a strong ground-state bleaching of the phthalocyanine and mono-styryl BODIPY bands at ca. 680 and 570 nm respectively. In addition, a new band at ca. 580 nm appeared, which can be attributed to the phthalocyanine radical anion.¹² This characteristic signal was not observed in the transient absorption spectra of the reference compounds 7.4 and 7.7. These observations supported that the quenching of Pc-part fluorescence was due to a photo-induced electron-transfer process in which the phthalocyanine serves as an acceptor.

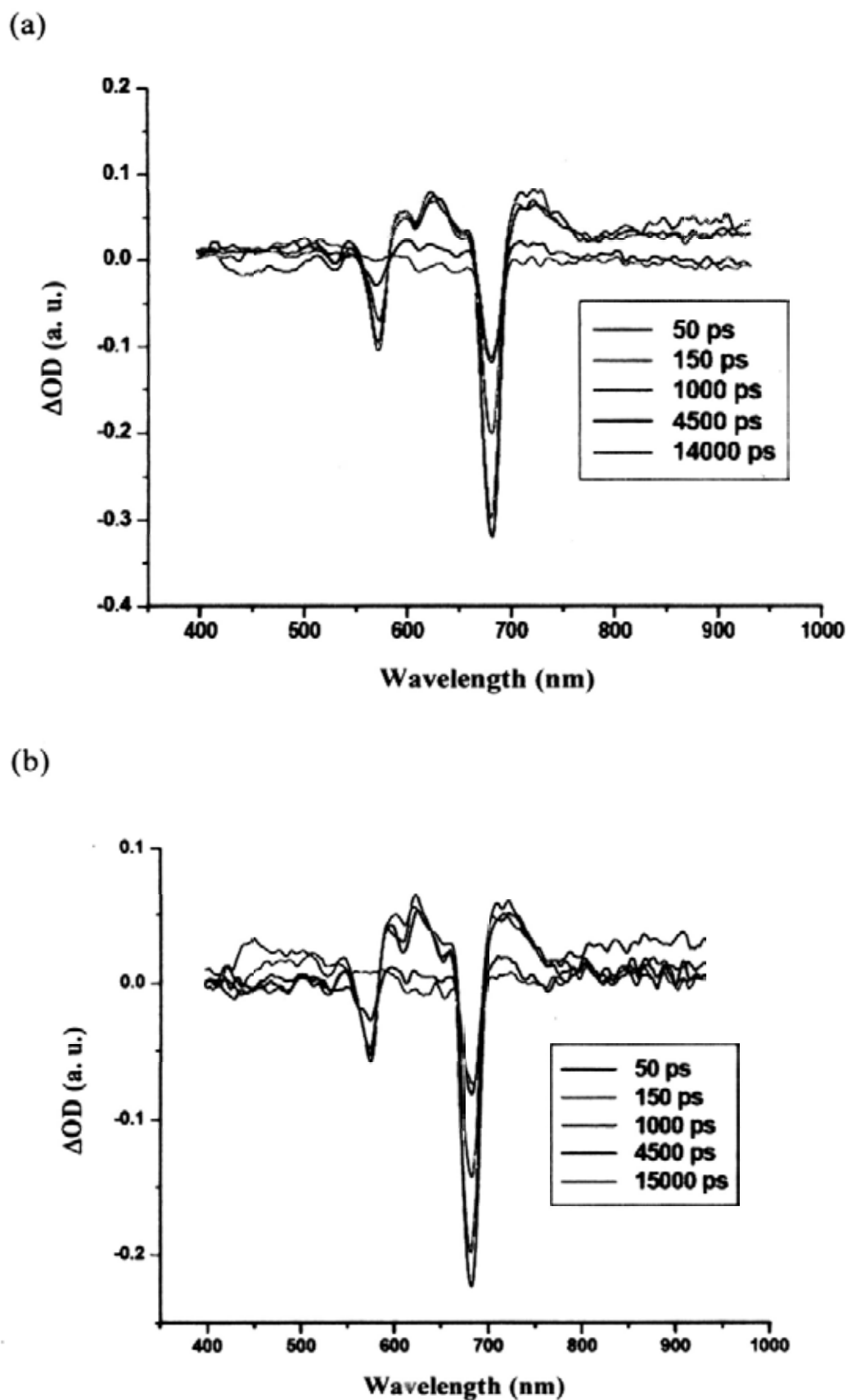


Figure 7.10. Transient absorption spectra of 7.5 in toluene at different delay times. The excitation was made at (a) 530 nm and (b) 615 nm.

The electrochemical properties of the reference compounds **6.1**, **7.4**, and **7.7** were studied by cyclic voltammetry and differential pulse voltammetry in DMF. They exhibited the first (quasi-reversible) reduction at -1.21, -1.05, and -0.57 V and the first (irreversible) oxidation at 1.05, 0.88, and 1.06 V (all vs. saturated calomel electrode) respectively. The conjugates **7.2** and **7.5** had limited solubility in DMF. Hence their electrochemical data were not measured. By using the electrochemical data and the Rehm-Weller equation¹³:

$$\Delta G_0^{D(A)} = e \left[E_{1/2}^{oxd} (D/D^+) - E_{1/2}^{red} (A/A^-) \right] - E_{0,0}^{D(A)} - \frac{e^2}{4\pi\epsilon_0\epsilon_s R_{DA}} - \frac{e^2}{8\pi\epsilon_0} \left[\frac{1}{r_{D^+}} + \frac{1}{r_{A^-}} \right] \left[\frac{1}{\epsilon_{ec}} - \frac{1}{\epsilon_s} \right],$$

the free energy change (ΔG^0) of charge-separation in **7.5** was estimated to be -0.40 eV for BODIPY-part excitation and -0.05 eV for Pc-part excitation. The negative values showed that electron transfer is thermodynamically favorable when either the mono-styryl BODIPY or phthalocyanine part in **7.5** is excited. The lifetime of the charge-separated state was also determined to be 1.7 ± 0.1 ns.

7.3 Conclusion

In conclusion, I have prepared two novel BODIPY-phthalocyanine triads **7.2** and **7.5** and studied their photophysical properties. Upon BODIPY-part excitation, both conjugates exhibit competitive energy and electron transfer processes. However, upon Pc-part excitation, an electron transfer process is switched off (for **7.2**) and on (for **7.5**) depending on the axial substituents.

7.4 Experimental Section

7.4.1 General

The general procedure for solvent purification and details for instrumental analysis have been described in Section 2.4.1.

7.4.2 Photophysical Studies

Steady-state fluorescence spectra were measured using a combination of a cw-xenon lamp (XBO 150) and a monochromator (Lot-Oriel, bandwidth 10 nm) for excitation and a polychromator with a cooled CCD matrix as the detector system (Lot-Oriel, Instaspec IV).¹⁴ Fluorescence quantum yields were determined by using *meso*-Tetraphenylporphyrin in *N,N*-dimethylformamide (DMF) [$\Phi_{F(\text{ref})} = 0.11$],¹⁰ rhodamine 110 in ethanol [$\Phi_{F(\text{ref})} = 0.94$]^{11b} and rhodamine 6G in ethanol [$\Phi_{F(\text{ref})} = 0.95$]^{11a} as the references. Time-resolved fluorescence spectroscopic studies were carried out using the set-up described previously.¹⁵

To measure transient absorption spectra, a white light continuum was generated as a test beam in a cell with a D₂O/H₂O mixture using intense 25 ps pulses from a Nd³⁺:YAG laser (PL 2143A, Ekspla) at 1064 nm. Before passing through the sample, the continuum radiation was split to obtain a reference spectrum. The transmitted as well as the reference beams were focused into two optical fibres and recorded simultaneously at different traces on a CCD-matrix (Lot-Oriel, Instaspec IV). Tunable radiation from an OPG/OPA (Ekspla PG 401/SH, tuning range 200-2300 nm) pumped by third harmonic of the same laser was used as an excitation beam. The mechanical

delay line allowed the measurement of light-induced changes of the absorption spectrum at different delays up to 15 ns after excitation. The OD of all samples was 1.0 at the maximum of the absorption band of lowest energy. The data were analysed using the compensation method.¹⁶

7.4.3 Electrochemical Studies

Electrochemical measurements were carried out with a BAS CV-50W voltammetric analyser. The cell comprised inlets for a platinum-sphere working electrode, a platinum-plate counter electrode and a silver-wire pseudo-reference electrode. Typically, a 0.1 M solution of [Bu₄N][PF₆] in DMF containing the sample was purged with nitrogen for 15 min, then the voltammograms were recorded at ambient temperature. Potentials were referenced to saturated calomel electrode (SCE) using ferrocene as an internal standard ($E_{1/2} = + 0.38$ V vs. SCE).

7.4.4 Synthesis

Bis(BODIPY) substituted phthalocyanine 7.2. A mixture of BODIPY-appended phenol **6.1** (102 mg, 0.30 mmol), silicon(IV) phthalocyanine dichloride (**7.1**) (92 mg, 0.15 mmol), and a small amount of pyridine (0.5 mL) in toluene (15 mL) was refluxed for 48 h. The mixture was evaporated to dryness under reduced pressure, then the residue was chromatographed using CHCl₃ as the eluent. The second green fraction was collected and rotary evaporated. The crude product was further purified by recrystallization from a mixture of CH₂Cl₂ and hexane to give

a gray-green solid (62 mg, 34%). ^1H NMR (300 MHz, CDCl_3): δ 9.62-9.66 (m, 8 H, Pc-H $_{\alpha}$), 8.38-8.42 (m, 8 H, Pc-H $_{\beta}$), 5.70 (s, 4 H, pyrrole-H), 5.50 (d, $J = 8.4$ Hz, 4 H, p -C $_6$ H $_4$), 2.60 (d, $J = 8.4$ Hz, 4 H, p -C $_6$ H $_4$), 2.34 (s, 12 H, CH $_3$), 0.57 (s, 12 H, CH $_3$); $^{13}\text{C}\{^1\text{H}\}$ NMR (75.4 MHz, CDCl_3): δ 154.7, 150.1, 149.7, 142.8, 141.5, 135.4, 131.5, 131.0, 127.0, 125.6, 123.9, 120.6, 118.4, 14.3, 14.2; MS (MALDI-TOF): several isotopic clusters peaking at m/z 1218 {8%, $[\text{M}]^+$ }, 1200 {24%, $[\text{M}-\text{F}+\text{H}]^+$ } and 880 {100%, $[\text{M}-\text{BODIPY}]^+$ }; HRMS (MALDI-TOF): m/z calcd for $\text{C}_{70}\text{H}_{52}\text{B}_2\text{F}_4\text{N}_{12}\text{O}_2\text{Si}$ $[\text{M}]^+$: 1218.4243, found: 1218.4265. Anal. Calcd for $\text{C}_{70}\text{H}_{52}\text{B}_2\text{F}_4\text{N}_{12}\text{O}_2\text{Si}$: C, 68.97; H, 4.30; N, 13.79. Found: C, 68.69; H, 4.77; N, 13.75.

Mono-styryl BODIPY 7.4. A mixture of BODIPY-appended phenol **6.1** (0.34 g, 1.0 mmol), 3,4,5-trimethoxybenzaldehyde (**7.3**) (0.20 g, 1.0 mmol), glacial acetic acid (2.0 mL, 34.9 mmol), piperidine (2.4 mL, 24.3 mmol), and a small amount of $\text{Mg}(\text{ClO}_4)_2$ in toluene (60 mL) was refluxed for 10 h. The water formed during the reaction was removed azeotropically with a Dean-Stark apparatus. The mixture was concentrated under reduced pressure, then the residue was purified by column chromatography using ethyl acetate/ CH_2Cl_2 (1:25 v/v) as the eluent. The pink fraction was collected and rotary evaporated to yield the desired product **7.4** (0.12 g, 23 %). ^1H NMR (300 MHz, CDCl_3): δ 7.55 (d, $J = 16.2$ Hz, 1 H, CH=CH), 7.16 (d, $J = 8.4$ Hz, 2 H, p -C $_6$ H $_4$), 7.15 (d, $J = 16.2$ Hz, 1 H, CH=CH), 6.97 (d, $J = 8.4$ Hz, 2 H, p -C $_6$ H $_4$), 6.80 (s, 2 H, ArH), 6.59 (s, 1 H, pyrrole-H), 6.02 (s, 1 H, pyrrole-H), 5.21 (s, 1 H, OH), 3.94 (s, 6 H, OCH $_3$), 3.89 (s, 3 H, OCH $_3$), 2.60 (s, 3 H, CH $_3$), 1.50 (s, 3 H, CH $_3$), 1.47 (s, 3 H, CH $_3$); $^{13}\text{C}\{^1\text{H}\}$ NMR (100.6 MHz, CDCl_3): δ 156.3, 155.4, 153.4, 152.4,

143.0, 142.4, 140.4, 139.1, 136.0, 133.2, 132.3, 129.6, 127.2, 121.3, 118.6, 117.5, 116.1, 104.6, 61.0, 56.2, 14.8, 14.7, 14.6 (two of the aromatic signals are overlapped); HRMS (MALDI-TOF): m/z calcd for $C_{29}H_{29}BF_2N_2NaO_4 [M+Na]^+$: 541.2086, found: 541.2104.

Bis(mono-styryl BODIPY) substituted phthalocyanine 7.5. According to the procedure for the preparation of 7.2, the mono-styryl BODIPY 7.4 (104 mg, 0.20 mmol) was treated with silicon(IV) phthalocyanine dichloride (7.1) (62 mg, 0.10 mmol) to give 7.5 as a purple solid (33 mg, 21%). 1H NMR (300 MHz, $CDCl_3$): δ 9.64-9.67 (m, 8 H, Pc- H_α), 8.39-8.43 (m, 8 H, Pc- H_β), 7.33 (d, $J = 16.2$ Hz, 2 H, CH=CH), 6.98 (d, $J = 16.2$ Hz, 2 H, CH=CH), 6.68 (s, 4 H, ArH), 6.31 (s, 2 H, pyrrole-H), 5.75 (s, 2 H, pyrrole-H), 5.53 (d, $J = 8.4$ Hz, 4 H, p - C_6H_4), 3.87 (s, 12 H, OCH_3), 3.84 (s, 6 H, OCH_3), 2.63 (d, $J = 8.4$ Hz, 4 H, p - C_6H_4), 2.39 (s, 6 H, CH_3), 0.61 (s, 6 H, CH_3), 0.60 (s, 6 H, CH_3); $^{13}C\{^1H\}$ NMR (75.4 MHz): δ 154.8, 153.3, 151.9, 150.1, 149.7, 142.6, 142.0, 140.2, 139.0, 135.6, 135.4, 132.4, 132.2, 131.5, 127.2, 125.7, 123.9, 120.8, 118.3, 116.9, 104.5, 60.9, 56.2, 14.5, 14.4, 14.2 (some of the signals are overlapped); MS (ESI): two isotopic clusters peaking at m/z 1598 {42%, $[M+Na]^+$ } and 1057 {100%, $[M - \text{mono-styryl BODIPY}]^+$ }; HRMS (ESI): m/z calcd for $C_{90}H_{72}B_2F_4N_{12}NaO_8Si [M+Na]^+$: 1597.5380, found: 1597.5378.

SiPc($OC_6H_4CO_2CH_3$)₂ (7.7). According to the procedure for the preparation of 7.2, silicon(IV) phthalocyanine dichloride (7.1) (61 mg, 0.10 mmol) was treated with methyl 4-hydroxybenzoate (7.6) (61 mg, 0.40 mmol) to give 7.7 as a blue solid (45 mg, 53%). 1H NMR (300 MHz, $CDCl_3$): δ 9.61-9.68 (m, 8 H, Pc- H_α),

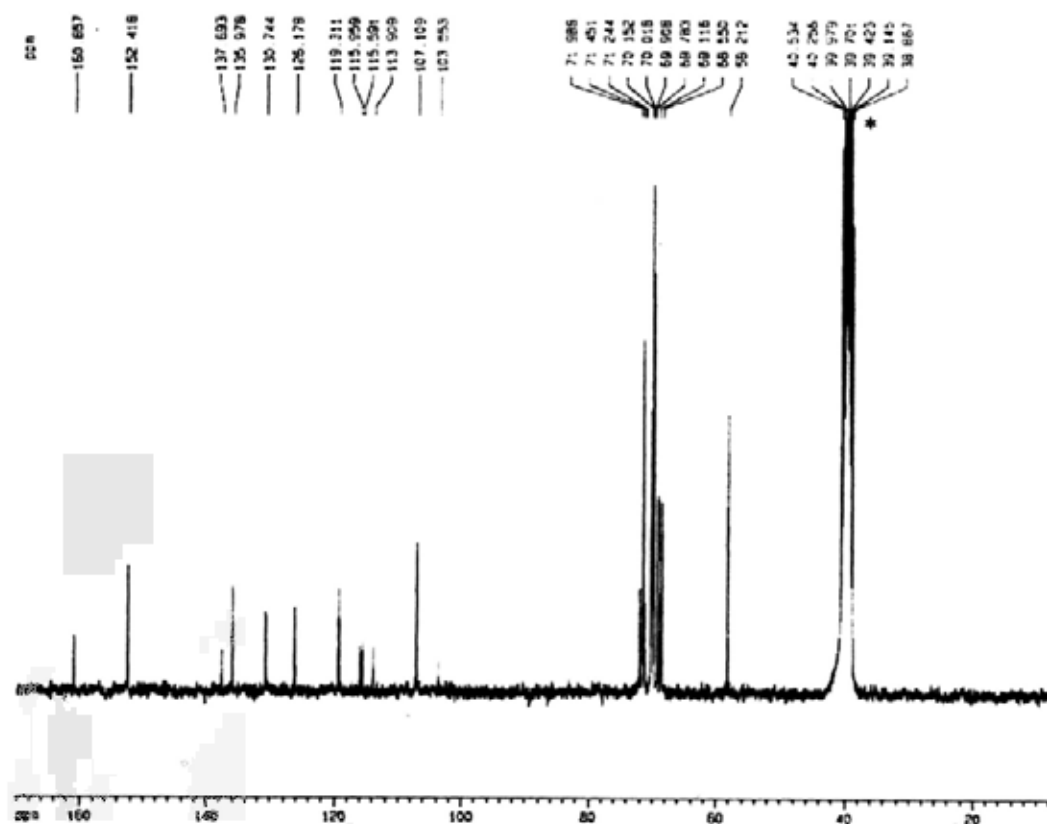
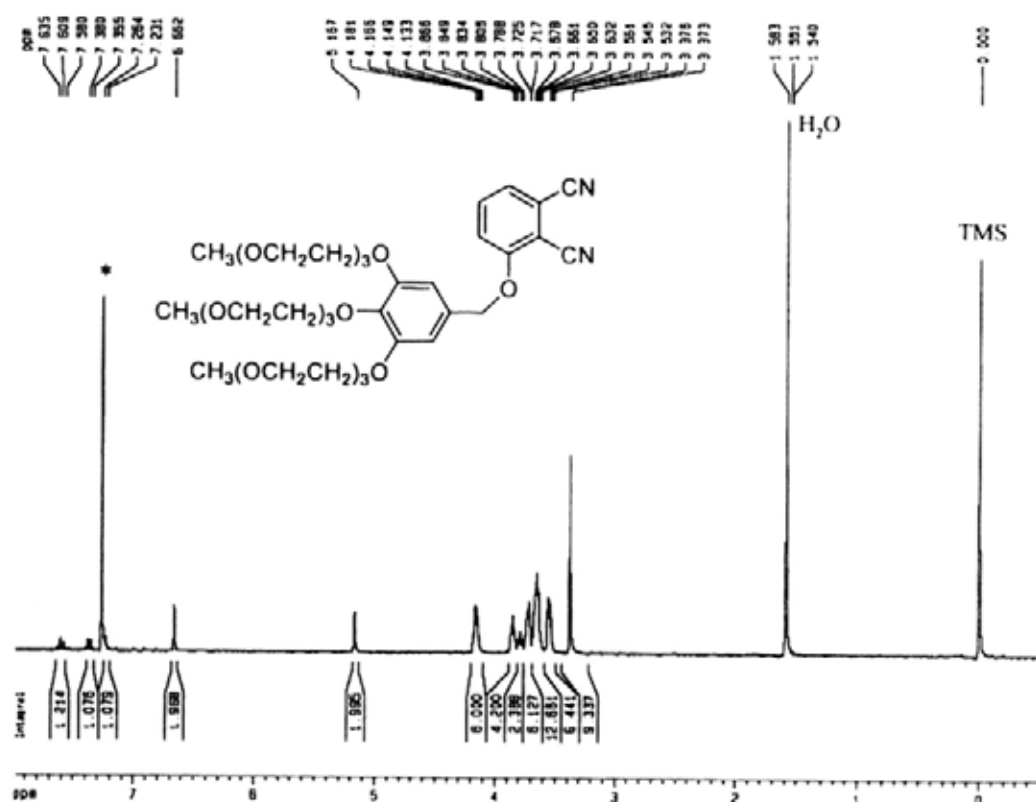
8.37-8.42 (m, 8 H, Pc-H β), 6.30 (d, $J = 7.8$ Hz, 4 H, p -C $_6$ H $_4$), 3.43 (s, 6 H, OCH $_3$), 2.45 (d, $J = 7.8$ Hz, 4 H, p -C $_6$ H $_4$); 13 C{ 1 H} NMR (75.4 MHz, CDCl $_3$): δ 154.0, 149.6, 135.3, 131.4, 129.2, 123.9, 120.9, 117.3, 51.3 (the carbonyl signal was too weak to be observed); MS (MALDI-TOF): an isotopic cluster peaking at m/z 843 {27%, [M+H] $^+$ }; HRMS (MALDI-TOF): m/z calcd for C $_{48}$ H $_{31}$ N $_8$ O $_6$ Si [M+H] $^+$: 843.2130, found: 843.2143.

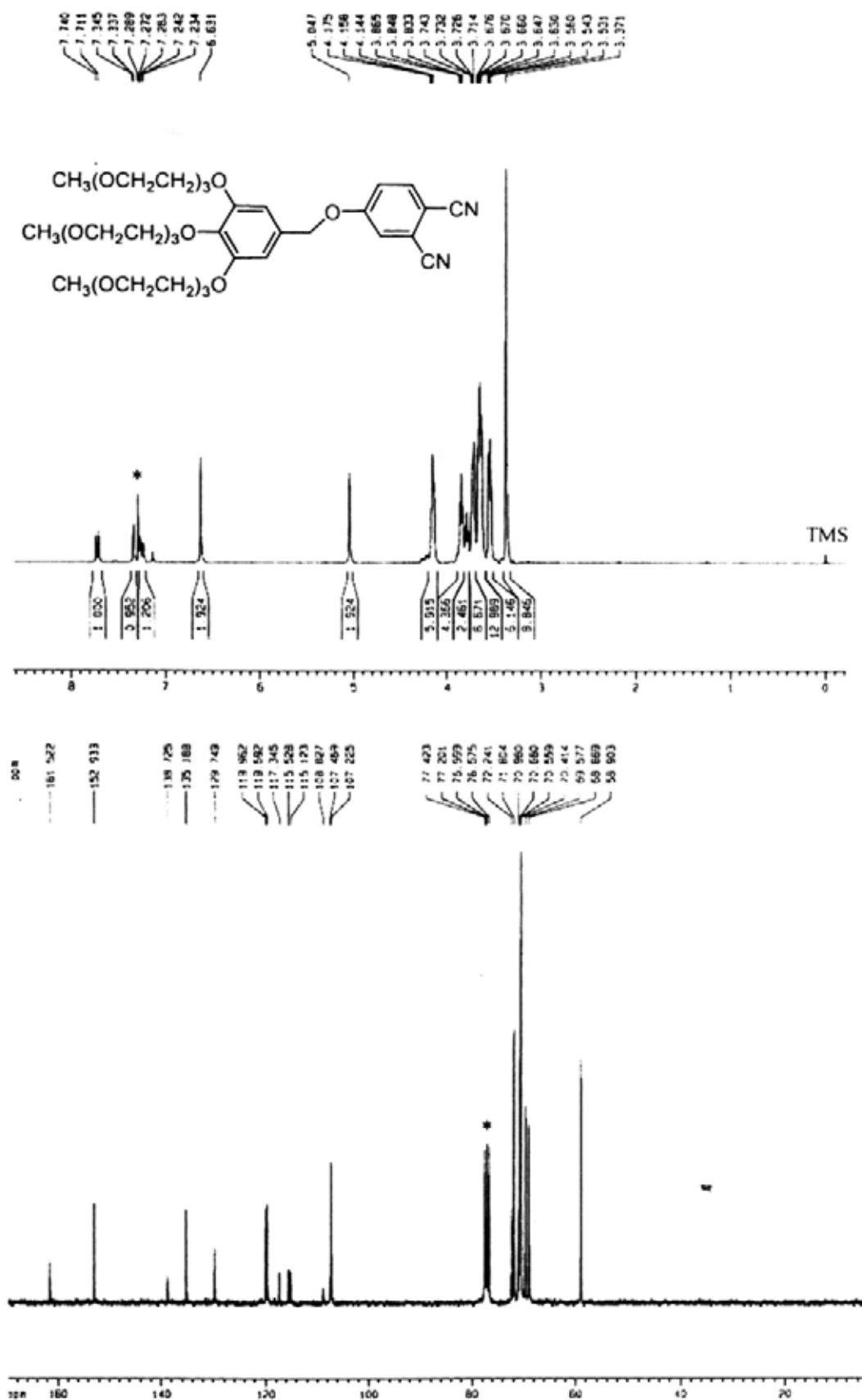
7.5 References

1. (a) Wasielewski, M. R. *J. Org. Chem.* **2006**, *71*, 5051. (b) Fukuzumi, S. *Phys. Chem. Chem. Phys.* **2008**, *10*, 2283.
2. Balzani, V.; Credi, A.; Venturi, M. *ChemSusChem* **2008**, *1*, 26.
3. Balzani, V.; Credi, A.; Venturi, M. *Chem. Eur. J.* **2008**, *14*, 26.
4. (a) de la Torre, G.; Claessens, C. G.; Torres, T. *Chem. Commun.* **2007**, 2000. (b) Claessens, C. G.; Hahn, U.; Torres, T. *Chem. Rec.* **2008**, *8*, 75.
5. (a) Loudet, A.; Burgess, K. *Chem. Rev.* **2007**, *107*, 4891. (b) Ulrich, G.; Ziesel, R.; Harriman, A. *Angew. Chem. Int. Ed.* **2008**, *47*, 1184.
6. See for example (a) D'Souza, F.; Smith, P. M.; Zandler, M. E.; McCarty, A. L.; Itou, M.; Araki, Y.; Ito, O. *J. Am. Chem. Soc.* **2004**, *126*, 7898. (b) de la Escosura, A.; Martínez-Díaz, M. V.; Guldi, D. M.; Torres, T. *J. Am. Chem. Soc.* **2006**, *128*, 4112. (c) Rodríguez-Morgade, M. S.; Torres, T.; Atienza-Castellanos, C.; Guldi, D. M. *J. Am. Chem. Soc.* **2006**, *128*, 15145.
7. Liu, J.-Y.; Yeung, H.-S.; Xu, W.; Li, X.; Ng, D. K. P. *Org. Lett.* **2008**, *10*, 5421.
8. Dost, Z.; Atilgan, S.; Akkaya, E. U. *Tetrahedron* **2006**, *62*, 8484.
9. Coskun, A.; Deniz, E.; Akkaya, E. U. *Org. Lett.* **2005**, *7*, 5187.
10. Seybold, P.; Gouterman, M. *J. Mol. Spectrosc.* **1969**, *31*, 1.
11. (a) Kubin, R. F.; Fletcher, A. N. *J. Luminescence* **1982**, *27*, 455. (b) Sens, R. Ph.D. thesis, University of Siegen, **1984**.

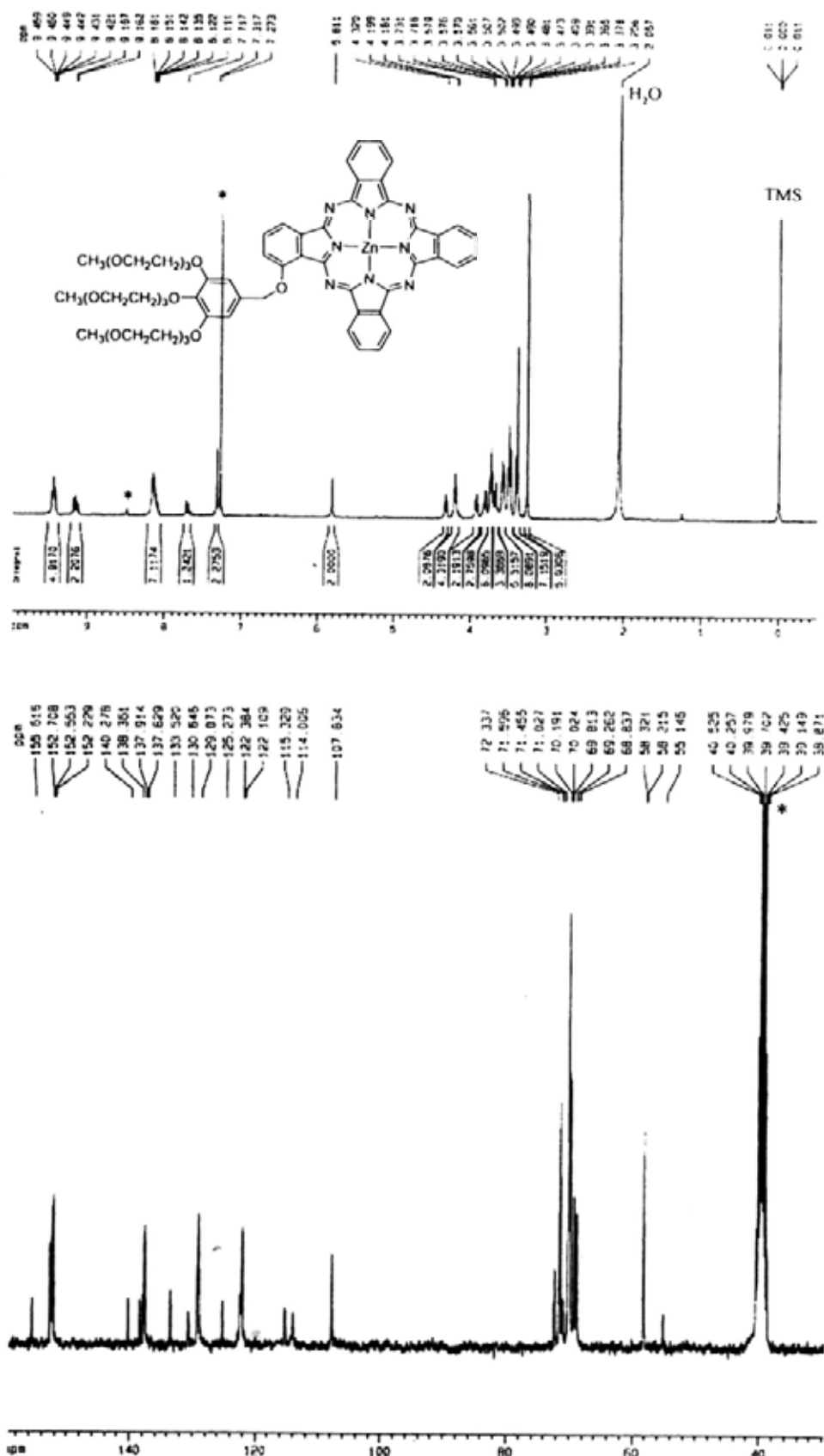
12. (a) Leng, X.; Choi, C.-F.; Lo, P.-C.; Ng, D. K. P. *Org. Lett.* **2007**, *9*, 231. (b) Tannert, S.; Ermilov, E. A.; Vogel, J. O.; Choi, M. T. M.; Ng, D. K. P.; Röder, B. *J. Phys. Chem. B* **2007**, *111*, 8053.
13. Rehm, D.; Weller, A. *Isr. J. Chem.* **1970**, *8*, 259.
14. Korth, O.; Hanke, T.; Rückmann, I.; Röder, B. *Exp. Tech. Phys.* **1995**, *41*, 25.
15. Tannert, S.; Ermilov, E. A.; Vogel, J. O.; Choi, M. T. M.; Ng, D. K. P.; Röder, B. *J. Phys. Chem. B* **2007**, *111*, 8053.
16. Rückmann, I.; Zeug, A.; Herter, R.; Röder, B. *Photochem. Photobiol.* **1997**, *66*, 576.

Appendix A-1 ^1H NMR (CDCl_3) and $^{13}\text{C}\{^1\text{H}\}$ NMR (DMSO-d_6) spectra of compound 2.5

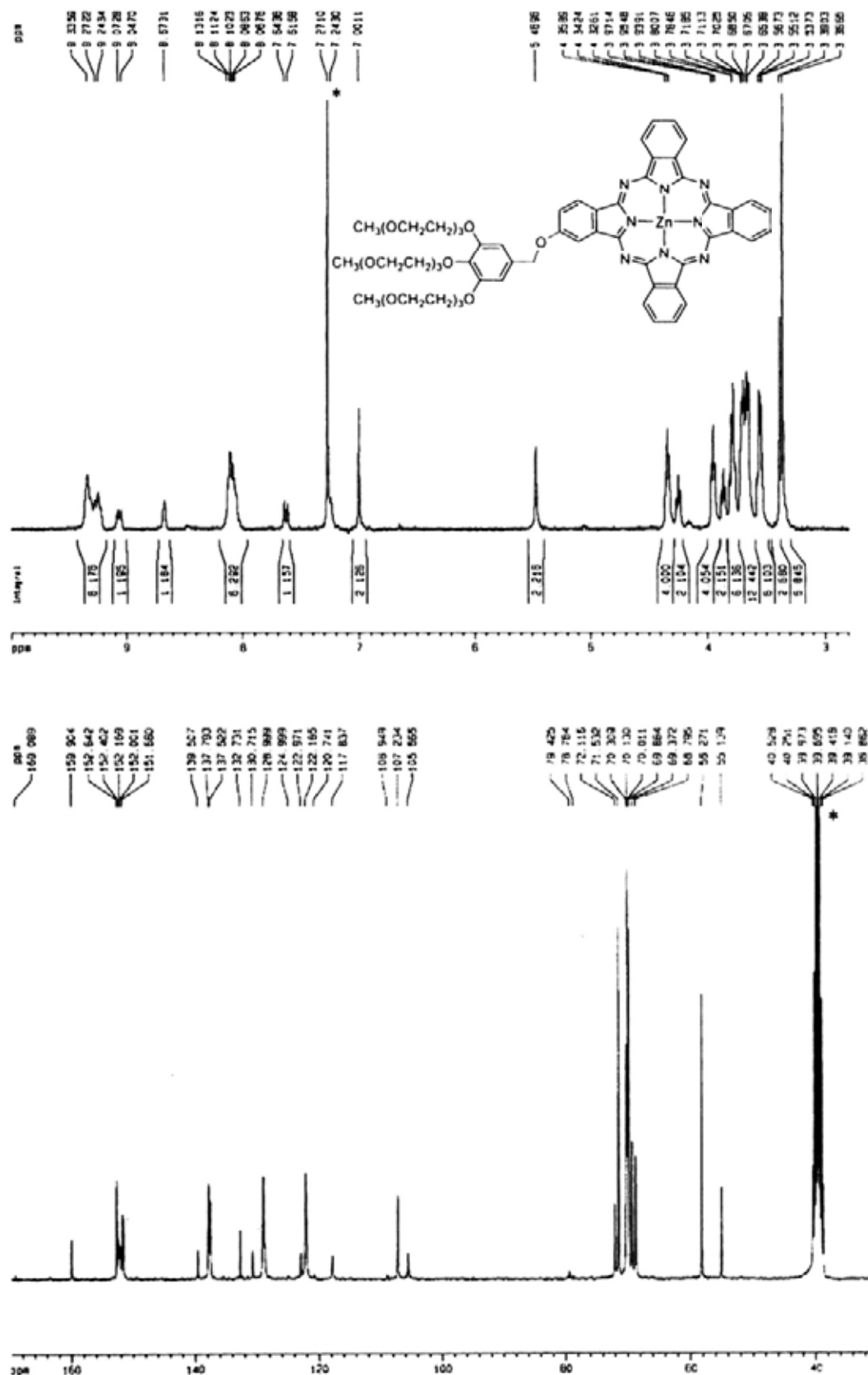


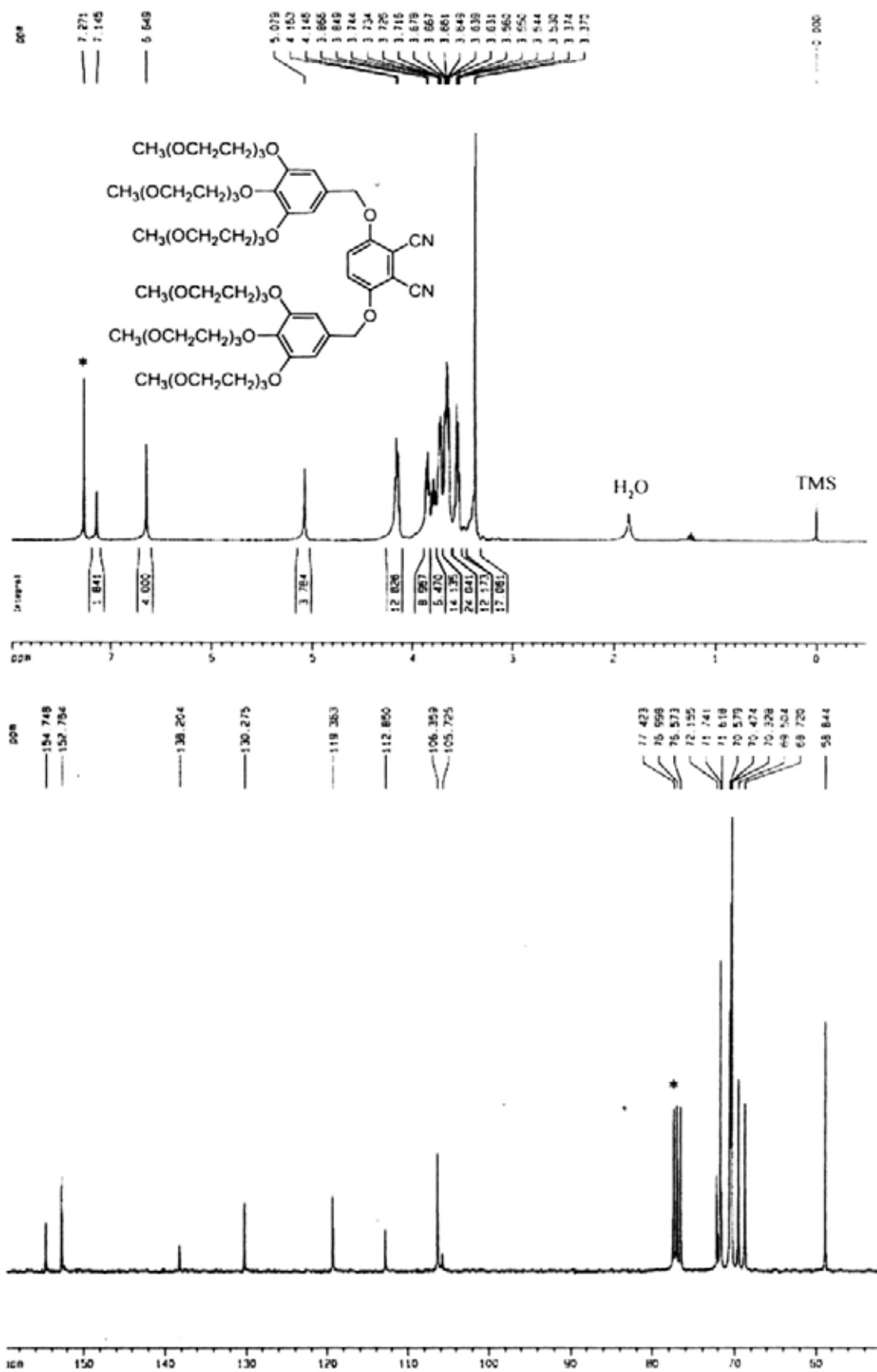
Appendix A-2 ^1H NMR and $^{13}\text{C}\{^1\text{H}\}$ NMR spectra of compound 2.6 in CDCl_3 

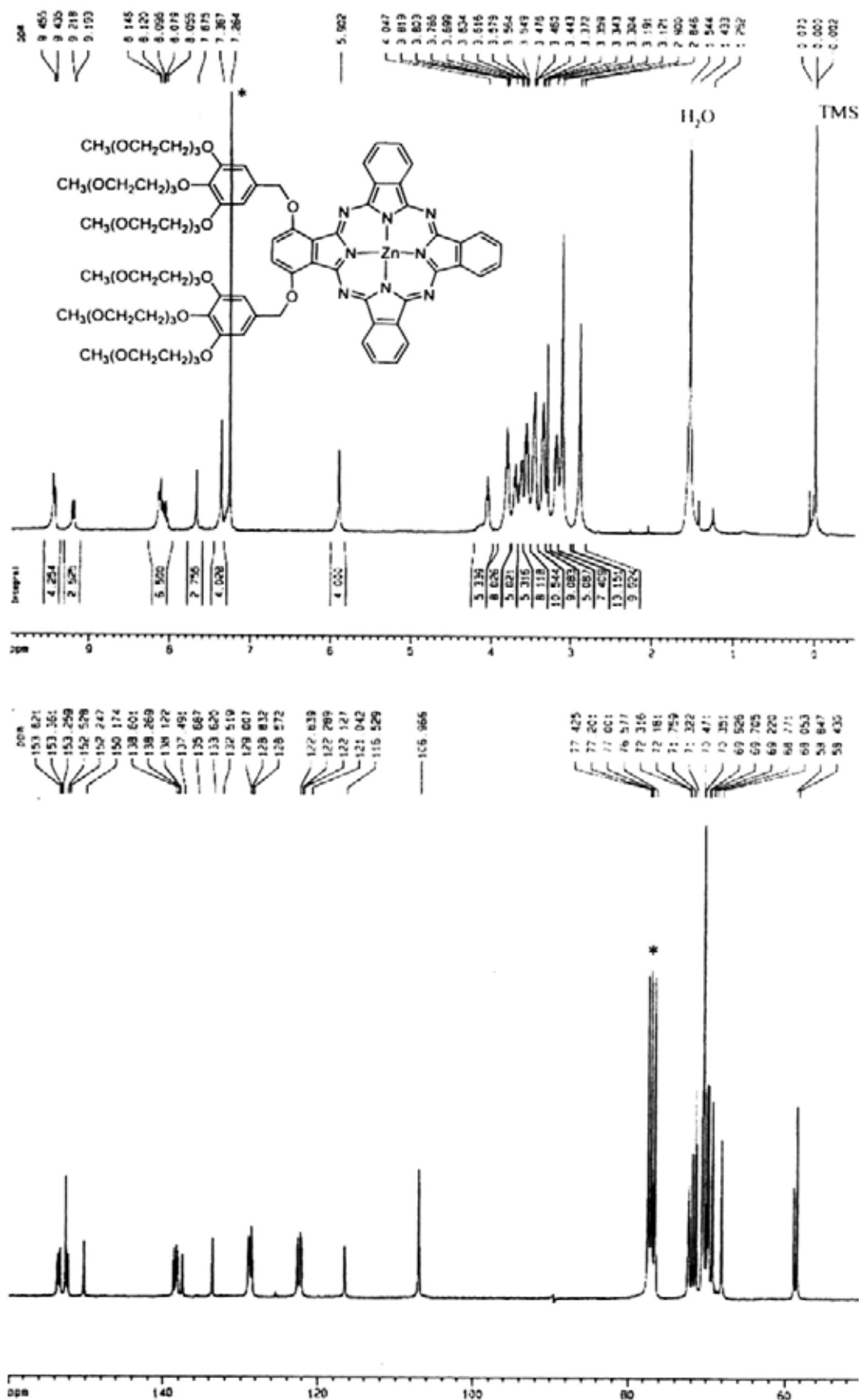
Appendix A-3 ^1H NMR (CDCl_3 with a trace amount of pyridine- d_5) and $^{13}\text{C}\{^1\text{H}\}$ NMR ($\text{DMSO}-d_6$) spectra of compound 2.7



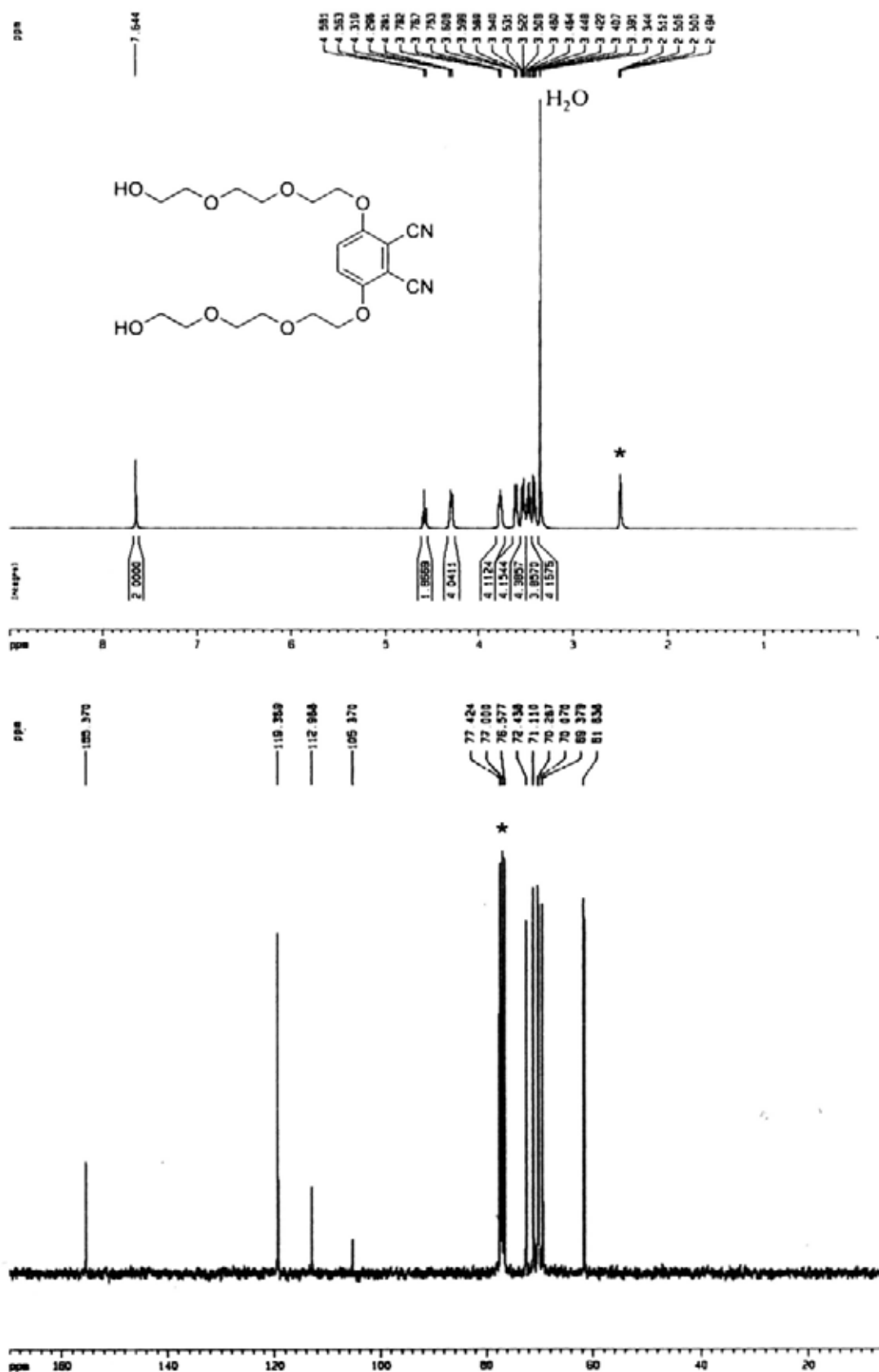
Appendix A-4 ^1H NMR (CDCl_3 with a trace amount of pyridine- d_5) and $^{13}\text{C}\{^1\text{H}\}$ NMR ($\text{DMSO}-d_6$) spectra of compound **2.8**



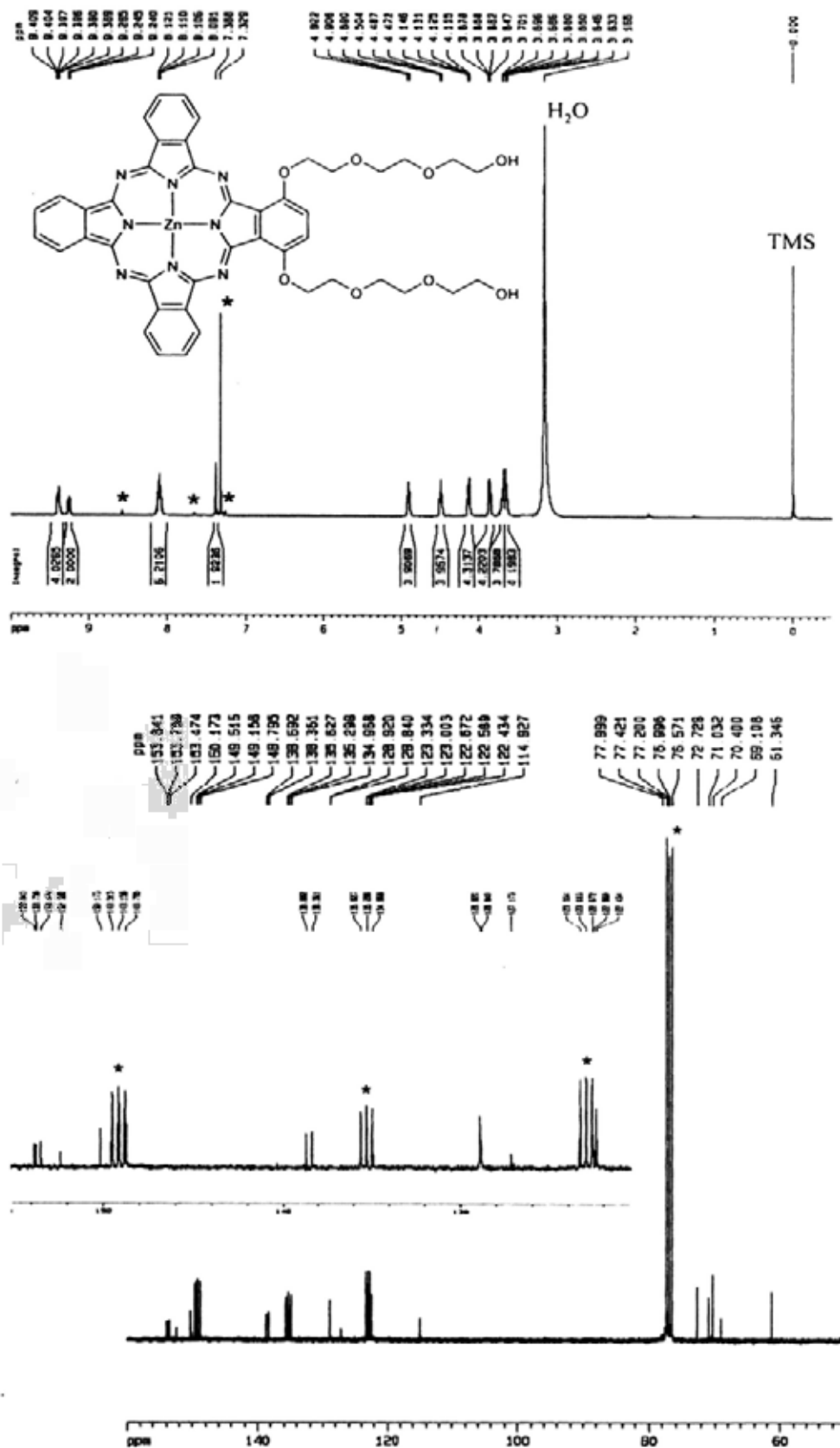
Appendix A-5 ^1H NMR and $^{13}\text{C}\{^1\text{H}\}$ NMR spectra of compound **2.10** in CDCl_3 

Appendix A-6 ^1H NMR and $^{13}\text{C}\{^1\text{H}\}$ NMR spectra of compound 2.11 in CDCl_3 .

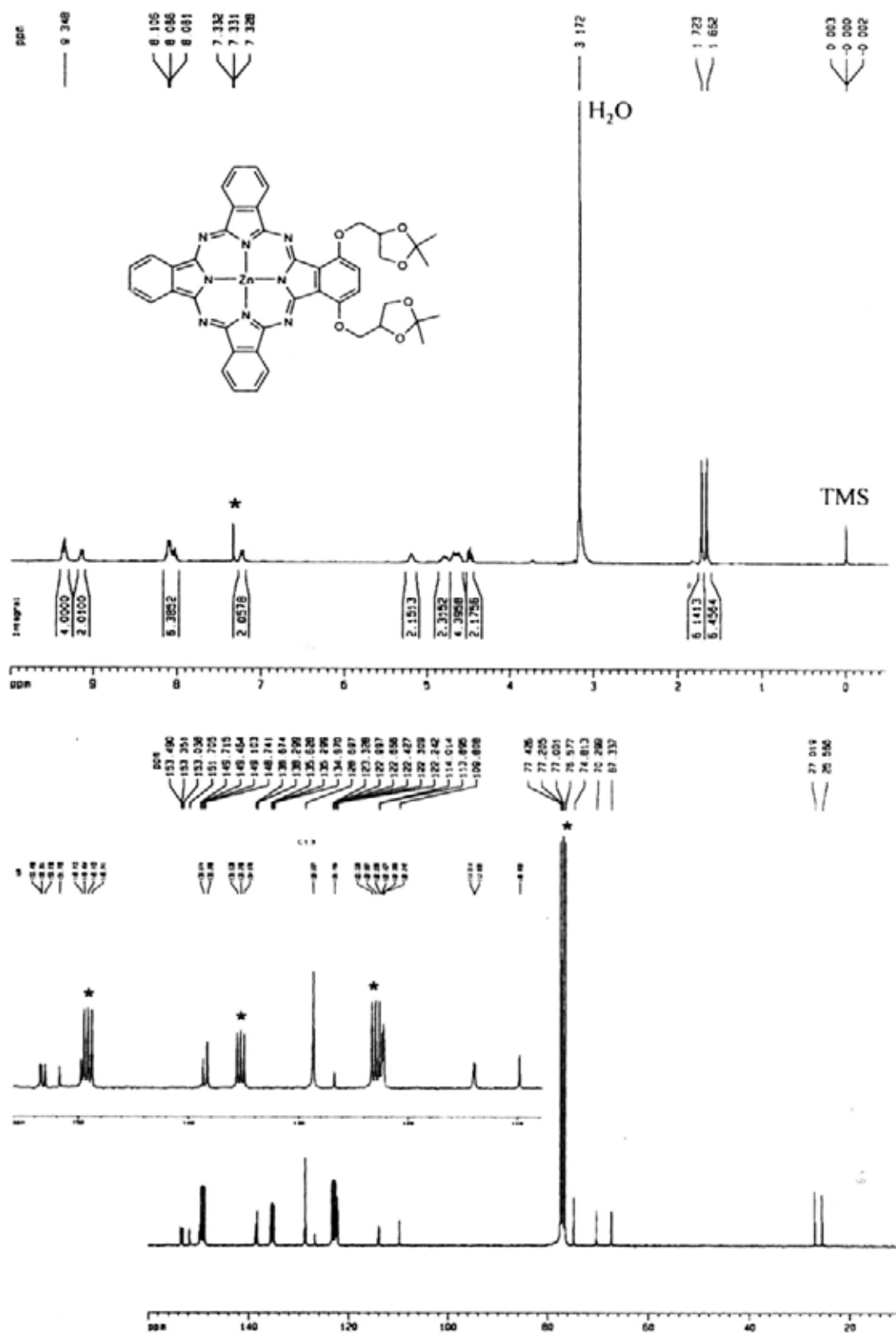
Appendix A-7 ^1H NMR (DMSO- d_6) and $^{13}\text{C}\{^1\text{H}\}$ NMR (CDCl_3) spectra of compound **3.3a**



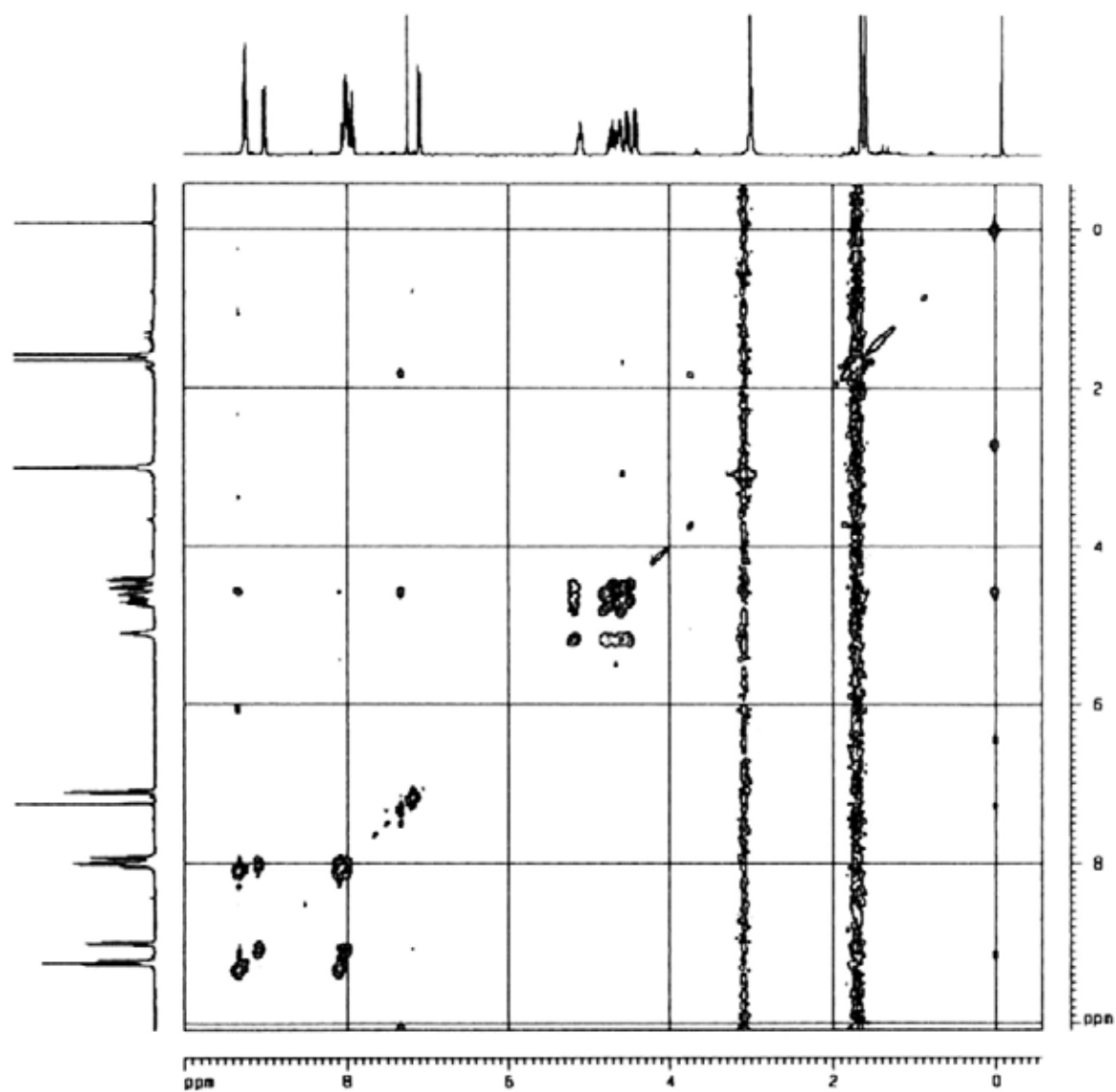
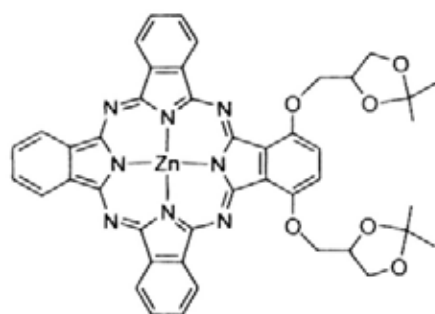
Appendix A-10 ^1H NMR and $^{13}\text{C}\{^1\text{H}\}$ NMR spectra of compound **3.4a** in CDCl_3 with a trace amount of pyridine- d_5



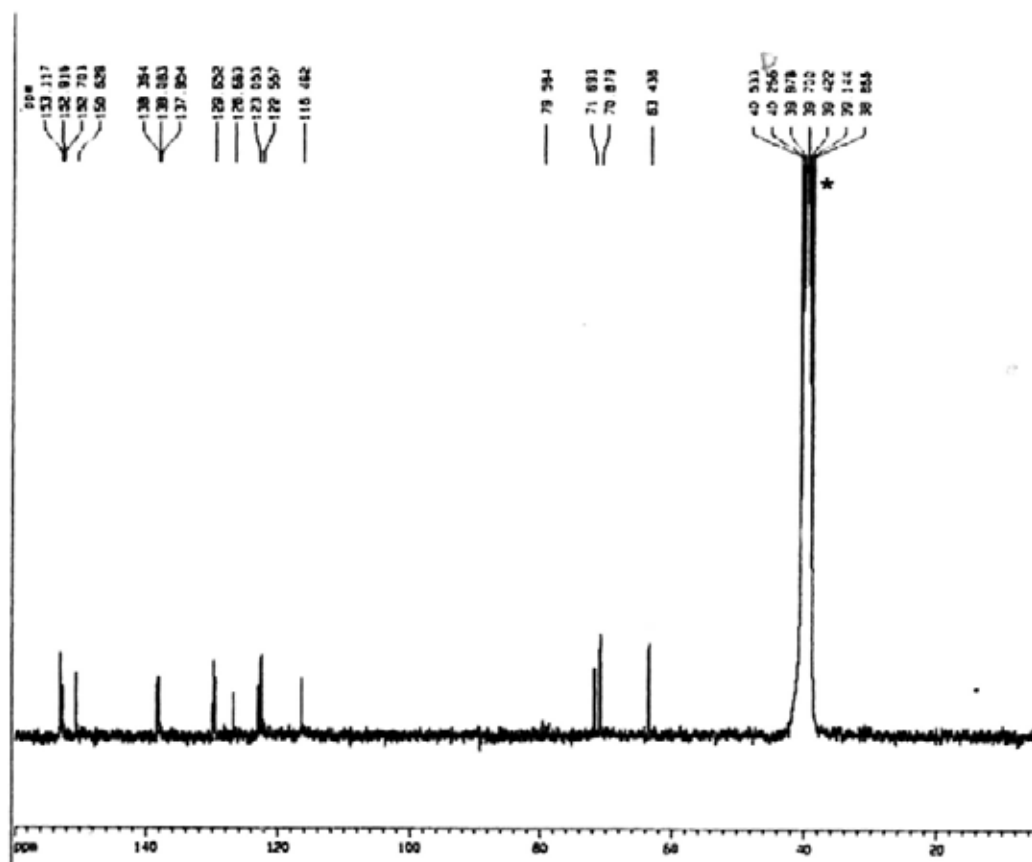
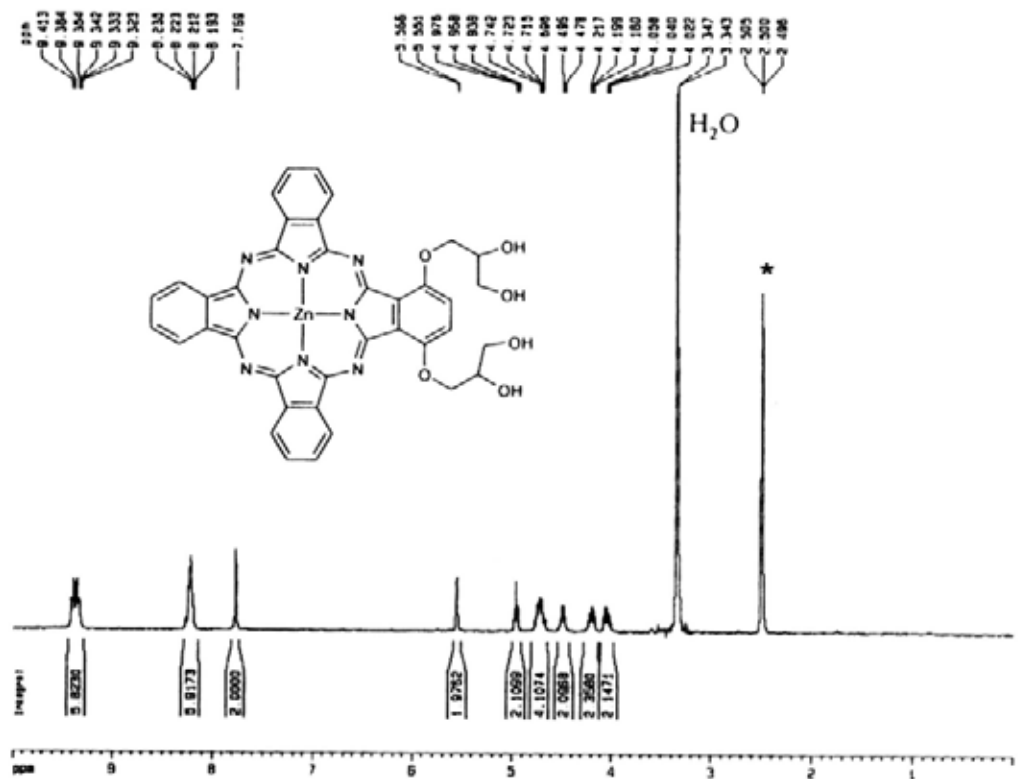
Appendix A-12 ^1H NMR and $^{13}\text{C}\{^1\text{H}\}$ NMR spectra of compound **3.4c** in CDCl_3 with a trace amount of pyridine- d_5

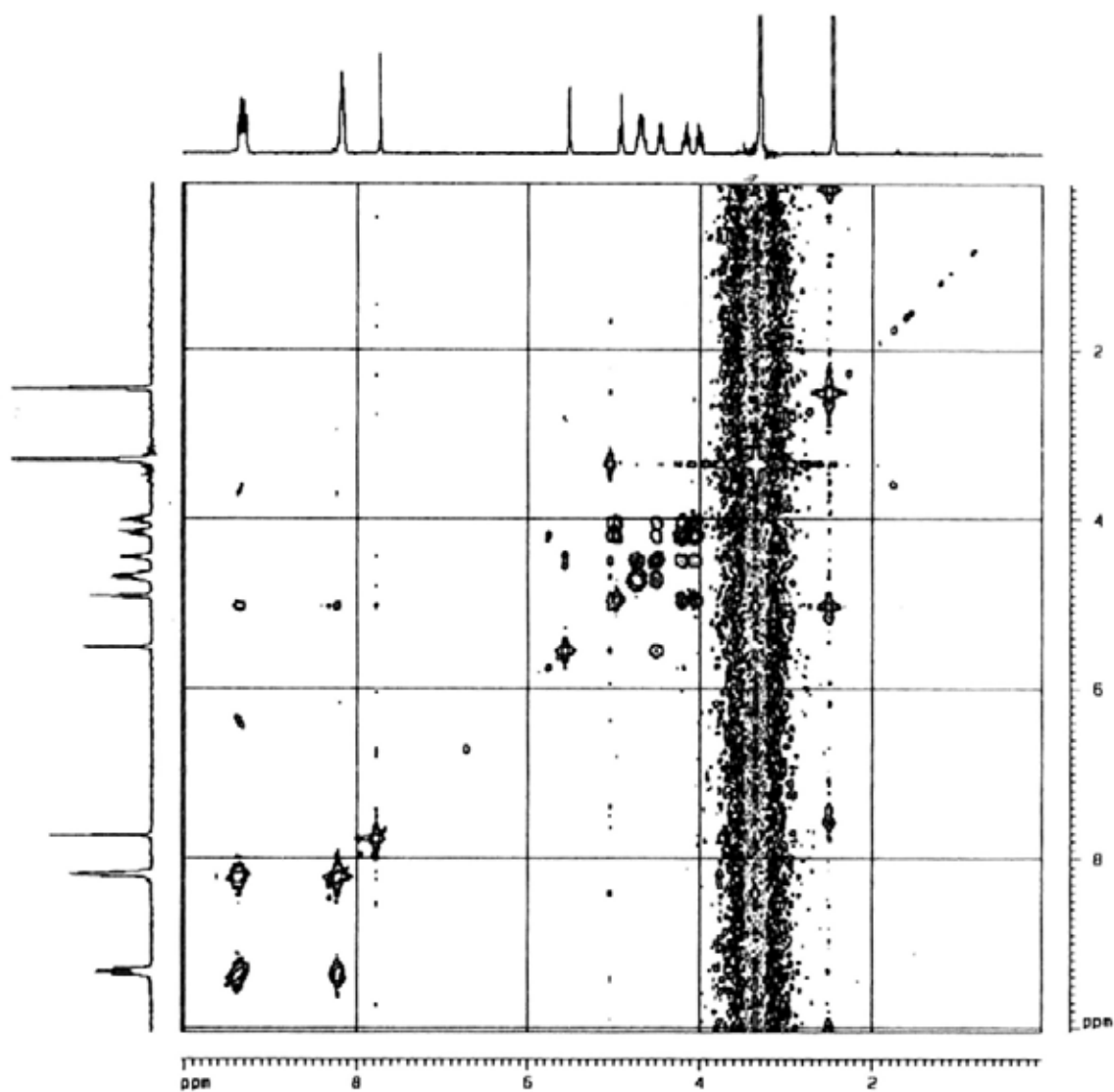
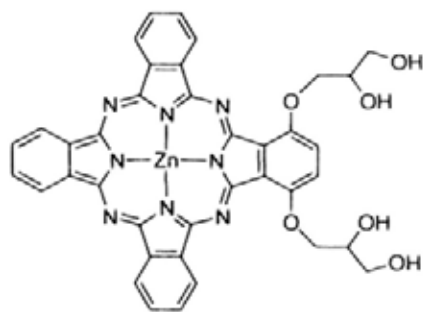


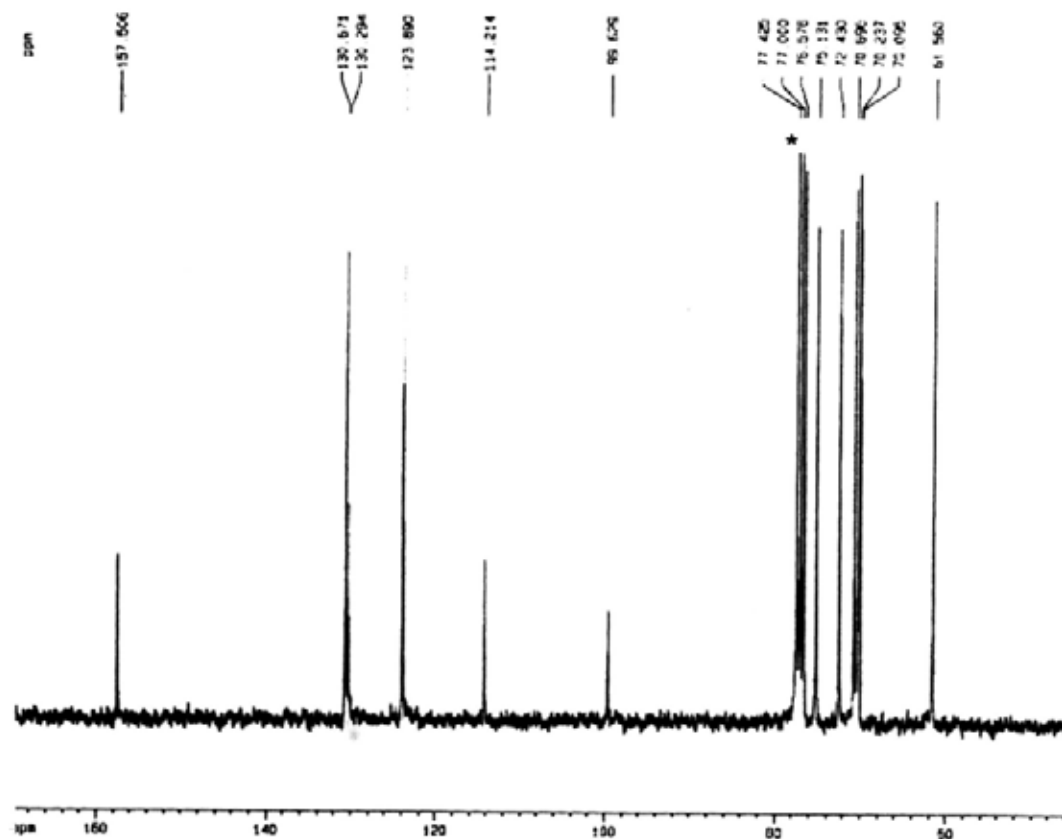
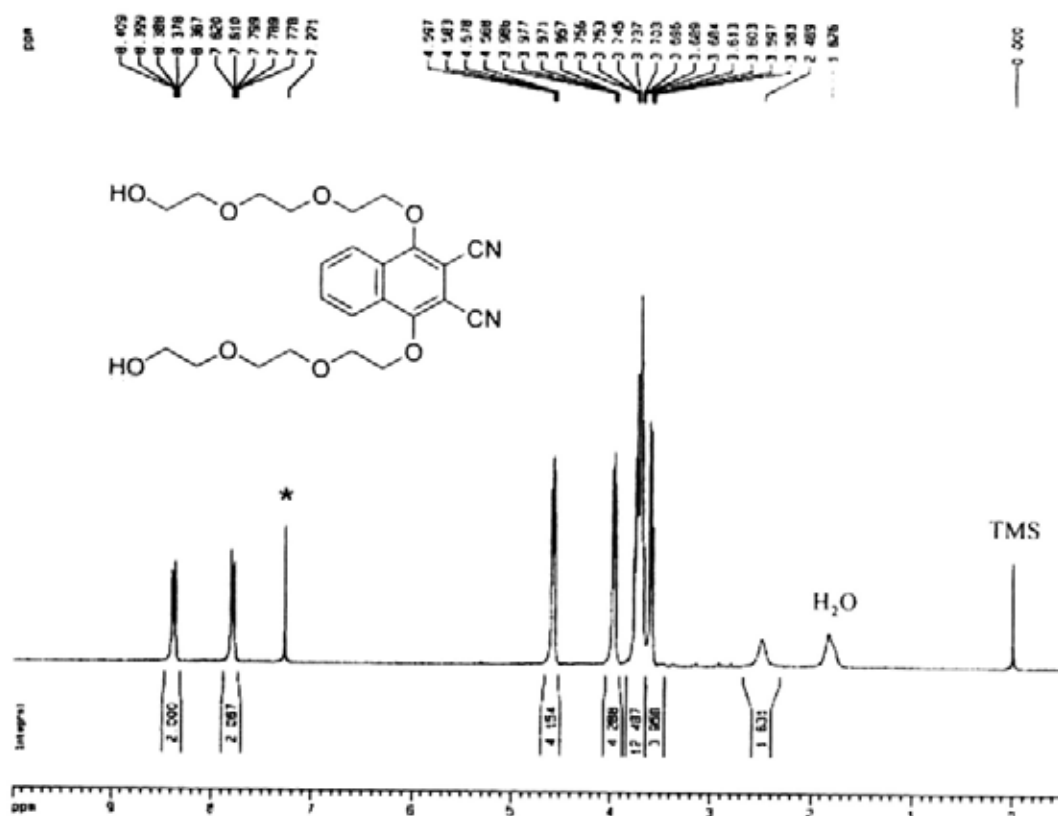
Appendix A-13 ^1H - ^1H COSY spectrum of **3.4c** in CDCl_3 with a trace amount of pyridine- d_5



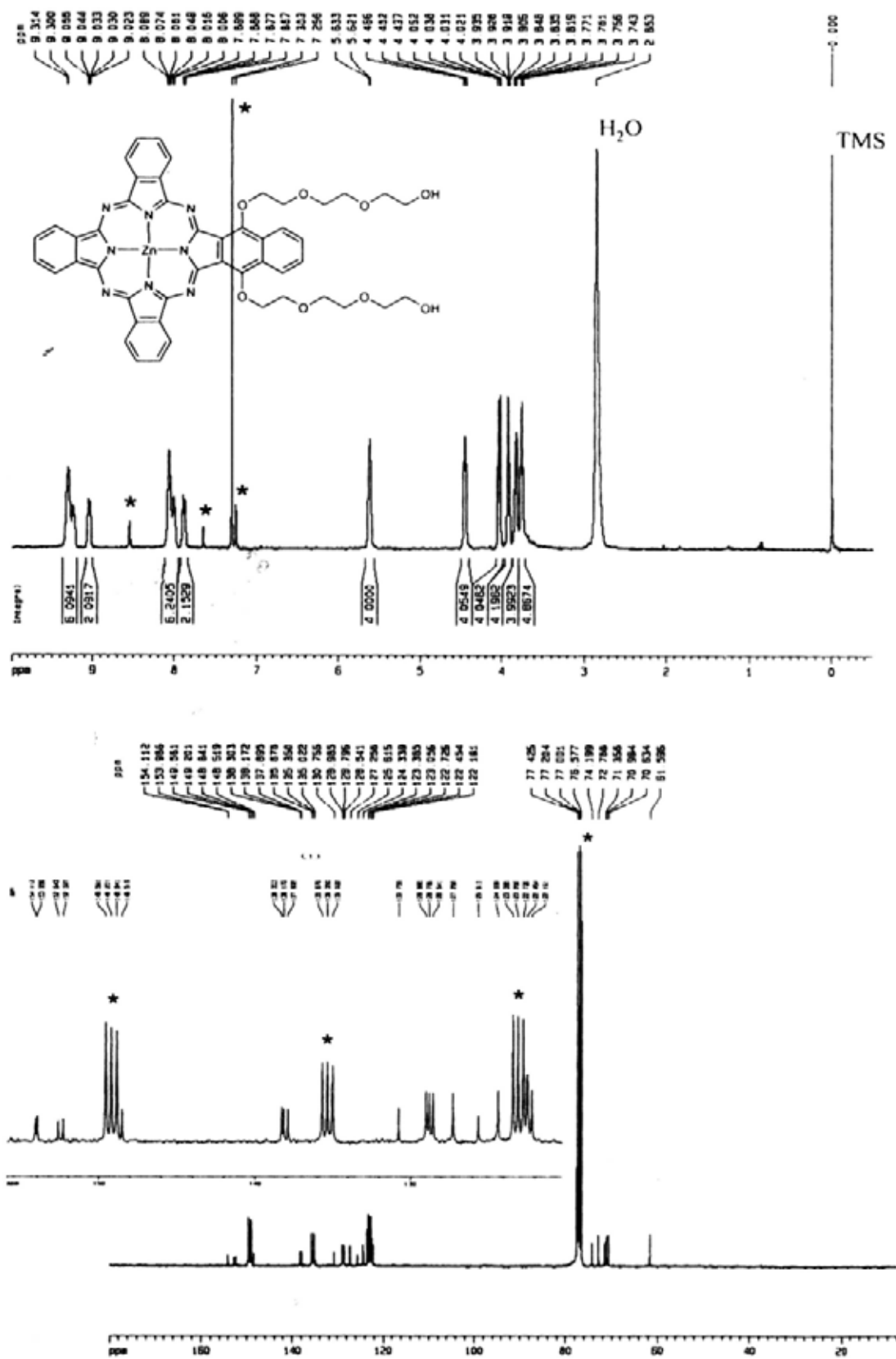
Appendix A-14 ^1H NMR and $^{13}\text{C}\{^1\text{H}\}$ NMR spectra of compound **3.4d** in DMSO-d_6



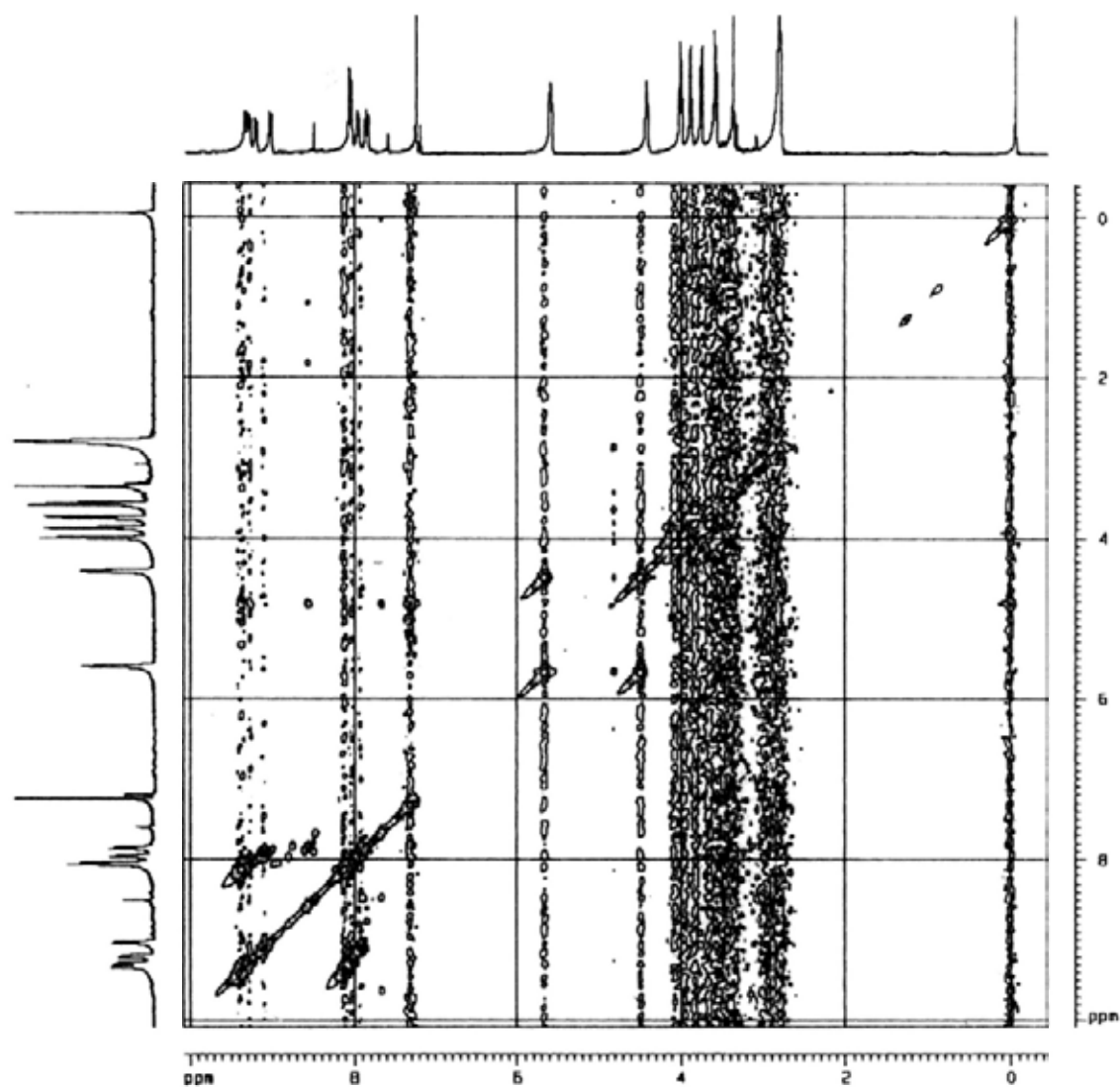
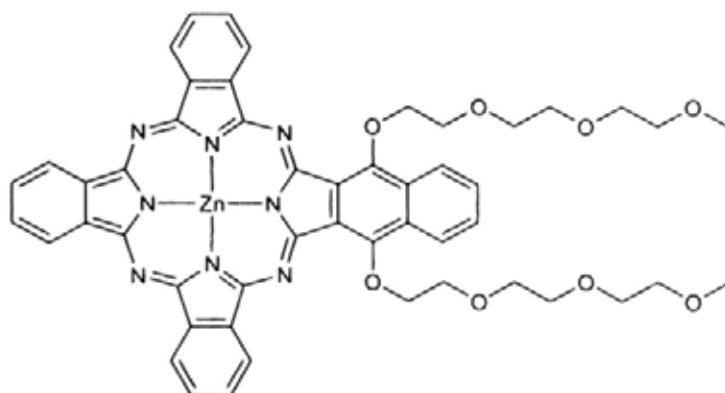
Appendix A-15 ^1H - ^1H COSY spectrum of compound **3.4d** in DMSO-d_6 

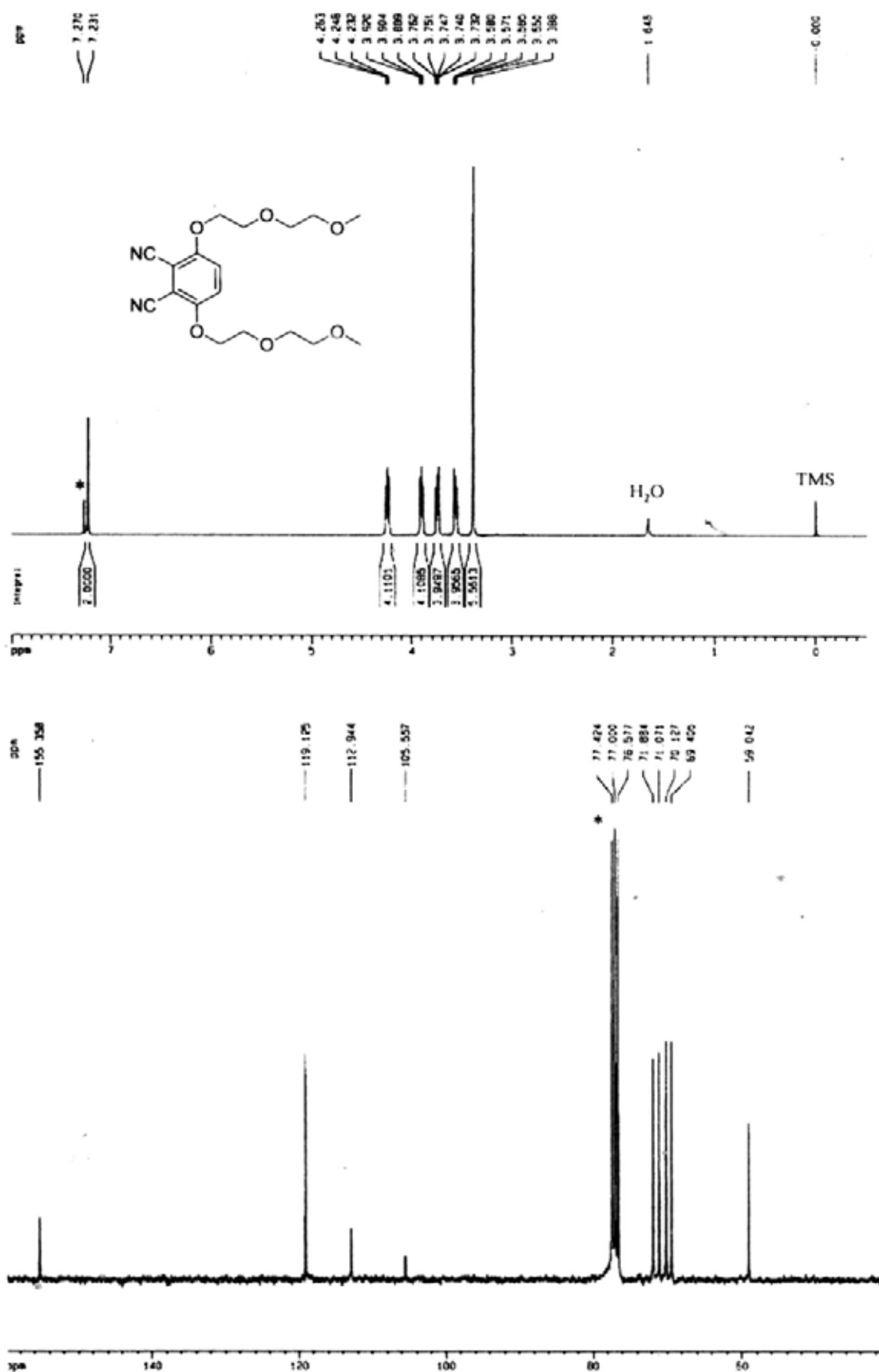
Appendix A-16 ^1H NMR and $^{13}\text{C}\{^1\text{H}\}$ NMR spectra of compound **3.6a** in CDCl_3 

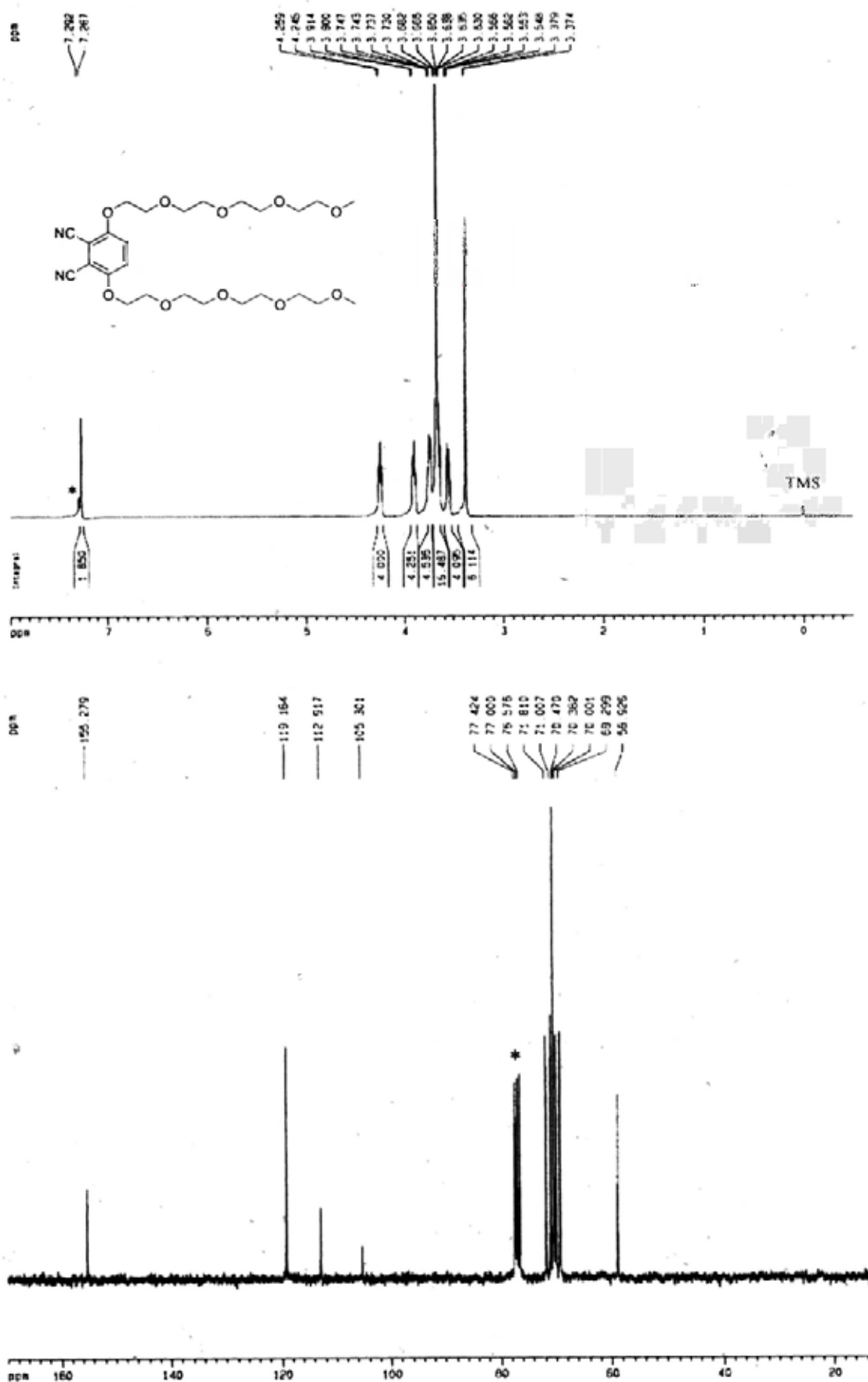
Appendix A-18 ^1H NMR and $^{13}\text{C}\{^1\text{H}\}$ NMR spectra of compound **3.7a** in CDCl_3 with a trace amount of pyridine- d_5

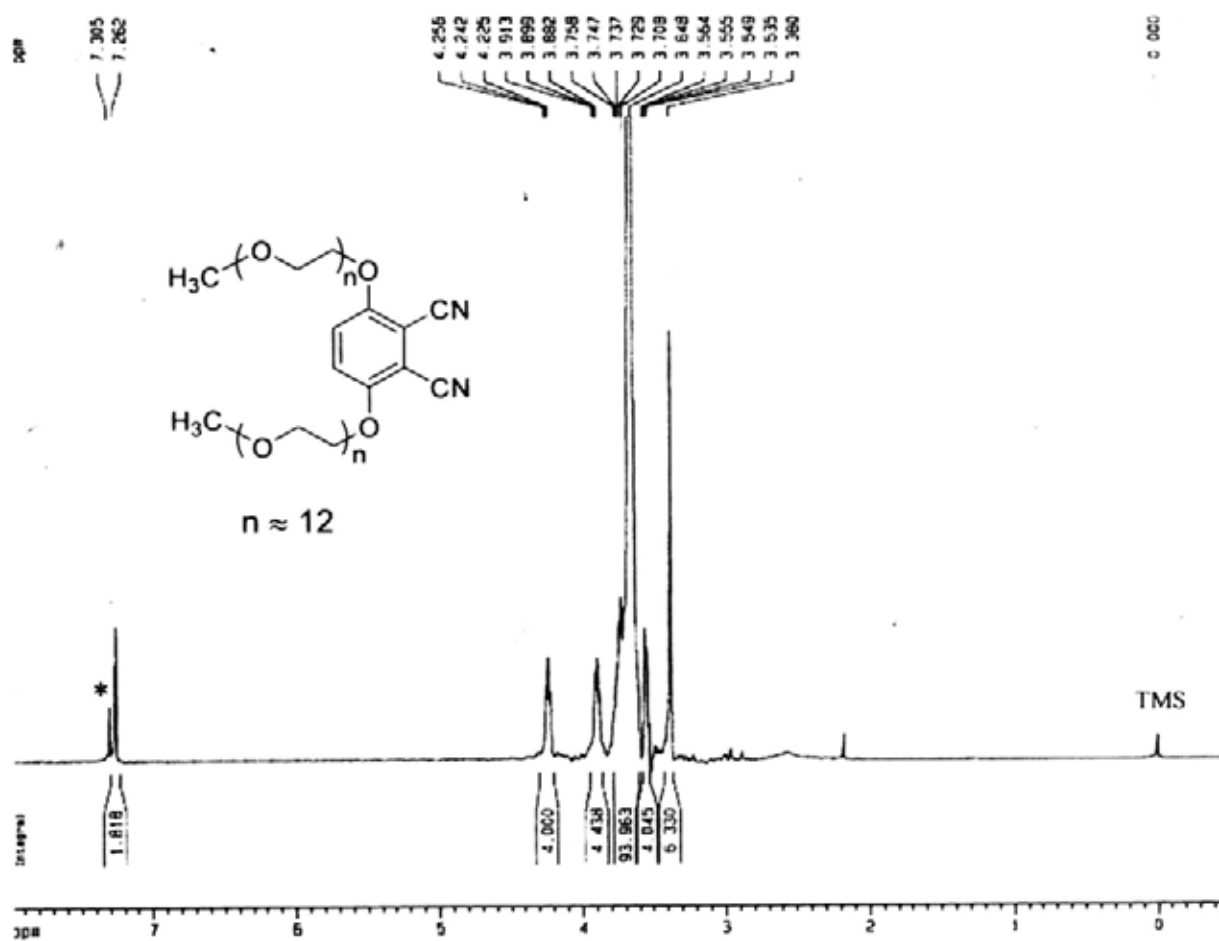


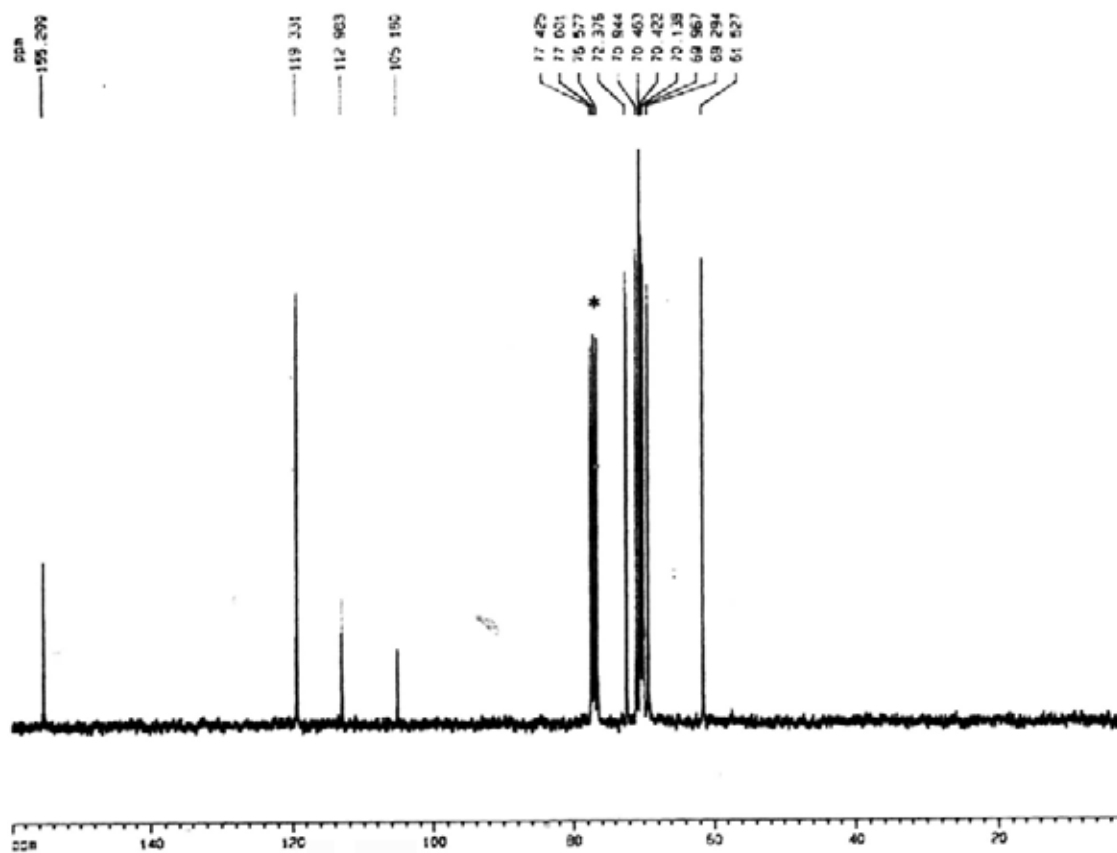
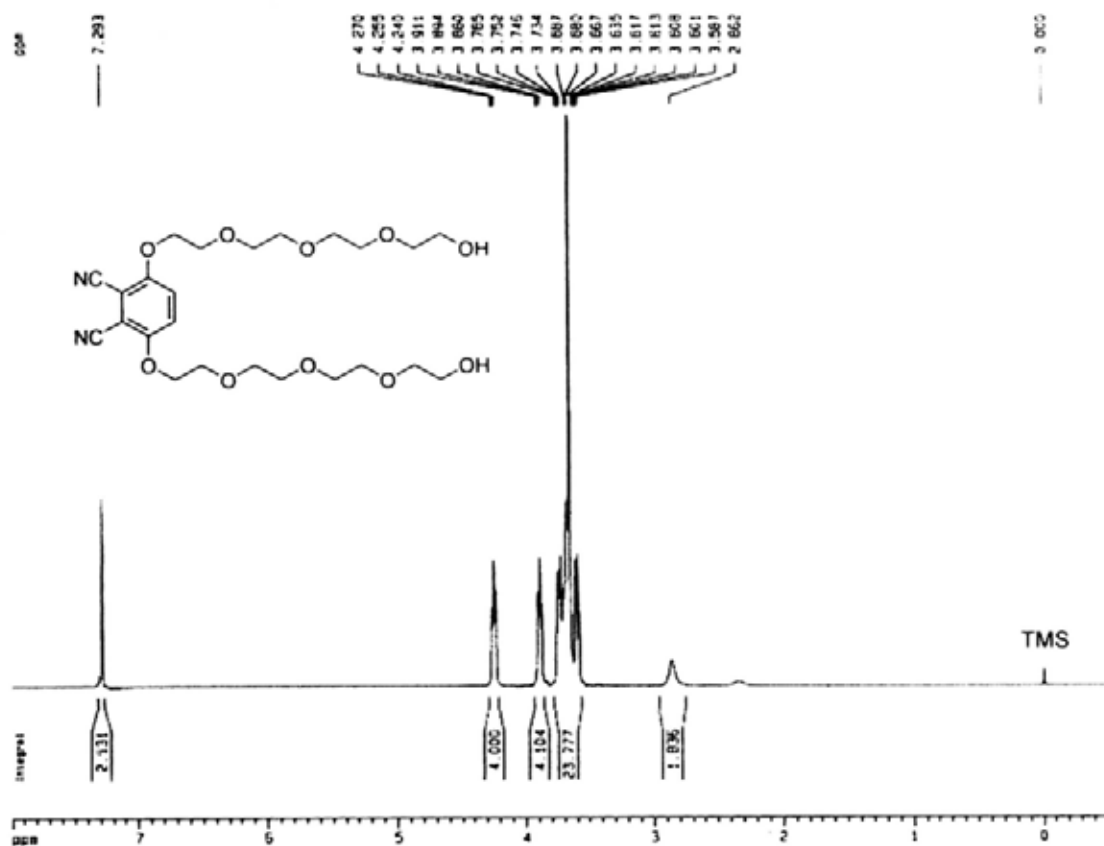
Appendix A-20 ^1H - ^1H COSY spectrum of **3.7b** in CDCl_3 with a trace amount of pyridine- d_5



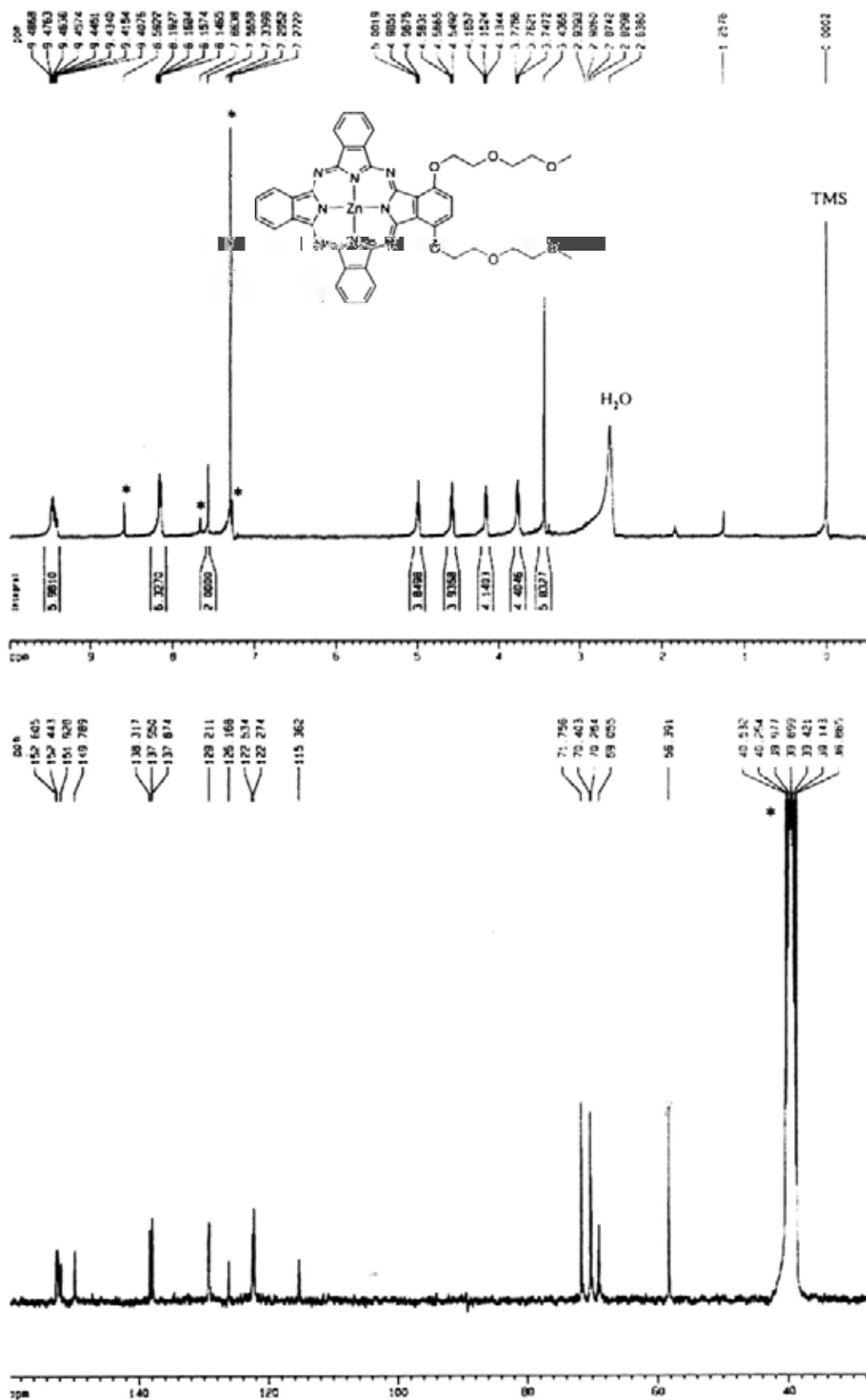
Appendix A-21 ^1H NMR and $^{13}\text{C}\{^1\text{H}\}$ NMR spectra of compound **4.2a** in CDCl_3 

Appendix A-22 ^1H NMR and $^{13}\text{C}\{^1\text{H}\}$ NMR spectra of compound **4.2b** in CDCl_3 

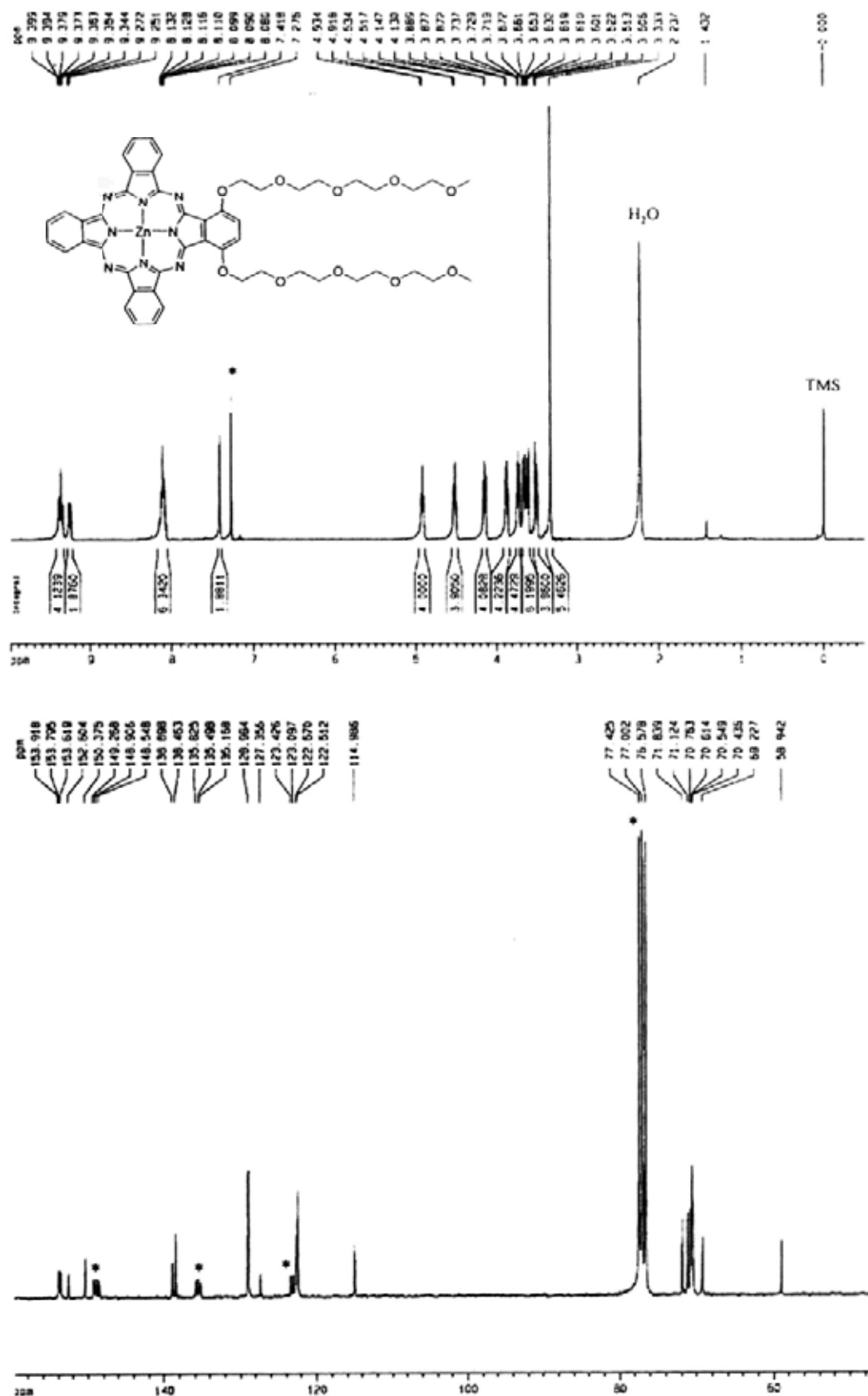
Appendix A-23 ^1H NMR spectrum of compound 4.2c in CDCl_3 

Appendix A-24 ^1H NMR and $^{13}\text{C}\{^1\text{H}\}$ NMR spectra of compound **4.2d** in CDCl_3 

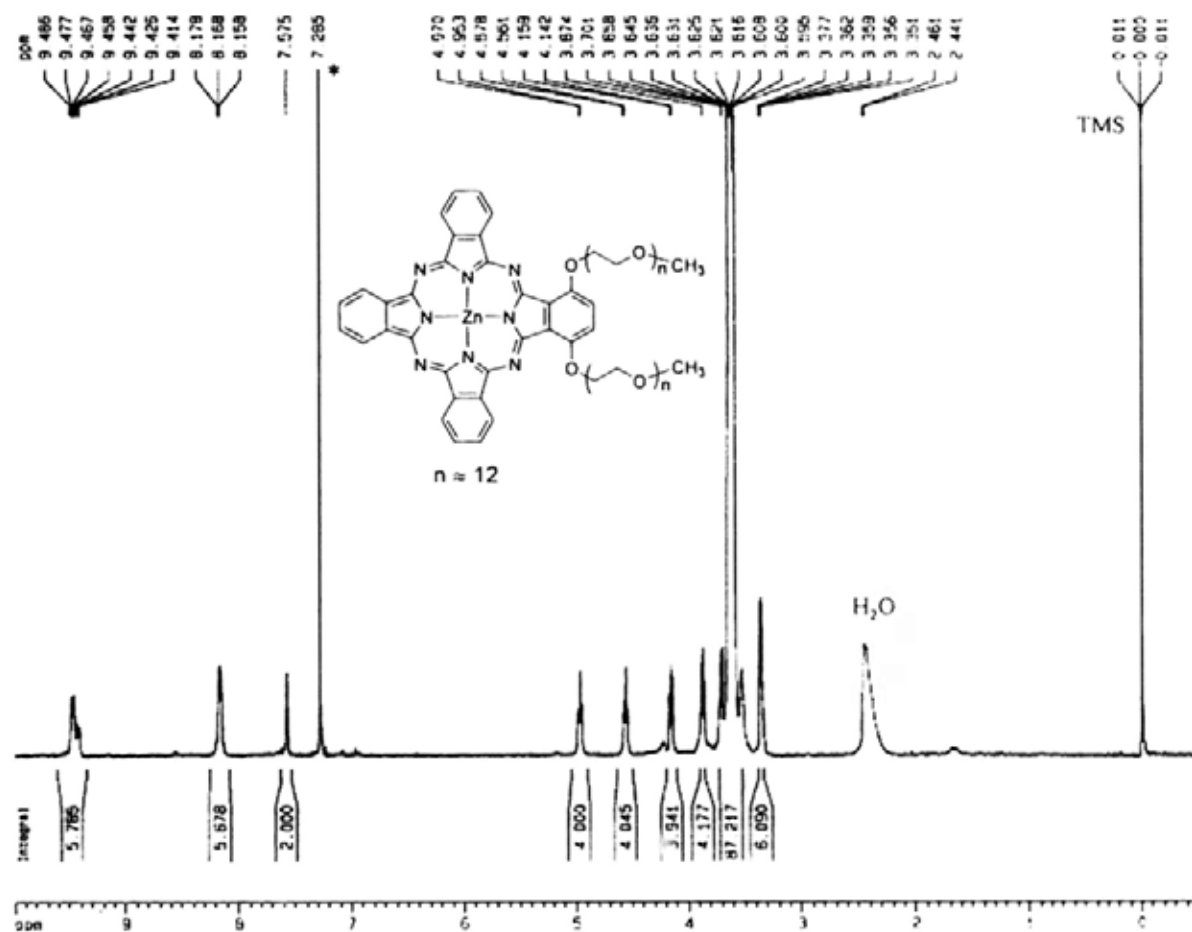
Appendix A-25 ^1H NMR (CDCl_3 with a trace amount of pyridine- d_5) and $^{13}\text{C}\{^1\text{H}\}$ NMR ($\text{DMSO}-d_6$) spectra of compound **4.3a**



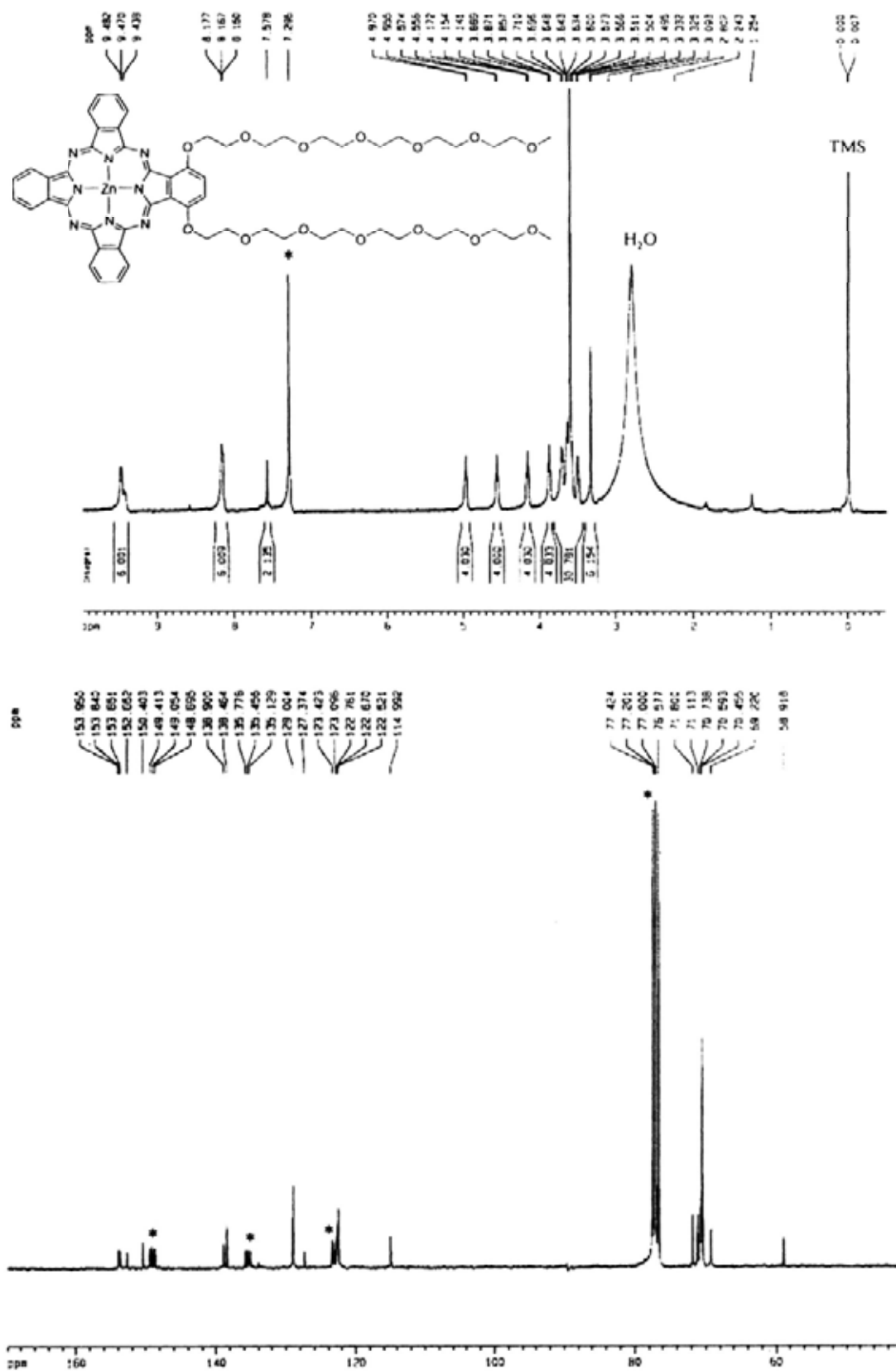
Appendix A-26 ^1H NMR and $^{13}\text{C}\{^1\text{H}\}$ NMR spectra of compound **4.3b** in CDCl_3 with a trace amount of pyridine- d_5



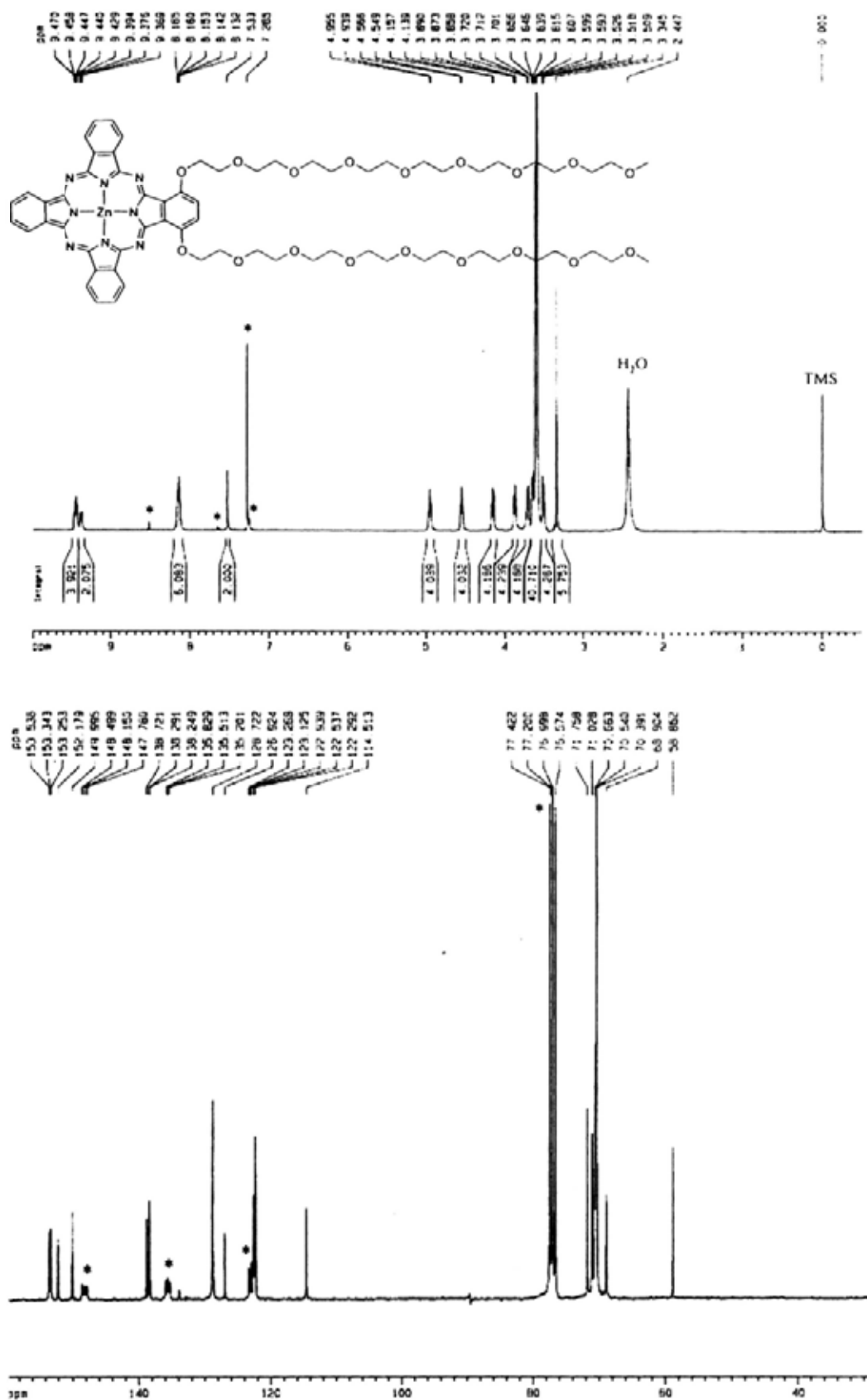
Appendix A-27 ^1H NMR spectrum of compound **4.3c** in CDCl_3 with a trace amount of pyridine- d_5



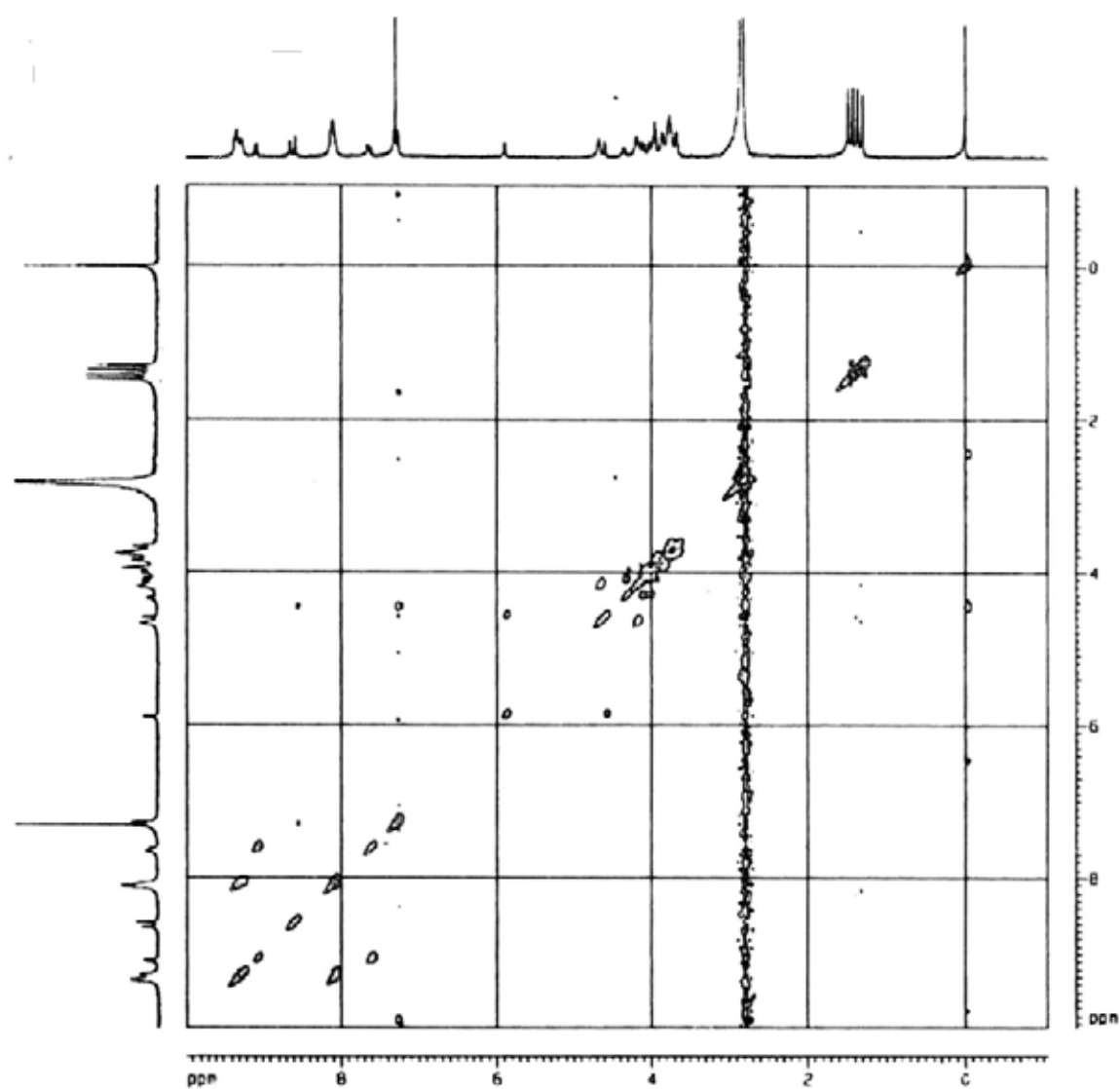
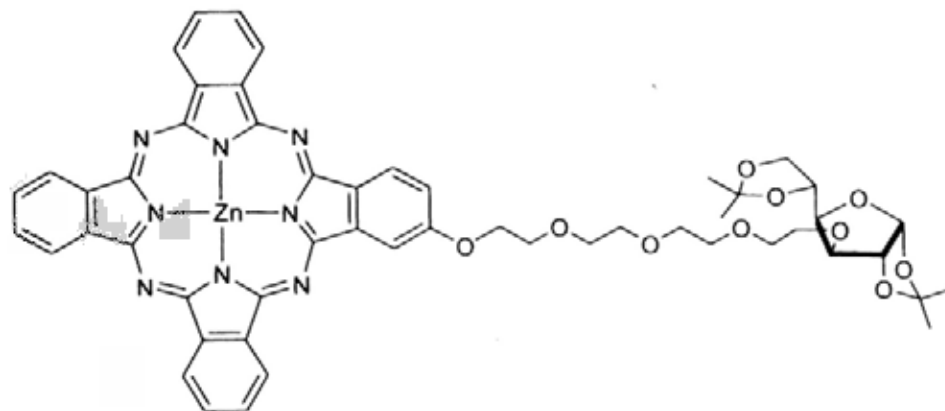
Appendix A-29 ^1H NMR and $^{13}\text{C}\{^1\text{H}\}$ NMR spectra of compound **4.3e** in CDCl_3 with a trace amount of pyridine- d_5

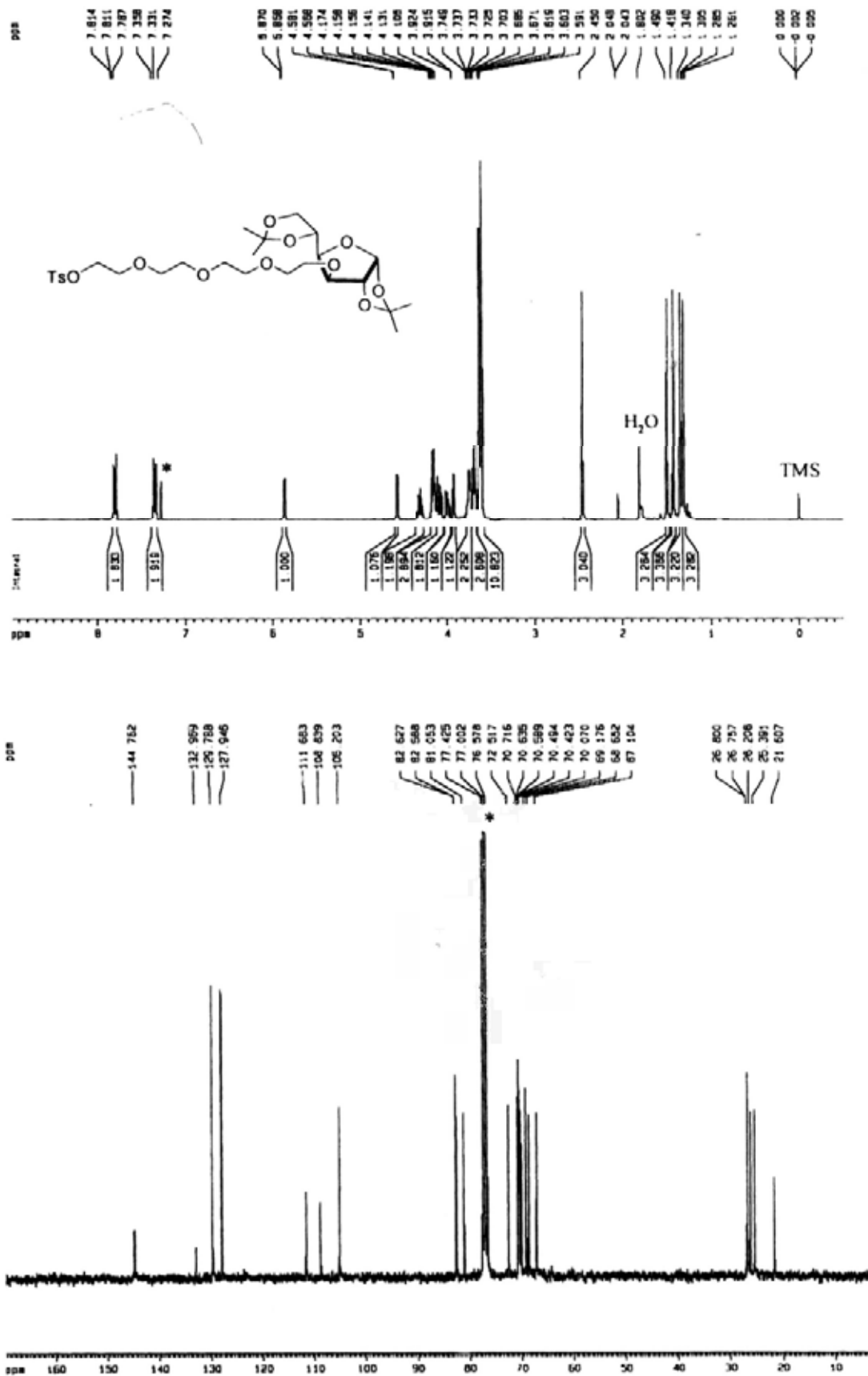


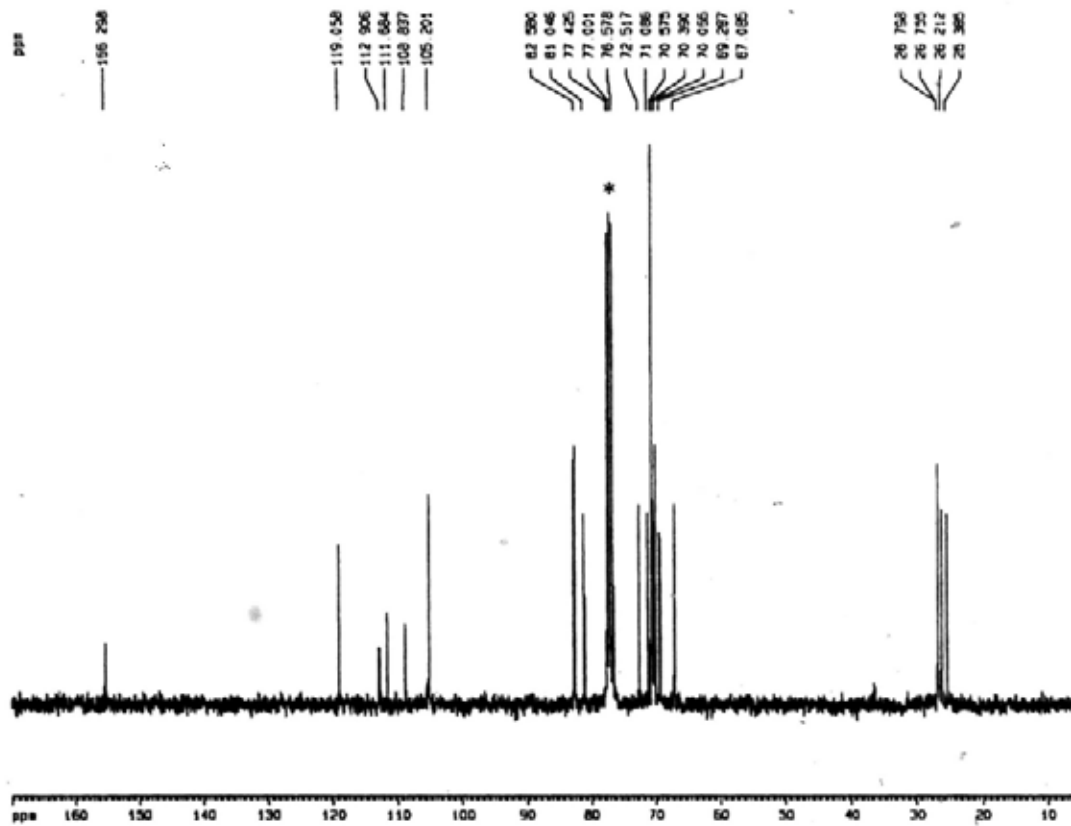
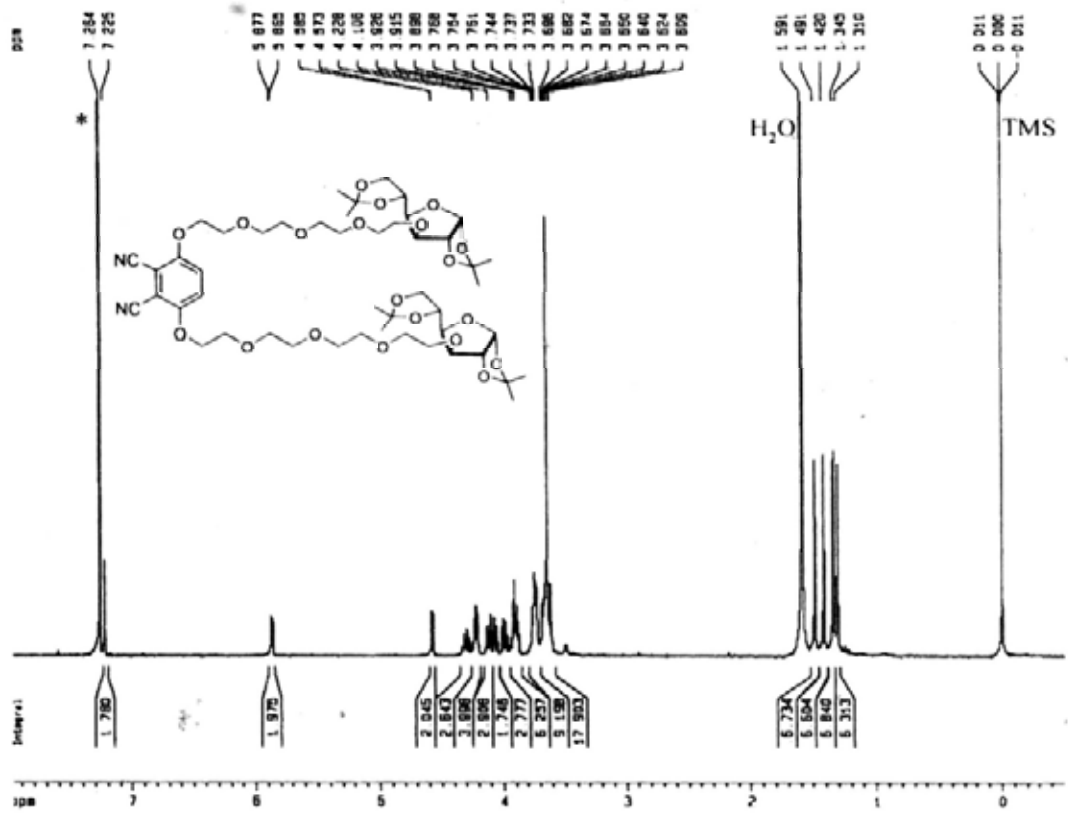
Appendix A-30 ^1H NMR and $^{13}\text{C}\{^1\text{H}\}$ NMR spectra of compound **4.3f** in CDCl_3 with a trace amount of pyridine- d_5



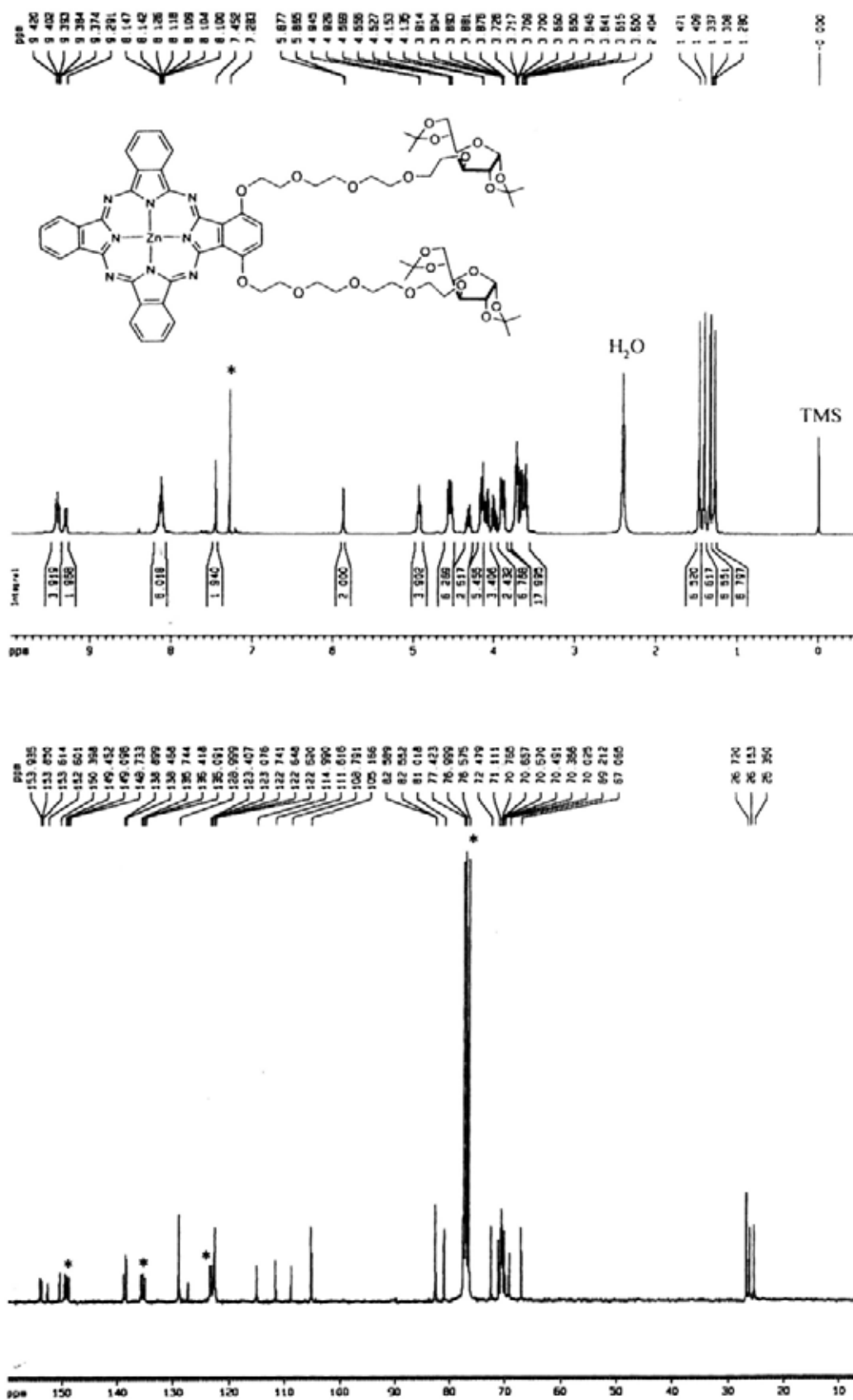
Appendix A-34 ^1H - ^1H COSY spectrum of 5.6 in CDCl_3 with a trace amount of pyridine- d_5

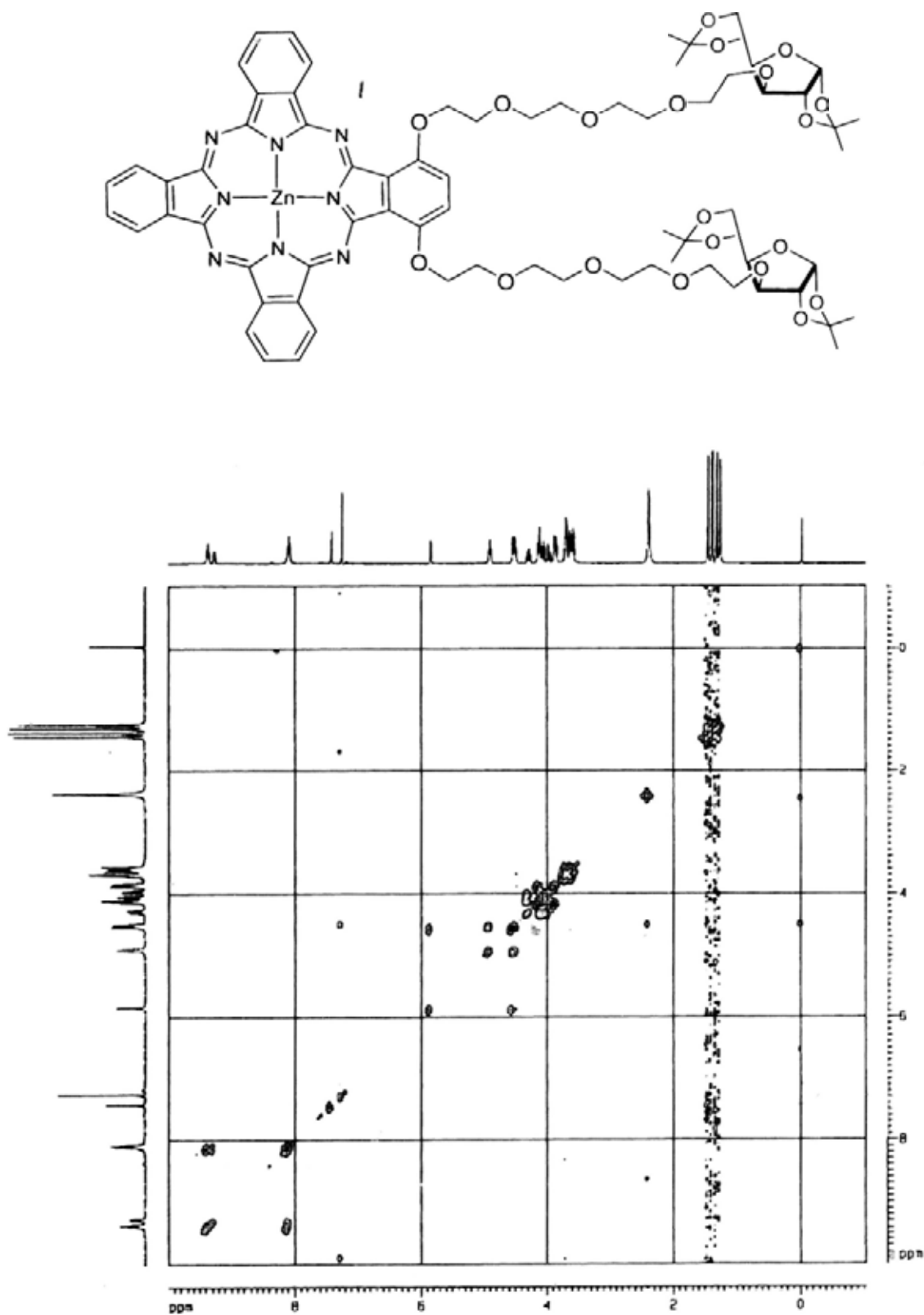


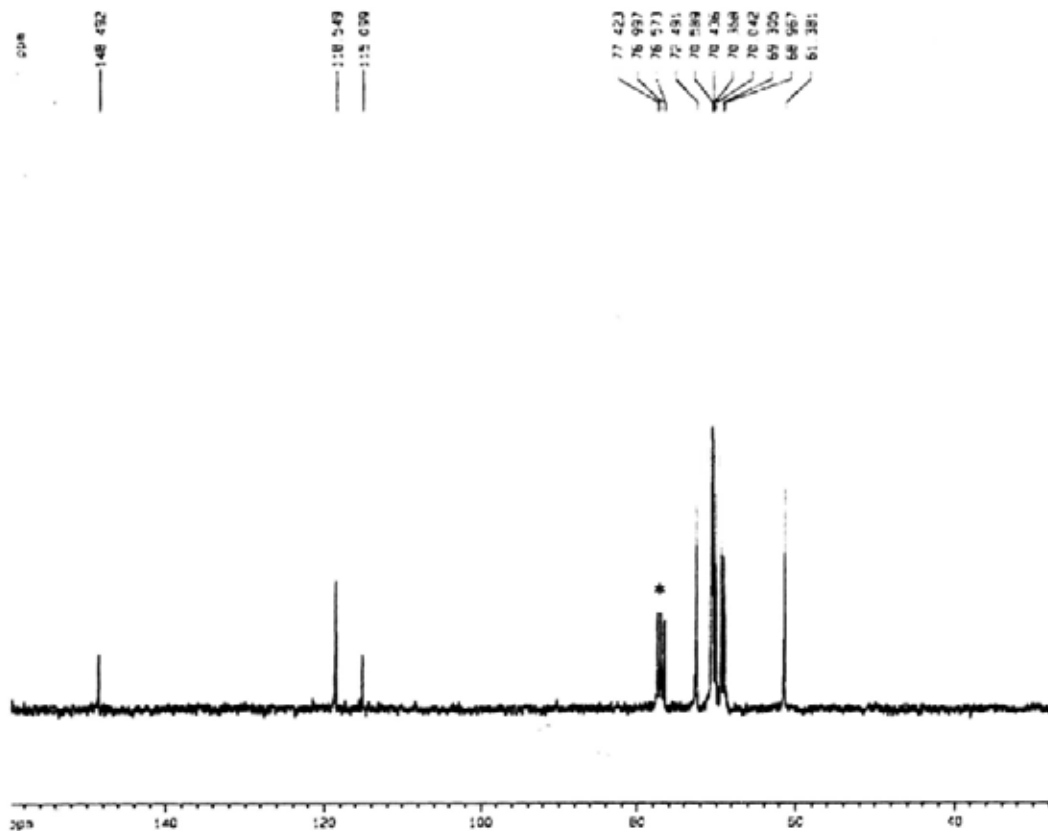
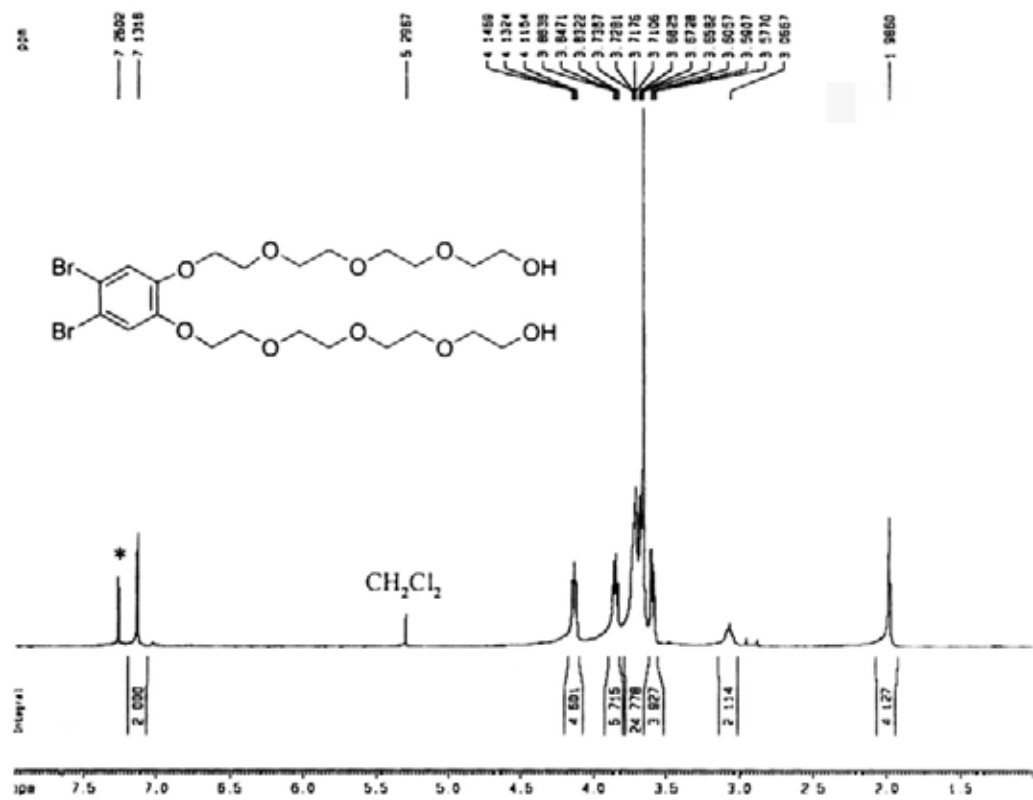
Appendix A-35 ^1H NMR and $^{13}\text{C}\{^1\text{H}\}$ NMR spectra of compound 5.7 in CDCl_3 

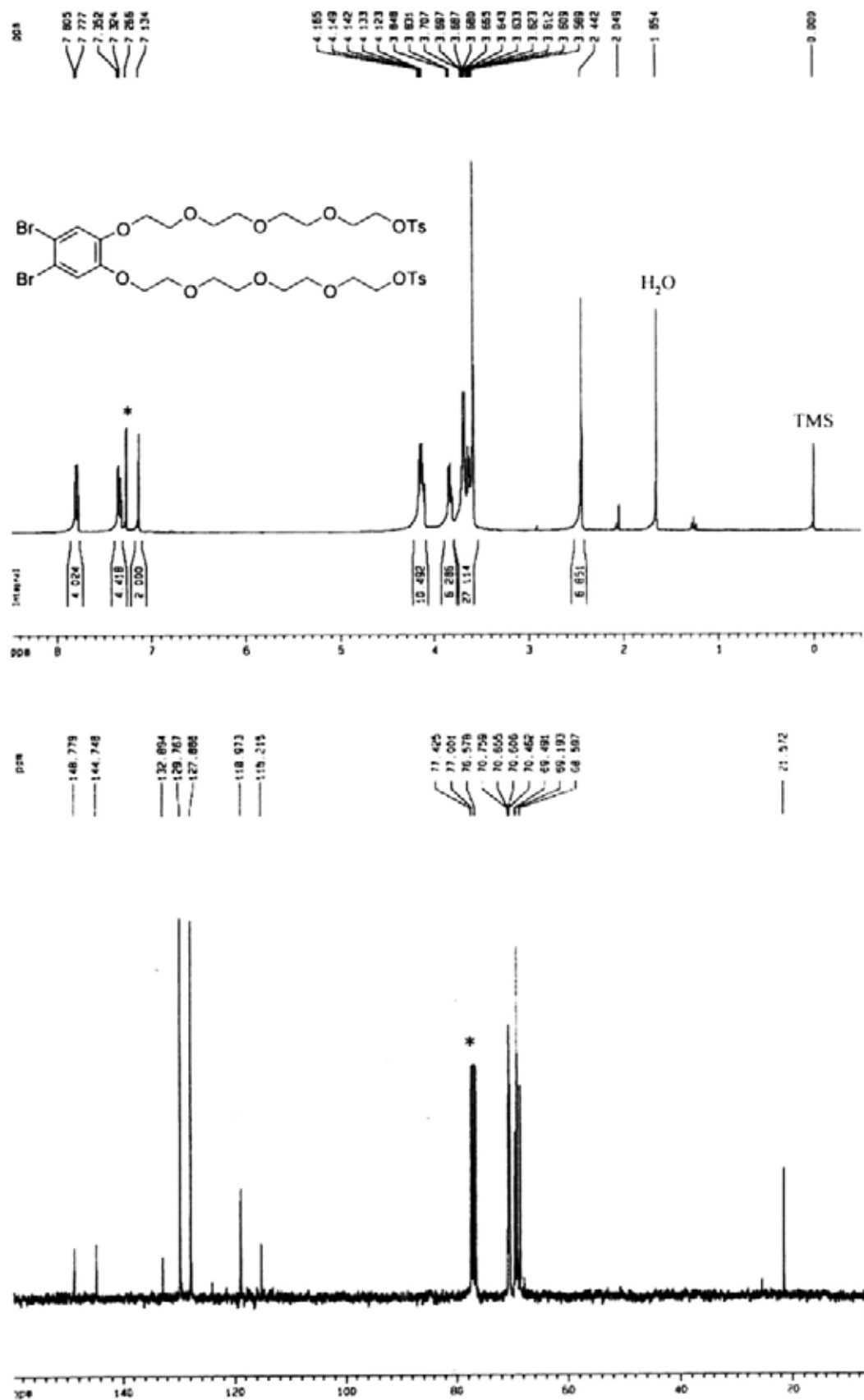
Appendix A-36 ^1H NMR and $^{13}\text{C}\{^1\text{H}\}$ NMR spectra of compound **5.8** in CDCl_3 

Appendix A-37 ^1H NMR and $^{13}\text{C}\{^1\text{H}\}$ NMR spectra of compound **5.9** in CDCl_3 with a trace amount of pyridine- d_5

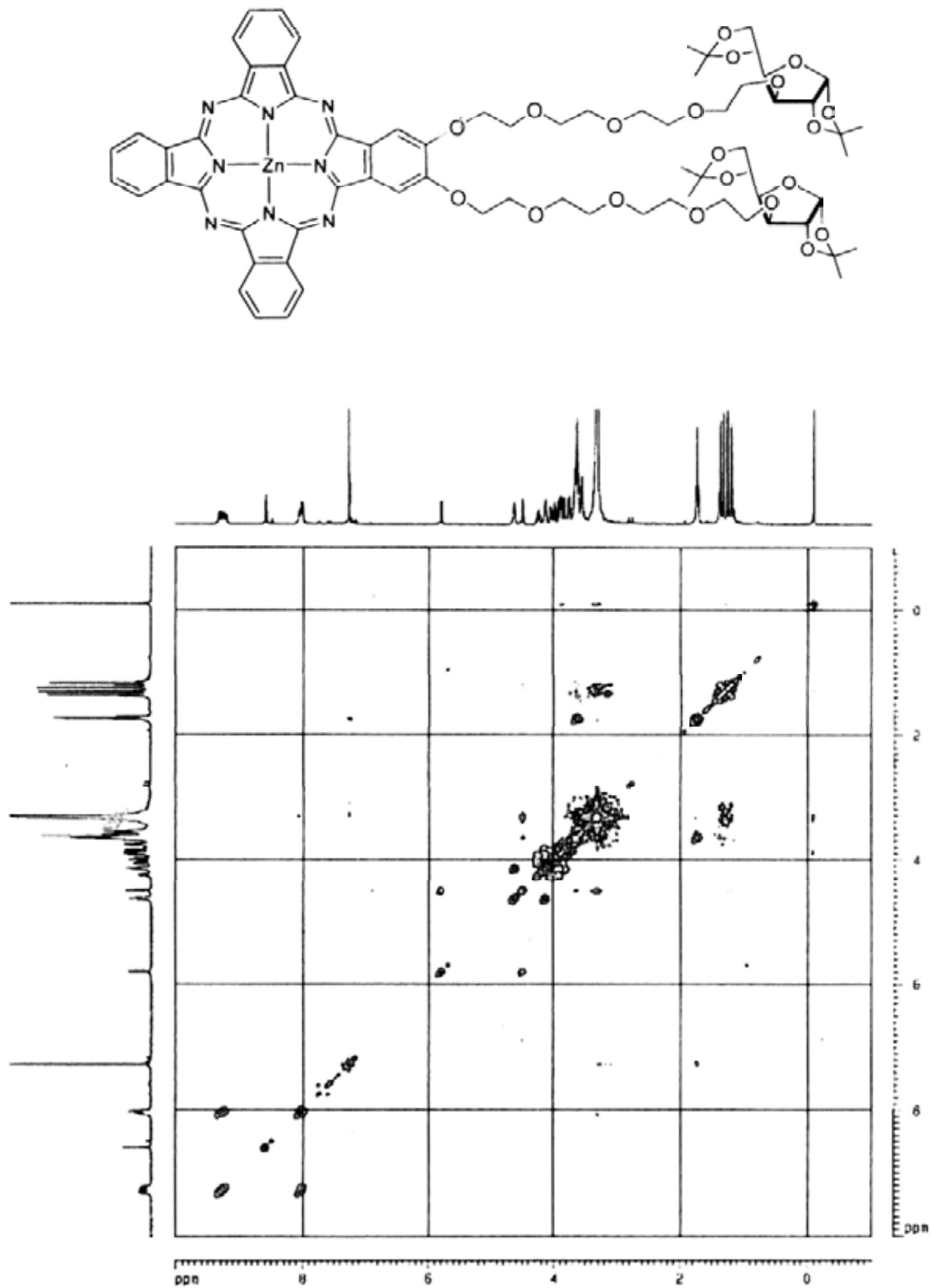


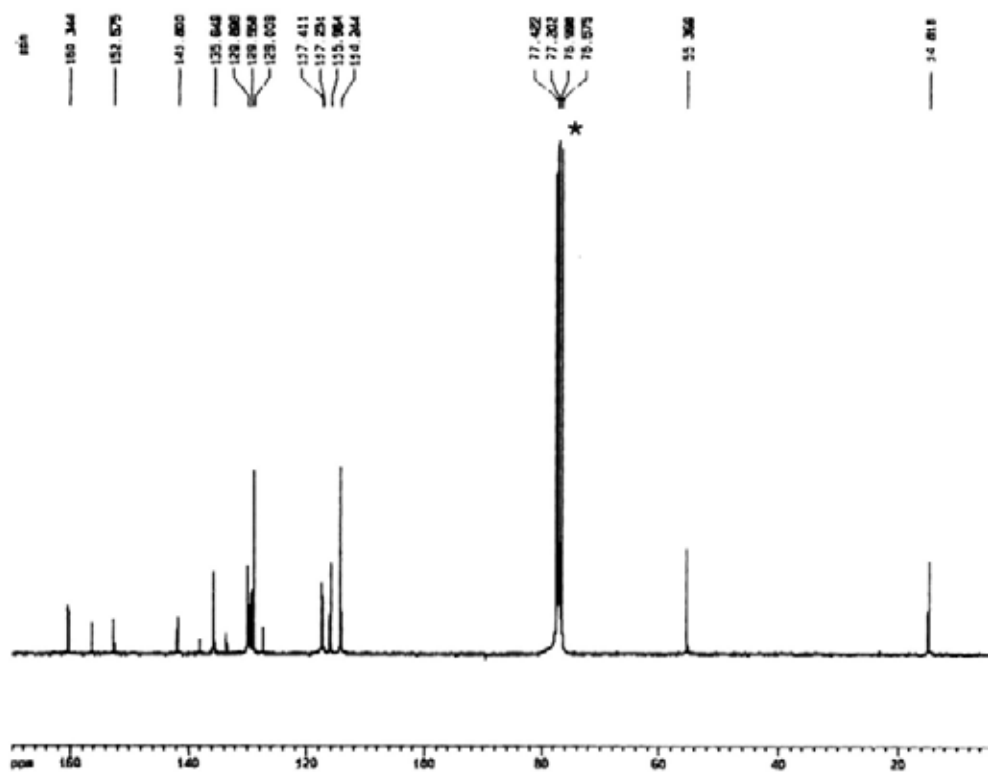
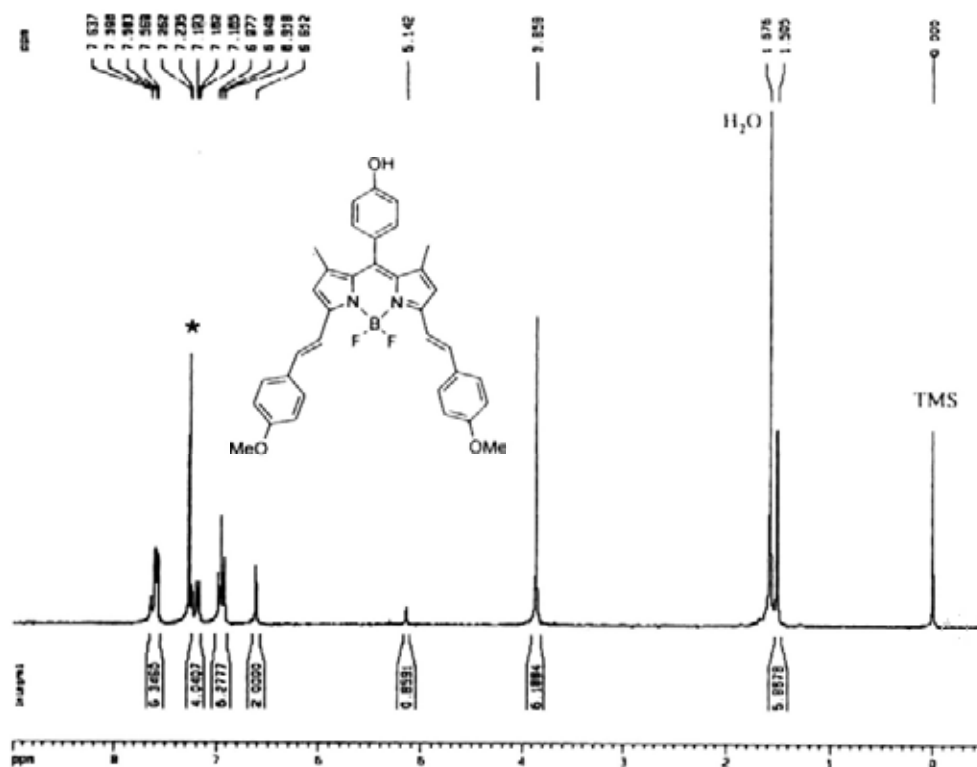
Appendix A-38 ^1H - ^1H COSY spectrum of **5.9** in CDCl_3 with a trace amount of pyridine- d_5 

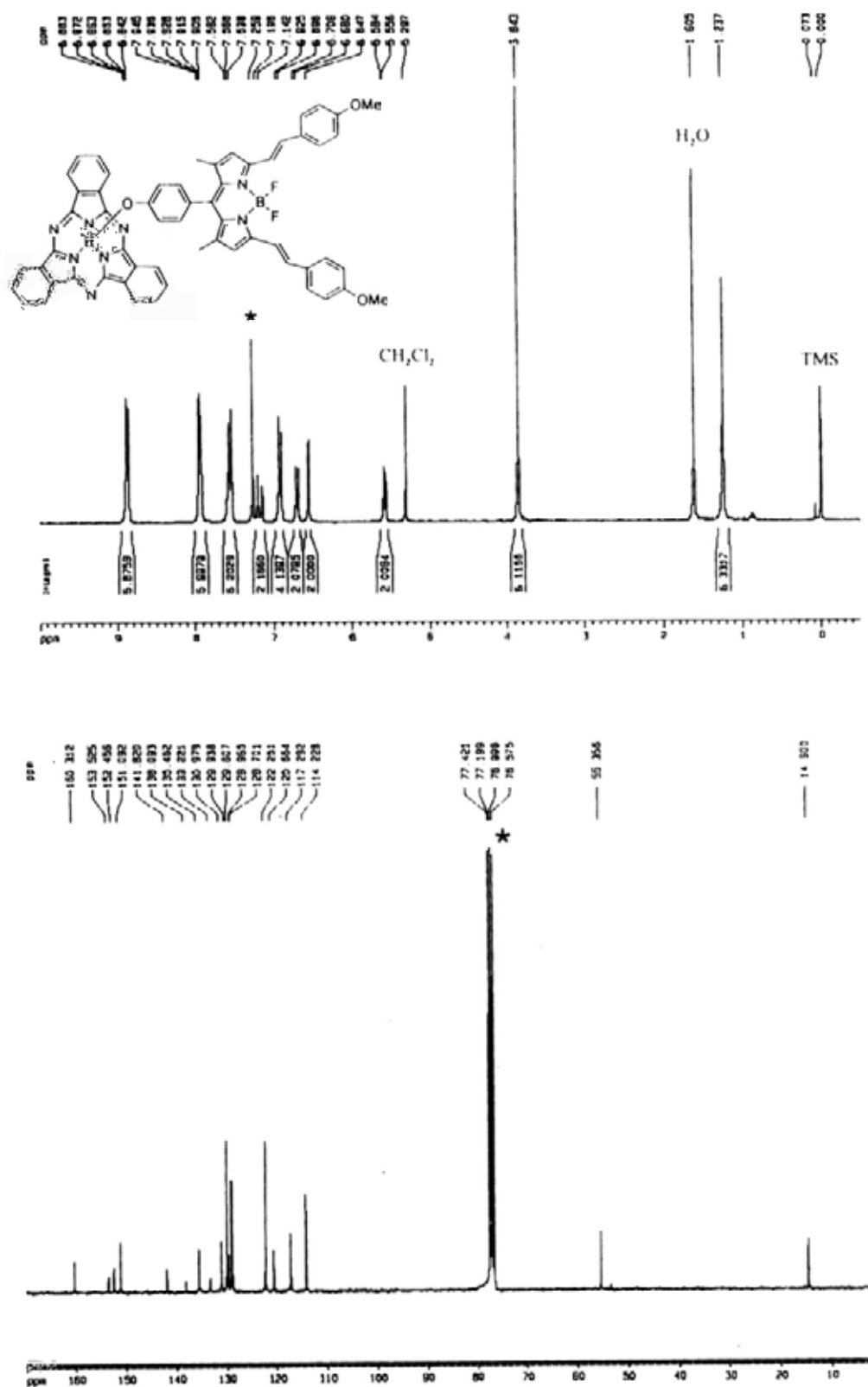
Appendix A-39 ^1H NMR and $^{13}\text{C}\{^1\text{H}\}$ NMR spectra of compound 5.12 in CDCl_3 

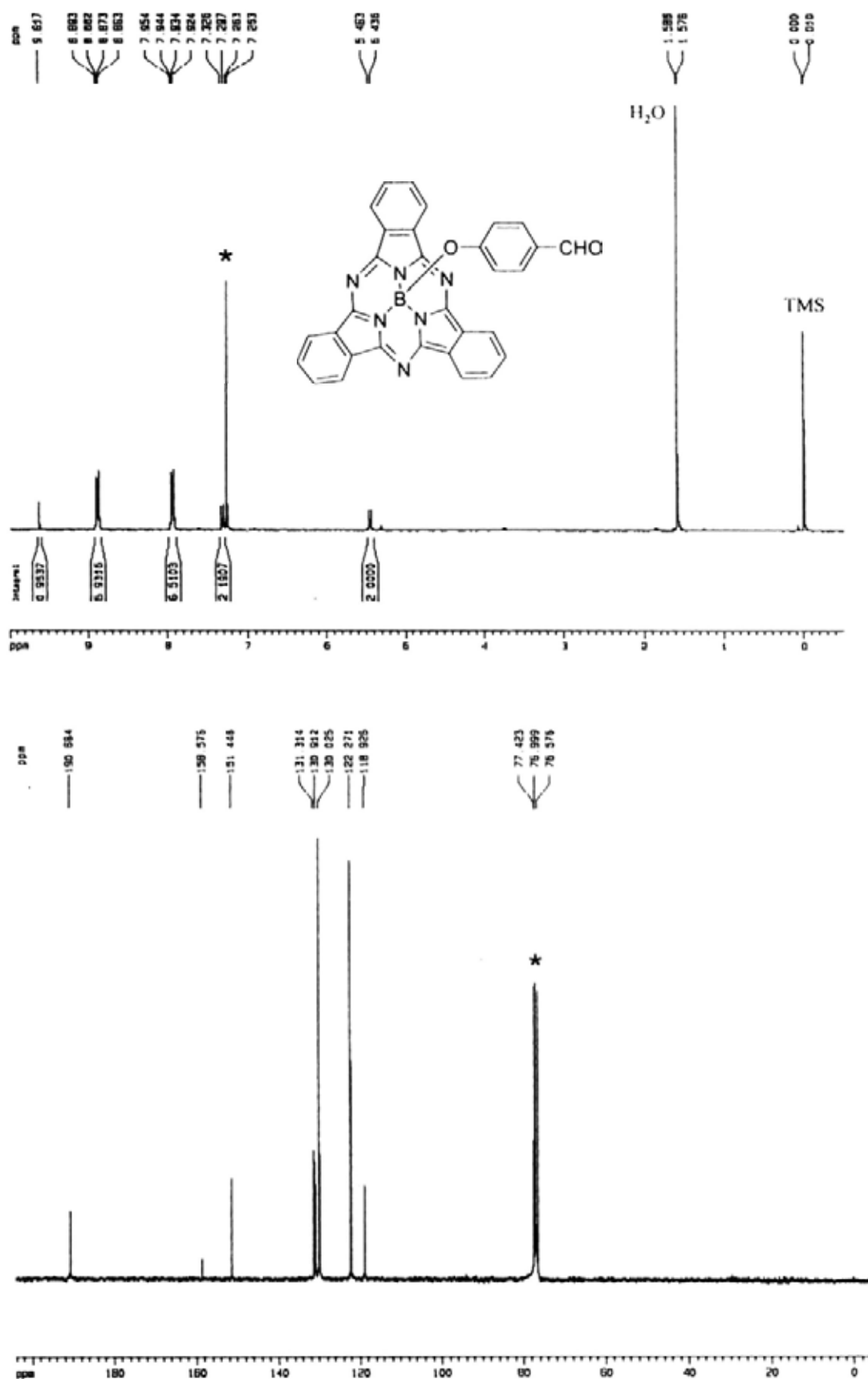
Appendix A-40 ^1H NMR and $^{13}\text{C}\{^1\text{H}\}$ NMR spectra of compound 5.13 in CDCl_3 

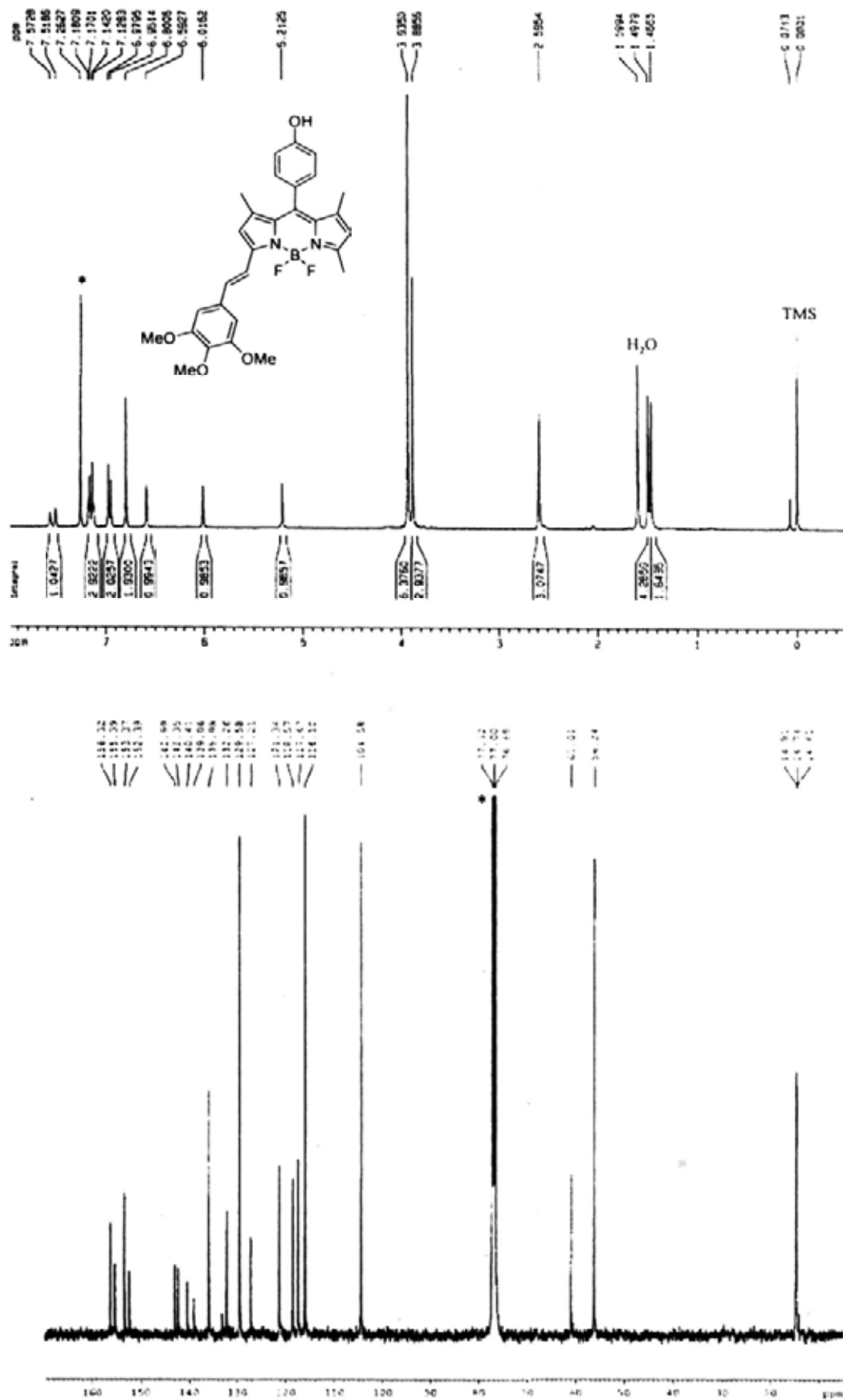
Appendix A-43 ^1H - ^1H COSY spectrum of **5.16** in CDCl_3 with a trace amount of pyridine- d_5

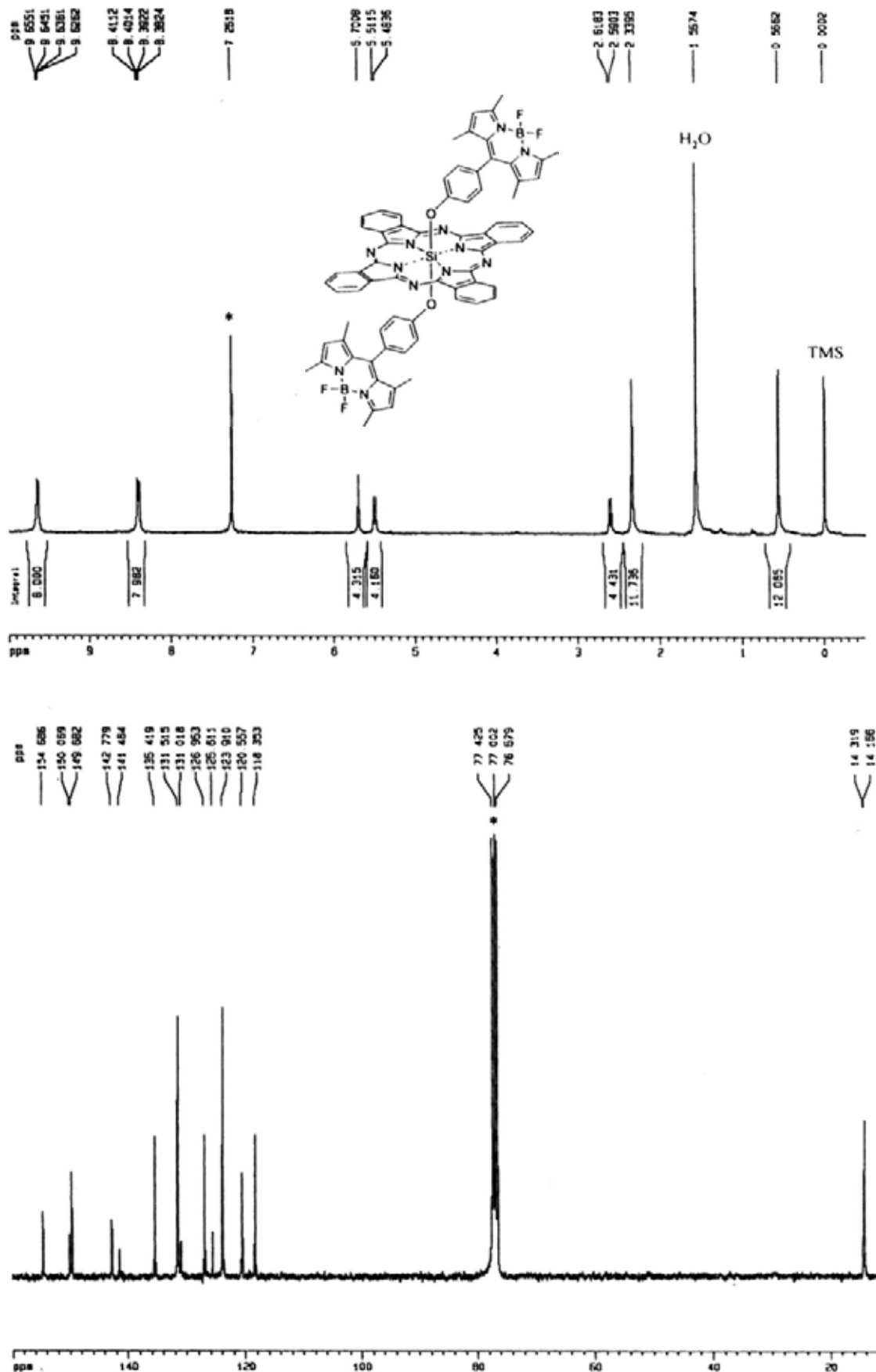


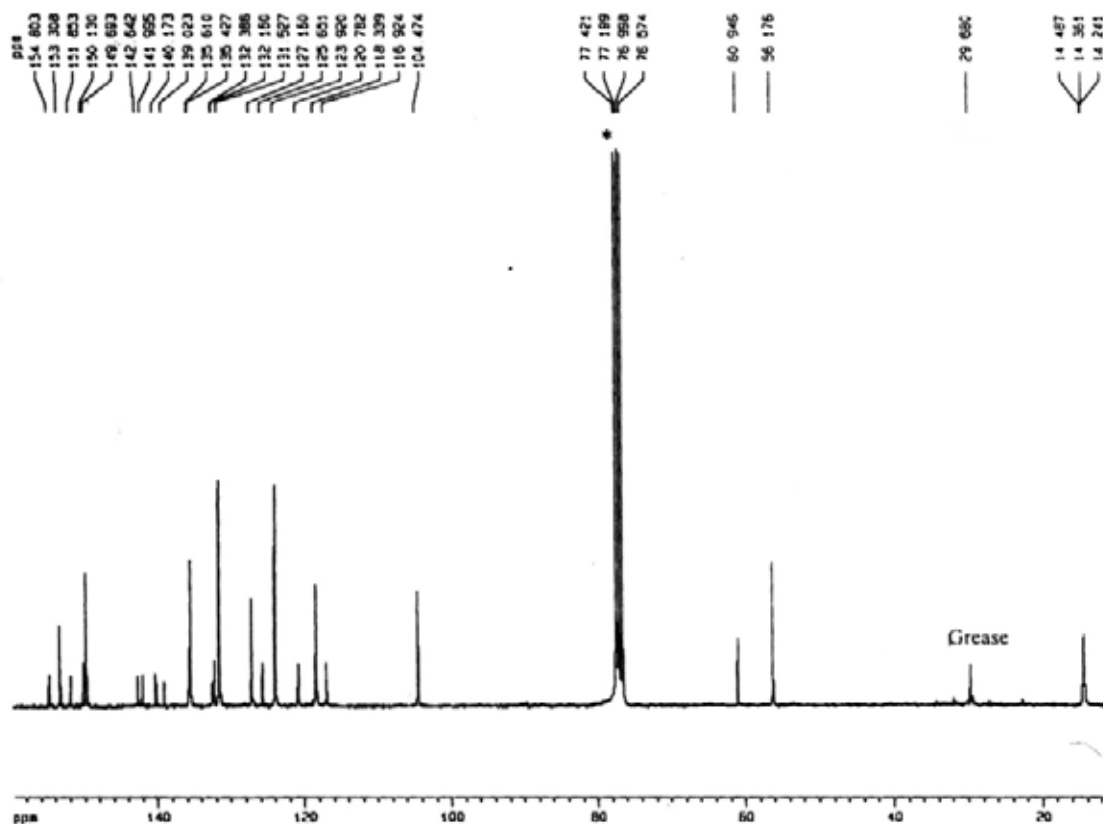
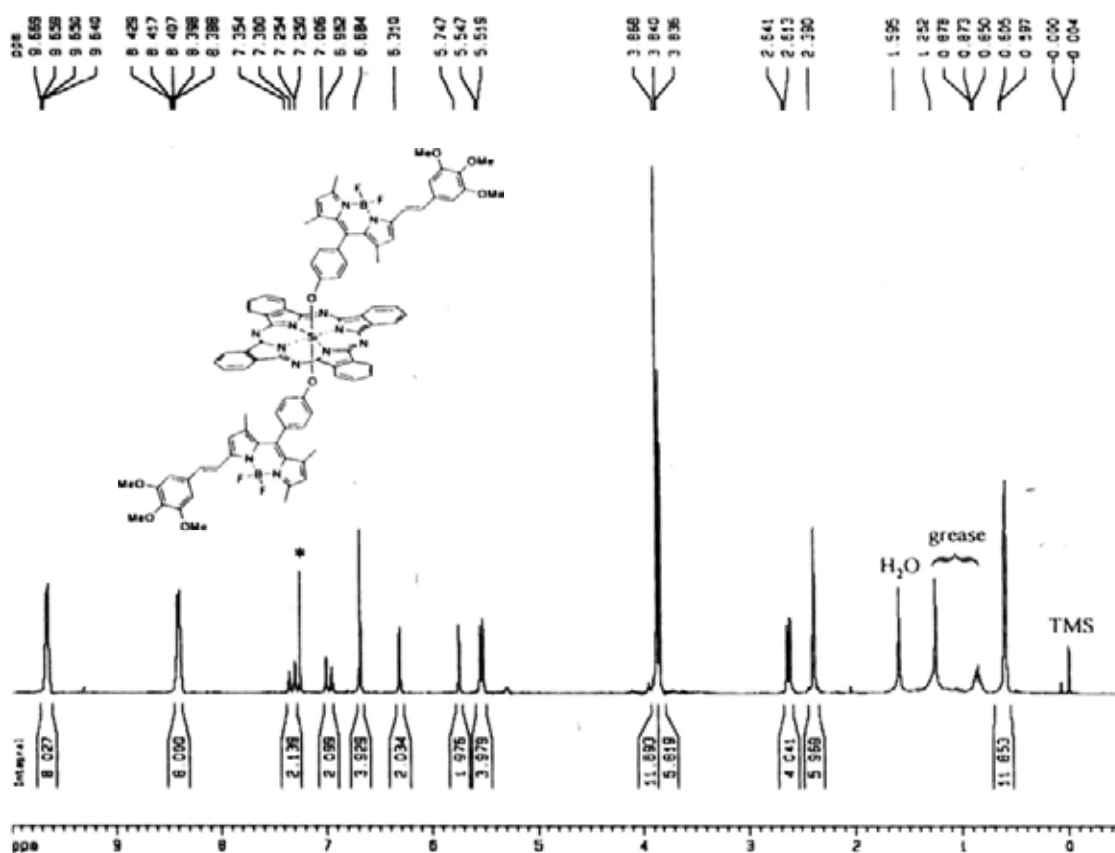
Appendix A-44 ^1H NMR and $^{13}\text{C}\{^1\text{H}\}$ NMR spectra of compound **6.2** in CDCl_3 

Appendix A-46 ^1H NMR and $^{13}\text{C}\{^1\text{H}\}$ NMR spectra of compound 6.5 in CDCl_3 

Appendix A-47 ^1H NMR and $^{13}\text{C}\{^1\text{H}\}$ NMR spectra of compound **6.6** in CDCl_3 

Appendix A-48 ^1H NMR and $^{13}\text{C}\{^1\text{H}\}$ NMR spectra of compound 7.4 in CDCl_3 

Appendix A-49 ^1H NMR and $^{13}\text{C}\{^1\text{H}\}$ NMR spectra of compound 7.2 in CDCl_3 

Appendix A-50 ^1H NMR and $^{13}\text{C}\{^1\text{H}\}$ NMR spectra of compound 7.5 in CDCl_3 

Appendix A-51 ^1H NMR and $^{13}\text{C}\{^1\text{H}\}$ NMR spectra of compound 7.7 in CDCl_3 

Appendix B-1 Crystallographic details of compound 6.2

Table 1. Crystal data and structure refinement for 6.2 (See Section 6.4.4 in Chapter 6).

Table 2. Atomic coordinates ($\times 10^4$) and equivalent isotropic displacement parameters ($\text{\AA}^2 \times 10^3$) for 6.2. $U(\text{eq})$ is defined as one third of the trace of the orthogonalized U_{ij} tensor.

| | x | y | z | U(eq) |
|-------|---------|---------|----------|--------|
| B(1) | 4010(3) | 3277(3) | 2783(2) | 56(1) |
| N(1) | 3891(2) | 3968(2) | 3491(2) | 58(1) |
| N(2) | 3505(2) | 2344(2) | 2992(1) | 51(1) |
| O(1) | 6893(2) | 7836(2) | 106(2) | 80(1) |
| O(2) | 2025(2) | 1595(2) | 7509(2) | 100(1) |
| O(3) | 5471(2) | 502(2) | -1901(2) | 87(1) |
| F(1) | 3610(2) | 3635(1) | 2037(1) | 88(1) |
| F(2) | 5057(2) | 3098(2) | 2711(1) | 86(1) |
| C(1) | 6777(4) | 7451(3) | -701(3) | 95(1) |
| C(2) | 6456(2) | 7355(2) | 732(2) | 61(1) |
| C(3) | 6082(3) | 6452(2) | 668(2) | 73(1) |
| C(4) | 5662(3) | 6050(2) | 1351(2) | 74(1) |
| C(5) | 5610(3) | 6538(2) | 2096(2) | 63(1) |
| C(6) | 5999(3) | 7438(2) | 2133(2) | 64(1) |
| C(7) | 6415(2) | 7845(2) | 1474(2) | 64(1) |
| C(8) | 5128(3) | 6135(2) | 2804(2) | 70(1) |
| C(9) | 4703(3) | 5305(3) | 2840(2) | 73(1) |
| C(10) | 4205(3) | 4882(2) | 3525(2) | 68(1) |
| C(11) | 3966(3) | 5254(3) | 4297(2) | 75(1) |
| C(12) | 3518(3) | 4570(2) | 4747(2) | 66(1) |
| C(13) | 3112(3) | 4710(3) | 5581(2) | 83(1) |
| C(14) | 3465(2) | 3744(2) | 4237(2) | 56(1) |
| C(15) | 3119(2) | 2826(2) | 4371(2) | 54(1) |
| C(16) | 2798(2) | 2554(2) | 5205(2) | 57(1) |
| C(17) | 1800(3) | 2576(3) | 5401(2) | 83(1) |
| C(18) | 1523(3) | 2271(3) | 6167(2) | 89(1) |
| C(19) | 2267(3) | 1934(3) | 6749(2) | 70(1) |
| C(20) | 3260(2) | 1927(2) | 6570(2) | 65(1) |
| C(21) | 3528(2) | 2242(2) | 5811(2) | 61(1) |
| C(22) | 3125(2) | 2133(2) | 3760(2) | 52(1) |
| C(23) | 2819(2) | 1159(2) | 3736(2) | 59(1) |
| C(24) | 2319(3) | 587(2) | 4372(2) | 74(1) |
| C(25) | 3037(2) | 809(2) | 2972(2) | 61(1) |
| C(26) | 3458(2) | 1547(2) | 2519(2) | 55(1) |
| C(27) | 3813(2) | 1525(2) | 1693(2) | 59(1) |
| C(28) | 4107(2) | 740(2) | 1317(2) | 63(1) |

| | | | | |
|-------|---------|---------|----------|--------|
| C(29) | 4467(2) | 683(2) | 484(2) | 58(1) |
| C(30) | 5054(3) | -76(2) | 264(2) | 69(1) |
| C(31) | 5421(3) | -163(2) | -509(2) | 71(1) |
| C(32) | 5169(3) | 526(2) | -1107(2) | 66(1) |
| C(33) | 4579(3) | 1278(2) | -910(2) | 69(1) |
| C(34) | 4245(3) | 1371(2) | -125(2) | 64(1) |
| C(35) | 6166(4) | -229(3) | -2108(2) | 102(1) |

Table 3. Bond lengths [Å] and angles [°] for **6.2**.

| | | | |
|------------------|----------|------------------|----------|
| B(1)-F(1) | 1.372(4) | B(1)-F(2) | 1.413(4) |
| B(1)-N(1) | 1.519(5) | B(1)-N(2) | 1.523(4) |
| N(1)-C(10) | 1.354(4) | N(1)-C(14) | 1.401(4) |
| N(2)-C(26) | 1.358(4) | N(2)-C(22) | 1.403(4) |
| O(1)-C(2) | 1.377(4) | O(1)-C(1) | 1.407(4) |
| O(2)-C(19) | 1.375(4) | O(3)-C(32) | 1.370(4) |
| O(3)-C(35) | 1.434(5) | C(2)-C(3) | 1.368(5) |
| C(2)-C(7) | 1.386(4) | C(3)-C(4) | 1.389(5) |
| C(4)-C(5) | 1.391(5) | C(5)-C(6) | 1.369(4) |
| C(5)-C(8) | 1.462(5) | C(6)-C(7) | 1.358(5) |
| C(8)-C(9) | 1.300(5) | C(9)-C(10) | 1.455(5) |
| C(10)-C(11) | 1.408(5) | C(11)-C(12) | 1.369(5) |
| C(12)-C(14) | 1.425(4) | C(12)-C(13) | 1.497(5) |
| C(14)-C(15) | 1.396(4) | C(15)-C(22) | 1.388(4) |
| C(15)-C(16) | 1.489(4) | C(16)-C(17) | 1.374(5) |
| C(16)-C(21) | 1.388(4) | C(17)-C(18) | 1.383(5) |
| C(18)-C(19) | 1.387(5) | C(19)-C(20) | 1.358(4) |
| C(20)-C(21) | 1.373(4) | C(22)-C(23) | 1.433(4) |
| C(23)-C(25) | 1.376(5) | C(23)-C(24) | 1.496(4) |
| C(25)-C(26) | 1.410(4) | C(26)-C(27) | 1.444(4) |
| C(27)-C(28) | 1.334(4) | C(28)-C(29) | 1.459(4) |
| C(29)-C(30) | 1.383(4) | C(29)-C(34) | 1.395(4) |
| C(30)-C(31) | 1.375(4) | C(31)-C(32) | 1.391(5) |
| C(32)-C(33) | 1.366(5) | C(33)-C(34) | 1.378(5) |
| F(1)-B(1)-F(2) | 107.7(3) | F(1)-B(1)-N(1) | 111.6(3) |
| F(2)-B(1)-N(1) | 109.4(2) | F(1)-B(1)-N(2) | 111.6(3) |
| F(2)-B(1)-N(2) | 107.9(3) | N(1)-B(1)-N(2) | 108.5(3) |
| C(10)-N(1)-C(14) | 108.7(3) | C(10)-N(1)-B(1) | 126.4(3) |
| C(14)-N(1)-B(1) | 124.8(3) | C(26)-N(2)-C(22) | 108.4(2) |
| C(26)-N(2)-B(1) | 126.4(3) | C(22)-N(2)-B(1) | 124.7(2) |
| C(2)-O(1)-C(1) | 117.8(3) | C(32)-O(3)-C(35) | 118.1(3) |
| C(3)-C(2)-O(1) | 124.9(3) | C(3)-C(2)-C(7) | 119.5(3) |
| O(1)-C(2)-C(7) | 115.7(3) | C(2)-C(3)-C(4) | 118.9(3) |
| C(3)-C(4)-C(5) | 122.0(3) | C(6)-C(5)-C(4) | 117.0(3) |

| | | | |
|-------------------|----------|-------------------|----------|
| C(6)-C(5)-C(8) | 120.7(3) | C(4)-C(5)-C(8) | 122.2(3) |
| C(7)-C(6)-C(5) | 122.0(3) | C(6)-C(7)-C(2) | 120.6(3) |
| C(9)-C(8)-C(5) | 126.8(3) | C(8)-C(9)-C(10) | 128.6(4) |
| N(1)-C(10)-C(11) | 107.7(3) | N(1)-C(10)-C(9) | 121.0(3) |
| C(11)-C(10)-C(9) | 131.4(3) | C(12)-C(11)-C(10) | 109.8(3) |
| C(11)-C(12)-C(14) | 106.0(3) | C(11)-C(12)-C(13) | 125.5(3) |
| C(14)-C(12)-C(13) | 128.5(3) | C(15)-C(14)-N(1) | 119.9(3) |
| C(15)-C(14)-C(12) | 132.2(3) | N(1)-C(14)-C(12) | 107.8(3) |
| C(22)-C(15)-C(14) | 121.6(3) | C(22)-C(15)-C(16) | 118.5(3) |
| C(14)-C(15)-C(16) | 119.8(3) | C(17)-C(16)-C(21) | 117.9(3) |
| C(17)-C(16)-C(15) | 122.8(3) | C(21)-C(16)-C(15) | 119.3(3) |
| C(16)-C(17)-C(18) | 121.3(3) | C(17)-C(18)-C(19) | 119.4(3) |
| C(20)-C(19)-O(2) | 118.5(3) | C(20)-C(19)-C(18) | 120.0(3) |
| O(2)-C(19)-C(18) | 121.5(3) | C(19)-C(20)-C(21) | 120.1(3) |
| C(20)-C(21)-C(16) | 121.3(3) | C(15)-C(22)-N(2) | 119.9(3) |
| C(15)-C(22)-C(23) | 132.8(3) | N(2)-C(22)-C(23) | 107.3(2) |
| C(25)-C(23)-C(22) | 107.0(3) | C(25)-C(23)-C(24) | 123.5(3) |
| C(22)-C(23)-C(24) | 129.5(3) | C(23)-C(25)-C(26) | 108.4(3) |
| N(2)-C(26)-C(25) | 108.9(3) | N(2)-C(26)-C(27) | 122.1(3) |
| C(25)-C(26)-C(27) | 129.0(3) | C(28)-C(27)-C(26) | 124.1(3) |
| C(27)-C(28)-C(29) | 126.1(3) | C(30)-C(29)-C(34) | 116.6(3) |
| C(30)-C(29)-C(28) | 120.4(3) | C(34)-C(29)-C(28) | 123.0(3) |
| C(31)-C(30)-C(29) | 122.9(3) | C(30)-C(31)-C(32) | 118.9(3) |
| C(33)-C(32)-O(3) | 116.5(3) | C(33)-C(32)-C(31) | 119.5(3) |
| O(3)-C(32)-C(31) | 124.0(3) | C(32)-C(33)-C(34) | 120.8(3) |
| C(33)-C(34)-C(29) | 121.2(3) | | |

Table 4. Anisotropic displacement parameters ($\text{\AA}^2 \times 10^3$) for **6.2**. The anisotropic displacement factor exponent takes the form: $-2 \pi^2[(ha^*)^2 U_{11} + \dots + 2hka^*b^* U_{12}]$.

| | U11 | U22 | U33 | U23 | U13 | U12 |
|------|--------|--------|-------|--------|--------|--------|
| B(1) | 53(2) | 64(2) | 51(2) | 3(2) | 4(2) | -11(2) |
| N(1) | 57(2) | 61(2) | 57(2) | 4(1) | 10(1) | -3(1) |
| N(2) | 52(2) | 54(1) | 48(2) | 4(1) | 7(1) | 1(1) |
| O(1) | 88(2) | 75(2) | 78(2) | 7(1) | 11(1) | -4(1) |
| O(2) | 81(2) | 161(3) | 60(2) | 41(2) | 20(1) | 26(2) |
| O(3) | 111(2) | 90(2) | 62(2) | 4(1) | 15(1) | 4(2) |
| F(1) | 124(2) | 78(1) | 58(1) | 18(1) | -19(1) | -30(1) |
| F(2) | 65(1) | 103(2) | 94(2) | -18(1) | 34(1) | -17(1) |
| C(1) | 105(4) | 100(3) | 79(3) | 9(2) | 10(2) | 11(2) |
| C(2) | 49(2) | 60(2) | 75(2) | 5(2) | 4(2) | 3(1) |
| C(3) | 73(2) | 64(2) | 81(3) | -11(2) | 11(2) | -2(2) |
| C(4) | 74(2) | 53(2) | 96(3) | -5(2) | 10(2) | -12(2) |
| C(5) | 55(2) | 58(2) | 75(2) | -1(2) | 3(2) | -1(2) |

| | | | | | | |
|-------|--------|--------|-------|--------|-------|--------|
| C(6) | 62(2) | 58(2) | 72(2) | -4(2) | -5(2) | -2(2) |
| C(7) | 56(2) | 53(2) | 83(3) | -1(2) | -2(2) | -4(1) |
| C(8) | 70(2) | 63(2) | 77(2) | -5(2) | -1(2) | -5(2) |
| C(9) | 78(2) | 66(2) | 76(2) | 5(2) | 4(2) | -10(2) |
| C(10) | 71(2) | 65(2) | 67(2) | 4(2) | 3(2) | -4(2) |
| C(11) | 88(3) | 60(2) | 78(3) | -12(2) | 1(2) | 4(2) |
| C(12) | 65(2) | 73(2) | 59(2) | -5(2) | 3(2) | 9(2) |
| C(13) | 92(3) | 93(3) | 64(2) | -14(2) | 14(2) | 18(2) |
| C(14) | 51(2) | 66(2) | 52(2) | 9(2) | 8(1) | 7(1) |
| C(15) | 40(2) | 71(2) | 51(2) | 11(2) | 5(1) | 8(1) |
| C(16) | 50(2) | 74(2) | 47(2) | 9(1) | 9(1) | 10(2) |
| C(17) | 49(2) | 140(4) | 61(2) | 28(2) | 11(2) | 28(2) |
| C(18) | 49(2) | 152(4) | 69(2) | 35(2) | 22(2) | 29(2) |
| C(19) | 61(2) | 99(3) | 51(2) | 14(2) | 13(2) | 15(2) |
| C(20) | 49(2) | 93(2) | 53(2) | 16(2) | 5(1) | 12(2) |
| C(21) | 41(2) | 85(2) | 59(2) | 7(2) | 8(1) | 6(1) |
| C(22) | 45(2) | 61(2) | 51(2) | 11(2) | 5(1) | 4(1) |
| C(23) | 50(2) | 65(2) | 61(2) | 17(2) | 4(2) | -1(1) |
| C(24) | 64(2) | 80(2) | 78(2) | 24(2) | 11(2) | -5(2) |
| C(25) | 62(2) | 57(2) | 65(2) | 8(2) | 1(2) | 0(2) |
| C(26) | 55(2) | 57(2) | 55(2) | 6(2) | 4(1) | 0(1) |
| C(27) | 58(2) | 66(2) | 54(2) | 1(2) | 2(2) | -3(2) |
| C(28) | 68(2) | 60(2) | 59(2) | 3(2) | -1(2) | -5(2) |
| C(29) | 59(2) | 55(2) | 58(2) | -4(1) | -2(2) | -2(1) |
| C(30) | 83(3) | 64(2) | 59(2) | 6(2) | -1(2) | 5(2) |
| C(31) | 80(3) | 70(2) | 64(2) | 1(2) | 5(2) | 10(2) |
| C(32) | 77(2) | 68(2) | 51(2) | -5(2) | 3(2) | -7(2) |
| C(33) | 84(3) | 63(2) | 57(2) | 4(2) | -6(2) | 2(2) |
| C(34) | 71(2) | 58(2) | 62(2) | 1(2) | -2(2) | 1(2) |
| C(35) | 116(4) | 122(3) | 71(3) | -7(2) | 22(2) | 24(3) |

Table 5. Hydrogen coordinates ($\times 10^4$) and isotropic displacement parameters ($\text{\AA}^2 \times 10^3$) for **6.2**.

| | x | y | z | U(eq) |
|--------|------|------|-------|-------|
| H(2A) | 2548 | 1424 | 7778 | 150 |
| H(1A) | 7121 | 7846 | -1075 | 142 |
| H(1B) | 6065 | 7418 | -881 | 142 |
| H(1C) | 7065 | 6826 | -697 | 142 |
| H(3A) | 6108 | 6112 | 176 | 87 |
| H(4A) | 5407 | 5436 | 1309 | 89 |
| H(6A) | 5977 | 7782 | 2624 | 77 |
| H(7A) | 6674 | 8457 | 1521 | 77 |
| H(8A) | 5125 | 6510 | 3278 | 84 |
| H(9A) | 4720 | 4934 | 2365 | 88 |
| H(11A) | 4093 | 5873 | 4474 | 90 |
| H(13A) | 3272 | 5340 | 5776 | 124 |
| H(13B) | 3419 | 4257 | 5968 | 124 |
| H(13C) | 2386 | 4625 | 5535 | 124 |
| H(17A) | 1301 | 2801 | 5011 | 100 |
| H(18A) | 844 | 2291 | 6291 | 107 |
| H(20A) | 3759 | 1708 | 6963 | 78 |
| H(21A) | 4212 | 2247 | 5701 | 74 |
| H(24A) | 2207 | -47 | 4170 | 111 |
| H(24B) | 1677 | 870 | 4477 | 111 |
| H(24C) | 2752 | 571 | 4879 | 111 |
| H(25A) | 2926 | 191 | 2787 | 74 |
| H(27A) | 3837 | 2095 | 1404 | 71 |
| H(28A) | 4080 | 177 | 1614 | 75 |
| H(30A) | 5208 | -549 | 655 | 82 |
| H(31A) | 5832 | -674 | -630 | 86 |
| H(33A) | 4401 | 1734 | -1312 | 82 |
| H(34A) | 3866 | 1900 | 2 | 77 |
| H(35A) | 6310 | -166 | -2681 | 154 |
| H(35B) | 5866 | -838 | -2023 | 154 |
| H(35C) | 6788 | -171 | -1760 | 154 |

Appendix B-2 Crystallographic details of compound 6.4·H₂O

Table 1. Crystal data and structure refinement for 6.4·H₂O (See Section 6.4.4 in Chapter 6).

Table 2. Atomic coordinates ($\times 10^4$) and equivalent isotropic displacement parameters ($\text{\AA}^2 \times 10^3$) for 6.4·H₂O. U(eq) is defined as one third of the trace of the orthogonalized U_{ij} tensor.

| | x | y | z | U(eq) |
|-------|----------|---------|---------|--------|
| O(1) | 8286(1) | 7789(2) | 3881(2) | 54(1) |
| F(1) | 4229(1) | 8033(2) | 1150(2) | 55(1) |
| F(2) | 4305(1) | 9080(2) | -242(2) | 61(1) |
| N(1) | 8506(1) | 6259(3) | 2782(2) | 55(1) |
| N(2) | 7701(2) | 5061(3) | 2677(3) | 62(1) |
| N(3) | 8210(1) | 5841(2) | 4335(3) | 49(1) |
| N(4) | 8924(1) | 5825(3) | 6018(2) | 53(1) |
| N(5) | 9128(1) | 6641(2) | 4486(2) | 49(1) |
| N(6) | 9520(2) | 6625(3) | 2951(3) | 63(1) |
| N(7) | 4985(1) | 9392(2) | 1474(2) | 42(1) |
| N(8) | 5060(1) | 7747(2) | 416(2) | 42(1) |
| B(1) | 8504(2) | 6705(4) | 3862(4) | 50(1) |
| B(2) | 4622(2) | 8572(3) | 672(3) | 42(1) |
| C(1) | 8982(2) | 6318(3) | 2359(3) | 61(1) |
| C(2) | 8812(2) | 5752(4) | 1326(3) | 70(1) |
| C(3) | 9126(3) | 5535(4) | 564(4) | 89(2) |
| C(4) | 8840(4) | 4864(5) | -292(4) | 109(2) |
| C(5) | 8279(3) | 4436(5) | -367(5) | 114(2) |
| C(6) | 7984(3) | 4646(4) | 380(4) | 91(2) |
| C(7) | 8248(2) | 5304(3) | 1239(3) | 67(1) |
| C(8) | 8084(2) | 5558(3) | 2225(3) | 59(1) |
| C(9) | 7790(2) | 5160(3) | 3739(4) | 57(1) |
| C(10) | 7618(2) | 4454(3) | 4513(4) | 59(1) |
| C(11) | 7198(2) | 3630(4) | 4391(4) | 73(1) |
| C(12) | 7168(2) | 3051(4) | 5283(5) | 91(2) |
| C(13) | 7550(2) | 3229(4) | 6273(5) | 90(2) |
| C(14) | 7971(2) | 4035(4) | 6408(4) | 75(1) |
| C(15) | 8000(2) | 4656(3) | 5526(3) | 56(1) |
| C(16) | 8399(2) | 5519(3) | 5387(3) | 51(1) |
| C(17) | 9295(2) | 6329(3) | 5541(3) | 50(1) |
| C(18) | 9929(2) | 6447(3) | 5851(3) | 54(1) |
| C(19) | 10336(2) | 6348(3) | 6844(4) | 63(1) |
| C(20) | 10923(2) | 6522(3) | 6870(4) | 73(1) |
| C(21) | 11104(2) | 6753(3) | 5950(5) | 75(1) |
| C(22) | 10708(2) | 6820(3) | 4961(4) | 68(1) |
| C(23) | 10116(2) | 6687(3) | 4921(3) | 56(1) |

| | | | | |
|-------|---------|----------|----------|--------|
| C(24) | 9590(2) | 6726(3) | 4029(3) | 56(1) |
| C(25) | 7706(2) | 7975(3) | 3356(3) | 44(1) |
| C(26) | 7272(2) | 7830(3) | 3892(3) | 46(1) |
| C(27) | 6693(2) | 8009(3) | 3362(3) | 41(1) |
| C(28) | 6538(1) | 8339(3) | 2301(3) | 38(1) |
| C(29) | 6980(2) | 8534(3) | 1788(3) | 50(1) |
| C(30) | 7561(2) | 8354(3) | 2309(3) | 52(1) |
| C(31) | 5908(2) | 8456(3) | 1728(3) | 39(1) |
| C(32) | 5588(2) | 9320(3) | 1955(3) | 40(1) |
| C(33) | 5750(2) | 10271(3) | 2595(3) | 47(1) |
| C(34) | 5243(2) | 10863(3) | 2499(3) | 52(1) |
| C(35) | 4782(2) | 10312(3) | 1812(3) | 49(1) |
| C(36) | 6354(2) | 10634(3) | 3195(3) | 66(1) |
| C(37) | 4163(2) | 10657(3) | 1458(3) | 70(1) |
| C(38) | 5651(1) | 7649(3) | 983(3) | 38(1) |
| C(39) | 5877(2) | 6683(3) | 645(3) | 43(1) |
| C(40) | 5421(2) | 6250(3) | -141(3) | 54(1) |
| C(41) | 4928(2) | 6898(3) | -274(3) | 46(1) |
| C(42) | 6466(2) | 6162(3) | 1035(3) | 55(1) |
| C(43) | 4333(2) | 6725(3) | -1008(3) | 66(1) |
| O(1W) | 9457(2) | 4275(4) | -2257(4) | 158(2) |

Table 3. Bond lengths [Å] and angles [°] for **6.4·H₂O**.

| | | | |
|-------------|----------|-------------|----------|
| O(1)-C(25) | 1.381(4) | O(1)-B(1) | 1.435(5) |
| F(1)-B(2) | 1.400(4) | F(2)-B(2) | 1.373(4) |
| N(1)-C(1) | 1.364(5) | N(1)-C(8) | 1.373(5) |
| N(1)-B(1) | 1.493(5) | N(2)-C(9) | 1.332(5) |
| N(2)-C(8) | 1.339(5) | N(3)-C(16) | 1.370(5) |
| N(3)-C(9) | 1.375(5) | N(3)-B(1) | 1.483(5) |
| N(4)-C(17) | 1.340(5) | N(4)-C(16) | 1.348(4) |
| N(5)-C(24) | 1.361(5) | N(5)-C(17) | 1.367(4) |
| N(5)-B(1) | 1.487(5) | N(6)-C(1) | 1.356(5) |
| N(6)-C(24) | 1.359(5) | N(7)-C(35) | 1.345(4) |
| N(7)-C(32) | 1.401(4) | N(7)-B(2) | 1.540(5) |
| N(8)-C(41) | 1.356(4) | N(8)-C(38) | 1.404(4) |
| N(8)-B(2) | 1.542(5) | C(1)-C(2) | 1.462(6) |
| C(2)-C(3) | 1.394(6) | C(2)-C(7) | 1.415(6) |
| C(3)-C(4) | 1.405(8) | C(4)-C(5) | 1.403(8) |
| C(5)-C(6) | 1.343(7) | C(6)-C(7) | 1.384(6) |
| C(7)-C(8) | 1.448(6) | C(9)-C(10) | 1.454(6) |
| C(10)-C(11) | 1.398(6) | C(10)-C(15) | 1.405(5) |
| C(11)-C(12) | 1.367(6) | C(12)-C(13) | 1.377(7) |
| C(13)-C(14) | 1.384(6) | C(14)-C(15) | 1.384(6) |

| | | | |
|-------------------|----------|--------------------------|----------|
| C(15)-C(16) | 1.459(5) | C(17)-C(18) | 1.452(5) |
| C(18)-C(19) | 1.394(5) | C(18)-C(23) | 1.404(5) |
| C(19)-C(20) | 1.392(6) | C(20)-C(21) | 1.383(6) |
| C(21)-C(22) | 1.375(6) | C(22)-C(23) | 1.391(5) |
| C(23)-C(24) | 1.460(5) | C(25)-C(26) | 1.380(5) |
| C(25)-C(30) | 1.382(5) | C(26)-C(27) | 1.379(4) |
| C(27)-C(28) | 1.379(4) | C(28)-C(29) | 1.385(5) |
| C(28)-C(31) | 1.488(4) | C(29)-C(30) | 1.381(5) |
| C(31)-C(32) | 1.378(4) | C(31)-C(38) | 1.408(4) |
| C(32)-C(33) | 1.428(5) | C(33)-C(34) | 1.380(5) |
| C(33)-C(36) | 1.504(5) | C(34)-C(35) | 1.391(5) |
| C(35)-C(37) | 1.475(5) | C(38)-C(39) | 1.417(4) |
| C(39)-C(40) | 1.383(5) | C(39)-C(42) ¹ | 1.494(5) |
| C(40)-C(41) | 1.384(5) | C(41)-C(43) | 1.493(5) |
| C(25)-O(1)-B(1) | 117.5(3) | C(1)-N(1)-C(8) | 112.6(4) |
| C(1)-N(1)-B(1) | 123.0(3) | C(8)-N(1)-B(1) | 123.0(4) |
| C(9)-N(2)-C(8) | 116.9(4) | C(16)-N(3)-C(9) | 112.4(3) |
| C(16)-N(3)-B(1) | 122.9(3) | C(9)-N(3)-B(1) | 123.8(3) |
| C(17)-N(4)-C(16) | 117.4(3) | C(24)-N(5)-C(17) | 112.8(3) |
| C(24)-N(5)-B(1) | 123.4(3) | C(17)-N(5)-B(1) | 123.1(3) |
| C(1)-N(6)-C(24) | 116.9(3) | C(35)-N(7)-C(32) | 108.3(3) |
| C(35)-N(7)-B(2) | 126.0(3) | C(32)-N(7)-B(2) | 125.6(3) |
| C(41)-N(8)-C(38) | 107.9(3) | C(41)-N(8)-B(2) | 126.4(3) |
| C(38)-N(8)-B(2) | 125.1(3) | O(1)-B(1)-N(3) | 117.1(3) |
| O(1)-B(1)-N(5) | 110.5(3) | N(3)-B(1)-N(5) | 104.0(3) |
| O(1)-B(1)-N(1) | 116.4(3) | N(3)-B(1)-N(1) | 103.1(3) |
| N(5)-B(1)-N(1) | 104.3(3) | F(2)-B(2)-F(1) | 108.3(3) |
| F(2)-B(2)-N(7) | 111.2(3) | F(1)-B(2)-N(7) | 109.6(3) |
| F(2)-B(2)-N(8) | 111.6(3) | F(1)-B(2)-N(8) | 109.4(3) |
| N(7)-B(2)-N(8) | 106.8(3) | N(6)-C(1)-N(1) | 122.4(4) |
| N(6)-C(1)-C(2) | 130.1(4) | N(1)-C(1)-C(2) | 105.7(4) |
| C(3)-C(2)-C(7) | 121.5(5) | C(3)-C(2)-C(1) | 131.0(5) |
| C(7)-C(2)-C(1) | 107.2(4) | C(2)-C(3)-C(4) | 115.3(6) |
| C(5)-C(4)-C(3) | 122.1(6) | C(6)-C(5)-C(4) | 121.7(6) |
| C(5)-C(6)-C(7) | 118.2(6) | C(6)-C(7)-C(2) | 121.1(5) |
| C(6)-C(7)-C(8) | 131.2(5) | C(2)-C(7)-C(8) | 107.3(4) |
| N(2)-C(8)-N(1) | 122.7(4) | N(2)-C(8)-C(7) | 129.5(4) |
| N(1)-C(8)-C(7) | 106.0(4) | N(2)-C(9)-N(3) | 122.1(4) |
| N(2)-C(9)-C(10) | 130.3(4) | N(3)-C(9)-C(10) | 105.7(3) |
| C(11)-C(10)-C(15) | 120.2(4) | C(11)-C(10)-C(9) | 132.0(4) |
| C(15)-C(10)-C(9) | 107.6(4) | C(12)-C(11)-C(10) | 118.0(5) |
| C(11)-C(12)-C(13) | 122.1(5) | C(12)-C(13)-C(14) | 120.7(5) |
| C(13)-C(14)-C(15) | 118.5(5) | C(14)-C(15)-C(10) | 120.5(4) |
| C(14)-C(15)-C(16) | 132.1(4) | C(10)-C(15)-C(16) | 107.4(4) |

| | | | |
|-------------------|----------|-------------------|----------|
| N(4)-C(16)-N(3) | 122.1(3) | N(4)-C(16)-C(15) | 130.6(4) |
| N(3)-C(16)-C(15) | 105.8(3) | N(4)-C(17)-N(5) | 121.8(3) |
| N(4)-C(17)-C(18) | 131.7(4) | N(5)-C(17)-C(18) | 105.1(3) |
| C(19)-C(18)-C(23) | 120.4(4) | C(19)-C(18)-C(17) | 131.6(4) |
| C(23)-C(18)-C(17) | 108.0(3) | C(20)-C(19)-C(18) | 117.3(4) |
| C(21)-C(20)-C(19) | 121.9(4) | C(22)-C(21)-C(20) | 121.3(4) |
| C(21)-C(22)-C(23) | 117.8(4) | C(22)-C(23)-C(18) | 121.3(4) |
| C(22)-C(23)-C(24) | 132.0(4) | C(18)-C(23)-C(24) | 106.7(3) |
| N(6)-C(24)-N(5) | 121.8(4) | N(6)-C(24)-C(23) | 131.1(4) |
| N(5)-C(24)-C(23) | 105.7(3) | C(26)-C(25)-O(1) | 120.0(3) |
| C(26)-C(25)-C(30) | 119.8(3) | O(1)-C(25)-C(30) | 120.1(3) |
| C(27)-C(26)-C(25) | 119.8(3) | C(26)-C(27)-C(28) | 121.1(3) |
| C(27)-C(28)-C(29) | 118.6(3) | C(27)-C(28)-C(31) | 119.9(3) |
| C(29)-C(28)-C(31) | 121.4(3) | C(30)-C(29)-C(28) | 120.7(3) |
| C(29)-C(30)-C(25) | 119.9(3) | C(32)-C(31)-C(38) | 121.8(3) |
| C(32)-C(31)-C(28) | 120.0(3) | C(38)-C(31)-C(28) | 118.1(3) |
| C(31)-C(32)-N(7) | 120.2(3) | C(31)-C(32)-C(33) | 132.5(3) |
| N(7)-C(32)-C(33) | 107.2(3) | C(34)-C(33)-C(32) | 106.5(3) |
| C(34)-C(33)-C(36) | 124.9(3) | C(32)-C(33)-C(36) | 128.4(3) |
| C(33)-C(34)-C(35) | 108.5(3) | N(7)-C(35)-C(34) | 109.5(3) |
| N(7)-C(35)-C(37) | 123.2(3) | C(34)-C(35)-C(37) | 127.3(4) |
| N(8)-C(38)-C(31) | 119.5(3) | N(8)-C(38)-C(39) | 108.3(3) |
| C(31)-C(38)-C(39) | 132.3(3) | C(40)-C(39)-C(38) | 105.4(3) |
| C(40)-C(39)-C(42) | 124.2(3) | C(38)-C(39)-C(42) | 130.4(3) |
| C(39)-C(40)-C(41) | 109.9(3) | N(8)-C(41)-C(40) | 108.5(3) |
| N(8)-C(41)-C(43) | 123.2(3) | C(40)-C(41)-C(43) | 128.3(3) |

Table 4. Anisotropic displacement parameters ($\text{\AA}^2 \times 10^3$) for **6.4·H₂O**. The anisotropic displacement factor exponent takes the form: $-2 \pi^2[(ha^*)^2U_{11} + \dots + 2hka^*b^*U_{12}]$.

| | U11 | U22 | U33 | U23 | U13 | U12 |
|------|-------|-------|-------|-------|-------|-------|
| O(1) | 38(1) | 49(2) | 68(2) | -8(1) | 0(1) | 4(1) |
| F(1) | 46(1) | 53(1) | 69(1) | 8(1) | 20(1) | -2(1) |
| F(2) | 65(1) | 63(1) | 47(1) | 14(1) | 1(1) | 12(1) |
| N(1) | 50(2) | 57(2) | 54(2) | -1(2) | 5(2) | 12(2) |
| N(2) | 54(2) | 59(2) | 62(2) | -8(2) | -5(2) | 10(2) |
| N(3) | 37(2) | 47(2) | 59(2) | -9(2) | 5(2) | 3(1) |
| N(4) | 44(2) | 60(2) | 54(2) | -8(2) | 9(2) | -3(2) |
| N(5) | 37(2) | 57(2) | 51(2) | 0(2) | 8(2) | 6(2) |
| N(6) | 61(2) | 65(2) | 65(2) | 11(2) | 22(2) | 13(2) |
| N(7) | 40(2) | 38(2) | 47(2) | 0(1) | 10(1) | 3(1) |
| N(8) | 40(2) | 40(2) | 45(2) | -2(1) | 9(1) | -2(1) |
| B(1) | 37(2) | 54(3) | 56(3) | -5(2) | 6(2) | 6(2) |
| B(2) | 41(2) | 40(2) | 44(2) | 9(2) | 9(2) | 3(2) |

| | | | | | | |
|-------|--------|--------|--------|--------|--------|--------|
| C(1) | 66(3) | 56(3) | 61(3) | 6(2) | 13(2) | 14(2) |
| C(2) | 99(4) | 64(3) | 44(2) | 8(2) | 15(3) | 34(3) |
| C(3) | 121(4) | 84(4) | 65(3) | 19(3) | 29(3) | 43(3) |
| C(4) | 188(7) | 95(5) | 47(3) | 5(3) | 35(4) | 64(5) |
| C(5) | 170(7) | 87(5) | 71(4) | -7(3) | 8(5) | 31(5) |
| C(6) | 133(5) | 71(3) | 54(3) | -10(3) | -4(3) | 30(3) |
| C(7) | 82(3) | 56(3) | 54(3) | 0(2) | -3(2) | 21(2) |
| C(8) | 60(3) | 52(3) | 54(3) | -11(2) | -5(2) | 18(2) |
| C(9) | 41(2) | 51(2) | 71(3) | -11(2) | -3(2) | 10(2) |
| C(10) | 43(2) | 50(3) | 81(3) | -6(2) | 12(2) | 3(2) |
| C(11) | 42(2) | 66(3) | 106(4) | -12(3) | 10(2) | -10(2) |
| C(12) | 58(3) | 83(4) | 130(5) | -3(4) | 20(3) | -18(3) |
| C(13) | 78(4) | 91(4) | 111(4) | 7(3) | 42(3) | -18(3) |
| C(14) | 67(3) | 84(3) | 80(3) | -4(3) | 32(3) | -10(3) |
| C(15) | 44(2) | 56(3) | 69(3) | -9(2) | 17(2) | 0(2) |
| C(16) | 40(2) | 59(3) | 55(3) | -12(2) | 12(2) | 2(2) |
| C(17) | 42(2) | 56(2) | 48(2) | -4(2) | 6(2) | 4(2) |
| C(18) | 43(2) | 49(2) | 64(3) | -1(2) | 2(2) | 3(2) |
| C(19) | 52(3) | 52(3) | 74(3) | 0(2) | -5(2) | -1(2) |
| C(20) | 44(3) | 58(3) | 99(4) | -3(3) | -13(3) | 4(2) |
| C(21) | 40(3) | 62(3) | 116(4) | -4(3) | 9(3) | 6(2) |
| C(22) | 43(3) | 62(3) | 101(4) | 2(2) | 20(3) | 3(2) |
| C(23) | 40(2) | 50(2) | 75(3) | 3(2) | 12(2) | 6(2) |
| C(24) | 46(2) | 58(3) | 65(3) | 6(2) | 15(2) | 9(2) |
| C(25) | 33(2) | 39(2) | 55(2) | -8(2) | 2(2) | 2(2) |
| C(26) | 49(2) | 48(2) | 41(2) | 0(2) | 11(2) | 3(2) |
| C(27) | 39(2) | 44(2) | 42(2) | 1(2) | 13(2) | -2(2) |
| C(28) | 37(2) | 35(2) | 41(2) | -2(2) | 10(2) | -2(2) |
| C(29) | 45(2) | 59(3) | 45(2) | 10(2) | 8(2) | 2(2) |
| C(30) | 47(2) | 57(3) | 58(3) | 7(2) | 22(2) | 0(2) |
| C(31) | 41(2) | 37(2) | 38(2) | 4(2) | 10(2) | -1(2) |
| C(32) | 43(2) | 36(2) | 39(2) | 0(2) | 8(2) | 2(2) |
| C(33) | 57(3) | 38(2) | 42(2) | 0(2) | 7(2) | -2(2) |
| C(34) | 62(3) | 41(2) | 54(2) | -6(2) | 15(2) | 9(2) |
| C(35) | 51(2) | 42(2) | 53(2) | 3(2) | 15(2) | 10(2) |
| C(36) | 64(3) | 48(2) | 77(3) | -12(2) | 5(2) | -7(2) |
| C(37) | 64(3) | 68(3) | 76(3) | 0(2) | 16(2) | 26(2) |
| C(38) | 38(2) | 36(2) | 40(2) | -1(2) | 10(2) | -1(2) |
| C(39) | 43(2) | 43(2) | 45(2) | -5(2) | 14(2) | 2(2) |
| C(40) | 56(3) | 48(2) | 60(3) | -15(2) | 20(2) | 1(2) |
| C(41) | 51(2) | 43(2) | 45(2) | -7(2) | 12(2) | -8(2) |
| C(42) | 53(2) | 48(2) | 66(3) | -5(2) | 20(2) | 9(2) |
| C(43) | 62(3) | 65(3) | 63(3) | -13(2) | 0(2) | -14(2) |
| O(1W) | 157(4) | 180(5) | 153(4) | 30(3) | 70(3) | 31(3) |

Table 5. Hydrogen coordinates ($\times 10^4$) and isotropic displacement parameters ($\text{\AA}^2 \times 10^3$) for **6.4-H₂O**.

| | x | y | z | U(eq) |
|--------|-------|-------|-------|-------|
| H(3A) | 9499 | 5815 | 618 | 107 |
| H(4B) | 9028 | 4698 | -827 | 131 |
| H(5A) | 8106 | 3996 | -949 | 136 |
| H(6B) | 7613 | 4356 | 322 | 109 |
| H(11A) | 6947 | 3481 | 3722 | 87 |
| H(12A) | 6881 | 2521 | 5220 | 109 |
| H(13A) | 7525 | 2802 | 6857 | 108 |
| H(14A) | 8229 | 4156 | 7077 | 89 |
| H(19A) | 10219 | 6172 | 7463 | 76 |
| H(20A) | 11203 | 6482 | 7526 | 87 |
| H(21A) | 11500 | 6864 | 6000 | 90 |
| H(22A) | 10832 | 6950 | 4339 | 82 |
| H(26A) | 7369 | 7612 | 4608 | 56 |
| H(27A) | 6401 | 7905 | 3725 | 49 |
| H(29A) | 6884 | 8790 | 1084 | 60 |
| H(30A) | 7854 | 8486 | 1957 | 63 |
| H(34A) | 5214 | 11520 | 2836 | 63 |
| H(36A) | 6326 | 11310 | 3548 | 98 |
| H(36B) | 6594 | 10726 | 2699 | 98 |
| H(36C) | 6527 | 10098 | 3722 | 98 |
| H(37A) | 3940 | 10118 | 989 | 105 |
| H(37B) | 4139 | 11334 | 1081 | 105 |
| H(37C) | 4006 | 10744 | 2075 | 105 |
| H(40A) | 5442 | 5617 | -523 | 65 |
| H(42A) | 6479 | 5510 | 634 | 82 |
| H(42B) | 6531 | 5989 | 1785 | 82 |
| H(42C) | 6765 | 6652 | 937 | 82 |
| H(43A) | 4077 | 7306 | -920 | 100 |
| H(43B) | 4176 | 6049 | -837 | 100 |
| H(43C) | 4362 | 6709 | -1740 | 100 |

Appendix B-3 Crystallographic details of compound 6.5·CH₂Cl₂

Table 1. Crystal data and structure refinement for 6.5·CH₂Cl₂ (See Section 6.4.4 in Chapter 6).

Table 2. Atomic coordinates ($\times 10^4$) and equivalent isotropic displacement parameters ($\text{\AA}^2 \times 10^3$) for 6.5·CH₂Cl₂. U(eq) is defined as one third of the trace of the orthogonalized U_{ij} tensor.

| | x | y | z | U(eq) |
|-------|----------|----------|---------|--------|
| F(1) | 7206(4) | 4420(4) | 3512(4) | 92(2) |
| O(1) | 1788(4) | 416(4) | 3106(3) | 68(1) |
| O(2) | 6341(5) | 9942(4) | 4012(4) | 86(2) |
| O(3) | 14359(6) | 5999(6) | 598(6) | 138(3) |
| N(1) | 1580(5) | -883(4) | 2642(4) | 60(2) |
| N(2) | -29(5) | -437(4) | 2115(4) | 61(2) |
| N(3) | 1546(5) | 760(4) | 1578(4) | 56(1) |
| N(4) | 3336(5) | 1681(5) | 465(4) | 68(2) |
| N(5) | 3306(5) | 203(5) | 1786(4) | 61(2) |
| N(6) | 3415(6) | -1517(5) | 2548(5) | 78(2) |
| N(7) | 5310(4) | 4424(4) | 3393(4) | 56(1) |
| N(8) | 6943(5) | 3756(4) | 2485(4) | 62(2) |
| F(2) | 7000(4) | 5469(3) | 2154(4) | 107(2) |
| C(1) | 2267(7) | -1646(5) | 2804(5) | 66(2) |
| C(2) | 1502(8) | -2517(6) | 3083(6) | 78(2) |
| C(3) | 1659(11) | -3517(6) | 3414(6) | 101(3) |
| C(4) | 797(12) | -4163(7) | 3593(7) | 106(3) |
| C(5) | -271(10) | -3856(6) | 3451(6) | 99(3) |
| C(6) | -434(8) | -2848(6) | 3110(5) | 80(2) |
| C(7) | 452(7) | -2183(5) | 2948(5) | 66(2) |
| C(8) | 562(6) | -1116(5) | 2588(5) | 61(2) |
| C(9) | 514(6) | 480(5) | 1569(5) | 58(2) |
| C(10) | 350(6) | 1263(5) | 747(5) | 59(2) |
| C(11) | -554(7) | 1391(6) | 396(6) | 77(2) |
| C(12) | -417(9) | 2213(7) | -447(7) | 93(3) |
| C(13) | 603(10) | 2857(7) | -929(7) | 104(3) |
| C(14) | 1520(7) | 2709(6) | -602(6) | 82(2) |
| C(15) | 1372(6) | 1915(5) | 253(5) | 64(2) |
| C(16) | 2181(6) | 1528(5) | 760(5) | 62(2) |
| C(17) | 3883(6) | 966(6) | 950(6) | 68(2) |
| C(18) | 5093(6) | 709(7) | 664(6) | 76(2) |
| C(19) | 6065(7) | 1219(8) | -120(7) | 98(3) |
| C(20) | 7084(8) | 750(11) | -206(8) | 105(4) |
| C(21) | 7090(10) | -167(12) | 456(12) | 123(5) |
| C(22) | 6126(9) | -721(9) | 1225(8) | 102(3) |
| C(23) | 5111(7) | -249(7) | 1322(7) | 78(2) |

| | | | | |
|-------|-----------|-----------|----------|---------|
| C(24) | 3928(7) | -591(7) | 1991(6) | 68(2) |
| C(25) | 2534(6) | 1104(5) | 3060(5) | 62(2) |
| C(26) | 3192(7) | 764(6) | 3647(6) | 73(2) |
| C(27) | 3958(7) | 1414(6) | 3628(6) | 73(2) |
| C(28) | 4069(6) | 2422(5) | 3043(5) | 55(2) |
| C(29) | 3408(6) | 2743(5) | 2479(6) | 70(2) |
| C(30) | 2626(6) | 2096(5) | 2491(6) | 69(2) |
| C(31) | 4928(6) | 3115(5) | 2997(5) | 58(2) |
| C(32) | 4533(6) | 3724(5) | 3476(5) | 53(2) |
| C(33) | 3409(6) | 3803(5) | 4057(5) | 56(2) |
| C(34) | 2303(6) | 3185(6) | 4400(6) | 77(2) |
| C(35) | 3530(6) | 4570(5) | 4271(5) | 61(2) |
| C(36) | 4706(6) | 4971(5) | 3848(5) | 56(2) |
| C(37) | 5243(6) | 5831(5) | 3802(5) | 65(2) |
| C(38) | 4652(6) | 6415(5) | 4199(5) | 64(2) |
| C(39) | 5151(6) | 7325(5) | 4129(5) | 62(2) |
| C(40) | 6264(7) | 7715(5) | 3602(6) | 73(2) |
| C(41) | 6721(7) | 8600(5) | 3517(6) | 77(2) |
| C(42) | 5996(7) | 9083(5) | 4027(5) | 66(2) |
| C(43) | 4864(7) | 8690(5) | 4571(6) | 73(2) |
| C(44) | 4445(7) | 7842(5) | 4615(6) | 72(2) |
| C(45) | 7500(9) | 10317(7) | 3541(9) | 122(4) |
| C(46) | 6108(6) | 3146(5) | 2497(5) | 64(2) |
| C(47) | 6709(7) | 2659(6) | 1923(6) | 82(2) |
| C(48) | 6205(8) | 1947(8) | 1668(8) | 112(4) |
| C(49) | 7862(7) | 2977(7) | 1600(7) | 89(3) |
| C(50) | 8002(7) | 3655(6) | 1946(6) | 73(2) |
| C(51) | 9051(7) | 4164(6) | 1806(6) | 78(2) |
| C(52) | 10104(7) | 4166(6) | 1210(6) | 79(2) |
| C(53) | 11189(6) | 4635(6) | 1082(6) | 72(2) |
| C(54) | 11312(7) | 4963(7) | 1699(7) | 92(3) |
| C(55) | 12350(8) | 5434(7) | 1556(8) | 99(3) |
| C(56) | 13296(8) | 5537(7) | 804(8) | 99(3) |
| C(57) | 13233(9) | 5217(9) | 172(8) | 123(4) |
| C(58) | 12183(8) | 4736(8) | 316(7) | 111(3) |
| C(59) | 14599(11) | 6083(10) | 1340(11) | 164(6) |
| B(1) | 2044(7) | 145(6) | 2331(6) | 57(2) |
| B(2) | 6644(7) | 4533(6) | 2890(7) | 63(2) |
| CI(1) | 828(6) | -3160(6) | 5546(5) | 271(3) |
| CI(2) | 481(10) | -1346(8) | 5345(9) | 434(6) |
| C(60) | 999(18) | -2343(10) | 6079(13) | 410(30) |

Table 3. Bond lengths [Å] and angles [°] for 6.5-CH₂Cl₂.

| | | | |
|-------------|-----------|-------------|-----------|
| F(1)-B(2) | 1.382(10) | O(1)-C(25) | 1.379(8) |
| O(1)-B(1) | 1.440(8) | O(2)-C(42) | 1.362(8) |
| O(2)-C(45) | 1.386(11) | O(3)-C(56) | 1.378(11) |
| O(3)-C(59) | 1.421(15) | N(1)-C(8) | 1.358(8) |
| N(1)-C(1) | 1.367(8) | N(1)-B(1) | 1.480(9) |
| N(2)-C(9) | 1.345(8) | N(2)-C(8) | 1.348(8) |
| N(3)-C(9) | 1.365(8) | N(3)-C(16) | 1.366(9) |
| N(3)-B(1) | 1.515(9) | N(4)-C(16) | 1.332(9) |
| N(4)-C(17) | 1.346(9) | N(5)-C(24) | 1.357(9) |
| N(5)-C(17) | 1.360(9) | N(5)-B(1) | 1.490(9) |
| N(6)-C(1) | 1.326(10) | N(6)-C(24) | 1.346(10) |
| N(7)-C(36) | 1.360(8) | N(7)-C(32) | 1.388(8) |
| N(7)-B(2) | 1.547(10) | N(8)-C(50) | 1.346(9) |
| N(8)-C(46) | 1.400(8) | N(8)-B(2) | 1.538(9) |
| F(2)-B(2) | 1.392(9) | C(1)-C(2) | 1.462(11) |
| C(2)-C(3) | 1.390(11) | C(2)-C(7) | 1.409(10) |
| C(3)-C(4) | 1.344(13) | C(4)-C(5) | 1.426(13) |
| C(5)-C(6) | 1.402(11) | C(6)-C(7) | 1.396(10) |
| C(7)-C(8) | 1.448(10) | C(9)-C(10) | 1.455(10) |
| C(10)-C(11) | 1.390(9) | C(10)-C(15) | 1.406(9) |
| C(11)-C(12) | 1.395(11) | C(12)-C(13) | 1.398(12) |
| C(13)-C(14) | 1.378(11) | C(14)-C(15) | 1.386(10) |
| C(15)-C(16) | 1.460(10) | C(17)-C(18) | 1.477(10) |
| C(18)-C(19) | 1.390(11) | C(18)-C(23) | 1.401(12) |
| C(19)-C(20) | 1.389(13) | C(20)-C(21) | 1.359(15) |
| C(21)-C(22) | 1.389(16) | C(22)-C(23) | 1.389(11) |
| C(23)-C(24) | 1.457(11) | C(25)-C(30) | 1.375(10) |
| C(25)-C(26) | 1.394(9) | C(26)-C(27) | 1.376(9) |
| C(27)-C(28) | 1.397(9) | C(28)-C(29) | 1.368(9) |
| C(28)-C(31) | 1.483(9) | C(29)-C(30) | 1.391(9) |
| C(31)-C(46) | 1.395(9) | C(31)-C(32) | 1.408(8) |
| C(32)-C(33) | 1.421(9) | C(33)-C(35) | 1.363(9) |
| C(33)-C(34) | 1.484(9) | C(35)-C(36) | 1.413(9) |
| C(36)-C(37) | 1.441(9) | C(37)-C(38) | 1.342(9) |
| C(38)-C(39) | 1.468(9) | C(39)-C(40) | 1.352(10) |
| C(39)-C(44) | 1.401(9) | C(40)-C(41) | 1.401(10) |
| C(41)-C(42) | 1.396(10) | C(42)-C(43) | 1.376(10) |
| C(43)-C(44) | 1.360(10) | C(46)-C(47) | 1.423(10) |
| C(47)-C(49) | 1.366(11) | C(47)-C(48) | 1.525(10) |
| C(49)-C(50) | 1.399(10) | C(50)-C(51) | 1.434(10) |
| C(51)-C(52) | 1.333(10) | C(52)-C(53) | 1.449(11) |
| C(53)-C(54) | 1.362(11) | C(53)-C(58) | 1.393(11) |
| C(54)-C(55) | 1.391(11) | C(55)-C(56) | 1.345(13) |

| | | | |
|-------------------|-----------|-------------------|-----------|
| C(56)-C(57) | 1.350(14) | C(57)-C(58) | 1.411(13) |
| Cl(1)-C(60) | 1.838(10) | Cl(2)-C(60) | 1.739(9) |
| C(25)-O(1)-B(1) | 119.6(5) | C(42)-O(2)-C(45) | 118.9(6) |
| C(56)-O(3)-C(59) | 118.0(9) | C(8)-N(1)-C(1) | 113.9(6) |
| C(8)-N(1)-B(1) | 123.3(6) | C(1)-N(1)-B(1) | 121.3(6) |
| C(9)-N(2)-C(8) | 116.9(6) | C(9)-N(3)-C(16) | 113.3(6) |
| C(9)-N(3)-B(1) | 122.5(6) | C(16)-N(3)-B(1) | 123.0(6) |
| C(16)-N(4)-C(17) | 116.5(7) | C(24)-N(5)-C(17) | 113.0(6) |
| C(24)-N(5)-B(1) | 121.8(7) | C(17)-N(5)-B(1) | 124.0(6) |
| C(1)-N(6)-C(24) | 117.2(6) | C(36)-N(7)-C(32) | 108.7(5) |
| C(36)-N(7)-B(2) | 126.2(5) | C(32)-N(7)-B(2) | 125.1(5) |
| C(50)-N(8)-C(46) | 109.0(5) | C(50)-N(8)-B(2) | 126.4(6) |
| C(46)-N(8)-B(2) | 123.9(6) | N(6)-C(1)-N(1) | 123.4(7) |
| N(6)-C(1)-C(2) | 130.7(7) | N(1)-C(1)-C(2) | 104.4(7) |
| C(3)-C(2)-C(7) | 120.8(8) | C(3)-C(2)-C(1) | 131.9(9) |
| C(7)-C(2)-C(1) | 107.3(6) | C(4)-C(3)-C(2) | 118.8(10) |
| C(3)-C(4)-C(5) | 122.3(9) | C(6)-C(5)-C(4) | 119.3(9) |
| C(7)-C(6)-C(5) | 118.1(9) | C(6)-C(7)-C(2) | 120.6(7) |
| C(6)-C(7)-C(8) | 131.6(7) | C(2)-C(7)-C(8) | 107.7(6) |
| N(2)-C(8)-N(1) | 123.0(6) | N(2)-C(8)-C(7) | 130.6(7) |
| N(1)-C(8)-C(7) | 105.1(6) | N(2)-C(9)-N(3) | 122.4(6) |
| N(2)-C(9)-C(10) | 130.8(6) | N(3)-C(9)-C(10) | 105.4(6) |
| C(11)-C(10)-C(15) | 121.2(7) | C(11)-C(10)-C(9) | 131.3(7) |
| C(15)-C(10)-C(9) | 107.3(6) | C(10)-C(11)-C(12) | 117.0(8) |
| C(11)-C(12)-C(13) | 121.1(8) | C(14)-C(13)-C(12) | 122.0(8) |
| C(13)-C(14)-C(15) | 117.2(8) | C(14)-C(15)-C(10) | 121.4(7) |
| C(14)-C(15)-C(16) | 130.7(7) | C(10)-C(15)-C(16) | 107.6(6) |
| N(4)-C(16)-N(3) | 123.0(6) | N(4)-C(16)-C(15) | 130.5(7) |
| N(3)-C(16)-C(15) | 104.9(6) | N(4)-C(17)-N(5) | 122.9(6) |
| N(4)-C(17)-C(18) | 130.6(8) | N(5)-C(17)-C(18) | 105.5(7) |
| C(19)-C(18)-C(23) | 122.3(8) | C(19)-C(18)-C(17) | 130.9(9) |
| C(23)-C(18)-C(17) | 106.6(7) | C(20)-C(19)-C(18) | 116.8(10) |
| C(21)-C(20)-C(19) | 119.9(11) | C(20)-C(21)-C(22) | 125.2(10) |
| C(21)-C(22)-C(23) | 115.1(11) | C(22)-C(23)-C(18) | 120.6(9) |
| C(22)-C(23)-C(24) | 131.6(10) | C(18)-C(23)-C(24) | 107.6(7) |
| N(6)-C(24)-N(5) | 122.3(7) | N(6)-C(24)-C(23) | 130.0(7) |
| N(5)-C(24)-C(23) | 105.9(8) | C(30)-C(25)-O(1) | 123.2(6) |
| C(30)-C(25)-C(26) | 119.5(6) | O(1)-C(25)-C(26) | 117.3(7) |
| C(27)-C(26)-C(25) | 120.0(7) | C(26)-C(27)-C(28) | 120.9(7) |
| C(29)-C(28)-C(27) | 118.3(6) | C(29)-C(28)-C(31) | 120.9(6) |
| C(27)-C(28)-C(31) | 120.7(6) | C(28)-C(29)-C(30) | 121.6(7) |
| C(25)-C(30)-C(29) | 119.7(7) | C(46)-C(31)-C(32) | 121.1(6) |
| C(46)-C(31)-C(28) | 119.9(6) | C(32)-C(31)-C(28) | 119.0(6) |
| N(7)-C(32)-C(31) | 119.9(6) | N(7)-C(32)-C(33) | 108.1(5) |

| | | | |
|-------------------|-----------|-------------------|-----------|
| C(31)-C(32)-C(33) | 132.0(6) | C(35)-C(33)-C(32) | 106.3(6) |
| C(35)-C(33)-C(34) | 124.9(6) | C(32)-C(33)-C(34) | 128.8(6) |
| C(33)-C(35)-C(36) | 109.5(6) | N(7)-C(36)-C(35) | 107.3(5) |
| N(7)-C(36)-C(37) | 122.3(6) | C(35)-C(36)-C(37) | 130.3(6) |
| C(38)-C(37)-C(36) | 123.3(7) | C(37)-C(38)-C(39) | 125.2(7) |
| C(40)-C(39)-C(44) | 117.0(7) | C(40)-C(39)-C(38) | 123.7(6) |
| C(44)-C(39)-C(38) | 119.3(7) | C(39)-C(40)-C(41) | 123.2(7) |
| C(42)-C(41)-C(40) | 118.0(8) | O(2)-C(42)-C(43) | 117.1(6) |
| O(2)-C(42)-C(41) | 123.6(7) | C(43)-C(42)-C(41) | 119.3(7) |
| C(44)-C(43)-C(42) | 120.9(7) | C(43)-C(44)-C(39) | 121.6(7) |
| C(31)-C(46)-N(8) | 121.1(6) | C(31)-C(46)-C(47) | 131.8(6) |
| N(8)-C(46)-C(47) | 107.1(6) | C(49)-C(47)-C(46) | 106.4(6) |
| C(49)-C(47)-C(48) | 125.0(7) | C(46)-C(47)-C(48) | 128.5(7) |
| C(47)-C(49)-C(50) | 109.5(7) | N(8)-C(50)-C(49) | 108.0(6) |
| N(8)-C(50)-C(51) | 122.9(6) | C(49)-C(50)-C(51) | 129.1(7) |
| C(52)-C(51)-C(50) | 125.3(7) | C(51)-C(52)-C(53) | 126.7(7) |
| C(54)-C(53)-C(58) | 116.6(8) | C(54)-C(53)-C(52) | 123.2(7) |
| C(58)-C(53)-C(52) | 120.1(8) | C(53)-C(54)-C(55) | 122.7(9) |
| C(56)-C(55)-C(54) | 119.7(9) | C(55)-C(56)-C(57) | 120.4(9) |
| C(55)-C(56)-O(3) | 124.0(11) | C(57)-C(56)-O(3) | 115.5(10) |
| C(56)-C(57)-C(58) | 120.0(10) | C(53)-C(58)-C(57) | 120.4(10) |
| O(1)-B(1)-N(1) | 112.0(6) | O(1)-B(1)-N(5) | 115.3(5) |
| N(1)-B(1)-N(5) | 105.3(5) | O(1)-B(1)-N(3) | 115.6(6) |
| N(1)-B(1)-N(3) | 104.4(5) | N(5)-B(1)-N(3) | 103.0(6) |
| F(1)-B(2)-F(2) | 108.2(6) | F(1)-B(2)-N(8) | 111.6(6) |
| F(2)-B(2)-N(8) | 108.8(7) | F(1)-B(2)-N(7) | 110.0(7) |
| F(2)-B(2)-N(7) | 109.9(6) | N(8)-B(2)-N(7) | 108.2(5) |
| Cl(2)-C(60)-Cl(1) | 93.9(8) | | |

Table 4. Anisotropic displacement parameters ($\text{\AA}^2 \times 10^3$) for **6.5-CH₂Cl₂**. The anisotropic displacement factor exponent takes the form: $-2 \pi^2[(ha^*)^2 U_{11} + \dots + 2hka^*b^* U_{12}]$.

| | U11 | U22 | U33 | U23 | U13 | U12 |
|------|-------|--------|--------|--------|--------|--------|
| F(1) | 59(3) | 134(4) | 130(4) | -94(4) | -41(3) | 17(3) |
| O(1) | 65(3) | 81(3) | 67(3) | -42(3) | -14(2) | -13(3) |
| O(2) | 93(4) | 68(3) | 108(5) | -52(3) | -27(4) | 6(3) |
| O(3) | 81(5) | 173(7) | 124(6) | -19(5) | -41(4) | -23(5) |
| N(1) | 60(4) | 66(4) | 66(4) | -37(3) | -23(3) | 6(3) |
| N(2) | 51(3) | 65(4) | 65(4) | -35(3) | -10(3) | 2(3) |
| N(3) | 50(3) | 61(3) | 65(4) | -32(3) | -23(3) | 2(3) |
| N(4) | 52(4) | 82(4) | 67(4) | -30(4) | -17(3) | -8(3) |
| N(5) | 53(4) | 80(4) | 62(4) | -39(4) | -23(3) | 9(3) |
| N(6) | 83(5) | 95(5) | 85(5) | -51(4) | -51(4) | 31(4) |

| | | | | | | |
|-------|---------|---------|---------|----------|---------|--------|
| N(7) | 52(3) | 58(3) | 70(4) | -38(3) | -22(3) | 6(3) |
| N(8) | 55(4) | 64(4) | 75(4) | -40(3) | -18(3) | 5(3) |
| F(2) | 92(4) | 65(3) | 119(4) | -30(3) | 9(3) | -7(2) |
| C(1) | 85(6) | 68(5) | 67(5) | -35(4) | -44(4) | 23(4) |
| C(2) | 107(7) | 67(5) | 75(6) | -34(4) | -43(5) | 14(5) |
| C(3) | 170(10) | 64(6) | 96(7) | -41(5) | -71(7) | 30(6) |
| C(4) | 164(11) | 63(6) | 97(8) | -34(5) | -52(7) | 20(7) |
| C(5) | 134(9) | 66(6) | 83(7) | -36(5) | -9(6) | -19(6) |
| C(6) | 101(6) | 71(5) | 60(5) | -33(4) | -11(4) | 1(5) |
| C(7) | 81(5) | 57(4) | 60(5) | -28(4) | -18(4) | -6(4) |
| C(8) | 64(5) | 68(5) | 57(4) | -34(4) | -18(4) | 3(4) |
| C(9) | 51(4) | 62(5) | 67(5) | -37(4) | -16(4) | 2(3) |
| C(10) | 54(4) | 58(4) | 67(5) | -30(4) | -19(4) | 8(3) |
| C(11) | 69(5) | 84(6) | 98(7) | -48(5) | -42(5) | 12(4) |
| C(12) | 101(7) | 92(6) | 96(7) | -27(6) | -60(6) | 2(6) |
| C(13) | 131(9) | 85(6) | 95(7) | -15(6) | -66(7) | 2(6) |
| C(14) | 87(6) | 77(5) | 74(6) | -20(5) | -30(5) | -17(4) |
| C(15) | 62(5) | 62(4) | 71(5) | -26(4) | -27(4) | -3(4) |
| C(16) | 59(5) | 67(5) | 61(5) | -26(4) | -17(4) | -10(4) |
| C(17) | 56(5) | 92(6) | 67(5) | -46(5) | -18(4) | -4(4) |
| C(18) | 49(5) | 125(7) | 78(6) | -68(6) | -21(4) | 1(5) |
| C(19) | 50(5) | 169(9) | 103(7) | -92(7) | -14(5) | -13(6) |
| C(20) | 53(6) | 185(12) | 120(9) | -113(9) | -17(6) | -2(7) |
| C(21) | 78(8) | 200(13) | 190(14) | -160(13) | -73(10) | 61(9) |
| C(22) | 71(6) | 167(10) | 131(9) | -109(8) | -56(7) | 40(7) |
| C(23) | 55(5) | 121(7) | 98(7) | -76(6) | -37(5) | 25(5) |
| C(24) | 69(5) | 86(6) | 73(5) | -48(5) | -36(5) | 21(5) |
| C(25) | 57(4) | 72(5) | 68(5) | -45(4) | -16(4) | 4(4) |
| C(26) | 82(5) | 66(5) | 89(6) | -36(4) | -47(5) | 12(4) |
| C(27) | 73(5) | 72(5) | 93(6) | -37(5) | -47(5) | 6(4) |
| C(28) | 57(4) | 57(4) | 62(4) | -30(4) | -25(4) | 4(3) |
| C(29) | 75(5) | 59(4) | 88(6) | -36(4) | -38(5) | 10(4) |
| C(30) | 67(5) | 66(5) | 87(6) | -37(4) | -39(4) | 10(4) |
| C(31) | 59(5) | 59(4) | 68(5) | -33(4) | -29(4) | 9(3) |
| C(32) | 52(4) | 54(4) | 62(4) | -29(4) | -22(3) | 4(3) |
| C(33) | 46(4) | 65(4) | 66(5) | -33(4) | -22(3) | 7(3) |
| C(34) | 61(5) | 89(5) | 88(6) | -51(5) | -13(4) | -7(4) |
| C(35) | 57(5) | 66(4) | 65(5) | -33(4) | -23(4) | 12(4) |
| C(36) | 59(4) | 55(4) | 63(4) | -30(4) | -26(4) | 8(3) |
| C(37) | 64(5) | 62(4) | 81(5) | -36(4) | -31(4) | 12(4) |
| C(38) | 68(5) | 59(4) | 76(5) | -36(4) | -31(4) | 15(4) |
| C(39) | 63(5) | 67(4) | 73(5) | -39(4) | -34(4) | 17(4) |
| C(40) | 70(5) | 71(5) | 97(6) | -54(5) | -26(5) | 10(4) |
| C(41) | 77(5) | 72(5) | 86(6) | -45(5) | -20(4) | 8(4) |

| | | | | | | |
|-------|---------|---------|---------|---------|----------|----------|
| C(42) | 78(5) | 54(4) | 77(5) | -35(4) | -29(4) | 13(4) |
| C(43) | 79(6) | 69(5) | 96(6) | -54(5) | -40(5) | 26(4) |
| C(44) | 60(5) | 77(5) | 101(6) | -57(5) | -31(4) | 20(4) |
| C(45) | 112(9) | 96(7) | 165(11) | -79(8) | -22(8) | -13(6) |
| C(46) | 61(5) | 70(5) | 82(5) | -47(4) | -29(4) | 8(4) |
| C(47) | 66(5) | 98(6) | 109(7) | -71(6) | -28(5) | 7(4) |
| C(48) | 85(6) | 152(9) | 157(10) | -123(8) | -36(6) | 8(6) |
| C(49) | 56(5) | 111(7) | 123(7) | -82(6) | -15(5) | 11(5) |
| C(50) | 57(5) | 83(5) | 89(6) | -53(5) | -17(4) | 8(4) |
| C(51) | 60(5) | 83(5) | 103(6) | -56(5) | -21(5) | 8(4) |
| C(52) | 63(5) | 104(6) | 87(6) | -57(5) | -24(5) | 13(4) |
| C(53) | 51(5) | 79(5) | 83(6) | -35(5) | -19(4) | 7(4) |
| C(54) | 52(5) | 120(7) | 111(7) | -65(6) | -13(5) | -1(5) |
| C(55) | 73(6) | 111(7) | 125(9) | -62(7) | -31(6) | 0(5) |
| C(56) | 65(6) | 110(7) | 96(8) | -18(6) | -27(6) | -9(5) |
| C(57) | 72(7) | 184(12) | 88(8) | -47(8) | -8(6) | -2(7) |
| C(58) | 70(6) | 169(10) | 87(7) | -55(7) | -15(5) | -4(6) |
| C(59) | 121(10) | 178(12) | 193(14) | -41(11) | -97(10) | -23(8) |
| B(1) | 52(5) | 69(5) | 63(5) | -40(5) | -18(4) | 2(4) |
| B(2) | 50(5) | 54(5) | 83(6) | -33(5) | -14(4) | -3(4) |
| Cl(1) | 210(5) | 347(7) | 278(6) | -140(5) | -98(4) | 19(5) |
| Cl(2) | 419(9) | 348(8) | 454(10) | -156(7) | -73(7) | 37(7) |
| C(60) | 330(30) | 300(30) | 420(40) | 190(30) | -310(30) | -150(20) |

Table 5. Hydrogen coordinates ($\times 10^4$) and isotropic displacement parameters ($\text{\AA}^2 \times 10^3$) for $6.5\text{-CH}_2\text{Cl}_2$.

| | x | y | z | U(eq) |
|--------|-------|-------|-------|-------|
| H(3A) | 2348 | -3736 | 3510 | 121 |
| H(4B) | 901 | -4833 | 3817 | 128 |
| H(5A) | -854 | -4321 | 3584 | 119 |
| H(6A) | -1114 | -2628 | 2994 | 96 |
| H(11A) | -1219 | 948 | 710 | 92 |
| H(12A) | -1014 | 2334 | -692 | 112 |
| H(13A) | 665 | 3402 | -1487 | 125 |
| H(14A) | 2209 | 3124 | -941 | 98 |
| H(19A) | 6036 | 1844 | -566 | 117 |
| H(20A) | 7759 | 1062 | -717 | 126 |
| H(21A) | 7796 | -445 | 390 | 147 |
| H(22A) | 6158 | -1361 | 1643 | 122 |
| H(26A) | 3113 | 98 | 4050 | 88 |
| H(27A) | 4408 | 1181 | 4010 | 87 |
| H(29A) | 3482 | 3410 | 2079 | 84 |
| H(30A) | 2169 | 2333 | 2116 | 82 |

| | | | | |
|--------|-------|-------|------|-----|
| H(34A) | 1691 | 3415 | 4787 | 116 |
| H(34B) | 2393 | 2510 | 4761 | 116 |
| H(34C) | 2112 | 3231 | 3872 | 116 |
| H(35A) | 2930 | 4796 | 4639 | 73 |
| H(37A) | 6041 | 5990 | 3480 | 78 |
| H(38A) | 3863 | 6228 | 4546 | 77 |
| H(40A) | 6750 | 7379 | 3280 | 88 |
| H(41A) | 7484 | 8859 | 3133 | 92 |
| H(43A) | 4380 | 9007 | 4914 | 87 |
| H(44A) | 3671 | 7600 | 4975 | 87 |
| H(45A) | 7608 | 10925 | 3582 | 183 |
| H(45B) | 7714 | 10435 | 2892 | 183 |
| H(45C) | 7979 | 9849 | 3821 | 183 |
| H(48A) | 6824 | 1751 | 1254 | 168 |
| H(48B) | 5666 | 2267 | 1359 | 168 |
| H(48C) | 5808 | 1373 | 2230 | 168 |
| H(49A) | 8462 | 2774 | 1210 | 107 |
| H(51A) | 8992 | 4522 | 2159 | 93 |
| H(52A) | 10147 | 3832 | 839 | 95 |
| H(54A) | 10677 | 4867 | 2239 | 111 |
| H(55A) | 12390 | 5677 | 1978 | 119 |
| H(57A) | 13882 | 5313 | -358 | 148 |
| H(58A) | 12154 | 4485 | -103 | 133 |
| H(59A) | 15350 | 6441 | 1098 | 246 |
| H(59B) | 14597 | 5436 | 1811 | 246 |
| H(59C) | 14014 | 6430 | 1614 | 246 |
| H(60A) | 512 | -2577 | 6736 | 495 |
| H(60B) | 1802 | -2212 | 5999 | 495 |
